



Graduation Project

Submitted to:

Prof. Osama

Prof. Gamal

By

Al-Sayed Azzat	Sec: 1	B.N : 19
Abdel-Kareem Shehata	Sec: 1	B.N : 32
Fatma Khalil	Sec: 2	B.N : 3
Mustafa Mahmoud	Sec: 2	B.N : 28
Yara Omar	Sec: 2	B.N : 36

AEROSPACE ENGINEERING DEPARTMENT,
FACULTY OF ENGINEERING,
CAIRO UNIVERSITY

June, 2018

ACKNOWLEDGEMENT

I would first like to thank my thesis advisor [title] [Name Surname] of the [School / Faculty name] at [University name]. The door to Prof. [Last name] office was always open whenever I ran into a trouble spot or had a question about my research or writing. He/She consistently allowed this paper to be my own work, but steered me in the right direction whenever he thought I needed it.

I would also like to thank the experts who were involved in the validation survey for this research project: [List professional Titles, Name and Surnames of the experts who participated/contributed]. Without their passionate participation and input, the validation survey could not have been successfully conducted.

I would also like to acknowledge [title] [Name Surname] of the [School / Faculty name] at [University name] as the second reader of this thesis, and I am gratefully indebted to his/her for his/her very valuable comments on this thesis.

Finally, I must express my very profound gratitude to my parents and to my [partner, spouse, girl/boyfriend] for providing me with unfailing support and continuous encouragement throughout my years of study and through the process of researching and writing this thesis. This accomplishment would not have been possible without them. Thank you.

Author

Contents

Acknowledgments	i
Table of Contents	ii
List of Tables	vii
List of Figures	viii
List of Codes	xvi
Chapter 1 Drones in Business	1
1.1 Introduction	1
1.2 Applicable Applications in Egypt	1
1.2.1 Using drones in Precision Agriculture	1
1.2.1.1 Introduction	1
1.2.1.2 Applications	2
1.2.1.3 Case Studies	8
1.2.2 Using drones in Media and Entertainment	26
1.2.2.1 Aerial photography	26
1.2.2.2 Advertising	29
1.2.3 Using drones in Search and Rescue	30
1.2.3.1 Introduction	30
1.2.3.2 Saving and Rescue UAS	30
1.2.3.3 Firefighting Drones	32
1.2.4 Using drones in Disaster Relief and Emergency Response	34
1.2.4.1 Introduction	34
1.2.4.2 Major Usage	34
1.2.4.3 Advantages in Disaster Relief and Emergency Response:	36
1.2.5 Using drones in Wind Turbine Inspection	37
1.2.6 Using drones in Other Applications	37
1.3 Conclusion	38
Chapter 2 Autopilot Overview	39
2.1 Introduction	39
2.2 Components of an Autopilot System	40
2.3 Professional Autopilot's Definitions	40
Auto Mode ⁴² Guided Mode ⁴² Land Mode ⁴³ Position Hold Mode ⁴³ Simple and Super Simple Modes ⁴³	
Brake Mode ⁴³ Circle Mode ⁴⁴ Sport Mode ⁴⁴ Follow Me Mode ⁴⁴	
2.4 Guidance System	44

Contents

2.4.1	Introduction	44	
2.5	Control System	49	
2.6	Navigation System	51	
2.7	Ground Control Station [1]	52	
2.7.1	Introduction	52	
2.7.2	Capabilities	52	
2.8	Telemetry	57	
2.8.1	Introduction	57	
Chapter 3	Drone Use in Aerial Images Application	58	
3.1	Introduction	58	
3.2	Cameras	60	
Hyperspectral vs. Multispectral Imaging Technology	71	Why Hyperspectral Over Multispectral for Precision Agriculture?	72
3.3	Images Analysis Software	75	
Chapter 4	Drone Use in Aerial Pesticide Application	78	
Chapter 5	Ground Control Station	82	
5.1	Introduction	82	
5.1.1	Features	82	
Chapter 6	Hardware	83	
6.1	Motor	83	
6.2	Connections	83	
6.3	First Iteration	85	
Chapter 7	Sizing	88	
7.1	Survey	88	
7.1.1	Charts [2]	96	
7.2	Coaxial vs Flat	99	
7.2.1	Experiment	100	
7.2.1.1	Side by Side	100	
7.2.1.2	Coaxial	100	
7.3	Requirements	100	
7.4	Sizing Procedure	101	
7.4.1	Data base	101	
7.4.2	Algorithm	103	
7.4.2.1	Requirements	103	
7.4.2.2	Motor selection	103	
7.4.2.3	Battery selection	103	
7.4.2.4	Weight check	103	
7.4.2.5	Flow chart	104	
7.5	Sizing Algorithm	106	
Chapter 8	Control and Simulation	108	
8.1	Open loop test	108	
8.1.1	Rig configuration	108	

Contents

8.1.2	Actual System Response in case of Δ_{Roll}	109
8.1.3	Actual System Response in case of Δ_{Pitch}	121
8.1.4	Actual System Response in case of Δ_{Yaw}	133
8.2	Non linear Simulation	144
8.2.1	Airplane Equations of Motion	144
8.2.2	Results for Nominal Thrust is 1650	147
8.2.2.1	Roll	148
8.2.2.2	Pitch	151
8.2.2.3	Yaw	154
8.2.3	Results for Nominal Thrust is 1700	157
8.2.3.1	Roll	157
8.2.3.2	Pitch	162
8.2.3.3	Yaw	165
8.3	Linearization	169
8.4	Comparing with Nonlinear Response	171
8.5	Control	178
8.6	Applying Controller on The Non Linear model	186
8.7	Testing on Actual System and Results	195
Chapter 9	Mechanical Design	196
9.1	Design Specifications	196
9.2	Constraints and Other Considerations	196
9.3	Major Components	197
9.3.1	Common Types of Materials Used For Drone Frames	198
9.3.2	Airframe Configuration	199
9.3.2.1	Quad , Hexa & Octa	199
9.3.2.2	Octoquad	200
9.3.2.3	Conclusion	200
9.3.3	Types of Motors	200
9.3.4	Propellers Types and Materials	201
9.3.5	Propeller Guards	203
9.3.6	Collision Tolerant	203
9.4	Design Layout	204
9.4.1	Structural Design	204
9.4.2	Material Selection	204
9.4.2.1	Why Foam?	204
9.4.3	Landing Leg Configuration	205
9.4.3.1	1st Iteration	205
9.4.3.2	2nd Iteration	205
9.4.4	Safety Frame	205
9.4.5	Motor Propellers Mounted	206
9.4.6	Design Alternatives	206
9.4.6.1	Overview of Conceptual Design Alternative	206
9.4.6.2	Design Alternative 1	207
9.4.6.3	Design Alternative 2	208
9.4.6.4	Design Alternative 3	209
9.4.6.5	Design Alternative 4	210

Contents

9.4.6.6	Design Alternative 5	211
9.4.6.7	Comparing Weights	211
9.5	Final Design	212
9.6	Manufacturing Process	212
9.7	Assembly Process	212
9.7.1	Jigs	212
9.7.2	Steps for Assembly	212
9.8	Stress Analysis	212
9.9	Strain Analysis	212
9.10	Vibrations Frequency Analysis	212
9.11	Suggestions to Enhance The Design	212
Chapter 10	Numerical Analysis of The Drone	213
10.1	Introduction	213
10.2	Model and Mesh	213
Chapter 11	Take-off Mode Analysis.	220
11.1	First Model Full Analysis	220
11.1.1	Geometry	220
11.1.2	Mesh	220
11.1.3	Setup	222
11.1.3.1	Model	222
11.1.3.2	Material	222
11.1.3.3	Boundary Conditions	223
11.1.4	Solution	224
11.1.5	Solution Methods	224
11.1.6	Results	225
11.2	Second Model Full Analysis	225
11.2.1	Geomtry	225
11.2.2	Mesh	226
11.2.3	Setup and solution	228
11.2.4	Results	228
Chapter 12	Forward Flight Mode Analysis	229
Bibliography		229
Appendix A Camera Terminology		232
Appendix B Ground Control Station		241
B.1	Windows API	251
B.2	Spline path	252
B.3	Manual	255
B.3.1	Make path	255
B.3.2	Modify way point	257
B.3.3	Make circle path	259
B.3.4	Make spline path	260
B.3.5	Delete last point	262

Contents

B.3.6 Delete all points	263
B.3.7 Refresh maps	263
B.3.8 Close the program	264
Appendix C Numerical Solution of differential equations using Runge-Kutta 4th order	265
C.1 Mat-lab code Implementation	266
Appendix D Moment of Inertia Estimation Using a Bifilar Pendulum	268
Appendix E Measuring Motors' Paramters	272
E.1 First Method	272
E.2 Second Method	277
E.3 Comparison	280

List of Tables

1.1	PWC' survey results[3]	1
1.2	AXIS Q8641-E detection ranges	31
3.1	Comparison between multi-spectral cameras	63
3.2	Consumer camera vs professional multi-spectral camera[4]	64
3.3	Comparison between consumer cameras	67
3.4	Survey 3 camera's specifications	68
6.1	Motor's specifications	83
7.1	Mission requirements	100
7.2	one of 30 motor in data base	102
7.3	battery data collection	102
7.4	Sizing's results	107
8.1	Equivalent transfer function for every test for roll rate	119
8.2	Equivalent transfer function for every test for roll angle	120
8.3	Equivalent transfer function for every test for pitch rate	131
8.4	Equivalent transfer function for every test for pitch angle	132
8.5	Equivalent transfer function for every test for yaw rate	143
8.6	Forces	145
8.7	Moments	146
9.1	Pros & Cons of different airframes configurations	199
D.1	Bifilar testing data	270
D.2	Moment of Inertia Results	270
E.1	Motors' constants	280
E.2	Comparison of motors' thrust constant using the two methods @ Nom.Thrust =1650	280
E.3	Comparison of motors' thrust constant using the two methods @ Nom.Thrust =1700	280

List of Figures

1.1	Fertilizers spreading drone	2
1.2	Reflection of light on plant	3
1.3	NDVI formula	3
1.4	NDVI image example	4
1.5	NDVI showing effects of compaction	5
1.6	True color and NIR showing nitrogen stress	6
1.7	VRA image	7
1.8	Weeded areas	8
1.9	Nonplanted areas	9
1.10	High vigor areas	10
1.11	NDVI zoning	11
1.12	Plugged center pivot emitters zones	12
1.13	Inefficient furrow irrigation zones	13
1.14	Spider mites zones	14
1.15	Targeted weed zone	15
1.16	Unevenly planted zones	16
1.17	Unevenly matured zones	17
1.18	Differing soil types zones	18
1.19	Infected powdery mildew zones	19
1.20	Infected zones	20
1.21	Weedy zones	21
1.22	Irrigation systems leak zones	22
1.23	Uneven field vigor zone #1	23
1.24	Uneven field vigor zone #2	24
1.25	Uneven vineyard vigor zone	25
1.26	Football match image taken by a drone	26
1.27	Cairo tower image taken by a drone	27
1.28	Road traffic image taken by a drone	28
1.29	Intel image #1	29
1.30	Intel image #2	29
1.31	TVIP-PHX-640-100HD camera specifications	30
1.32	AXIS Q8641-E PT camera specifications	31
1.33	Dropping life vests drone	32
1.34	Thermal image taken by a Drone	33
1.35	Wind Turbine inspection	37
1.36	Pipeline inspections	38
2.1	Components of an Autopilot System	40
2.2	RTL mode	41

List of Figures

2.3	Auto Mode	42
2.4	Guided Mode	42
2.5	Guidance principles line of sight (LOS), pure pursuit (PP), and constant bearing (CB).	45
2.6	The main variables associated with steering laws for straight-line paths.	46
2.7	Navigation in x-y plane with circle of acceptance	47
2.8	Block diagram of a guidance system[5]	48
2.9	Navigation map	48
2.10	PID controller scheme	49
2.11	Block diagram of a guidance, navigation and control system	51
2.12	INS validation	52
2.13	Mission planner user interface	53
2.14	GCS Flight Data Screen #1	54
2.15	GCS Flight Data Screen #2	55
2.16	Typical log file	56
2.17	Waypoints specified map	56
2.18	Telemetry module	57
3.1	Parrot SEQUOIA	60
3.2	Parrot SEQUOIA's specifications	60
3.3	MicaSense RedEdge	61
3.4	MicaSense RedEdge's specifications	61
3.5	The Sentera Double 4K	62
3.6	NIR filter	63
3.7	Right image from red edge camera and left image from consumer camera with filter	64
3.8	Canon S110 RGB/NIR/RE camera's images	66
3.9	Mapir Survey 3 camera	68
3.10	GSD vs Height	69
3.11	Velocity vs Height	69
3.12	Corning micro HSI 410 camera	70
3.13	Light bands	72
3.14	FLIR VUE camera	73
3.15	Flir Vue specifications	73
3.16	Motion blur	74
3.17	Basic free services	75
3.18	Price plan	76
4.1	Drone used to spray fertilizers	78
4.2	Water Pump	79
4.3	Tank	79
4.4	Nozzle kit	80
4.5	Radar system	80
4.6	Aliexpress Spraying kit	81
6.1	Connections #1	83
6.2	Connections #2	84
6.3	Connections #3	84
6.4	PCB #1	85
6.5	PCB #2	86

List of Figures

6.6	PCB #3	86
6.7	PCB #4	87
7.1	3DR X8+ Multicopter	88
7.2	Mk8-3500 Agrar	89
7.3	Mk8-3500 Agrar's specifications	89
7.4	Mk8-3500 Agrar's flight times	90
7.5	Agras MG-1S	91
7.6	Agras MG-1S's specifications #1	91
7.7	Agras MG-1S's specifications #2	92
7.8	Agras MG-1S's specifications #3	92
7.9	Agras MG-1S's specifications #4	93
7.10	Matrice 200 Series	94
7.11	Matrice 200 Series's specifications #1	95
7.12	Matrice 200 Series's specifications #2	95
7.13	Empty weight vs payload (quad copter)	96
7.14	Empty weight vs payload (coax copter)	97
7.15	Empty weight vs payload (octa copter)	97
7.16	Empty weight vs payload (hexa copter)	98
7.17	Empty weight vs payload (tri copter)	98
7.18	Coaxial vs Flat #1	99
7.19	Coaxial vs Flat #2	99
7.20	Experiment #1	100
7.21	Performance Testing Data Sheet for KDE2814XF-515	101
7.22	flow chart part 1	104
7.23	flow chart part 2	105
8.1	3DOF Test Jig	108
8.2	Nominal thrust = 1650 , $\Delta_{Roll} = 10$	109
8.3	Nominal thrust = 1700 , $\Delta_{Roll} = 10$	110
8.4	Nominal thrust = 1650 , $\Delta_{Roll} = -10$	110
8.5	Nominal thrust = 1700 , $\Delta_{Roll} = -10$	111
8.6	Nominal thrust = 1650 , $\Delta_{Roll} = 20$	111
8.7	Nominal thrust = 1700 , $\Delta_{Roll} = 20$	112
8.8	Nominal thrust = 1650 , $\Delta_{Roll} = -20$	112
8.9	Nominal thrust = 1700 , $\Delta_{Roll} = -20$	113
8.10	Nominal thrust = 1650 , $\Delta_{Roll} = 30$	114
8.11	Nominal thrust = 1700 , $\Delta_{Roll} = 30$	114
8.12	Nominal thrust = 1650 , $\Delta_{Roll} = -30$	115
8.13	Nominal thrust = 1700 , $\Delta_{Roll} = -30$	116
8.14	Positive step response for roll rate	117
8.15	Negative step response for roll rate	117
8.16	Positive step response for roll angle	118
8.17	Negative step response for roll angle	119
8.18	Nominal thrust = 1650 , $\Delta_{Pitch} = 10$	121
8.19	Nominal thrust = 1700 , $\Delta_{Pitch} = 10$	121
8.20	Nominal thrust = 1650 , $\Delta_{Pitch} = -10$	122
8.21	Nominal thrust = 1700 , $\Delta_{Pitch} = -10$	123

List of Figures

8.22 Nominal thrust = 1650 , $\Delta_{Pitch} = 20$	123
8.23 Nominal thrust = 1700 , $\Delta_{Pitch} = 20$	124
8.24 Nominal thrust = 1650 , $\Delta_{Pitch} = -20$	124
8.25 Nominal thrust = 1700 , $\Delta_{Pitch} = -20$	125
8.26 Nominal thrust = 1650 , $\Delta_{Pitch} = 30$	126
8.27 Nominal thrust = 1700 , $\Delta_{Pitch} = 30$	126
8.28 Nominal thrust = 1650 , $\Delta_{Pitch} = -30$	127
8.29 Nominal thrust = 1700 , $\Delta_{Pitch} = -30$	128
8.30 Positive step response for pitch rate	129
8.31 Negative step response for pitch rate	130
8.32 Positive step response for pitch angle	130
8.33 Negative step response for pitch angle	131
8.34 Nominal thrust = 1650 , $\Delta_{Yaw} = 10$	133
8.35 Nominal thrust = 1700 , $\Delta_{Yaw} = 10$	134
8.36 Nominal thrust = 1650 , $\Delta_{Yaw} = -10$	134
8.37 Nominal thrust = 1700 , $\Delta_{Yaw} = -10$	135
8.38 Nominal thrust = 1650 , $\Delta_{Yaw} = 20$	136
8.39 Nominal thrust = 1700 , $\Delta_{Yaw} = 20$	136
8.40 Nominal thrust = 1650 , $\Delta_{Yaw} = -20$	137
8.41 Nominal thrust = 1700 , $\Delta_{Yaw} = -20$	138
8.42 Nominal thrust = 1650 , $\Delta_{Yaw} = 30$	138
8.43 Nominal thrust = 1700 , $\Delta_{Yaw} = 30$	139
8.44 Nominal thrust = 1650 , $\Delta_{Yaw} = -30$	140
8.45 Nominal thrust = 1700 , $\Delta_{Yaw} = -30$	140
8.46 Positive step response for yaw rate	141
8.47 Negative step response for yaw rate	142
8.48 Positive step response for yaw angle	142
8.49 Negative step response for yaw angle	143
8.50 Equivalent transfer function for every test for yaw angle	144
8.51 Nominal thrust = 1650 , $\Delta_{Roll} = 10$	148
8.52 Nominal thrust = 1650 , $\Delta_{Roll} = -10$	148
8.53 Nominal thrust = 1650 , $\Delta_{Roll} = 20$	149
8.54 Nominal thrust = 1650 , $\Delta_{Roll} = -20$	149
8.55 Nominal thrust = 1650 , $\Delta_{Roll} = 30$	150
8.56 Nominal thrust = 1650 , $\Delta_{Roll} = -30$	150
8.57 Nominal thrust = 1650 , $\Delta_{Pitch} = 10$	151
8.58 Nominal thrust = 1650 , $\Delta_{Pitch} = -10$	152
8.59 Nominal thrust = 1650 , $\Delta_{Pitch} = 20$	152
8.60 Nominal thrust = 1650 , $\Delta_{Pitch} = -20$	153
8.61 Nominal thrust = 1650 , $\Delta_{Pitch} = 30$	153
8.62 Nominal thrust = 1650 , $\Delta_{Pitch} = -30$	154
8.63 Nominal thrust = 1650 , $\Delta_{Yaw} = 10$	154
8.64 Nominal thrust = 1650 , $\Delta_{Yaw} = -10$	155
8.65 Nominal thrust = 1650 , $\Delta_{Yaw} = 20$	155
8.66 Nominal thrust = 1650 , $\Delta_{Yaw} = -20$	156
8.67 Nominal thrust = 1650 , $\Delta_{Yaw} = 30$	156
8.68 Nominal thrust = 1650 , $\Delta_{Yaw} = -30$	157

List of Figures

8.69 Nominal thrust = 1700 , $\Delta_{Roll} = 10$	158
8.70 Nominal thrust = 1700 , $\Delta_{Roll} = -10$	159
8.71 Nominal thrust = 1700 , $\Delta_{Roll} = 20$	159
8.72 Nominal thrust = 1700 , $\Delta_{Roll} = -20$	160
8.73 Nominal thrust = 1700 , $\Delta_{Roll} = 30$	160
8.74 Nominal thrust = 1700 , $\Delta_{Roll} = -30$	161
8.75 Nominal thrust = 1700 , $\Delta_{Pitch} = 10$	162
8.76 Nominal thrust = 1700 , $\Delta_{Pitch} = -10$	162
8.77 Nominal thrust = 1700 , $\Delta_{Pitch} = 20$	163
8.78 Nominal thrust = 1700 , $\Delta_{Pitch} = -20$	163
8.79 Nominal thrust = 1700 , $\Delta_{Pitch} = 30$	164
8.80 Nominal thrust = 1700 , $\Delta_{Pitch} = -30$	164
8.81 Nominal thrust = 1700 , $\Delta_{Yaw} = 10$	165
8.82 Nominal thrust = 1700 , $\Delta_{Yaw} = -10$	166
8.83 Nominal thrust = 1700 , $\Delta_{Yaw} = 20$	166
8.84 Nominal thrust = 1700 , $\Delta_{Yaw} = -20$	167
8.85 Nominal thrust = 1700 , $\Delta_{Yaw} = 30$ test #1	167
8.86 Nominal thrust = 1700 , $\Delta_{Yaw} = 30$ test #2	168
8.87 Nominal thrust = 1700 , $\Delta_{Yaw} = -30$	168
8.88 Response #!	171
8.89 Response #2	172
8.90 Response #3	173
8.91 Response #4	174
8.92 Response #5	175
8.93 Response #6	176
8.94 Response #7	177
8.95 Response #8	178
8.96 Z vs time	179
8.97 p vs time	179
8.98 ϕ vs time	180
8.99 q vs time	180
8.100 θ vs time	181
8.101r vs time	181
8.102 ψ vs time	182
8.103p vs time	182
8.104 ϕ vs time	183
8.105q vs time	183
8.106 θ vs time	184
8.107r vs time	184
8.108 ψ vs time	185
8.109Response at Nom. Thrust = 1650	186
8.110Control actions at Nom. Thrust = 1650	187
8.111Response at Nom. Thrust = 1650	188
8.112Control actions at Nom. Thrust = 1650	189
8.113Response at Nom. Thrust = 1650	190
8.114Control actions at Nom. Thrust = 1650	191
8.115Response at Nom. Thrust = 1650	192

List of Figures

8.116 Control actions at Nom. Thrust = 1650	193
8.117 Response at Nom. Thrust = 1650	194
8.118 Control actions at Nom. Thrust = 1650	195
9.1 Matrice	196
9.2 Wooden frame	198
9.3 Carbon Fiber frame	198
9.4 Metal Frame	198
9.5 Plastic frame	199
9.6 Octoquad	200
9.7 Brushed DC Motors	201
9.8 Brushless Motors	201
9.9 Carbon Fiber propellers	202
9.10 Wooden propellers	202
9.11 Plastic propellers	202
9.12 Phantom drone with prop guards	203
9.13 Elios Inspection Drone	203
9.14 Landing leg first iteration	205
9.15 Safety frame progress	205
9.16 A simple connection and its geometry parameters of a co-axis form with two propellers	206
9.17 Design alternative (1) SOLIDWORKS model	207
9.18 Design alternative (1) prototype	207
9.19 Design alternative(2) SOLIDWORKS model	208
9.20 Design alternative(2) prototype	208
9.21 Design alternative(3) SOLIDWORKS model	209
9.22 Design alternative(4) SOLIDWORKS model	210
9.23 Design alternative (5) SOLIDWORKS model	211
10.1 First Model	214
10.2 Second Model	215
10.3 control volume	215
10.4 Sphere of influence	216
10.5 Sphere of influence in mesh	216
10.6 3D view of Mesh	217
10.7 Mesh	217
10.8 Section plane in Mesh	218
10.9 3D Mesh of Third Model	218
10.10view from Y-Z plane of Mesh	219
10.11Section plane in Third Model	219
11.1 First Model Geometry	220
11.2 3D Model of First Mesh	221
11.3 view from Y-Z plane for First Model	221
11.4 section plane for First Model	221
11.5 Model	222
11.6 Material	222
11.7 Boundary conditions	223
11.8 Inlet and outlet only	224

List of Figures

11.9 solution method	225
11.10 Second Model Geometry	226
11.11 3D Mesh of Second Model	227
11.12 view from Y-Z plane of Mesh	227
11.13 Section plane in Second Model	228
A.1 Focal length and flight height effect on area covered	233
A.2 Image rate and flight height effect on overlap	233
A.3 Meter resolution	234
A.4 12 inch resolution	235
A.5 6 inch resolution	235
A.6 3 inch resolution	236
A.7 3 inch resolution	236
A.8 JPEG image vs RAW image	237
A.9 Ideal image acquisition plan	238
A.10 Overlap	238
A.11 Sensor width placed perpendicular to the flight direction.	239
A.12 Sensor width placed perpendicular to the flight direction.	240
B.1 Program sequence diagram	242
B.2 Placemark example	244
B.3 Style example	247
B.4 Path example	249
B.5 Network link example	251
B.6 Aera of interest	252
B.7 Front panel #1	253
B.8 Block diagram #1	254
B.9 Front panel #2	254
B.10 Block diagram #2	255
B.11 Dialog box #1	255
B.12 Dialog box #2	256
B.13 Dialog box #3	256
B.14 Screen shoot #1	257
B.15 Dialog box #2	257
B.16 Screen shoot #2	258
B.17 Dialog box #3	258
B.18 Screen shoot #3	259
B.19 Screen shoot #4	259
B.20 Dialog box #4	260
B.21 Screen shoot #5	260
B.22 Screen shoot #4	261
B.23 Screen shoot #6	261
B.24 Screen shoot #7	262
B.25 Screen shoot #4	262
B.26 Screen shoot #4	263
B.27 Screen shoot #8	263
B.28 Screen shoot #8	264

List of Figures

C.1	RK4 flow chart	265
C.2	Analytic solution vs numerical solution	267
D.1	Bifilar Pendulum Experiment installation	268
D.2	Bifilar Pendulum Experiment cycles	269
D.3	Rectangular prism	270
E.1	Loadcell #1	272
E.2	Load Cell #1	273
E.3	Load Cell calibration	274
E.4	Motor 1	275
E.5	Motor 2	275
E.6	Motor 3	276
E.7	Motor 4	276
E.8	Motor testing	277
E.9	Motor 1	278
E.10	Motor 2	278
E.11	Motor 3	279
E.12	Motor 4	279

List of Codes

0D __ Graduation _ project _ Matlab–project–files _ Non _ linear _ simulation _ RK4.m	266
1D __ Graduation _ project _ Matlab–project–files _ Numerical _ integration _ f.m	266
2D __ Graduation _ project _ Matlab–project–files _ Numerical _ integration _ test _ runge _ kutta.m	267

1. Drones in Business

1.1. Introduction

Drones are taking off across all business sectors. according to PWC ¹, it is estimated that the total addressable value of drone powered solutions in all applicable industries is estimated at over \$127bn. The industry with the best prospects for drone applications is infrastructure, with total addressable value of just over \$45bn.

2015	
Infrastructure	45.2
Transport	13.0
Insurance	6.8
Media & Ent.	8.8
Telecommunication	6.3
Agriculture	32.4
Security	10.5
Mining	4.3
Total	127.3

Table 1.1.: PWC' survey results[3]

1.2. Applicable Applications in Egypt

1.2.1. Using drones in Precision Agriculture

1.2.1.1. Introduction

Agricultural drones have been changing the face of farming and cultivation heavily the past 3-5 years, and completely changing the way that many farmers and other entities go about their business. This

¹PWC is a multinational professional services network corporation, which focuses on audit and assurance, tax and consulting services. they help resolve complex issues and identify opportunities.

1. Drones in Business

drones have the ability to check storm damage, monitor crop progress, and make sure that both crops and herds are healthy.

Precision agriculture is a farming management concept that uses drones for agriculture to measure, observe, and respond to variability found in crops.

When you implement all of the new technology that is available out there including drones in agriculture, you can apply resources (even if limited), to make sure that the farm has a very maximum yield.



Figure 1.1.: Fertilizers spreading drone

1.2.1.2. Applications

Crop Health

It is no secret that there is a strong need for increased agricultural production given the increase expected in population around the globe. There are finite agriculture resources and growers are expected to produce more with less. The need for improved management practices is acute. In order to implement improved practices reliable, timely, and actionable data is required. Enter in-season on-demand aerial imagery.

Aerial imagery is used by consultants (CCAs, scouts, agronomists), cooperatives, and agriculture service providers to assist in calculating the economic differences between the “good” and “bad” crop condition zones enabling improved management decisions. Often times, determining crop health without the “bird’s eye view” from aerial imagery is difficult.

One of the main image types to determine crop health is the Near Infrared (NIR) image. The NIR is most effective to determine the vegetative health of the crop as the other imagery bands (Red, Blue, Green) are “absorbed” by the plant to create food.

1. Drones in Business

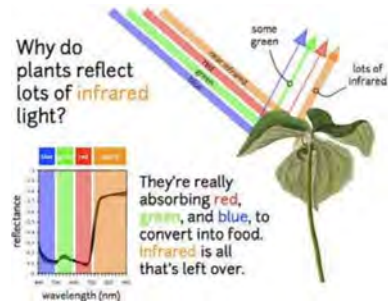


Figure 1.2.: Reflection of light on plant

The NIR band used in conjunction with the red band is utilized to create a vegetation index commonly called a Normalized Difference Vegetation Index (NDVI).

The NDVI provides quantitative information on the health of the crop in the field. The green colored zones have the most robust and volume of vegetation while the yellow and red zones represent less vegetation. This information can be used to make management decisions on the application of inputs like fertilizer and fungicide.

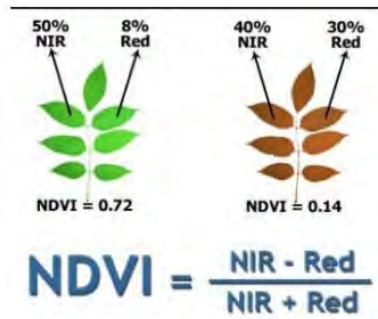


Figure 1.3.: NDVI formula

1. Drones in Business

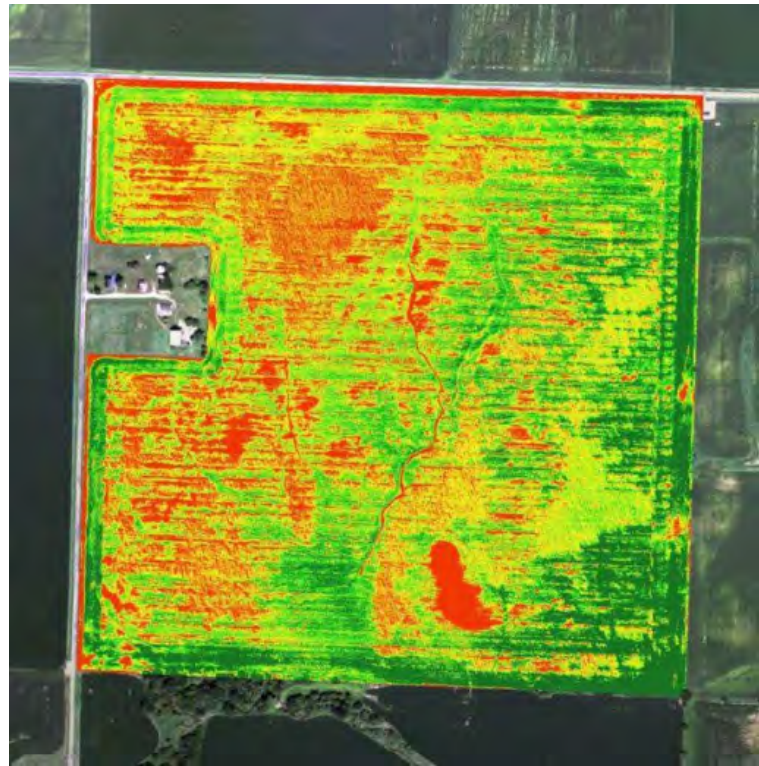


Figure 1.4.: NDVI image example

Compaction

The term “soil compaction” refers to a change in state of the soil that increases its bulk density. Soil compaction is becoming more and more important due to the fact that:

- Equipment is larger
- Uncontrolled traffic
- Earlier field operations
- Operating on wet soils

Identifying compacted areas within a field with the naked eye is difficult and compaction is a difficult variable to measure from the ground without equipment (eg soil penetrometer) and high labor costs.

If a soil is over-compacted there is significant risk of yield reductions as compacted soils affect both soil and plant growth alike:

Effects On Soil	Effects on Plant Growth
Porosity	Root growth
Aeration	Nutrient uptake
Structure	Water Infiltration/Utilization

1. Drones in Business

Aerial imagery shows subtle patterns of soil compaction that are almost impossible to see from the ground. By comparing patterns of traffic and irregular crop growth, problem areas due to compaction are easily identifiable. In Figure 1 above, the red areas on the north side of the field showed yield losses of 45-65 bushels per acre while the red strip on the east side showed yield losses of 20-30 bushels per acre

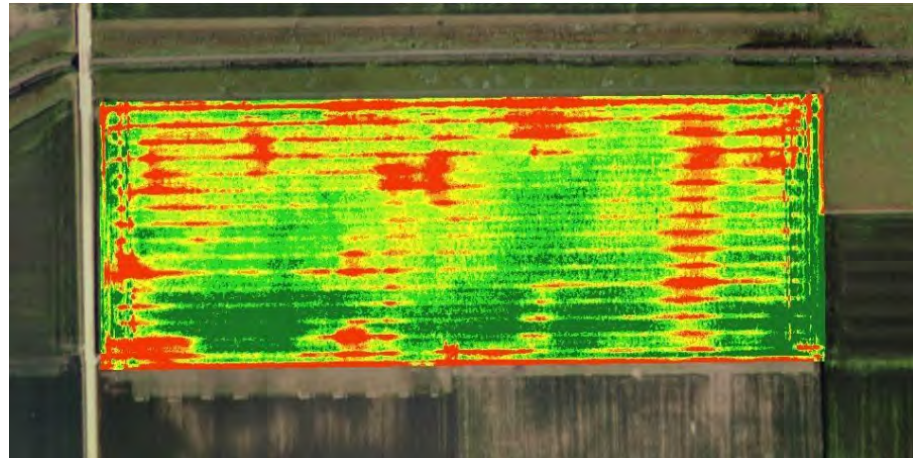


Figure 1.5.: NDVI showing effects of compaction

1. Drones in Business

Variable Rate Application

Variable rate application (VRA) is the method of applying varying rates of inputs in the appropriate zones within an individual field. The ultimate goals of VRA are:

- Maximize farm profitability
- Increase efficiencies in the application of crop inputs
- Ensure environmental safety and sustainability

The management of in-season nitrogen application(s) is a critical component to land management. Mismanagement can result in yield loss and negative impacts to the environment. Given this importance, companies and individuals alike are turning toward aerial imagery as a means to develop nitrogen management zones and the corresponding VRA. The economical nitrogen rate can vary substantially within individual fields. It is difficult to assess these differences in a timely manner without the use of remote sensing. An aerial image, when analyzed appropriately, can provide the agronomist with key insights on the crop. For example, the near-infrared (NIR) light reflecting off a nitrogen stressed corn crop is quite less than a non-nitrogen stressed crop.

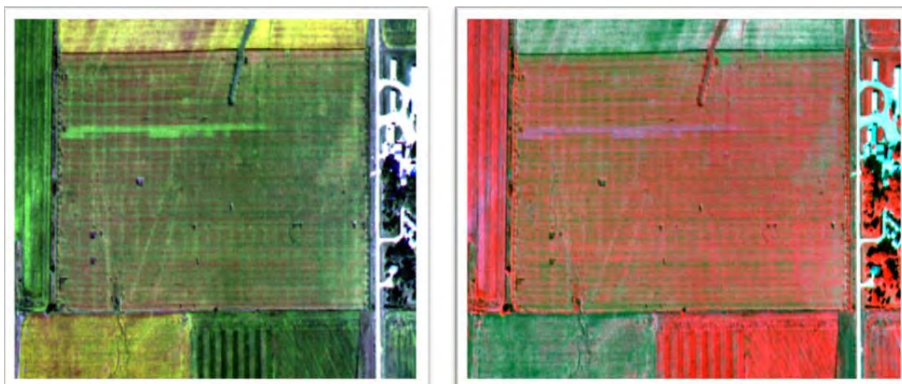


Figure 1.6.: True color and NIR showing nitrogen stress

1. Drones in Business

Once aerial images have been utilized to target scouting efforts, a VRA fertilization file can be created using precision agriculture software (ie Mapshots, SST, AgFleet, etc...) Another application of aerial imagery for VRA is using the bare soil image to create zones to apply soil nutrients and/or amendments. Whether you are looking at VR seeding, VRA for fertilization, or VRA for herbicide/fungicide and aerial image is the data layer to use to enable better management decisions and increase profitability.

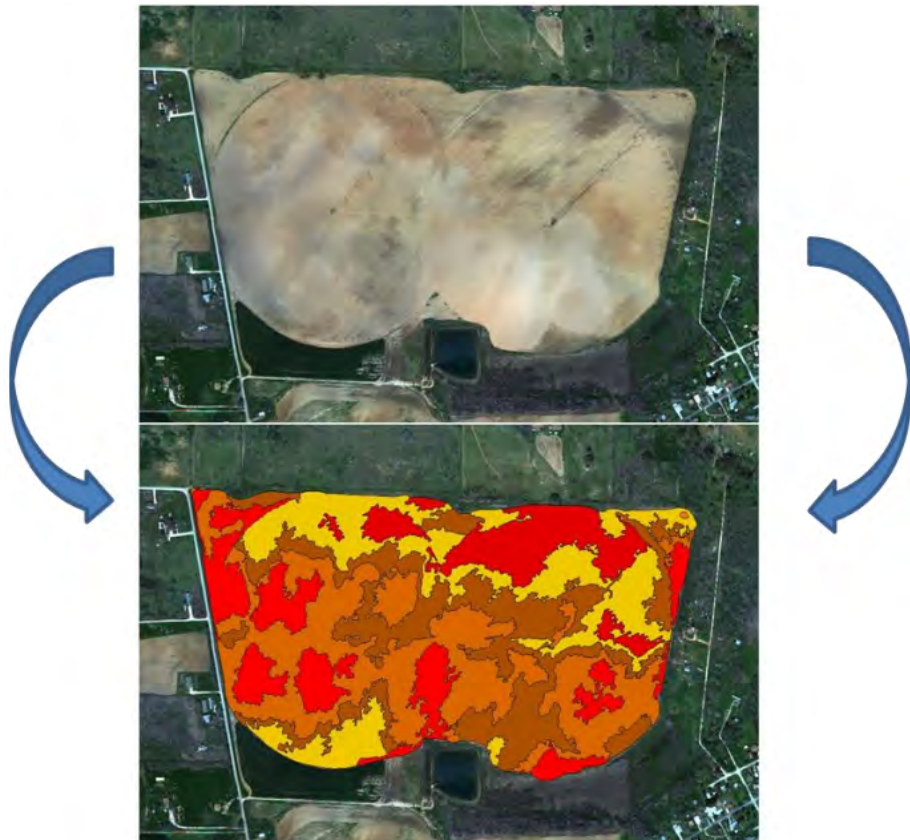


Figure 1.7.: VRA image

1. Drones in Business

1.2.1.3. Case Studies

Cotton

Situation

Farmers apply herbicides uniformly across fields before planting to ensure good field conditions for planting

Action

Use NDVI imagery to identify weeded areas, Apply herbicide only in weeded areas or intensify herbicide applications in heavily weeded areas.

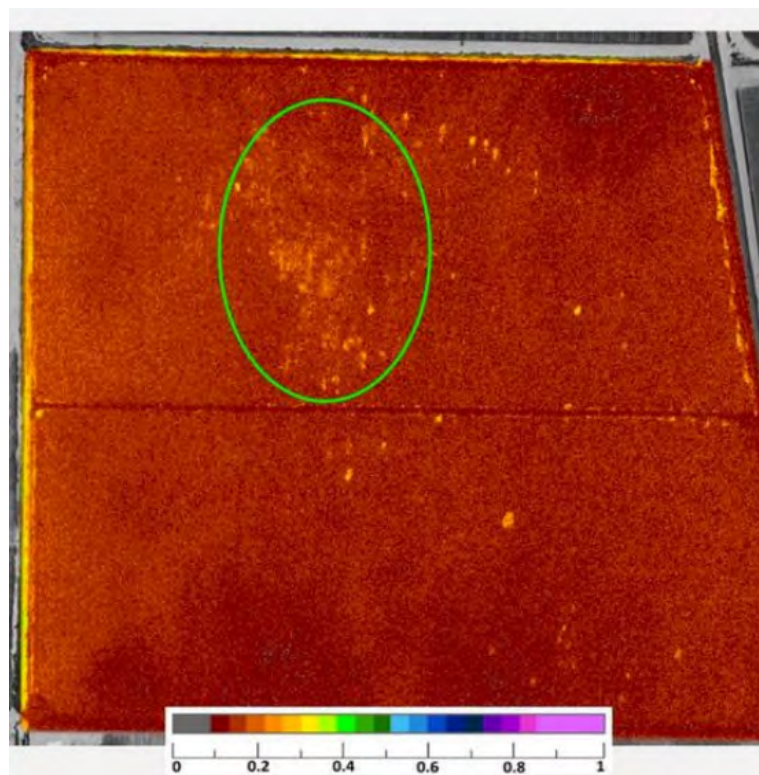


Figure 1.8.: Weeded areas

1. Drones in Business

Planter malfunction

Situation

Malfunctioning planter can cause 100% loss in nonplanted areas, but such areas can be difficult to locate and quantify.

Action

Use imagery to Identify areas to re-plant

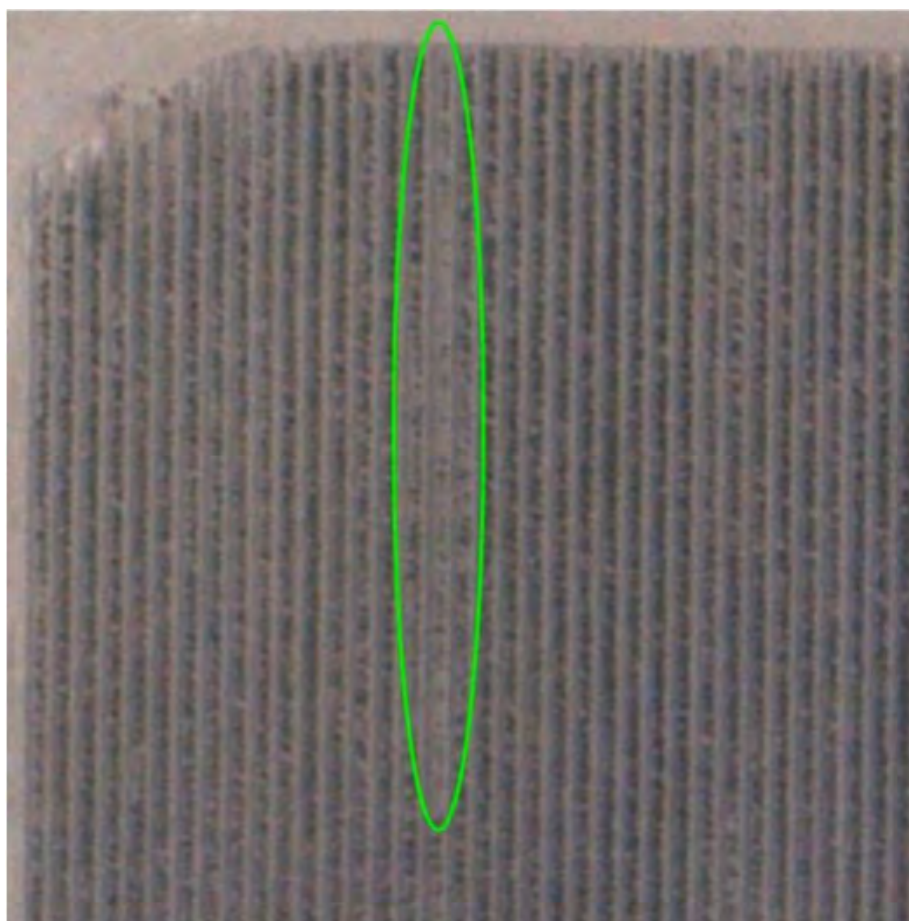


Figure 1.9.: Nonplanted areas

1. Drones in Business

Targeted insecticide applications(plant bugs)

Situation

Farmers generally apply insecticides uniformly, although early stage plant bugs generally only attack high vigor areas

Action

Use NDVI imagery to identify high vigor areas, thus applying insecticide where needed

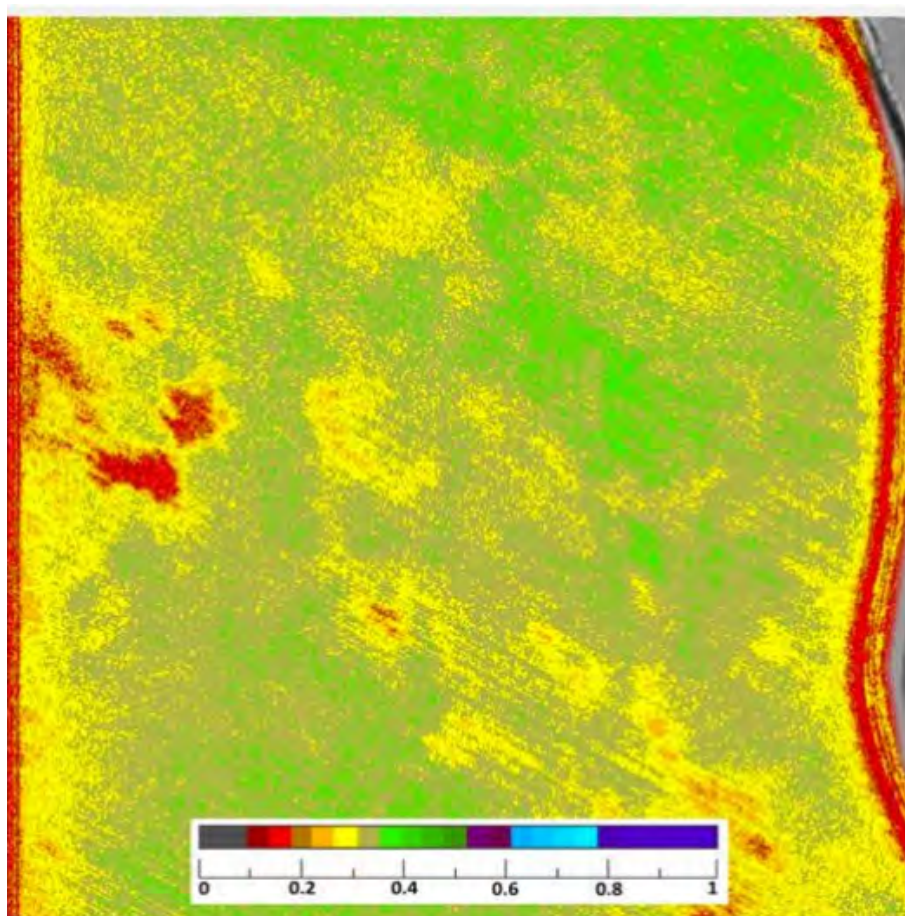


Figure 1.10.: High vigor areas

1. Drones in Business

Fertilizer second application

Situation

Farmers generally make second nitrogen application uniformly or based on soil maps, where NDVI imagery may provide better representation of nitrogen needs

Action

Use NDVI imagery to provide accurate assessment of relative vigor in field to develop fertilizer zones

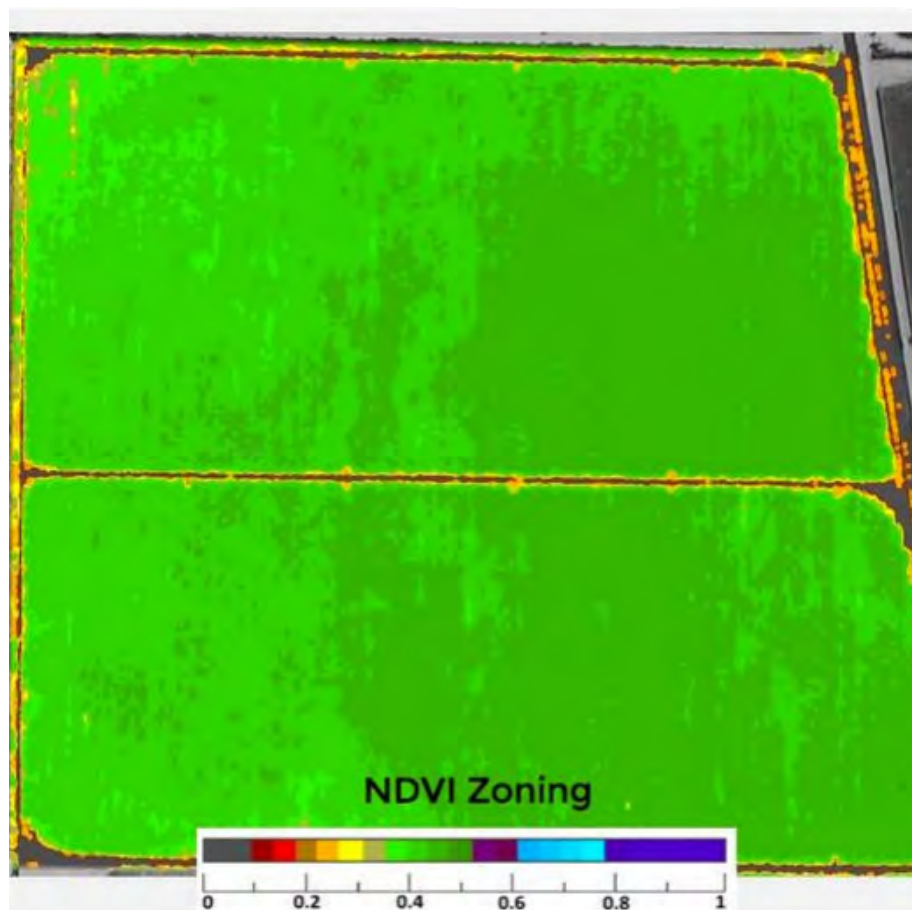


Figure 1.11.: NDVI zoning

1. Drones in Business

Center pivot emitter failure

Situation

Plugged center pivot emitters not visible by visual inspection, but revealed through NDVI and Thermal Imagery

Action

Repair plugged sprinklers

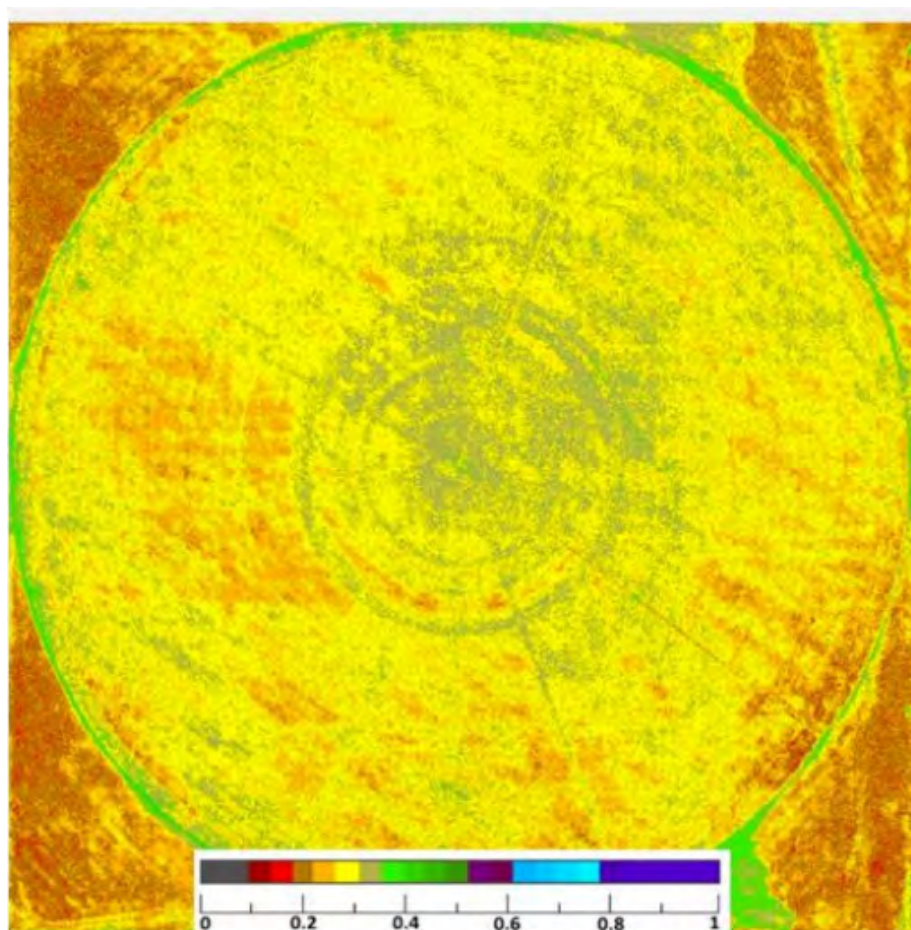


Figure 1.12.: Plugged center pivot emitters zones

1. Drones in Business

Inefficient furrow irrigation

Situation

Furrows do not flow efficiently, resulting in uneven application of irrigation water. Difficult to assess from the ground with naked eye, but thermal and NDVI imagery enable problem areas to be identified and repaired

Action

Repair furrow irrigation efficiencies

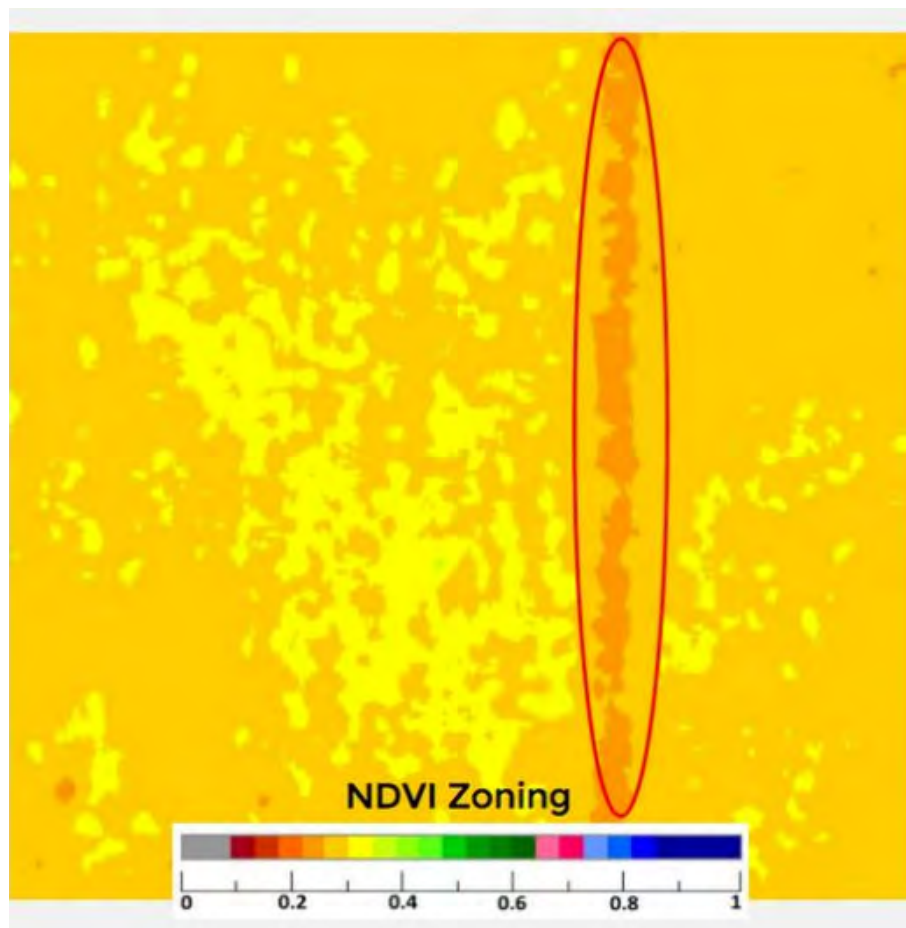


Figure 1.13.: Inefficient furrow irrigation zones

1. Drones in Business

Targeted insecticide application (spider mites)

Situation

Farmers generally do not apply insecticides, unless scouting identifies a problem, NDVI imagery enable problem areas to be identified and sprayed

Action

Use NDVI imagery to identify infested areas, thus applying insecticide when needed

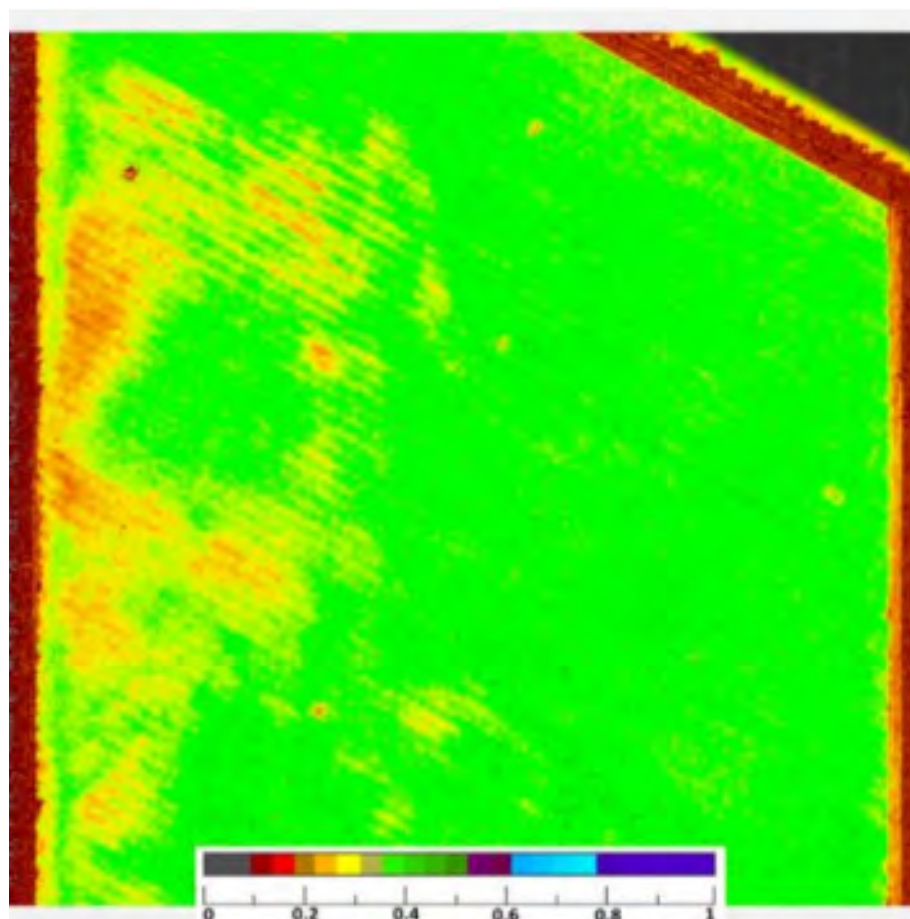


Figure 1.14.: Spider mites zones

1. Drones in Business

Targeted weed control

Situation

Scouts currently sample the field randomly to discover potential issues or to assess crops. Aerial imagery allows for targeted scouting.

Action

Identify areas for scout to visit to discover issues or accurately assess crop, allowing for targeted pest and weed applications

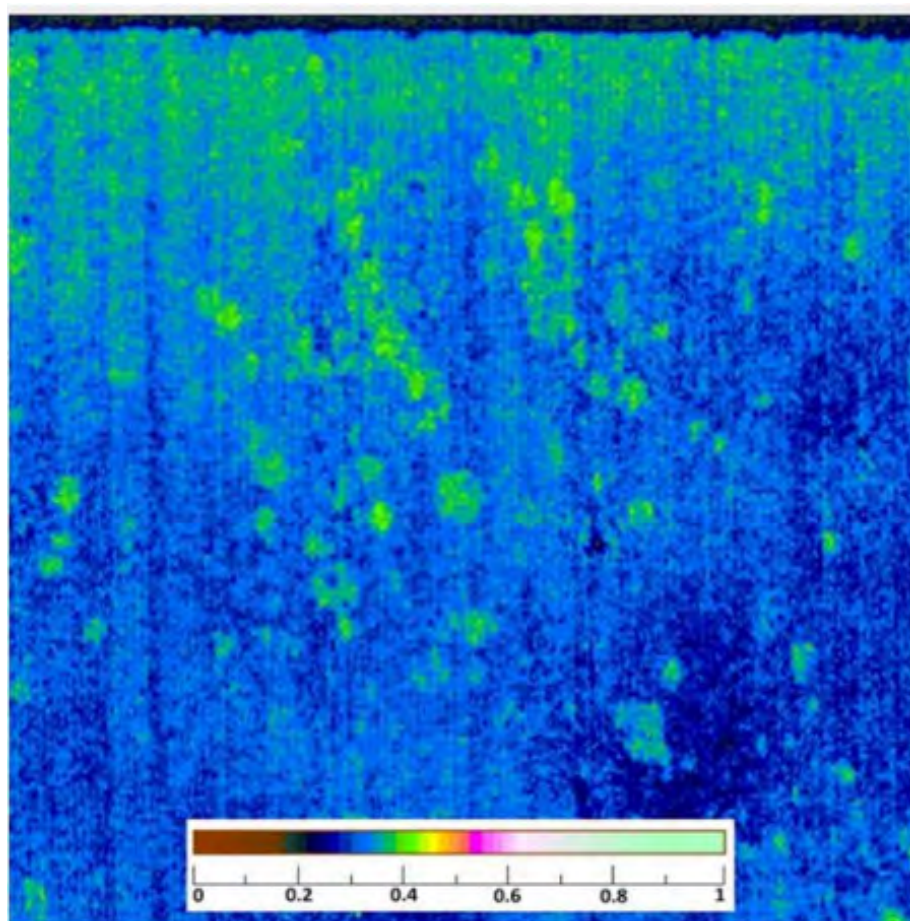


Figure 1.15.: Targeted weed zone

1. Drones in Business

Plant growth regulator

Situation

Field grows unevenly, necessitating variable applications of PGRs in different areas of field

Action

Identify PGR application zones, Apply different rates of PGR in different zonested pest and weed applications

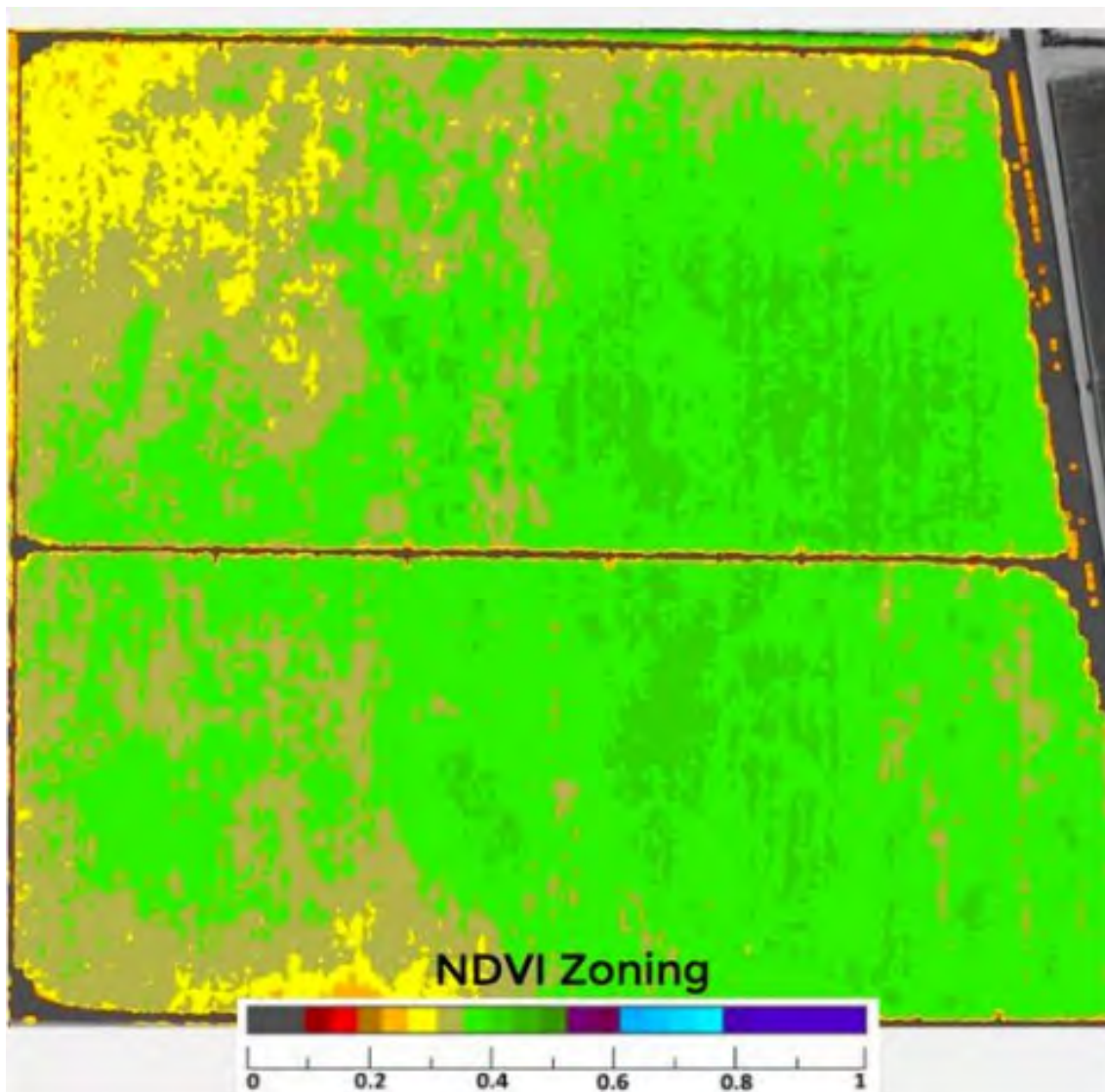


Figure 1.16.: Unevenly planted zones

1. Drones in Business

Defoliant application

Situation

Field matures unevenly, resulting in difficult balance between defoliant efficacy, yield levels, and harvest requirements

Action

Time defoliant application to achieve maximum efficacy to achieve optimal yields and lint quality

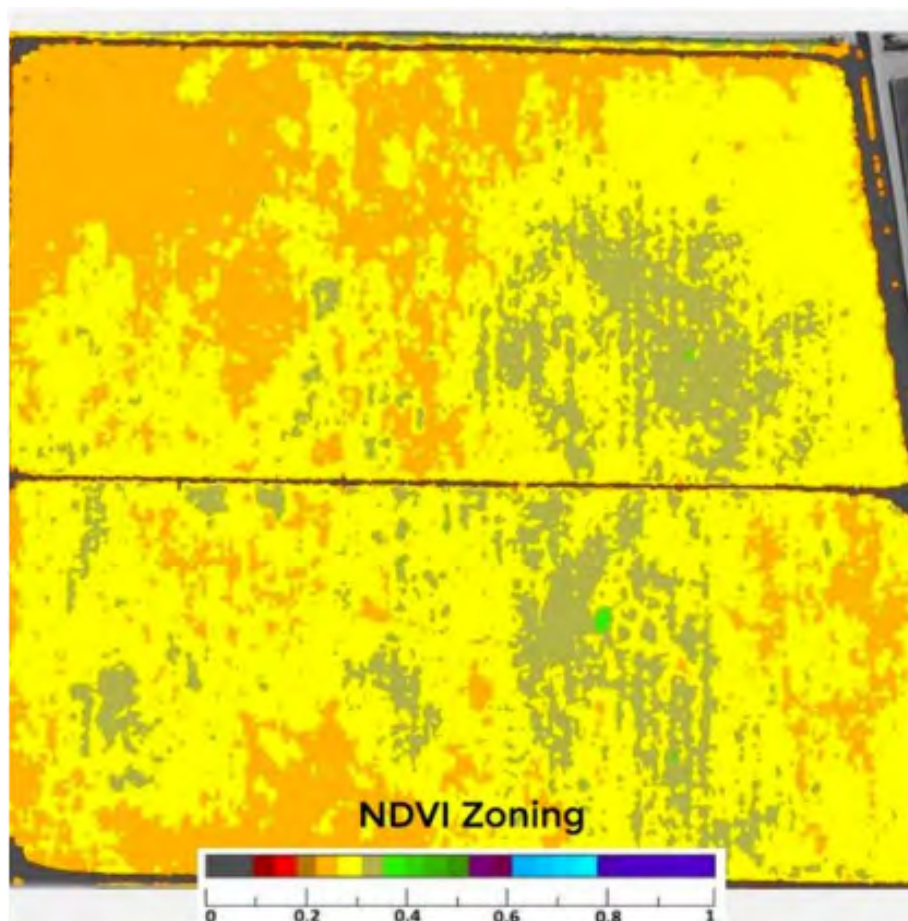


Figure 1.17.: Unevenly matured zones

1. Drones in Business

Soil amendments

Situation

Soils greatly affect yield and value, but it is very difficult to discern geospatial distribution of soils without aerial imagery

Action

Infrared and NDVI imagery highlights differing soil types, allowing for targeted soil amendments

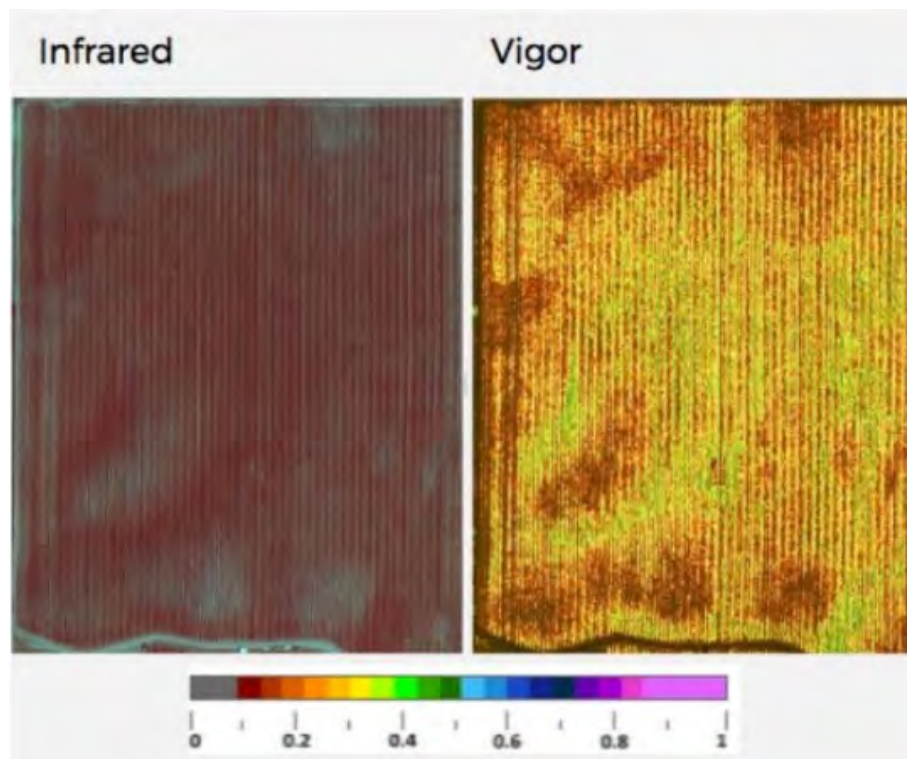


Figure 1.18.: Differing soil types zones

1. Drones in Business

powdery mildew

Situation

Scouts randomly scout the vineyard for powdery mildew colonies throughout the season

Action

NDVI imagery highlights high-vigor areas that are susceptible to powdery mildew, enabling targeted scouting, treatments or thinning.

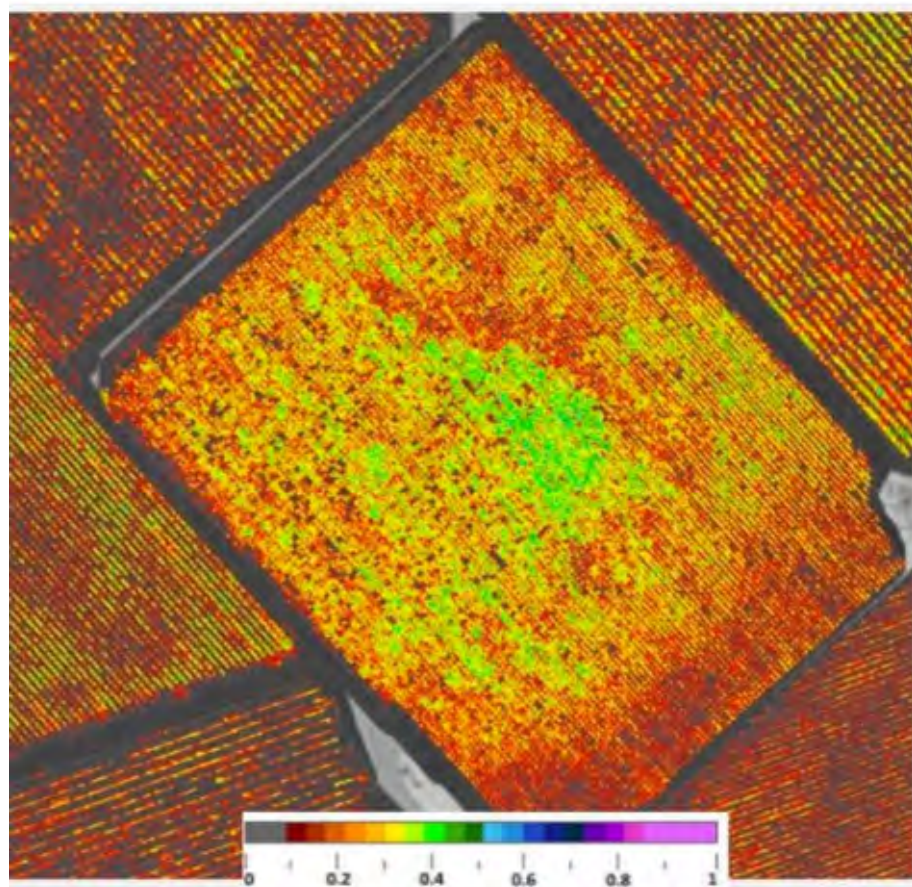


Figure 1.19.: Infected powdery mildew zones

1. Drones in Business

Diseases control

Situation

Diseases can adversely affect yield, but diseased areas can be difficult to identify

Action

Use NDVI imagery to identify infected areas, thus applying fungicide when and where needed



Figure 1.20.: Infected zones

1. Drones in Business

Weed control

Situation

Weeds can adversely affect yield, but weedy areas can be difficult to locate and target

Action

Use NDVI imagery to identify weedy areas, thus applying herbicides when and where needed

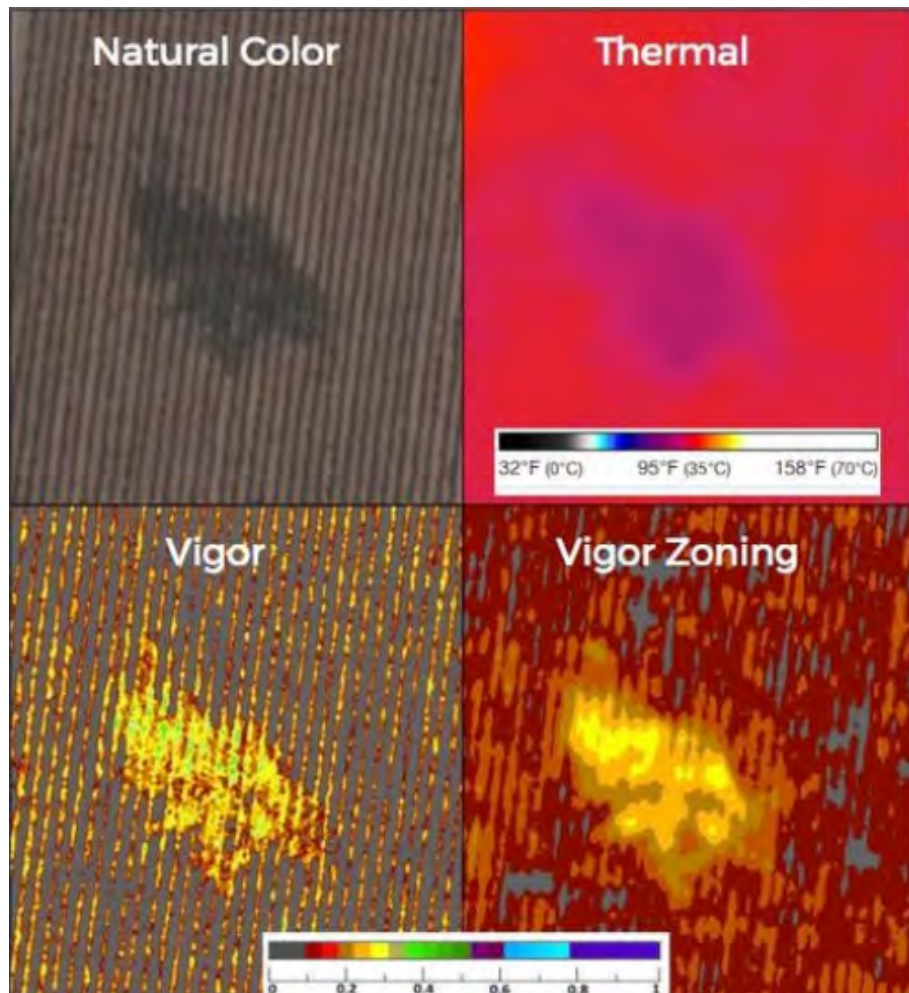


Figure 1.21.: Weedy zones

1. Drones in Business

Irrigation leaks

Situation

Irrigation systems leak, causing excess vine vigor which diminishes grape quality and thus adversely affects price. Irrigation leaks are difficult to identify without aerial imagery.

Action

Use thermal and NDVI imagery to identify irrigation leaks to be repaired, resulting in higher grape quality across vineyard

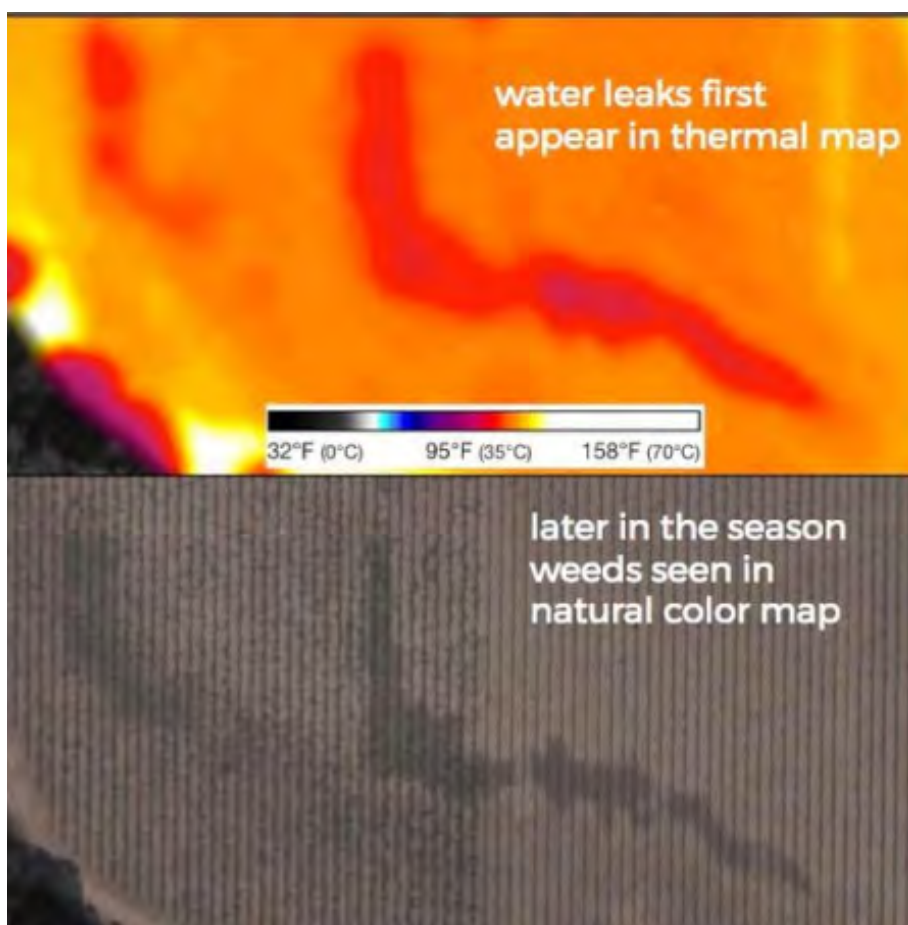


Figure 1.22.: Irrigation systems leak zones

1. Drones in Business

Irrigation optimization

Situation

Uneven field vigor results in sub-optimal irrigation deliveries (i.e., some parts of vineyard get too much water, other parts get too little)

Action

Use NDVI to create irrigation zones, enabling differential irrigation to ensure appropriate irrigation applications in each part of vineyard.

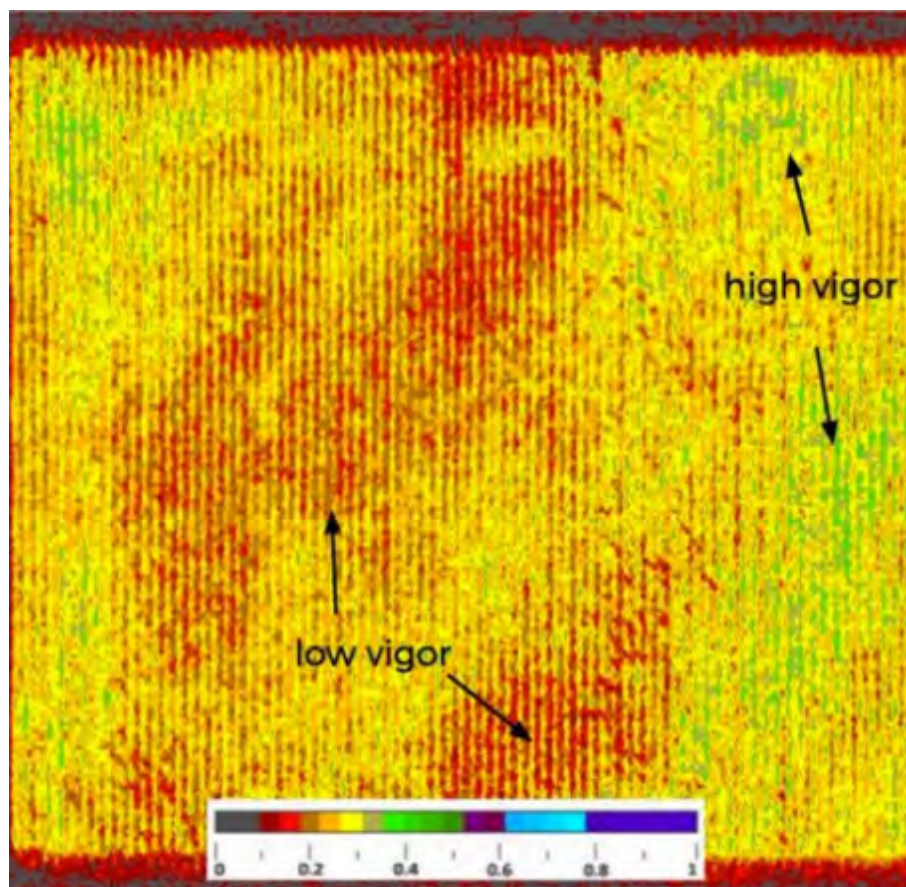


Figure 1.23.: Uneven field vigor zone #1

1. Drones in Business

Harvest zones

Situation

Uneven field vigor results in mixed quality grape harvest.

Action

Use NDVI to create harvest zones, enabling differential harvesting to avoid mixing high and low quality grapes.

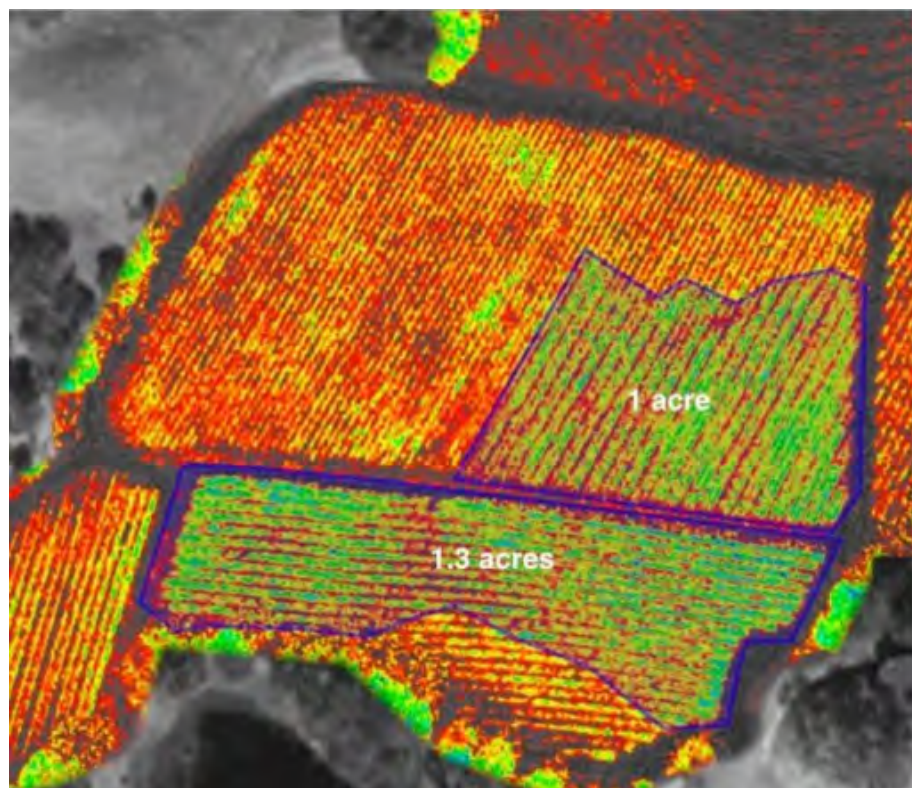


Figure 1.24.: Uneven field vigor zone #2

1. Drones in Business

Cover crops

Situation

Uneven vineyard vigor results in sub-optimal cover crop planting decisions (i.e., cover crop based upon average vineyard needs as opposed to cover crops matching particular areas)

Action

Create in-season vigor zones to inform off-season cover crop decisions

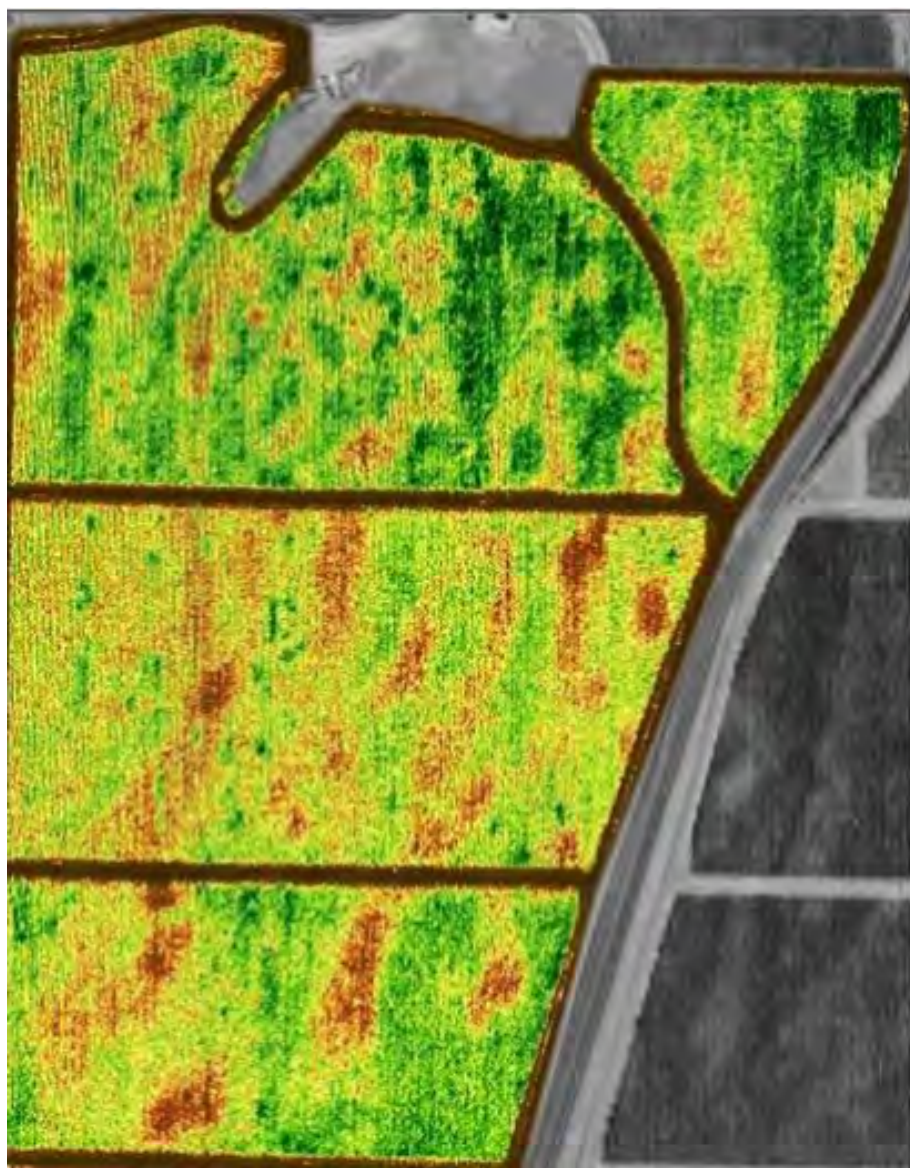


Figure 1.25.: Uneven vineyard vigor zone

1. Drones in Business

1.2.2. Using drones in Media and Entertainment

1.2.2.1. Aerial photography

In 2016 , An Egyptian company called “IFLY EGYPT” [6], started up which is specialized in developing UAVs used in aerial photography.they used drones in applications such as

- Football matches



Figure 1.26.: Football match image taken by a drone

1. Drones in Business

- Tourism industry



Figure 1.27.: Cairo tower image taken by a drone

1. Drones in Business

- Road traffic



Figure 1.28.: Road traffic image taken by a drone

Challenges they have faced:

- permissions for using RC devices
- Exporting a lot of advanced equipment
- Maintenance of these equipment Local
- Developing for some equipment to meet the requirements

1. Drones in Business

1.2.2.2. Advertising

Intel used the squadron of drones to advertise its logo



Figure 1.29.: Intel image #1



Figure 1.30.: Intel image #2

1. Drones in Business

1.2.3. Using drones in Search and Rescue

1.2.3.1. Introduction

Drones aren't always mentioned in the same breath as saving lives, but a new report from one drone manufacturer says they should be.

Civilian drones have been used to save at least 59 people in 18 different incidents around the world since 2013, DJI, a China-based company that manufacturers popular civilian drones, said in a statement on Tuesday. The company added that 38 of those individuals were saved within in the last 10 months thanks to rescue teams and civilians employing their unmanned aerial vehicles (UAV) to aid people facing life-threatening emergencies.

Now, DJI says a drone is saving nearly one person's life a week on average.

1.2.3.2. Saving and Rescue UAS

The mission

The initial design is a fixed wing UAS with an IR camera for night vision. The UAS surfs the ocean and the Mediterranean Sea in order to search for any people stuck in the middle of the sea and rescue them. This can be done by installing the following devices:

- Long Range IR PTZ system

Specifications:		
Model /specification	RANGE	LENS
	Human Detection: Day: over 3.7 miles (5950 m) Night: 0.7 Miles (1000 m)	 Optical zoom: 37 X zoom lens with max zoom to 129 mm
TVIP-PHX-640-30X-100HD	Recognition Day: 1 mile (1600 m) Night: 0.19 Miles (309 m)	Thermal lens: Fixed 100 mm
Dual sensor medium range camera system, includes up to 129 mm optical zoom lens, and 640 x 480 thermal camera with 100 mm fixed thermal lens	Identification: Day: 0.49 mile (793 m) Night: 0.09 Miles (153 m)	

Figure 1.31.: TVIP-PHX-640-100HD camera specifications

- AXIS Q8641-E PT Thermal Network Camera

1. Drones in Business

Reliable thermal detection
Outstanding thermal contrast
Responsive positioning with quick, smooth pan and tilt capabilities
Save bandwidth with Zipstream
Smooth and steady video with electronic image stabilization



Figure 1.32.: AXIS Q8641-E PT camera specifications

- AXIS Q8641-E lets operators choose between really slow or super-fast pan (from 0.05 to 120 degrees per second) and tilt movement (from 0.05 to 65 degrees per second). So they get smooth and jerk-free panoramic viewing when they need it and can respond quickly to events. The camera can be column-mounted, on poles or walls for a 360° panoramic view and a ground-to-sky view from -90° to +45°. It can withstand high winds when it's in motion of up to 47-meter per second (106 mph).
 - Detection Ranges

	Focal length mm	Viewing angle Horizontal	Detection			
			Human: 1.8 x 0.5 m		Vehicle: 4 x 1.5 m	
			m	yards	m	yards
Detection (1.5 pixels on target)	35	10.7°	1028	1124	3153	3448
Recognition (6 pixels on target)	35	10.7°	257	281	788	862
Identification (12 pixels on target)	35	10.7°	129	141	394	431

Table 1.2.: AXIS Q8641-E detection ranges

- This camera can be a better option as it has a local seller in Egypt. As the camera belongs to Axis communications and has a seller “Quantum Digital Technologies, Cairo”, “HitekNofal Solutions, Cairo” and “C&CC, Cairo”.

1. Drones in Business

Types of UAS that can be used in search and rescue

Fixed Wing UAS

The first trial maybe a fixed wing UAS able to carry the payload of the camera system, compatible with the battery and having a GPS system to detect the one drowning in the sea and send its location to The responsible Authority for saving him.

Multi-Rotor Drone

This design can be taken into consideration as it's easy to manufacture. This option is a better one.

Another Function may be added to this Multi-Rotor Drone which is dropping life vests and ropes to people stuck in the sea like in the following picture.



Figure 1.33.: Dropping life vests drone

1.2.3.3. Firefighting Drones

In search and rescue operations, drones allow greater coverage of a search area – and thermography allows rescue teams to work through the night, significantly increasing the potential for success. Thermal imaging cameras give teams the power to “see in total darkness,” says FLIR, the global leader in

1. Drones in Business

thermo-graphic imaging sensors. Added to that is the ability to discern figures difficult to find with traditional cameras even in daylight- like one stranded hiker lost against the backdrop of a snowy field. This capacity is one of several reasons that law enforcement organizations around the world are using drones. Firefighting may provide one of the most compelling applications for drones equipped with thermal imaging equipment. From New York City's famous FDNY to volunteer departments in small towns around the country, fire departments are utilizing drone technology to save structures and victims, and minimize risk to firefighters. The aerial perspective through a thermal imaging camera allows teams to pinpoint hotspots, identify victims on the scene, and quickly establish a plan of attack. It provides a level of visibility in the midst of a fire that is impossible with the naked eye or traditional cameras. (You can see how a fire looks through the lens of one of these thermo-graphic tools here – experiencing a firefighters view through dark and smoke.) Drones not only make firefighters more effective – they keep them safe.



Figure 1.34.: Thermal image taken by a Drone

Main components

Drones may have the same cameras mentioned above or more accurate thermal cameras for optimizing its missions. But it may be designed to be Multi-Rotor Drone in order to be more flexible to fly above the burnt areas.

1. Drones in Business

1.2.4. Using drones in Disaster Relief and Emergency Response

1.2.4.1. Introduction

Aerial drones are one of the most promising and powerful new technologies to improve disaster response and relief operations. Drones naturally complement traditional manned relief operations by helping to ensure that operations can be conducted safer, faster, and more efficiently.

When a disaster occurs, drones may be used to provide relief workers with better situational awareness, locate survivors amidst the rubble, perform structural analysis of damaged infrastructure, deliver needed supplies and equipment, evacuate casualties, and help extinguish fires among many other potential applications.

In advance of an emergency, drones are able to assist with risk assessment, mapping, and planning [7]. When individuals, businesses, and communities are able to understand and manage risks and plan effectively, they reduce overall damage and losses. Rebuilding and recovery are then able to begin more quickly and ultimately strengthening the resiliency of communities.

Drones have long been described as optimally suited to perform the “3-D” missions, often described as dirty, dull, and dangerous. They can provide needed aerial data in areas considered too hazardous for people on the ground or for manned aircraft operation, such as sites with nuclear radiation contamination or in close proximity to wildfires. Drones can also deliver needed supplies and relay Wi-Fi and cellular phone service when communications are needed the most.

Disaster relief and emergency response (DRER) efforts are inclusive of all actions by first responders and subsequent aid efforts during and immediately following a catastrophic event which threatens human life. The primary purpose of DRER efforts is to save human lives. Secondary purposes of DRER efforts are to preserve and maintain the environment, protect property, keep the peace, and uphold governmental authority.

UAV systems have the potential to improve the effectiveness of DRER efforts by enhancing first responder.

Modern manned DRER systems include ground vehicles, conventional aircraft, and rotorcraft capabilities and providing advanced predictive capabilities and early warning. A wide variety of system types of all sizes with varying capabilities already exist with even more under development.

Disasters or emergencies for which DRER UAV systems could be implemented include: severe storms, tornados, hurricanes, wild fires, tsunamis, floods, earthquakes, avalanches, civil disturbances, oil or chemical spills, and urban disasters.

Civil unmanned aerial vehicle systems have potential to augment disaster relief and emergency response efforts. Optimal design of aerial systems for such applications will lead to unmanned vehicles which provide maximum potentiality for relief and emergency response while accounting for public safety concerns and regulatory requirements.

1.2.4.2. Major Usage

Reconnaissance and Mapping

The need for regular mapping of disaster-prone areas cannot be overstated. Flood maps help coordinate disaster response efforts after events like the Superstorm Sandy storm surge; 3D topographical mapping can help identify areas prone to mudslide; high-resolution visual imaging can help first responders flag critical infrastructure that needs to be secured immediately after a disaster; and advances in remote sensing technology have opened new possibilities in developing early warning signs for potential disasters. For example, British researchers operating in Malaysia have used drones to map patterns of deforestation that have been correlated with increased incidences of malaria.

1. Drones in Business

Maps constructed quickly in the wake of a disaster are also useful tools for identifying and assessing damage, especially when combined with images of the area before a disaster. For this to be most efficacious in assisting relief operations, “before” maps must be very recent, while “after” maps must be created as swiftly as possible.

Unfortunately, in the aftermath of a disaster, mapping may take too long using satellites or traditional manned aircraft. Satellite imaging technology cannot currently penetrate cloud cover, often leading to delays in image capture after extreme weather events.

Structural Integrity Assessment

Natural disasters such as earthquakes, hurricanes, tornadoes, tsunamis, and floods, as well as man-made disasters such as explosions and arson, can all cause immense damage to the structural integrity of buildings and infrastructure. Even small-scale events can cause serious damage. For example, the 2011 Virginia Earthquake, though measuring only 5.8 on the Richter scale, caused significant structural damage to such famous landmarks as the Washington Monument and the National Cathedral.

Assessing structural damage after a disaster comes with many potential risks. Assessors may have to enter buildings in danger of collapse or access hard-to-reach places like the undersides of bridges. Drones have proven their usefulness in assessing structural damage over a wide area, locally, and even in building interiors.

Chemical, Biological, Radiological, Nuclear, or Explosive (CBRNE) Events

Heavy industry and power generation relies on hazardous chemicals and fuels, including fissile material to create nuclear power. Malfunctions in factories or power plants, accidents while transporting hazardous materials, terrorism and criminal sabotage all have the potential to create unexpected chemical, biological or nuclear disasters. These devastating events require fast and effective disaster response and relief efforts, but by their nature are extremely unsafe for relief workers. Characteristics of CBRNE events are:

- Toxic / radioactive / explosive environments.
- Unprepared / disrupted surfaces.
- Rapidly changing environmental situations.
- Lack of information and data on the extent of the disaster.

Drones significantly reduce human exposure to unsafe environments while providing continuous monitoring and data validation in the most extreme conditions. Sending drones into a CBRNE area can help rescue workers quickly and safely locate sources of contamination/danger and the scope of the damage, providing invaluable situational awareness. Drones can also be used to repair damage, quickly deliver needed equipment to disaster teams, and apply chemical retardants or dispersants. Additionally, most drones can be deployed from unimproved locations, ensuring that even if airfields are not present or are unusable, aircraft can still be deployed to the area.

While drones have been used primarily in post-CBRNE disaster damage assessment and establishing situational awareness, the uses of drones in these environments are nearly endless.

For example, drones could have been used to distribute goods to the family of Thomas Duncan, the man infected with the Ebola virus in Liberia, who returned to Dallas, Texas, in fall 2014.

Drones have many uses in the preparedness and prevention stages of disaster, as well. For instance, drones fitted with methane sniffers could detect a gas leak in a storage tank before it ignited.

1. Drones in Business

Search and Rescue Operations

Many dynamic tactical challenges accompany search and rescue operations [8]. Searching for people or wreckage over vast areas like deserts, oceans, rugged mountainous and forested terrain can be very time consuming and difficult. This can lead to crew fatigue, decreasing their effectiveness in searching and increasing the likelihood of pilot error. Furthermore, once survivors are located, many rescue / evacuation operations must be carried out in hazardous environments (CBRNE, low visibility, rugged terrain, etc.). The use of unmanned systems in these situations allows operations to be conducted without exposing a flight crew to unnecessary danger. Search and rescue operations often embody the “3-D” model (Dull, Dirty, Dangerous) of missions best suited to drones.

Insurance Claims Response and Risk Assessment

Insurance companies play an invaluable role in assisting disaster relief efforts. When people lose their homes and possessions and when businesses suffer property damage and business interruption, insurance companies are there to provide them with the material support they need to begin the rebuilding process. Insurance coverage can help disaster-stricken areas recover much more quickly and comprehensively than would have been possible otherwise. For these reasons, it is imperative that insurance companies act as effectively and efficiently as possible in the wake of a disaster. Insurance companies could use drones to fly over an affected area, assessing damage to insured property, developing situational awareness for deploying additional claims adjusters on the ground, and supporting the claims response process. Using drones will also reduce the inherent dangers of inspecting damaged properties. Drones provide more options to review properties, which otherwise would be inaccessible due to safety concerns.

Logistics Support

The damage to infrastructure that occurs after major disasters is often one of the most significant obstacles to efficient disaster relief. Blocked roads, damaged rail, and destroyed sea and airports can severely curtail disaster recovery by delaying delivery of needed supplies and equipment.

Drones provide an alternative for logistical support after a disaster. Drones can fly above destroyed infrastructure, and many, particularly rotary-wing craft, do not require runways for takeoff.

Drone logistics support will also help disaster responders directly. Any extra time that disaster responders can devote to actively mitigating a disaster or searching for and rescuing survivors will save lives and reduce costs. Many rescue workers currently devote substantial time to establishing logistical support for other responders, ferrying equipment and essential supplies like food and water. Drones can help speed up this process.

1.2.4.3. Advantages in Disaster Relief and Emergency Response:

- Drone technology can reduce disaster worker exposure to unnecessary danger:
 - Drones function in environments that are unsafe for humans.
- Drones enhance the effectiveness of responders
 - In addition to relieving disaster responders from some of their most dangerous duties, drones can perform dull and dirty tasks to allow responders to focus on more important matters.
- Drones provide unique viewing angles at low altitudes not possible from manned aircraft

1. Drones in Business

- For example, a team from several European universities, called NIFTi, used two small rotary-wing drones to assess damage to cathedrals in Mirandola, Italy, after an earthquake in 2012. Such an assessment is impossible with manned systems.
- Drone technology is highly deployable
 - Drones, particularly small models, can be launched in a variety of environments without the need for a runway.
- Drone technology is cost-efficient
 - While a robust drone system can require significant upfront capital cost, drones are still often cheaper than manned aircraft to purchase and operate. Furthermore, by developing relationships with drone service companies, emergency response organizations can pay only for the tools that they need before and after disasters, lowering costs.

1.2.5. Using drones in Wind Turbine Inspection

Wind Turbine Inspections involve identification of defects such as: Dents, Cracks, Delamination, Gel-coat degradation, Paint peel-off, Lightning Strike damage, Lightning Receptor damage, Vortex Generator damage, Fiber Wrinkles, Manufacturing anomalies, installation damage, etc.



Figure 1.35.: Wind Turbine inspection

1.2.6. Using drones in Other Applications

- Meteorological Monitoring (Humidity – Wind – Pressure – Temperature - . . .) in various locations to get a Meteorological map
- Police or Military reconnaissance Especially in mountainous areas
- Industrial roof inspections
- Surveying & Mapping

1. Drones in Business

- Solar panels inspections
- Civil inspection
- Pipeline and power line inspections

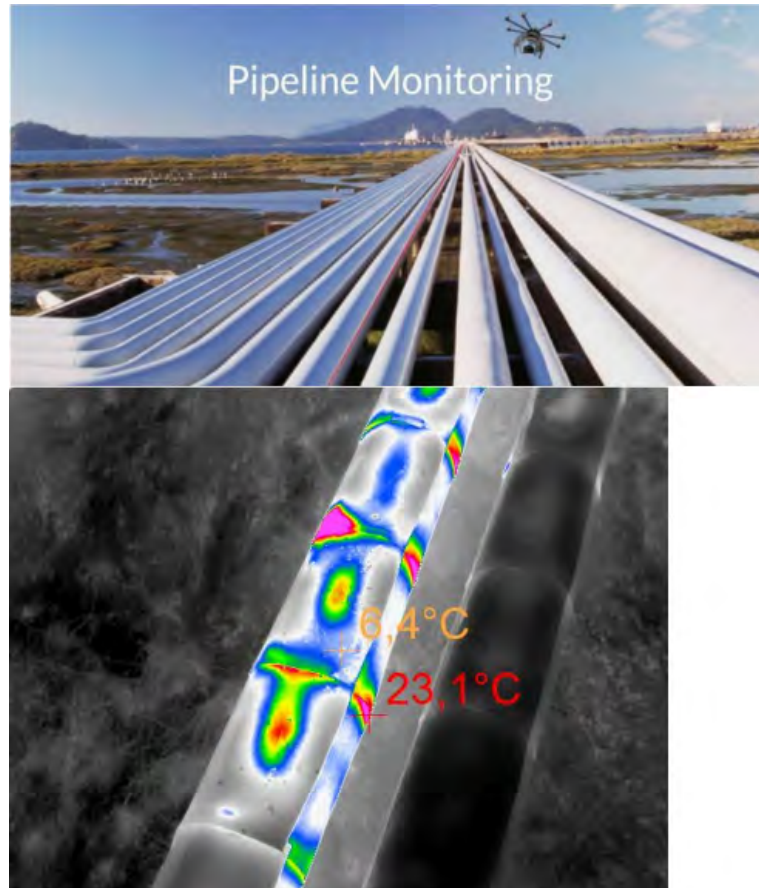


Figure 1.36.: Pipeline inspections

- Tunnels inspections Especially narrow ones
- Racing Besides it can be integrated with VR (virtual reality)

1.3. Conclusion

We settled on precision agriculture field as it has so much potential whether or not drones are used to capture aerial images of the crops or spraying fertilizers, the two applications have so many benefits.

2. Autopilot Overview

2.1. Introduction

The basis for autopilot system operation is error correction. When an aircraft fails to meet the conditions selected, an error is said to have occurred. The autopilot system automatically corrects that error and restores the aircraft to the flight attitude desired by the pilot. There are two basic ways modern autopilot systems do this. One is position based and the other is rate based. A position based autopilot manipulates the aircraft's controls so that any deviation from the desired attitude of the aircraft is corrected. This is done by memorizing the desired aircraft attitude and moving the control surfaces so that the aircraft returns to that attitude. Rate based autopilots use information about the rate of movement of the aircraft, and move control surfaces to counter the rate of change that causes the error. Most large aircraft use rate-based autopilot systems. Small aircraft may use either.

Any autopilot consists of three different things

- Guidance system
- Control system
- Navigation system

These systems aim to make the any aircraft full autonomous.

2. Autopilot Overview

2.2. Components of an Autopilot System

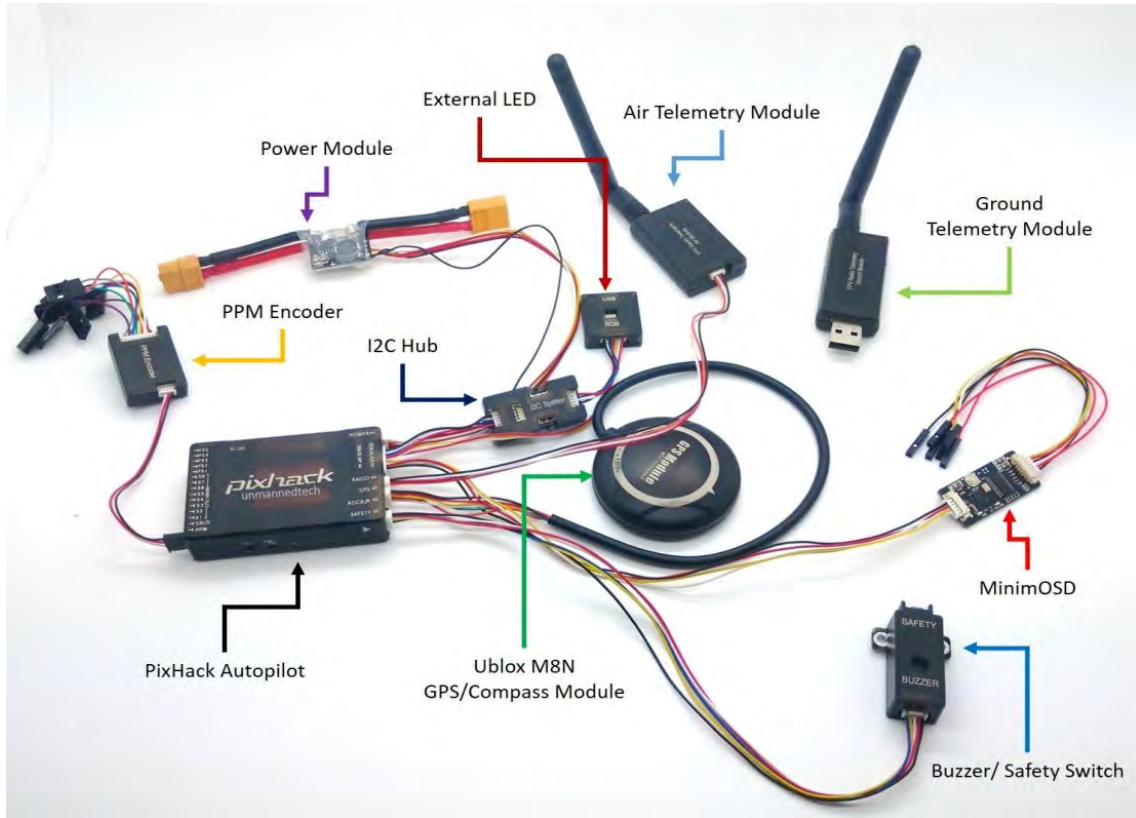


Figure 2.1.: Components of an Autopilot System

2.3. Professional Autopilot's Definitions

Professional Autopilots such as ArduPilot and Pixhawk Autopilot defined these definitions (modes) so that other companies or individuals working in the same field follow their standard of Autopilot

Basic Autopilot control modes

Stabilize Mode

Stabilize mode allows you to fly your vehicle manually, but self-levels the roll and pitch axis.

- Pilot's roll and pitch input control the lean angle of the copter. When the pilot releases the roll and pitch sticks the vehicle automatically levels itself.
- Pilot will need to regularly input roll and pitch commands to keep the vehicle in place as it is pushed around by the wind.
- Pilot's yaw input controls the rate of change of the heading. When the pilot releases the yaw stick the vehicle will maintain its current heading.

2. Autopilot Overview

- Pilot's throttle input controls the average motor speed meaning that constant adjustment of the throttle is required to maintain altitude. If the pilot puts the throttle completely down the motors will go to their minimum rate and if the vehicle is flying it will lose attitude control and tumble.
- The throttle sent to the motors is automatically adjusted based on the tilt angle of the vehicle (i.e. increased as the vehicle tilts over more) to reduce the compensation the pilot must do as the vehicle's attitude changes.

Altitude Hold Mode

In altitude hold mode, Copter maintains a consistent altitude while allowing roll, pitch, and yaw to be controlled normally.

When altitude hold mode is selected, the throttle is automatically controlled to maintain the current altitude. Roll, Pitch and yaw operate the same as in Stabilize mode meaning that the pilot directly controls the roll and pitch lean angles and the heading.

Loiter Mode

Loiter Mode automatically attempts to maintain the current location, heading and altitude. The pilot may fly the copter in Loiter mode as if it were in a more manual flight mode but when the sticks are released, the vehicle will slow to a stop and hold position.

A good GPS lock, low magnetic interference on the compass and low vibrations are all important in achieving good loiter performance.

RTL Mode

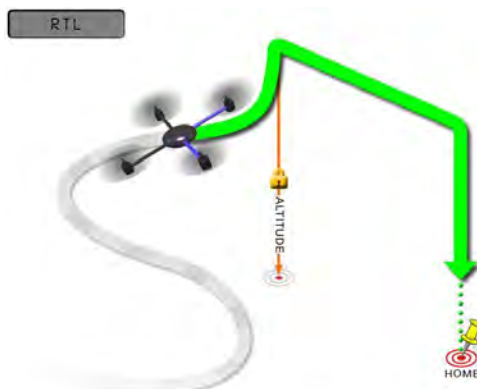


Figure 2.2.: RTL mode

RTL mode (Return To Launch mode) navigates Copter from its current position to hover above the home position.

When RTL mode is selected, the copter will return to the home location. The copter will first rise to specified altitude before returning home or maintain the current altitude if the current altitude is higher than the specified altitude. The default value for the specified altitude is 15m.

2. Autopilot Overview

RTL is a GPS-dependent move, it will command the copter to return to the home position, meaning that it will return to the location where it was armed. Therefore, the home position is always supposed to be your copter's actual GPS takeoff location, unobstructed and away from people.(barometer & GPS & sonar for 20 feet)

Agriculture modes

Auto Mode

Auto Mode



Figure 2.3.: Auto Mode

In Auto mode, the copter will follow a pre-programmed mission script stored in the autopilot which is made up of navigation commands (i.e. waypoints) .

AUTO mode incorporates the altitude control from Altitude Hold mode and position control from Loiter mode and should not be attempted before these modes are flying well.

Guided Mode

Guided Mode



Figure 2.4.: Guided Mode

2. Autopilot Overview

Guided mode is a capability of Copter to dynamically guide the copter to a target location wirelessly using a telemetry radio module and ground station application.

Guided mode is not a traditional flight mode that would be assigned to a mode switch like other flight modes

Pilot point of view modes

Land Mode

Land Mode

LAND Mode attempts to bring the copter straight down and has these features:

- descends to 10m (or until the sonar senses something below the copter)

Position Hold Mode

Position Hold Mode

The Position Hold flight is similar to Loiter in that the vehicle maintains a constant location, heading, and altitude but is generally more popular because the pilot stick inputs directly control the vehicle's lean angle providing a more "natural" feel.

Good GPS position, low magnetic interference on the compass and low vibrations are all important in achieving good loiter performance.

Simple and Super Simple Modes

Simple and Super Simple Modes

"Simple" and "Super Simple" modes allow the pilot to control the movement of the copter from the pilot's point of view regardless of which way the copter is facing. This is useful for new pilots who have not mastered adjusting their roll and pitch inputs depending upon which way the vehicle is facing and for cases when the copter is far enough away that it's heading is not apparent.

- "Simple" and "Super Simple" modes can be used in combination with nearly all flight
- Simple Mode allows you to control the copter relative to the copters heading at takeoff and relies only on a good compass heading.
- Super Simple Mode allows you to control the copter relative to its direction from home (i.e. where it was armed) but requires a good GPS position.

Brake Mode

Brake Mode

This very simple flight mode simply stops the vehicle as soon as possible using the Loiter controller. Once invoked, this mode does not accept any input from the pilot.

When switched on, Brake mode will attempt to stop the vehicle as quickly as possible. Good GPS position, low magnetic interference on the compass and low vibrations are all important in achieving good performance.

2. Autopilot Overview

Photographing modes

Circle Mode

Circle Mode

Circle will orbit a point located with specified radius in front of the vehicle with the nose of the vehicle pointed at the center.

Setting the radius to zero will cause the copter to simply stay in place and slowly rotate (useful for panorama shots).

Sport Mode

Sport Mode

- It was designed to be useful for flying FPV and filming dolly shots or fly by because you can set the vehicle at a particular angle and it will maintain that angle.
- The pilot's roll, pitch and yaw sticks control the rate of rotation of the vehicle so when the sticks are released the vehicle will remain in its current attitude.
- The vehicle will not lean more than 45 degrees.
- The altitude is maintained with the altitude hold controller so the vehicle will attempt to hold its current altitude when the sticks are placed with 10% of mid-throttle.
- It will climb or descend at up to 2.5m/s.

Follow Me Mode

Follow Me Mode

Follow Me mode makes it possible for you to have your copter follow you as you move, using a telemetry radio and a ground station. (GPS dongle)

2.4. Guidance System

2.4.1. Introduction

Guidance is defined as: The process for guiding the path of an object towards a given point, which in general may be moving.

- Determines a path to follow based on commanded signals (waypoints – altitude - speed) by the operator.
- Many methods to make a guidance system depends on what the autopilot supposed to do (tracking a moving target which is time-dependent) or (follow a predefined path which is time-independent).
- The guidance system of any aerial vehicle must handle three dimensions. It will be decoupled into two parts:
 - Horizontal(East-West)
 - Vertical(alitude)

2. Autopilot Overview

Guidance laws are composed of speed and steering laws, which can be combined in different ways to achieve different motion control objectives. We must know about the different motion control scenarios in order to find what suits our application.

motion control scenarios

motion control scenarios are typically divided into the following categories: point stabilization, trajectory tracking, and path following.

- The control objective of a target-tracking scenario is to track the motion of a target that is either stationary (analogous to point stabilization) or that moves such that only its instantaneous motion is known, i.e., such that no information about the future target motion is available. Thus, in this case it is impossible to separate the spatio-temporal constraint associated with the target into two separate constraints.
- The control objective of a path-following scenario is to follow a predefined path, which only involves a spatial constraint. No restrictions are placed on the temporal propagation along the path. However, the control objective of a path-tracking scenario is to track a target that moves along a predefined path (analogous to trajectory tracking), which means that it is possible to separate the related spatio-temporal constraint into two separate constraints. Often, the spatial constraint is considered more important than the temporal constraint, such that if both cannot be satisfied simultaneously, the spatial constraint takes precedence (i.e., to move along the path, albeit at a distance behind the target).
- The control objective of a path-maneuvering scenario is to employ knowledge about vehicle maneuverability to feasibly negotiate (or somehow optimize the negotiation of) a predefined path. As such, path maneuvering represents a subset of path following, but is less constrained than path tracking since spatial constraints always take precedence over temporal constraints.

There are three terminal guidance strategies will be presented in the following, namely line of sight, pure pursuit, and constant bearing.

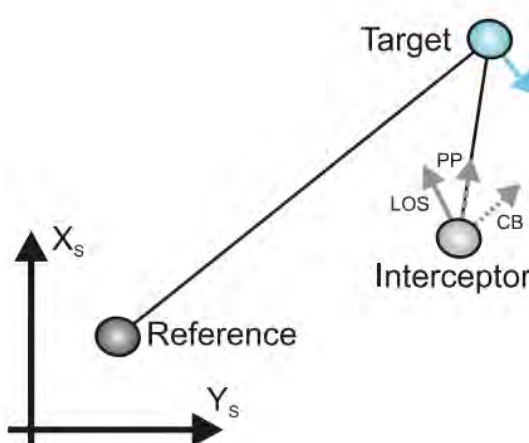


Figure 2.5.: Guidance principles line of sight (LOS), pure pursuit (PP), and constant bearing (CB).

2. Autopilot Overview

- Line of Sight Guidance

Line of sight (LOS) guidance is classified as a so-called three-point guidance scheme since it involves a (typically stationary) reference point in addition to the interceptor and the target. The LOS denotation stems from the fact that the interceptor is supposed to achieve an intercept by constraining its motion along the line of sight between the reference point and the target.

- Pure Pursuit Guidance

Pure pursuit (PP) guidance belongs to the so-called two point guidance schemes, where only the interceptor and the target are considered in the engagement geometry. Simply put, the interceptor is supposed to align its velocity along the line of sight between the interceptor and the target.

- Constant Bearing Guidance

Constant bearing (CB) guidance is also a two-point guidance scheme, with the same engagement geometry as PP guidance. However, in a CB engagement the interceptor is supposed to align the relative interceptor-target velocity along the line of sight between the interceptor and the target.

conclusion

Int the end we know that the LOS guidance is what we want to use as in the ground control station is supposed to be used to specify way points and upload it the Guidance system.

Steering Laws for path following

In LOS guidance, There are a lot of Steering laws to use according to type of the path that is being followed

- Steering Laws for Straight Lines

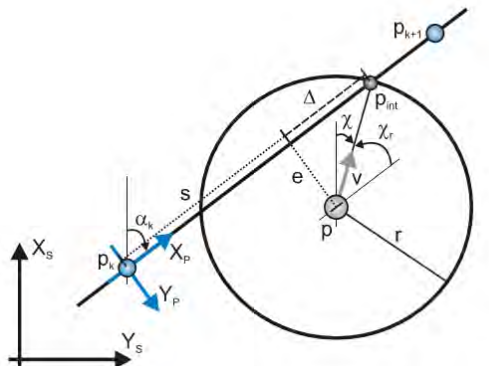


Figure 2.6.: The main variables associated with steering laws for straight-line paths.

Consider a straight-line path implicitly defined by two waypoints through which it passes. Denote these waypoints as p_k and p_{k+1} , respectively. Also, consider a path-fixed reference frame with origin in p_k .

2. Autopilot Overview

Only the cross-track error is relevant since $e(t) = 0$ means that the vehicle has converged to the straight line.

$$\begin{aligned} e(t) &= -[x(t) - x_K] \sin(\alpha_K) + [y(t) - y_K] \cos(\alpha_K) \\ \alpha_K &:= \text{atan2}(y_{k+1} - y_K, x_{k+1} - x_K) \\ \lim_{t \rightarrow \infty} e(t) &= 0 \end{aligned}$$

- there are two methods to do so
 - Enclosure-Based Steering
 - Lookahead-Based Steering

the lookahead-based scheme has several advantages over the enclosure-based approach as it's less computationally intensive than the enclosure-based approach.

- Lookahead-Based Steering

$$\Psi_R = \alpha_K - \arctan(K_p e)$$

where

K_p is just a gain

there are other of Steering laws for Piecewise Linear Paths , Circles and Regularly Parameterized Paths.

Circle of Acceptance

Circle of acceptance is a method for knowing when to switch to the next waypoint [5].

When the aircraft is inside a circle with radius R_{k+1} around the point $[x_{k+1}, y_{k+1}]$, as can be seen in the following figure

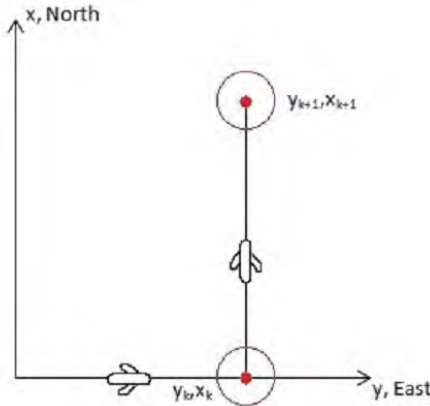


Figure 2.7.: Navigation in x-y plane with circle of acceptance

The guidance system should change to the next waypoint. The position of the aircraft has to satisfy:

$$[x_{k+1} - x(t)]^2 + [y_{k+1} - y(t)]^2 \leq R_{k+1}^2$$

2. Autopilot Overview

Altitude Guidance

First we must make sure that the multi rotor is stable then we work on controlling the altitude.

What we hope to do

The guidance system could be implemented and looks like the following figure.

- LOS is used for calculating desired heading angle
- the kinematic controller has been used for desired pitch angle
- a 1st order LP filter for speed.

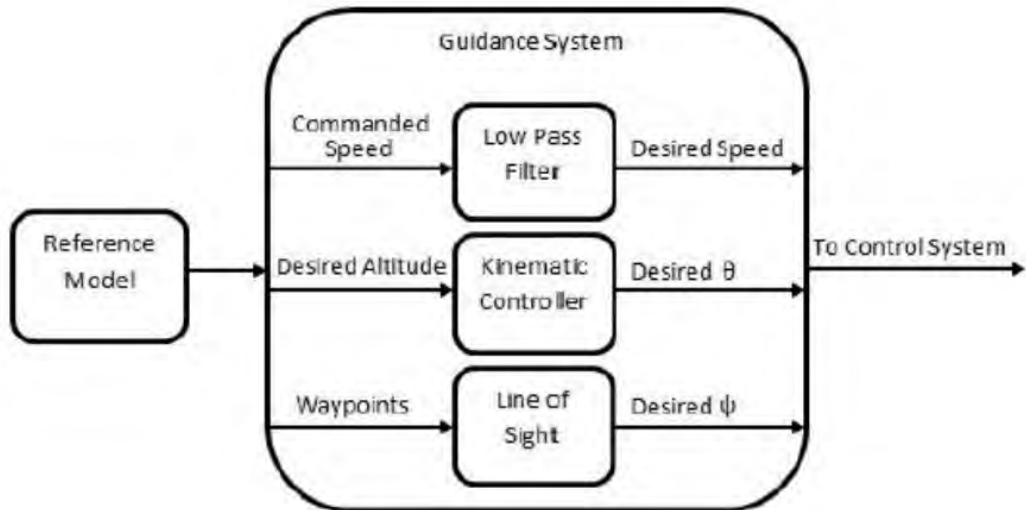


Figure 2.8.: Block diagram of a guidance system[5]

and we hope we could create something like this

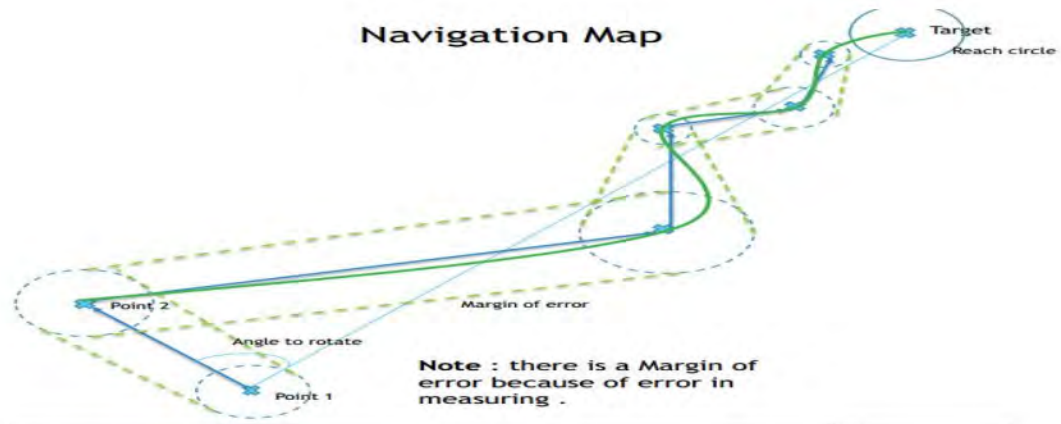


Figure 2.9.: Navigation map

2. Autopilot Overview

2.5. Control System

We'll design the control system using any design methods that we studied in the previous years.
here is a summery of these methods

PID Controller Design

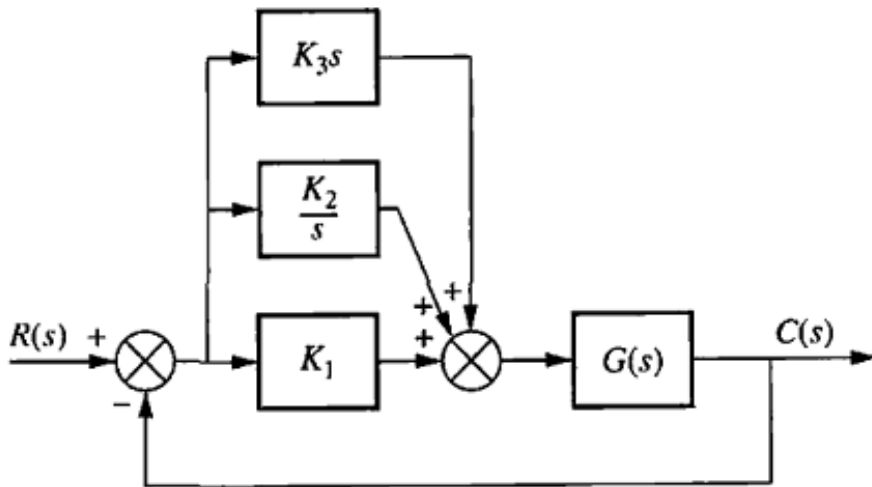


Figure 2.10.: PID controller scheme

A PID controller transfer function is

$$G_c(s) = K_1 + \frac{K_2}{s} + K_3 s = \frac{K_1 s + K_2 + K_3 s^2}{s} = \frac{K_3(s^2 + \frac{K_1}{K_3}s + \frac{K_2}{K_3})}{s}$$

which has two zeros plus a pole at the origin. One zero and the pole at the origin can be designed as the ideal integral compensator; the other zero can be designed as the ideal derivative compensator.

Controller Design procedure[9]

The design technique consists of the following steps :

1. Model the system using Newton equations or Lagrange equations
2. Linearize around your operating point.
3. Take Laplace transform
4. Get open loop transfer function (G_{open})

2. Autopilot Overview

5. Evaluate the performance of the uncompensated system to determine how much improvement in transient response is required.

6. Design a P controller to meet your requirement.

7. Simulate the system to be sure all requirements have been met.

8. If it doesn't meet. Change the type of the controller to PI controller

$$a) PI = K_p + \frac{K_i}{s} = K_p \frac{s + \frac{K_i}{K_p}}{s} = K_p \frac{s + zero}{s}$$

9. Put the zero so that the phase at your required pole is -180 (Root Locus condition)

10. Get gain so that the open loop poles move to your required pole.

11. The new open loop transfer function is $G_{open_{new}} = \frac{G_{open}}{s}$

12. Simulate the system to be sure all requirements have been met.

13. If it doesn't meet. Change the type of the controller to PID controller

$$a) PID = K_p + \frac{K_i}{s} + K_d * s = K_d \frac{s^2 + \frac{K_p}{K_d} * s + \frac{K_i}{K_d}}{s} = K_d \frac{(s + zero1)(s + zero2)}{s}$$

14. Make each zero compensate half of the phase required

15. Simulate the system using nonlinear simulation.

16. If you increased the input and the response become unstable, you should linearize around a different operating point and consider using gain scheduling

State Feedback Controller Design

Pole Placement

- Assume that the single-input system dynamics are given by

$$\dot{x} = Ax + Bu$$

$$y = Cx + Du$$

and $D = 0$.

- Recall that the system poles are given by eigenvalues of A .

– Want to use the input $u(t)$ to modify the eigenvalues of A to change the system dynamics.

- Assume a full state feedback of the form:

$$u = r - Kx$$

where r is some reference input.

- Find the closed loop dynamics:

$$\dot{x} = Ax + B(r - Kx) = (A - BK)x + Br = A_{cl}x + Br$$

$$y = Cx$$

- Pick K so that A_{closed} has the desired properties.

- Note that it's not always easy, as the issue of the controllability must be checked.

2. Autopilot Overview

Ackermann's Formula

- Ackermann's Formula gives us a method of doing this entire design process as one step.

$$K = [\begin{array}{cccc} 0 & \dots & 0 & 1 \end{array}] M_c^{-1} \Phi_d(s)$$

where

$$- M_c = [\begin{array}{cccc} B & AB & \dots & A^{n-1}B \end{array}]$$

- $\Phi_d(s)$ is the characteristic equation for the closed-loop poles, which we then evaluate for $s = A$.

- It's explicit that the system must be controllable because we are inverting the controllability matrix.

Flight Qualities

The flying qualities of an airplane are related to the stability and control characteristics and can be defined as those stability and control characteristics.

Unfortunately there is no flying qualities for multi-copters published in any text book as the main focus is manned airplanes so our design points be set according to our preferences.

2.6. Navigation System

As previously said, Guidance takes care of input to the system, inputs as waypoints and desired speed, and determine the desired path from the current location of the aircraft to the desired waypoint.

Guidance is often decoupled onto reference model and guidance system where reference model deals with commanded signals and guidance determines the path.

Navigation determines the location and altitude of the aircraft at a given time.

The control system ensures that the aircraft follows the desired path and altitude by manipulating the control surfaces.

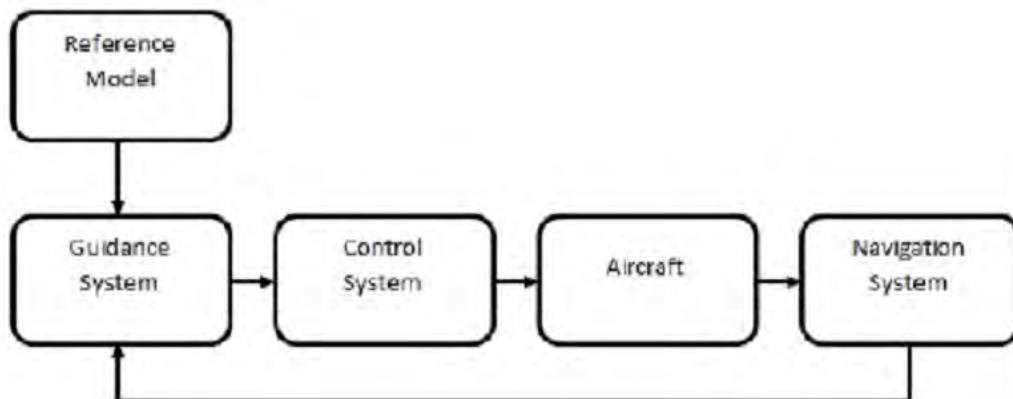


Figure 2.11.: Block diagram of a guidance, navigation and control system

2. Autopilot Overview

We should take advantage of the previous year work of INS as their work have been verified.

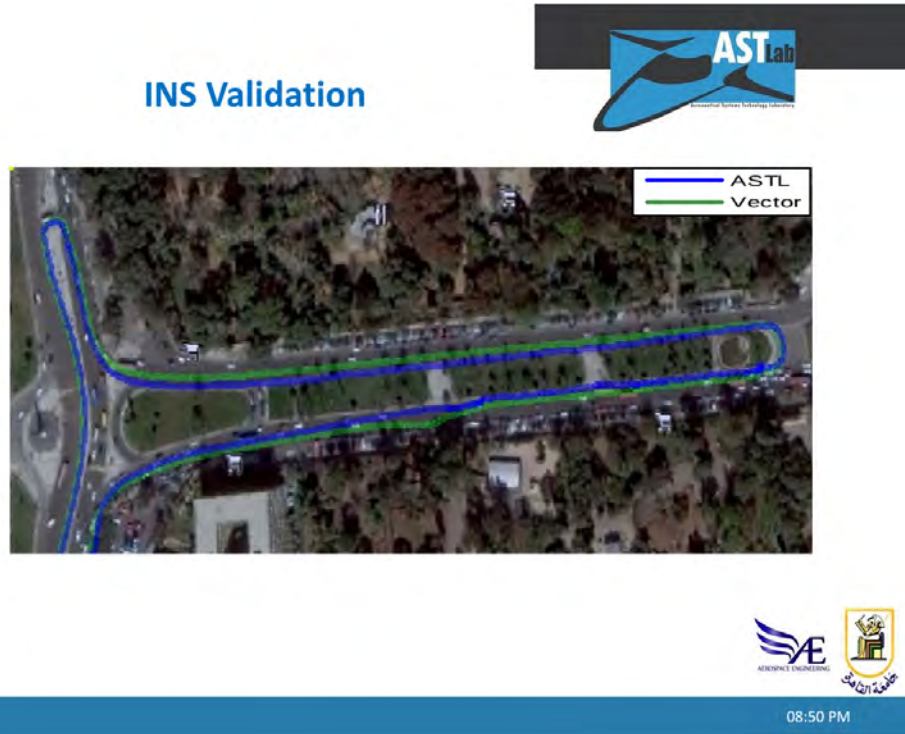


Figure 2.12.: INS validation

2.7. Ground Control Station [1]

2.7.1. Introduction

A ground station is typically a software application, running on a ground-based computer, that communicates with your UAV via wireless telemetry. It displays real-time data on the UAVs performance and position and can serve as a virtual cockpit, showing many of the same instruments that you would have if you were flying a real plane. A GCS can also be used to control a UAV in flight, uploading new mission commands and setting parameters. It is often also used to monitor the live video stream from a UAV's cameras.

For Desktop, there is (Mission Planner, APM Planner 2, MAVProxy, QGroundControl and UgCS.

For Tablet/Smartphone, there is Tower (DroidPlanner 3), MAVPilot, AndroPilot and SidePilot that can be used to communicate with ArduPilot.

Now we are going to talk about Mission Planner as it's a full-featured ground station application for the ArduPilot open source autopilot project.

2.7.2. Capabilities

- Point-and-click waypoint entry
- using Google Maps/Bing/Open street maps/Custom WMS.

2. Autopilot Overview

- Select mission commands from drop-down menus
- Download mission loges and analyze them Congure APM settings for your airframe
- Interface with a PC flight simulator to create a full hardware-in-the-loop UAV simulator.
- See the output from APM's serial terminal • With appropriate telemetry hardware you can: Monitor your vehicle's status while in operation. Record telemetry logs which contain much more information the the on-board autopilot logs. View and analyze the telemetry logs. Operate your vehicle in FPV (rst person view)
- Auto grid You can also have the Mission Planner create a mission for you, which is useful for function like mapping missions, where the aircraft should just go back and forth in a lawnmower pattern over an area to collect photographs.
- MAVLink protocol defines a large number of commands that the mission planners uses
- Planning a camera mission • Setting Up Rally Points(Return yo home points)
- Radio Control Calibration in Mission Planner

User Interface

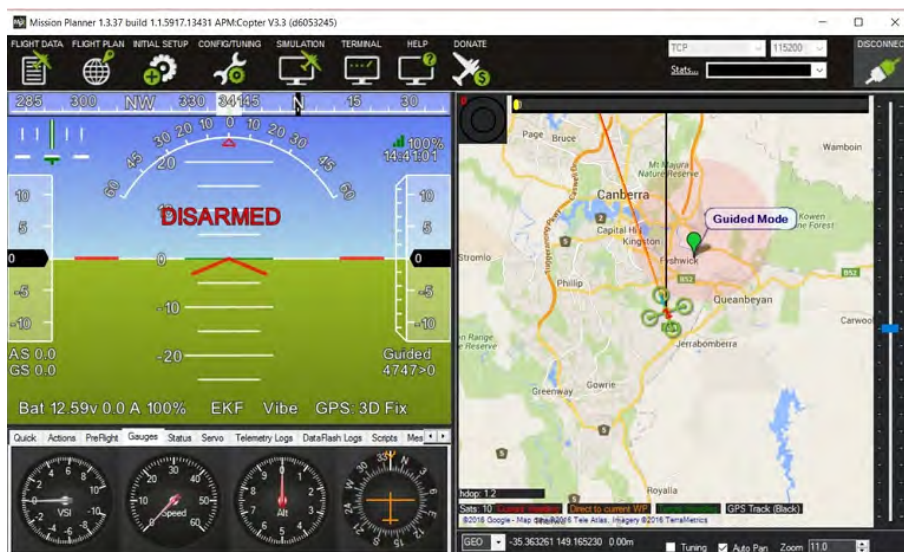


Figure 2.13.: Mission planner user interface

2. Autopilot Overview

GCS Flight Data Screen



Figure 2.14.: GCS Flight Data Screen #1

2. Autopilot Overview

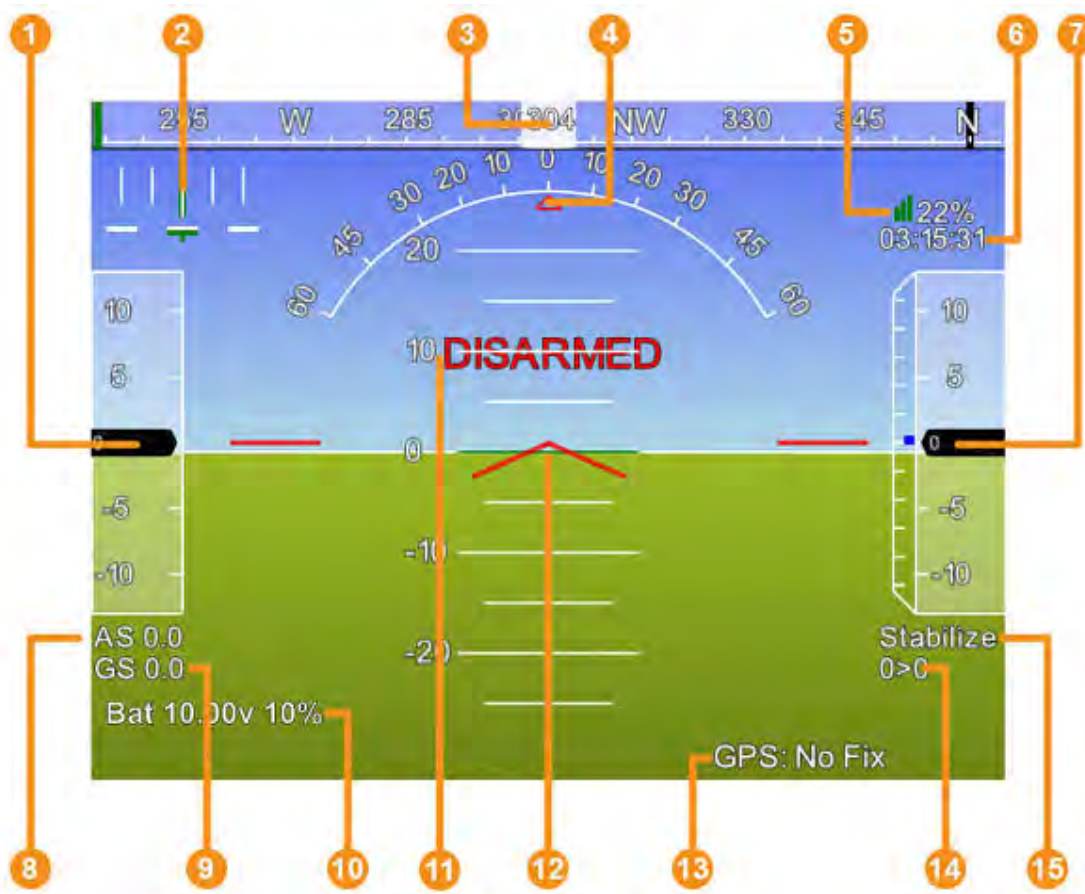


Figure 2.15.: GCS Flight Data Screen #2

Where

- | | |
|--------------------------------------------------|----------------------------------------------|
| 1. Air speed | 6. GPS time |
| 2. Cross track error and turn rate (T) | 7. Altitude
(blue bar is rate of climb) |
| 3. Heading direction | 8. Air speed |
| 4. Bank angle | 9. Ground speed |
| 5. Wireless telemetry connection (% bad packets) | 10. Battery status |
| | 11. Artificial Horizon |

2. Autopilot Overview

Typical log file

	A	B	C	D	E	F	G	H	I	J
1	Date	Time	mavlink_gps_r aw_t.eph	mavlink_ra w_imu_t.xm ag	mavlink_r w_imu_t.ymag ag	mavlink_ra w_imu_t.zm ag	mavlink_attit ude_t.yaw	mavlink_v fr_hud_ta irspeed	mavlink_vfr _hud_t.grou ndspeed	mavlink_v fr_hud_t. heading
2	02/05/2012	7:27:09		0	0	0	-2.744607	0	0	0
3	02/05/2012	7:27:09		0	0	0	-2.744607	0	0	202
4	02/05/2012	7:27:09		0	-82	64	289	-2.744607	0	0
5	02/05/2012	7:27:09	7.813966	-82	64	289	-2.744607	0	0	202
6	02/05/2012	7:27:09	7.813966	-82	64	289	-2.745121	0	0	202
7	02/05/2012	7:27:09	7.813966	-82	64	289	-2.745121	0	0	202
8	02/05/2012	7:27:09	7.813966	-85	61	289	-2.745121	0	0	202
9	02/05/2012	7:27:10	8.87957	-85	61	289	-2.745121	0	0	202
10	02/05/2012	7:27:10	8.87957	-85	61	289	-2.745434	0	0	202
11	02/05/2012	7:27:10	8.87957	-85	61	289	-2.745434	0	0	202
12	02/05/2012	7:27:10	8.87957	-82	62	289	-2.745434	0	0	202
13	02/05/2012	7:27:10	9.617817	-82	62	289	-2.745434	0	0	202
14	02/05/2012	7:27:10	9.617817	-82	62	289	-2.745587	0	0	202
15	02/05/2012	7:27:10	9.617817	-82	62	289	-2.745587	0	0	202
16	02/05/2012	7:27:10	9.617817	-86	62	288	-2.745587	0	0	202
17	02/05/2012	7:27:10	8.652532	-86	62	288	-2.745587	0	0	202
18	02/05/2012	7:27:10	8.652532	-86	62	288	-2.747233	0	0	202
19	02/05/2012	7:27:10	8.652532	-86	62	288	-2.747233	0	0	202
20	02/05/2012	7:27:10	8.652532	-86	62	287	-2.747233	0	0	202
21	02/05/2012	7:27:11	6.307695	-86	62	287	-2.747233	0	0	202

Figure 2.16.: Typical log file

What we hope to do

- Connecting GCS software with the autopilot and making configuring waypoints and upload them to the aircraft through the communication system.



Figure 2.17.: Waypoints specified map

2.8. Telemetry

2.8.1. Introduction

Telemetry is what you use to send and receive data between your drone and your ground station. Adding telemetry to your drone is very useful, but is not always necessary.

Telemetry modules are the actual radio devices that transmit and receive the data. You will have one onboard your drone, and one on the ground plugged onto your ground station device. The most important thing when using telemetry modules for your given autopilot, is that they will often need to be paired together so they can communicate.



Figure 2.18.: Telemetry module

3. Drone Use in Aerial Images Application

3.1. Introduction

vegetation index is a simple graphical indicator that can be used to analyze remote sensing measurements, typically, but not necessarily, from a space platform, and assess whether the target being observed contains live green vegetation or not.

There are many indexes that can be used to extract valuable information from captured images Here are some of them :

- Enhanced Normalized Difference Vegetation Index [10]
 - Description: ENDVI is a close equivalent and modified version of NDVI, designed for low altitude monitoring systems, such as UAVs. ENDVI is an indicator of live green vegetation, and can be used for crops in all growth stages.
- Green Normalized Difference Vegetation Index
 - Description: GNDVI is a modified version of the NDVI to be more sensitive to the variation of chlorophyll content in the crop. It is useful for assessing the canopy variation in biomass, and is an indicator of senescence in case of stress or late maturity stage. This index can be used to analyze crops in mid to late growth stages.
- Difference Vegetation Index[11]
 - Description: DVI is a simple vegetation index, and distinguishes between the soil and vegetation. This index can be used for crops in all growth stages.
- Field Uniformity Tool
 - Description: The Field Uniformity Tool makes it possible to quantify plot-level statistics on plant count, height, vigor, leaf area and canopy cover. Drawing data from your other licensed algorithms (Row-Based Plant Counting Tool, Plant Height, Canopy Cover, Leaf Area and Vegetation Indices) , it calculates the maximum, minimum, mean and standard deviation for each plot or user-defined grid cell.
- Optimized Soil Adjusted Vegetation Index
 - Description: OSAVI is a simplified version of SAVI to minimize the influence of soil brightness. This index is recommended to analyze crops in early to mid growth stages, in areas with relatively sparse vegetation where soil is visible through the canopy.
- Green Leaf Index
 - Description: GLI was designed to adjust for the greenness and yellowness of the crop, and was designed for low altitude monitoring systems, such as UAVs. This index can be used for crops in all growth stages.
- Visual NDVI

3. Drone Use in Aerial Images Application

- Description: Visual NDVI, also known as NGRDI, is an indicator of surface greenness and it is an index to detect live green plant canopies. This index can be used to analyze crops in all growth stages.
- Visible atmospherically resistant index
 - Description: VARI was designed to introduce an atmospheric correction and is a good index to estimate the vegetation fraction from the visible range of the spectrum. This index can be used to analyze crops in all growth stages.

Note

- NIR (Near-infrared) image is more valuable than its counterpart RGB (Red, Green and Blue) image as vegetation stress occurs in the NIR region first.

3. Drone Use in Aerial Images Application

3.2. Cameras

Multi-Spectral Cameras

Parrot SEQUOIA [12]



Figure 3.1.: Parrot SEQUOIA

Sequoia captures information from both visible and invisible light, providing data to optimally monitor the health and vigor of your crops.

Price: \$3500 USD

Figure 3.2.: Parrot SEQUOIA's specifications

3. Drone Use in Aerial Images Application

MicaSense RedEdge[13]



Figure 3.3.: MicaSense RedEdge

RedEdge is a rugged, built-to-last, professional multispectral sensor that captures specific wavebands needed for accurate plant health analysis. With various integration options, it's also one of the most flexible solutions on the market. Additionally, optimized GSD, a downwelling light sensor, a low power requirement, and a global shutter for distortion-free images make this sensor the multispectral powerhouse.

Price: \$5195 USD

Weight:	180 grams (6.3 oz.) (including DLS and cable)
Dimensions:	12.1 cm x 6.6 cm x 4.6 cm (4.8 in x 2.6 in x 1.8 in)
External Power:	5.0 V DC, 4 W nominal (8 W peak)
Spectral Bands:	Blue, green, red, red edge, near IR (global shutter, narrowband)
RGB Color Output:	3.6 MP (global shutter, aligned with all bands)
Ground Sample Distance (GSD):	8 cm per pixel (per band) at 120 m (~400 ft) AGL
Capture Rate:	1 capture per second (all bands), 12-bit RAW
Interfaces:	Serial, Ethernet, WiFi, External Trigger, GPS
Field of View:	47.2° HFOV
Custom Bands:	400nm - 900nm (QE of 10% at 900nm)

Figure 3.4.: MicaSense RedEdge's specifications

3. Drone Use in Aerial Images Application

Sequoia and RedEdge are both powerful multispectral sensors with the capability to yield accurate and calibrated results [?]. Sequoia is simple to operate, fully capable yet lightweight and cost-effective. The additional band (blue), improved GSD, and multiple integration options make RedEdge an ideal solution for research and advanced integrations.

The Sentera Double 4K[14]



Figure 3.5.: The Sentera Double 4K

The Sentera Double 4K is a small, fully customizable twin-imager sensor that is universally compatible with any UAV.

Fitting in the footprint of a GoPro® HERO 4, the rugged, high-throughput Double 4K Sensor is designed for use in harsh environments with configuration options that make it ideal for use in agriculture and infrastructure inspection applications.

The camera is capable of capturing high-megapixel color stills, near-infrared (NIR), and normalized difference vegetation index (NDVI) data, and 4K video.

Price: \$1999-\$2949 USD

3. Drone Use in Aerial Images Application

Comparison Between Multi-Spectral Cameras

Camera	Number of bands	Light sensor	Price	Weight	Power usage	IMU & GPS
MicaSense	5 bands (Blue, Green, Red, Red Edge, Nearinfrared)	✓	5900\$	180 grams (with DLS and cable)	4 W nominal, 8 W peak	✓
RedEdge						
Parrot	4 bands	✓	3500\$	135 grams (with Sunshine Sensor and cable)	8 W nominal, 12 W peak	✓
Sequoia	(Green, Red, Red Edge, Nearinfrared)					
Sentera Double 4K	Spectral Bands: (Blue-Green - Red- Red Edge Near Infrared)	Need additional one	2,499\$~ 4,299\$	80 grams	8W typical / 12W maximum	

Table 3.1.: Comparison between multi-spectral cameras

We can see that the price of any professional cameras is so high. but you can overcome this by buying a consumer camera and convert to NIR camera through NIR filter in front of its lenses .Nevertheless this modified camera is in the same level as other professional cameras due to additional hardware and their specific user online help.



Figure 3.6.: NIR filter

3. Drone Use in Aerial Images Application

Consumer Camera Vs Professional Multi-Spectral Camera

	Consumer camera	Professional multispectral camera
Calibration	needs to be calibrated (ISO,Aperture,shutter speed)	A real and calibrated NDVI camera will account for differences in lighting and maintain consistent and comparable outputs between multiple visits to the same site, regardless of lighting.
Both need	calibrated against reflectance panels	calibrated against reflectance panels
Price	400\$	3500\$ ~7000\$

Table 3.2.: Consumer camera vs professional multi-spectral camera[4]

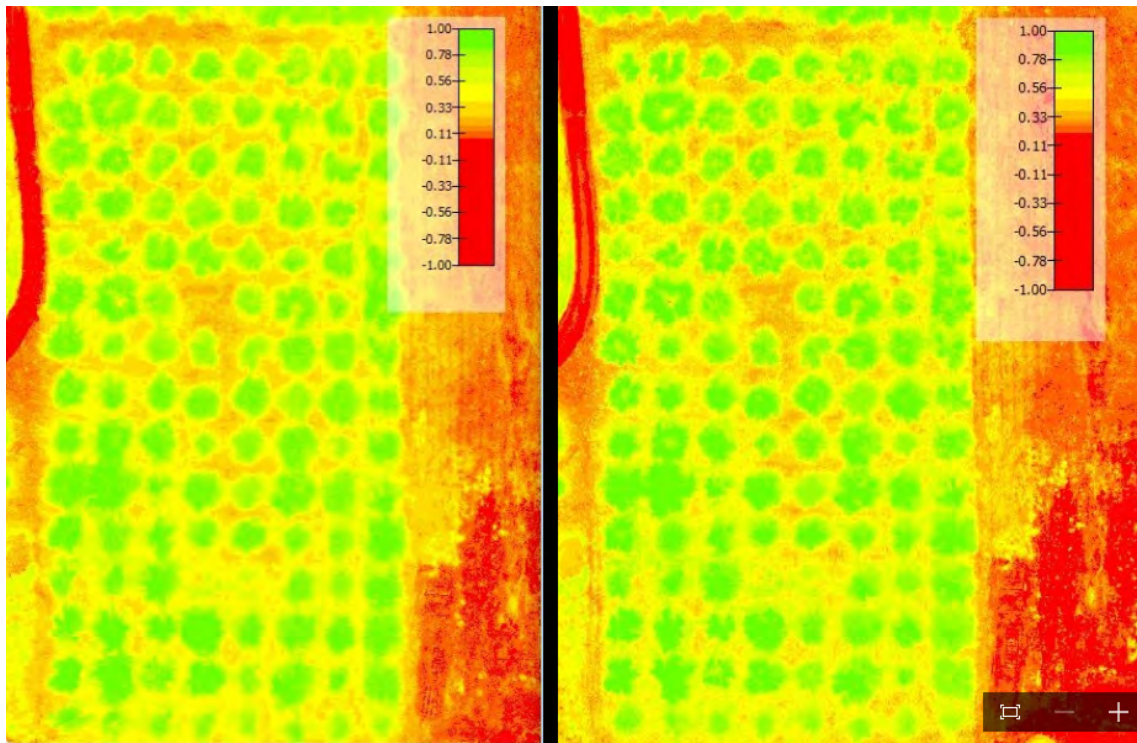


Figure 3.7.: Right image from red edge camera and left image from consumer camera with filter

3. Drone Use in Aerial Images Application

Recommended Consumer Camera and Filters

- Canon SX260, SX280, S100, S110, and S120
 - They are used by companies such as Agribotix, Sensefly, Roboflight, Quest UAV etc. To simplify operation.
 - Camera SX260HS, as this has an on-board GPS, allowing for captured image to be geo-tagged with GPS coordinates. This can help with the image processing later\
 - price : \$399.00 and it can be bought from any supplier in Egypt.
 - Filter [15]
 - * Custom NGB Filter Glass for DIY SX260, SX280, S100, S110, and S120 Camera Conversions.
 - * Price: \$89.00
- Canon S110 RGB/NIR/RE camera
 - Price: \$699.00
 - Filter
 - * Normal view (RGB), Near Infrared (NIR), or Red-Edge (RE)

3. Drone Use in Aerial Images Application



S110 RGB camera: The RGB variant corresponds to the original S110 camera. Colours are unmodified and look natural, e.g., when looking through the camera's LCD screen the vegetation appears green and the sky blue



S110 NIR camera: The NIR variant features custom filters, which capture Near Infrared information in the blue channel. On the camera's LCD screen the vegetation therefore looks violet and the sky appears yellow/orange.



S110 RE camera: The RE variant's custom filters capture Red-Edge information in the red channel. On the camera's LCD screen, the vegetation appears red and the sky blue.

Figure 3.8.: Canon S110 RGB/NIR/RE camera's images

- Sony WX500
 - Price: \$499.00 “lower prices may be found on amazon”
 - Filters may be removed from the camera to convert it to IR camera or adding a NGB filter
- Mapir Survey 2 , Survey 3 [16]
 - When buying a camera, it has 6 options of filters and you can get with the camera only one these filters.
 - Price : 400\$

3. Drone Use in Aerial Images Application

Comparison Between Consumer Cameras

Camera	Sensor width	Focal length	Image width	Image height	Mode	Offers	Cost
Survey 3 w	6.2	3.37	4000	3000	jpg or jpg + raw	GPS + IMU	400\$
Survey 2 w	6.17	3.97	4608	3456	jpg or jpg + raw	No GPS or IMU	400\$
Canon Sx260	6.17	4.5	4000	3000	jpg + raw (requires library)	GPS	4000~2000 bounds + filter 99\$
Canon Sx280	6.16	4.5	4000	3000	jpg + raw (requires library)	GPS	4000~2000 bounds + filter 99\$
Canon Sx100,Sx110 ,Sx120 series	7.6	5.2	4000	3000	jpg + raw (requires library)	Sx100 only have GPS	4000~2000 bounds+ filter 99\$

Table 3.3.: Comparison between consumer cameras

3. Drone Use in Aerial Images Application

Recommendation

We recommend buying Mapir Survey 3 camera.



Figure 3.9.: Mapir Survey 3 camera

- Specifications [17]

- Dimensions 59 x 41.5 x 36mm (Length x Height x Depth)
- Image Dimensions (pixels) 4032 x 3024
- Weight 50g (Without Battery), 76g (With Battery)
- Power Draw 5.2V 0.2A (Without Battery), 5.2V 0.4A (With Battery)
- External GPS Tags (Included)
- IMU
- Internal Battery
- Price : 400\$

For Survey3 camera, the manufacturer recommends[18]

"For best stitching results, we recommend a survey overlap of at least 70% front-lap and 70% side-lap and a maximum 5mph (8kmh) speed for every 65ft (20m) of altitude (AGL) for RAW+JPG mode, and a maximum 10mph (16kmh) speed for every 65ft (20m) of altitude (AGL) for JPG only mode."

Sensor Width (SW)	6.2 m.m
Focal Length (FL)	3.37 m.m
Image Width (imW)	4000 px
Image Height (imH)	3000 px
$Ovelap_{front}$	0.7
$Ovelap_{side}$	0.7

Table 3.4.: Survey 3 camera's specifications

3. Drone Use in Aerial Images Application

We can generate the following figures using the relations in [appendix A](#)

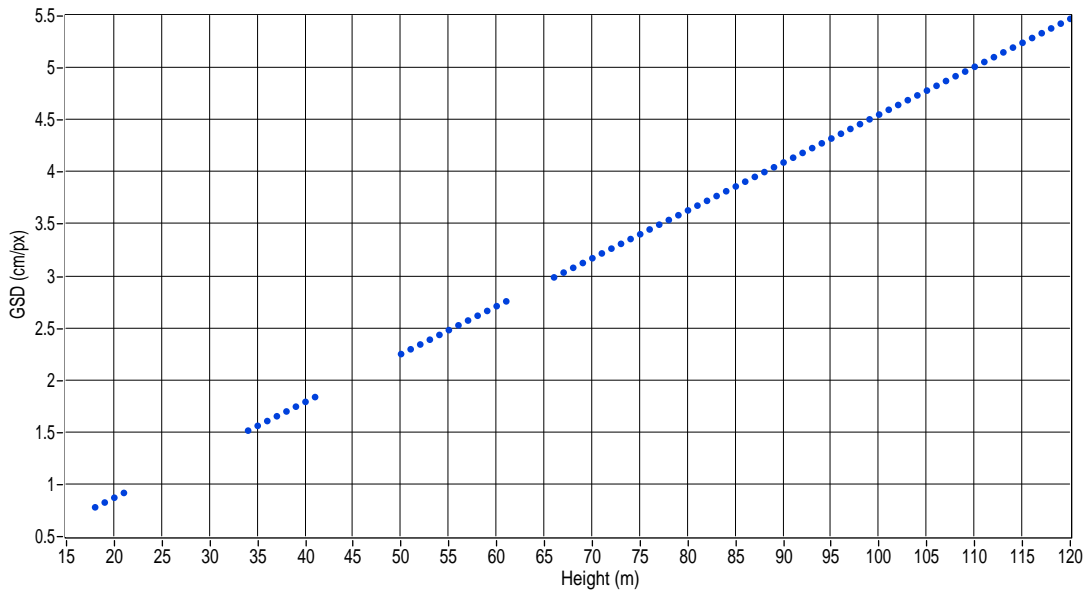


Figure 3.10.: GSD vs Height

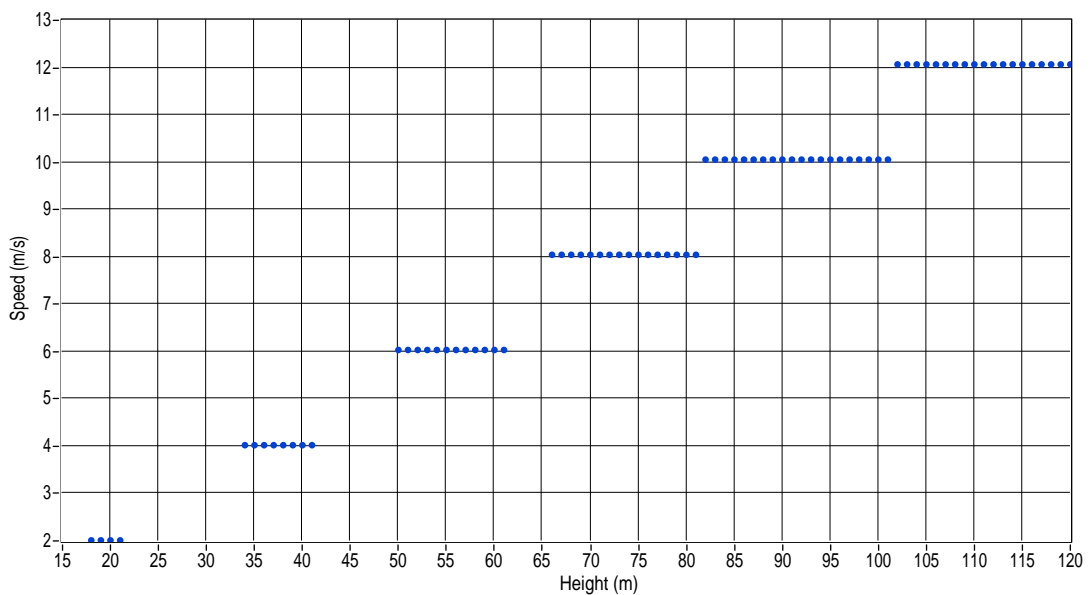


Figure 3.11.: Velocity vs Height

3. Drone Use in Aerial Images Application

We can determine for a given height and velocity the area that we can cover without causing problems like motion blur.

Hyper-Spectral Cameras

Corning micro HSI 410 SHARK Hyperspectral Sensor for UAV Drones



Figure 3.12.: Corning micro HSI 410 camera

Corning Hyperspectral Imaging provides hyperspectral sensors and full hyperspectral systems for all applications including precision agriculture, industrial, environmental monitoring, mining, and mineralogy. Corning's microHSI™ family of hyperspectral sensors and systems combine the lowest size, weight and power (SWaP) in the industry with uncompromising performance, enabling deployment for challenging applications in limited payload and/or size constrained environments.

A few of the 410 SHARK's innovative features include:

- First complete, coherent HSI sensor system designed specifically for small UAS/UAV drones.
- System includes:
 - visNIR microHSI™ 410 sensor
 - Lens
 - GPS/Inertial navigation system (INS)
 - Microprocessor control
 - Data acquisition and storage
- Dimensions: 136.4 x 87.4 x 70.4mm (with lens) / 95.8 x 87.4 x 70.4mm (without lens)
- Weight: 730 grams
- Web interface for system management and control

3. Drone Use in Aerial Images Application

- Flight planning and execution software enables pre-programming of image collection plan
 - Automated waypoint operation, frame rate, binning, selectable image recording options
- Operating and maintenance documentation
- API interface (upon request)
- Designed for minimum 30 minute operating/recording time.
 - Consistent with performance of most small UAS
 - Hot-swap battery optional; larger battery available
- For more effective data management, the user can choose to collect the entire 155 band hyperspectral image cube, or only the spectral bands needed for a specific mission or application.
- Digital Elevation Maps (DEM) can be loaded into the system pre-flight for the area to be imaged to improve image georegistration during post-processing.

Hyperspectral vs. Multispectral Imaging Technology

Hyperspectral vs. Multispectral Imaging Technology

- Hyperspectral imagers cover many dozens to hundreds of spectral bands contiguously
- Multispectral imagers cover a selected set of bands non-contiguously
 - Spectral information critical for characterization, research and development of specific applications may be missing.

Number of spectral bands is insufficient to address multitude of developed and proven applications and indices

3. Drone Use in Aerial Images Application

Why Hyperspectral Over Multispectral for Precision Agriculture?

Why Hyperspectral Over Multispectral for Precision Agriculture?

- Agricultural market demand for hyperspectral sensor systems is growing to address a growing catalog of vegetation indices used for vegetation/crop analysis and diagnostics.
 - There are currently over proven 65 vegetation indices, and growing
- New crop specific, application specific indices are being developed and introduced each year.
- Multispectral sensor systems can utilize only a small subset of indices, and cannot take advantage of new indices as they are introduced.
- Hyperspectral sensors enable the research and development of new vegetation indices – multispectral sensors do not.

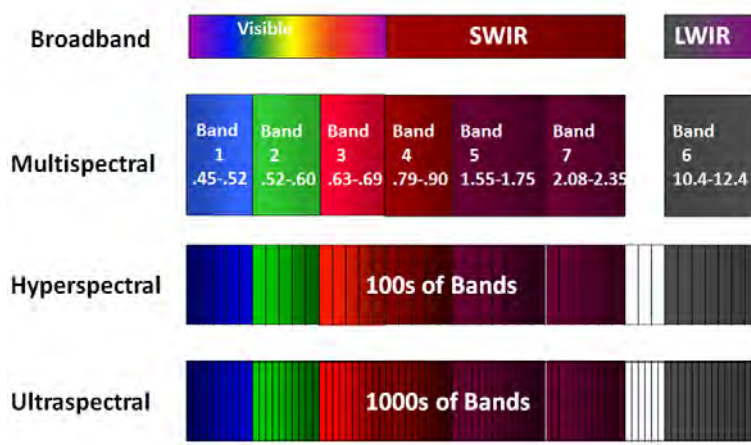


Figure 3.13.: Light bands

3. Drone Use in Aerial Images Application

Thermal Cameras



Figure 3.14.: FLIR VUE camera

Price: \$1199.2

FLIR VUE SPECIFICATIONS

Overview		
Thermal Imager	Uncooled VOx Microbolometer	
Resolution	640x512	336x256
Lens Options	9 mm; 69° x 56° 13 mm; 45° x 37° 19 mm; 32° x 26°	6.8 mm; 44° x 36° 9 mm; 35° x 27° 13 mm; 25° x 19°
Spectral Band	7.5 - 13.5 μm	
Full Frame Rates	30 Hz (NTSC); 25 Hz (PAL) <i>US only, not for Export</i>	
Exportable Frame Rates	7.5 Hz (NTSC); 8.3 Hz (PAL)	
Physical Attributes		
Size	2.26" x 1.75" x 1.75" (57.4 x 44.4 mm x 44.4 mm) (including lens)	
Weight	3.25-4 oz (92.1 – 113.4 g) (configuration dependent)	
Precision Mounting Holes	Two M2x0.4 on each of two sides & bottom One 1/4-20 threaded hole on top	

Figure 3.15.: Flir Vue specifications

3. Drone Use in Aerial Images Application

Notes

- A gimballed system compensates for effects like blurred or oblique images and lack of overlap.
- The camera needs to be isolated from vibrations of the multi-rotor and this can be achieved using rubber isolation grommets between the camera gimbal and the airframe.
- Preplan your mission, do a site visit or use Google Earth for site info
- The higher you fly, the less images you need which means less processing time
- The higher you fly, the larger the area you can map
- Always check your images when in the field
- Fly at noon to limit shadows from the vines
- Use an observer
- Crop analysis is 20% flying and 80% data processing
- Image processing takes lots of computing power, get a fast processor with lots of memory
- High quality images equates to high quality crop analysis, poor images mean poor data
- Aerial images and analysis needs to be correlated with ground data to be effective
- Normal photographs and video in RGB is almost as invaluable as NGB to the vineyard owner
- Drone NDVI mapping becomes effective with vineyards greater than 50 acres[19]

Problems [20]

Motion Blur

This is caused by fast-moving drones or vibration- this either means the shutter speed isn't fast enough, or that you are flying too fast. The best way to solve this is to improve shutter speed, but flying slower or higher will help as well. Here is an example of what motion blur looks like:

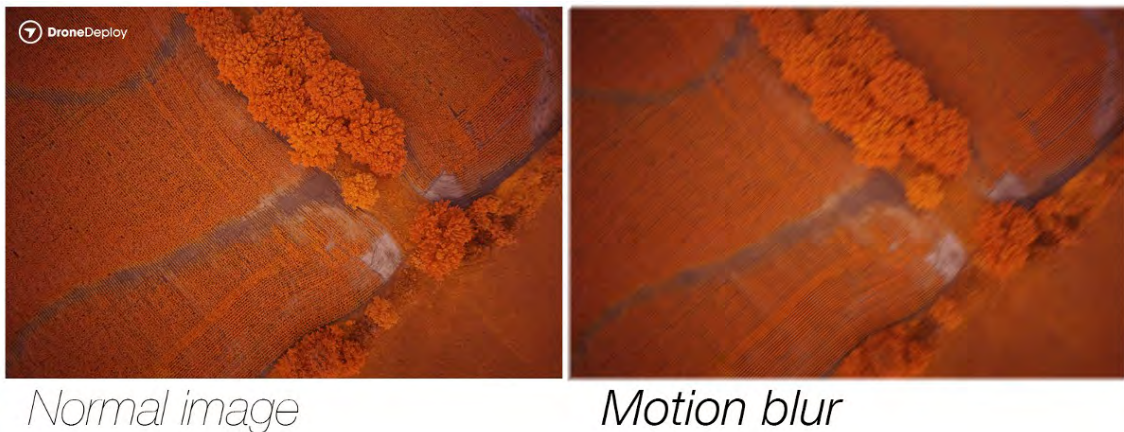


Figure 3.16.: Motion blur

3. Drone Use in Aerial Images Application

Photos taken at low altitude

Taking photos at a low altitude lowers the surface area per image, which will make them difficult to stitch together. This can result in blurry maps. It is difficult to cover as much ground in one flight as you could from a higher altitude.

3.3. Images Analysis Software

Software On Server [10]

There are some websites that offer some tools on their server for free.



Figure 3.17.: Basic free services

3. Drone Use in Aerial Images Application

Other services are available according to their price plan.

	FREE	STANDARD	STANDARD +	BUSINESS
	\$ 0 /MO	\$ 95 /MO	\$ 240 /MO	\$ 450 /MO
CLOUD-BASED 2D/3D MAPS (Any Resolution)	5/mo Visual Only	10/mo	10/mo	50/mo
STORAGE	300 GB	450 GB	450 GB	Unlimited
EXPORT	✓	✓	✓	✓
PRECISIONVIEWER Instant Data Review	✓	✓	✓	✓
VOLUMETRICS	✓	✓	✓	✓
UNLIMITED BASIC VEGETATIVE INDICES <small>Learn more</small>	✓	✓	✓	✓
UNLIMITED ADVANCED VEGETATIVE INDICES <small>Learn more</small>	✗	✓	✓	✓
OFFLINE IMAGE PROCESSING	✗	✗	✓	✓
MULTIPLE USER ACCESS	✗	✗	✗	✓
ADD-ON ADVANCED ANALYSIS TOOLS <small>Learn more</small>	\$4.99-\$19/mo	\$9.99-\$29/mo	\$9.99-\$29/mo	\$49-\$149/mo
	GET STARTED	GET STARTED	GET STARTED	GET STARTED

Figure 3.18.: Price plan

Desktop Application

There are some software that can run on your machine.

- ArcGIS

- ArcGIS Desktop Basic- Visualize, build maps, edit data, import CAD, perform data conversions, generate maps, query data. Cost is \$1,500 for a single use license / \$3,500 for concurrent.
- ArcGIS Desktop Standard- Allows everything found in the basic version but allows additional capabilities for multi-user platforms and editing enterprise level geodatabases. This level is required to take advantage of many custom editing tools published by esri. Cost is \$7,000 for a single use or concurrent license.

3. Drone Use in Aerial Images Application

- Envi
 - ENVI image analysis software uses scientifically proven analytics to deliver expert-level results.

Build our own software

We could use any image processing packages to analyze any image and compute the desired vegetation index as any index has their own formula such as

- Normalized difference vegetation index (NDVI)

$$NDVI = \frac{NIR - Red}{NIR + Red}$$

- Global environmental monitoring index (GEMI)

$$eta = \frac{2(NIR^2 - Red^2) + 1.5 * NIR + 0.5 * Red}{NIR + Red + 0.5}$$

$$GEMI = eta(1 - 0.25 * eta) - \frac{Red - 0.125}{1 - Red}$$

4. Drone Use in Aerial Pesticide Application

Spraying System



Figure 4.1.: Drone used to spray fertilizers

4. Drone Use in Aerial Pesticide Application

Components

- Water Pump
 - Quantity: 2
 - Input: 11-25.5v
 - Power: 45 watts
 - N.W: 284 gm
 - Dual pump system
 - Price : 95 \$ /one



Figure 4.2.: Water Pump

- Tank
 - Volume : 10 liter
 - Max payload: 10kg
 - Coverage per tank using standard spray nozzle: 2.47 Acres (10,000 m²)
 - Price : 15 \$



Figure 4.3.: Tank

4. Drone Use in Aerial Pesticide Application

- Nozzle kit
 - Quantity: 2
 - Industry-standard ceramic nozzle
 - 360° degrees atomized spray pattern
 - Includes 2 nozzles and tubes
 - Max spray speed: 0.43L/min(per nozzle for water)
 - Spray width: 4-6M (4 nozzles,1.5-3M above the crops)
 - Droplet size : 130-150(droplet size vary according to operation environment and spraying speed)
 - Price : 87 \$



Figure 4.4.: Nozzle kit

- Radar system
 - Quantity:3
 - Weight: 0.17 kg



Figure 4.5.: Radar system

4. Drone Use in Aerial Pesticide Application

- Aliexpress Spraying kit
 - Operating voltage: 12VDC
 - Net weight: 2.2KG-3kg
 - Water tank capacity 15L / 20L * 1(Optional) Quick disassembly Nozzle * 4 pcs
 - Spray rod * 2
 - Water pump * 1
 - Remote control switch (adjustable speed) * 1
 - Aluminum tripod and body connector * 1
 - Price: US \$432.25 - 441.75 / piece



Figure 4.6.: Aliexpress Spraying kit

- System capabilities
 - It can cover around 65-80 acres for one day
 - It takes the farmer to cover 0.65 acres in full day but with UAV it can do it in just 2 minutes.
 - Spray rate may vary according to the nozzle model and viscosity of liquid, For water, when using four XR11001 nozzles, the minimum rate is 1.2L/min and the maximum rate is 1.7L/min.

5. Ground Control Station

5.1. Introduction

We considered the design of our own ground control station (GCS), we build it considering the features mentioned in [2.7](#).

5.1.1. Features

- Point-and-click waypoint entry
- The map is from Google Earth .
 - Google Earth can work semi offline by cashing 2 gigabyte worth imagery on the hard desk.
- Select mission commands from drop-down menus
 - Current missions include
 - * Survey
 - * Circular Path
- You can see a how it was designed and a quick tutorial about it in [appendix B](#)

6. Hardware

6.1. Motor

Description	kV	Constant Watts	Burst Watts	3D
RimFire .15	1200	500	650	1135 g

Table 6.1.: Motor's specifications

6.2. Connections

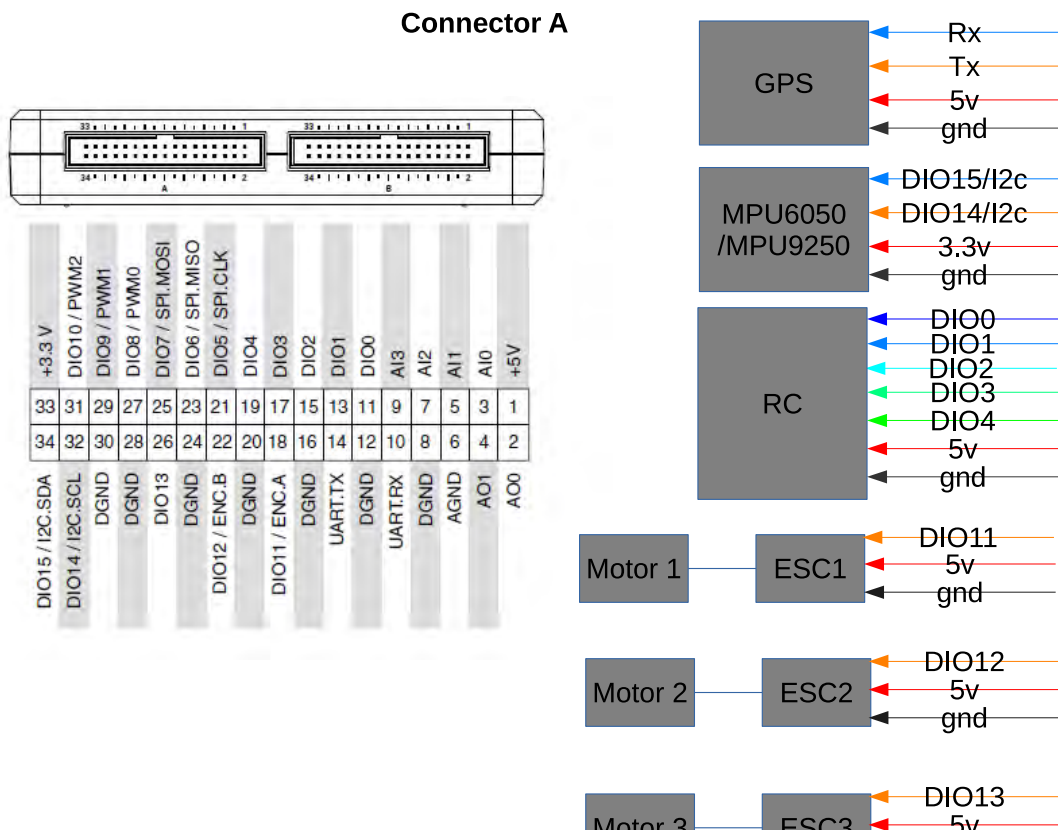


Figure 6.1.: Connections #1

6. Hardware

Connector B

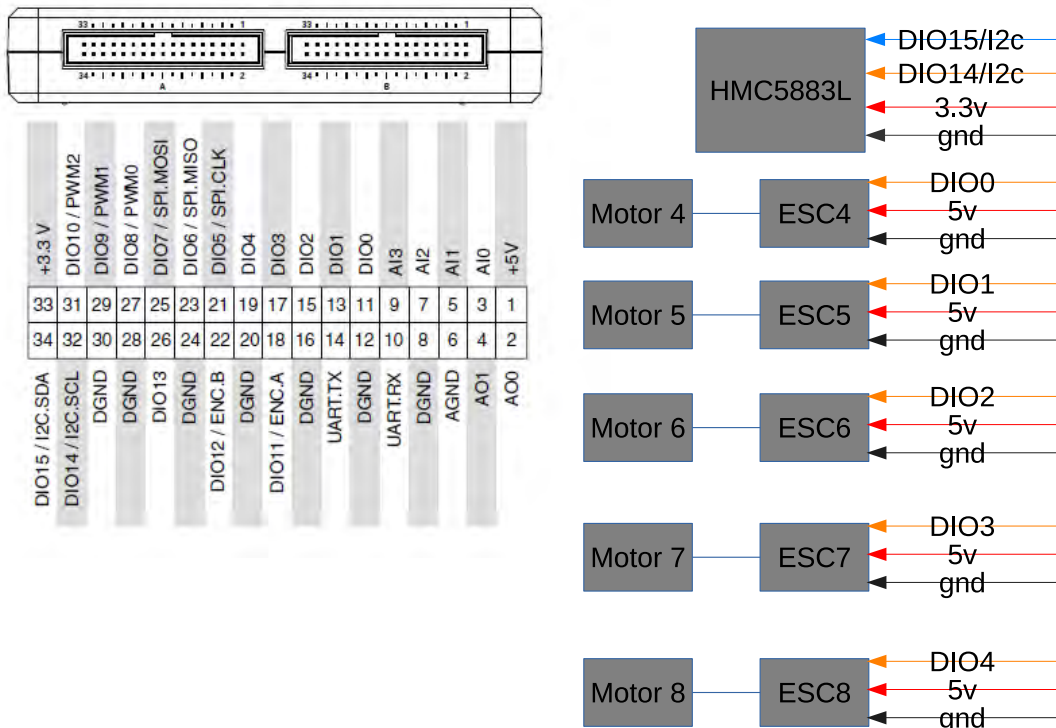


Figure 6.2.: Connections #2

Connector C

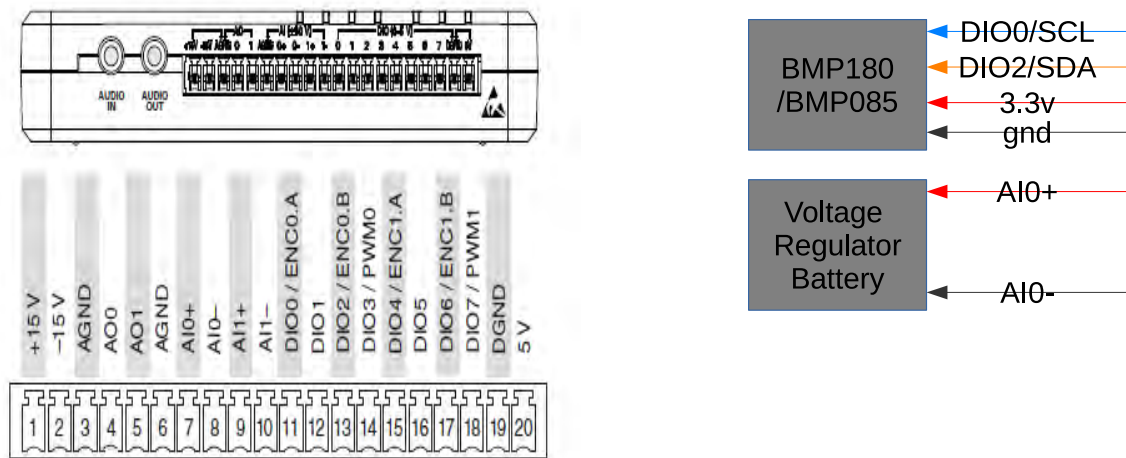


Figure 6.3.: Connections #3

6. Hardware

6.3. First Iteration

A PCB is used to gather all sensor boards into one board for these reasons:

- Wiring problems
- Fixing boards
- Collect their power sources in one specified power source
- Makes communication wires a lot easier to connect

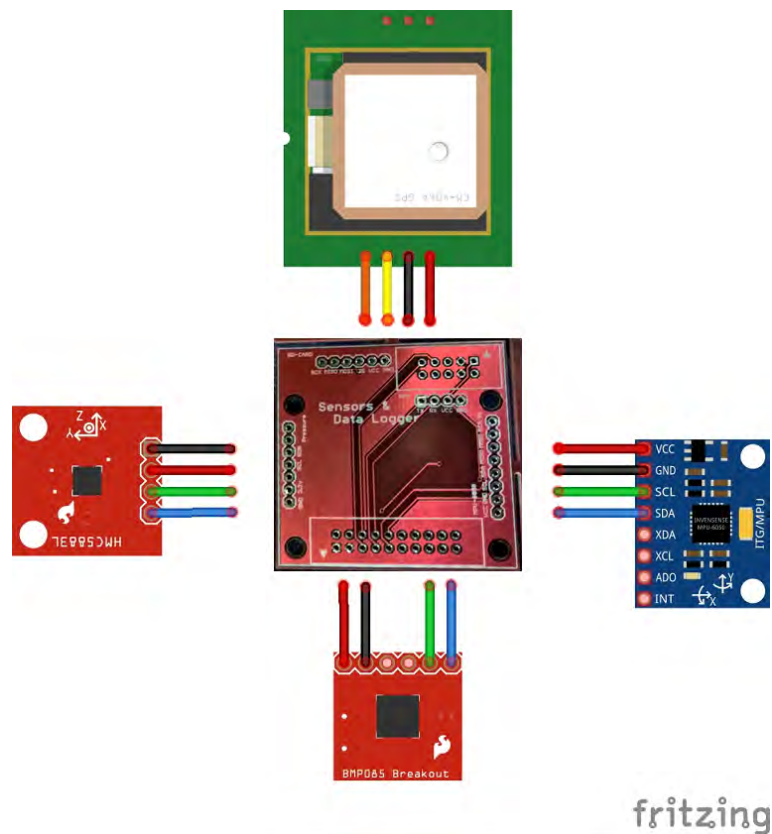


Figure 6.4.: PCB #1

Actuators

6. Hardware

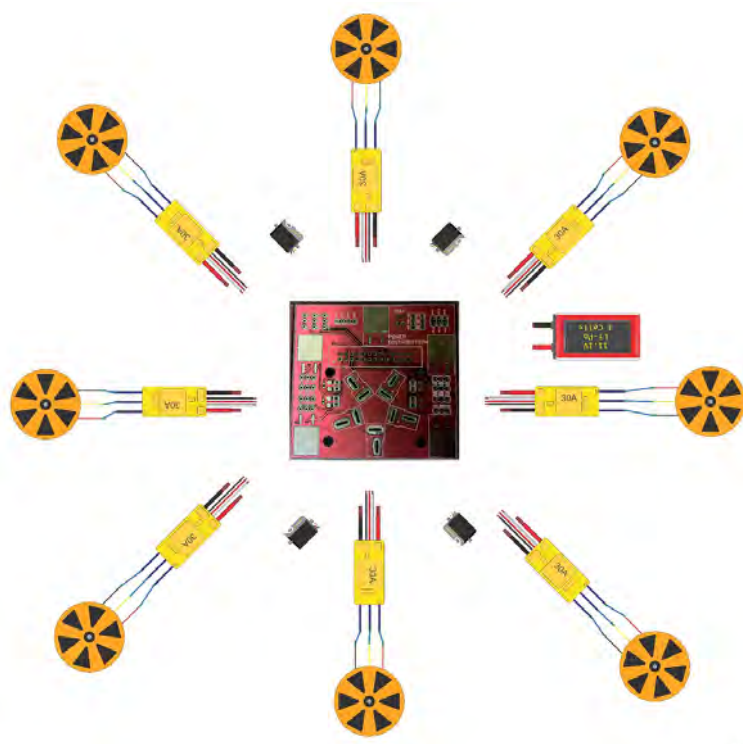


Figure 6.5.: PCB #2

Boards after components

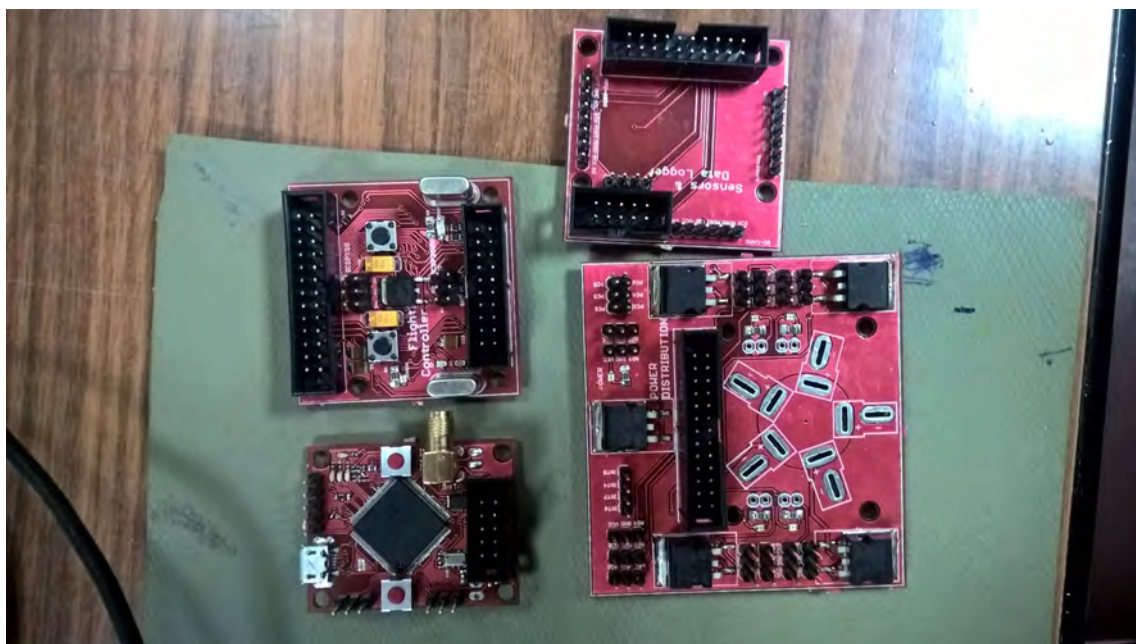


Figure 6.6.: PCB #3

6. Hardware



Figure 6.7.: PCB #4

7. Sizing

7.1. Survey

3DR X8+ Multicopter



Figure 7.1.: 3DR X8+ Multicopter

- Aircraft weight (with battery): 7.7 lbs (3.5 kg)
- Aircraft dimensions: 13.7 in x 20.1 in x 11.8 in (35 cm x 51 cm x 30 cm)
- Case dimensions: 60.7 in x 14.5 in x 15.5 in (154 cm x 37 cm x 39 cm)
- Payload capacity: .4 lbs (200 g)
- Flight time: 14 min*
- Maximum operational wind speed: 25 mph (11 m/s)
- Recommended flight speed: 11 mph (5 m/s)

7. Sizing

Mk8-3500 Agrar[21]



Figure 7.2.: Mk8-3500 Agrar

model designation	MK8-3500 Agrar
base weight ind. 2 batteries	4350g
weight ind. 2 batteries & SLR2 gimbal	4637g
weight ind. 2 batteries, gimbal & camera	4978g
weight ind. 4 batteries	5732g
weight ind. 4 batteries & SLR2 Gimbal	5989g
weight ind. 4 batteries, Gimbal & camera	6330g
max. payload	3500g (with 2 batteries) 2150g (with 4 batteries)
Drive	8 single driven brushless motors (with 16" CFK propellers)
Dimensions MK8-3500	aprox. 1085mm x 1160mm x 450mm
Dimensions transport case	aprox. 700mm x 600mm x 400mm
Flight time	approximately 30 minutes (ind. cameras, 4 batteries and gimbal)
Range	Depending on the used transmitter / receiver (Range Graupner MX-20/MC-32 ind. receiver GR-16 = 4km (acc. to manufacturer))
Altitude	up zu 5000m above sea level
Operating temperature range	-5°C up to +40°C Batteries loses performance in cold weather performance. The flight time can be reduced accordingly.
Recommended max. Wind speed	up to 3 Beaufort Copter is airworthy up to 6 Beaufort (requires enhanced flight skills)
camrea mount	MK HISight SLR2, 2 axis (Nick & Roll), Servogimbal
Camera	Multispectral "RedEdge" from Micasense, CMOS Kamera
dlimb rate	---
battery pack	High current lithium polymer battery, 4500mAh, 6S

Figure 7.3.: Mk8-3500 Agrar's specifications

7. Sizing

Flight times

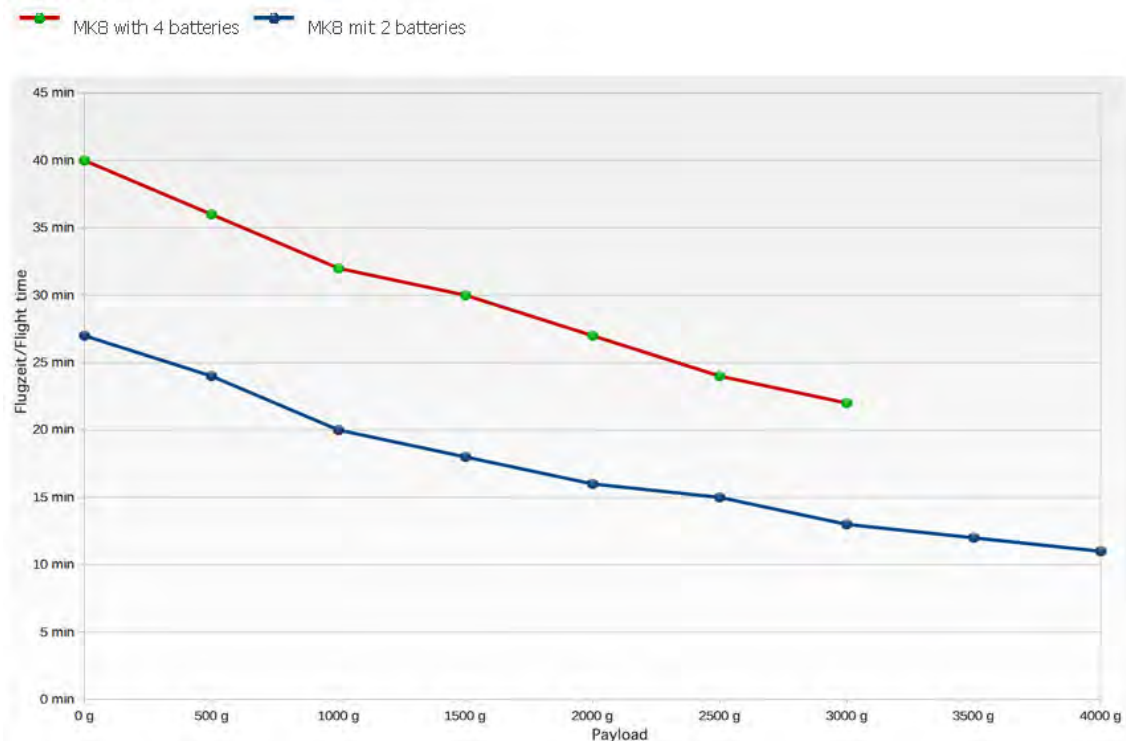


Figure 7.4.: Mk8-3500 Agrar's flighth times

7. Sizing

Agras MG-1S[22]



Figure 7.5.: Agras MG-1S

AIRCRAFT FRAME

Diagonal Wheelbase	1515 mm
Frame Arm Length	625 mm 1471 mm×1471 mm×482 mm (arm unfolded, without propellers)
Dimensions	1471 mm×1471 mm×482 mm (arm unfolded, without propellers) 780 mm×780 mm×482 mm (arm folded)

Figure 7.6.: Agras MG-1S's specifications #1

7. Sizing

RADAR MODULE			
		Detection Range	1-5 m
Total Weight	10 kg (without battery)	Working Range	1.5-3.5 m
Standard Takeoff Weight	23.8 kg	Precision	<10 cm
Max Takeoff Weight	24.8 kg (at sea level)		
Max Thrust-Weight Ratio	1.71 (with 23.8 kg takeoff weight)		
Power Battery	DJI Designated Battery (MG-12000S)		
Max Power Consumption	6400 W		
Hanging Power Consumption	3800 W (@with 23.8 kg takeoff weight)		
Hovering Time*	22 min (@12000 mAh & 13.8 kg takeoff weight) 10 min (@12000 mAh & 23.8 kg takeoff weight) <small>*Hovering time acquired at sea level with wind speeds lower than 3 m/s.</small>	Model	A14-057N1A
Max Operating Speed	7 m/s	Voltage	17.4 V
Max Flying Speed	12 m/s (P & F Mode, with GPS) ; 15 m/s (A Mode)	Rated Power	57 W
Max Service Ceiling Above Sea Level	2000 m		
Recommended Operating Temperature	0°C to 40°C		

REMOTE CONTROLLER CHARGER			
		Model	A14-057N1A

Figure 7.7.: Agars MG-1S's specifications #2

PROPELLION SYSTEM

MOTOR		ESC	
Stator Size	60×10 mm	Max Allowable Current (Continuous)	25 A
KV	130 rpm/V	Operating Voltage	50.4 V (12S LiPo)
Max Thrust	5.1 kg/rotor	Drive PWM Frequency	12 kHz
Max Power	770 W		
Weight	280g (with cooling fan)		

FOLDABLE PROPELLER

Material	High-performance engineered plastics
Diameter/Pitch	21×7 inch
Weight	58 g

Figure 7.8.: Agars MG-1S's specifications #3

7. Sizing

SPRAY SYSTEM

LIQUID TANK

Volume	10 L
Standard Operating Payload	10 kg
Max Battery Size	151 mm×195 mm×70 mm

NOZZLE

Model	XR11001VS (0.379L/min)
Recommend Model	XR11001VS (0.591L/min)
	TK-VK6 (0.393L/min)
	TK-VK8 (0.525L/min)
Quantity	4
Droplet Size	XR11001VS : 130-250 µm (subject to working environment and spraying speed)

Figure 7.9.: Agras MG-1S's specifications #4

7. Sizing

Matrice 200 Series [23]



Figure 7.10.: Matrice 200 Series

7. Sizing

Model	M200
Package Dimensions	31.1×15.4×11.4inch(790×390×290mm)
Dimensions(unfolded)	34.9×34.6×14.9 inch(887×880×378 mm)
Dimensions(folded)	28.2×8.7×9.3 inch(716×220×236 mm)
Folding Method	Folded Inward
Diagonal Wheelbase	25.3 inch(643 mm)
Number of Batteries	2
Weight(TB50)	Approx. 3.80 kg
Weight(TB55)	Approx. 4.53 kg
MaxTakeoff Weight	6.14KG
Max Payload(2 TB50)	Approx.2.34kg(with two standard batteries)
Max Payload(2 TB55)	Approx.1.61kg(with two standard batteries)
Hovering Accuracy(P-mode with GPS)	Vertical: ±1.64 feet(0.5m) or ±0.33 feet(0.1m, Downward Vision System enabled) Horizontal: ±4.92 feet(1.5m) or ±0.98 feet(0.3m,Downward Vision System enabled)

Figure 7.11.: Matrice 200 Series's specifications #1

Max Angular Velocity	Pitch: 300°/s ; Yaw: 150°/s
Max Pitch Angle	P Mode: 30° (Forward Vision System enabled: 25°) ; A Mode: 35° ; S Mode: 35°
Max Ascent Speed	16.4 ft/s(5 m/s)
Max Descent Speed	Vertical: 9.8 ft/s(3 m/s)
Max Speed	S Mode: 51.4mph(82.8kph) P Mode: 38mph(61.2kph) A Mode: 51.4mph(82.8kph)
Max Service Ceiling Above Sea Level	1.86 mi(3000 m)
Max Wind Resistance	39.4 ft/s(12 m/s)
Max Flight Time(No Payload, with TB50)	27min
Max Flight Time(No Payload, with TB55)	38min
Max Flight Time(Full Payload, with TB50)	13min
Max Flight Time(Full Payload, with TB55)	24min

Figure 7.12.: Matrice 200 Series's specifications #2

7. Sizing

7.1.1. Charts [2]

The following figures were generated based on a survey on professional drones.

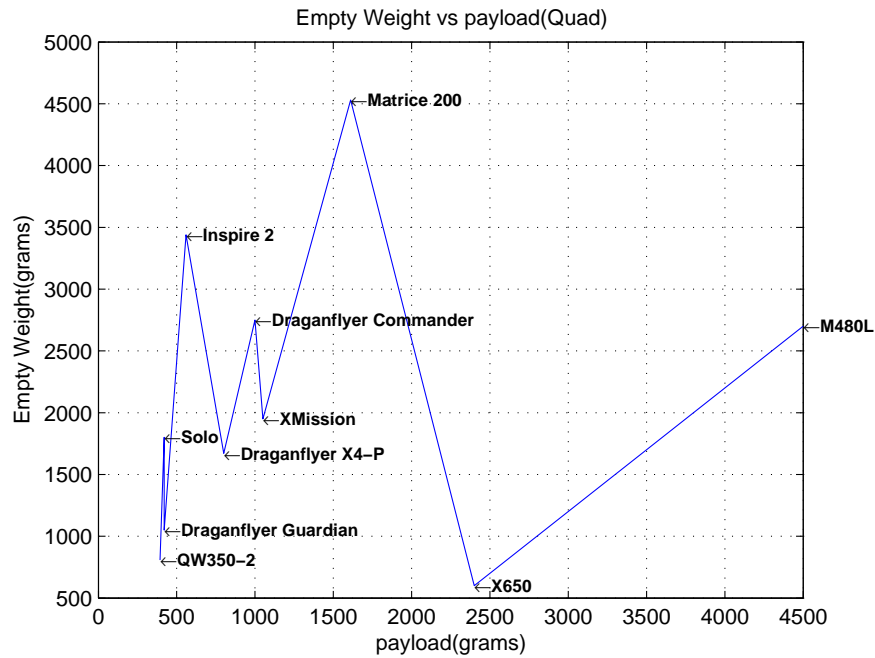


Figure 7.13.: Empty weight vs payload (quad copter)

7. Sizing

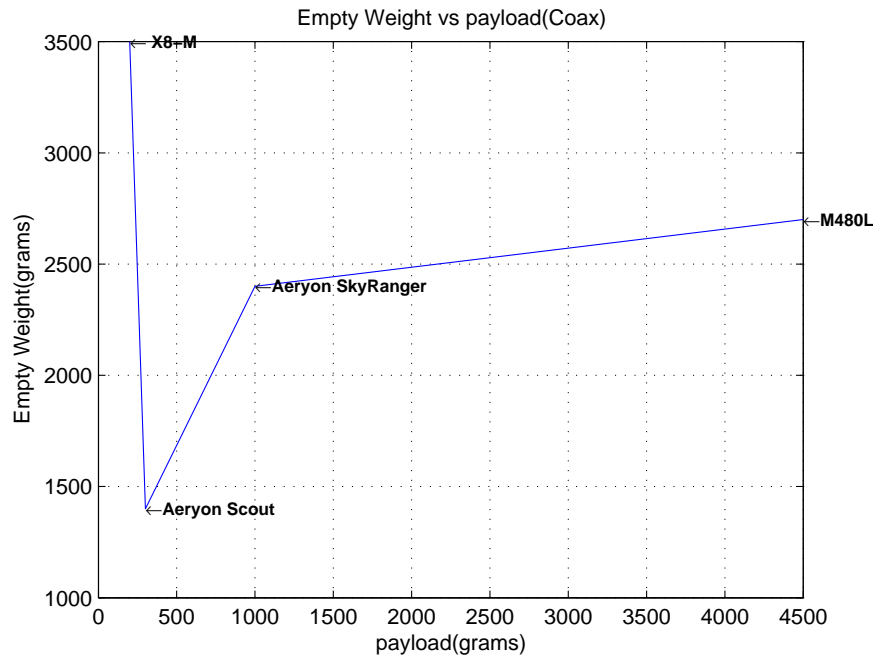


Figure 7.14.: Empty weight vs payload (coax copter)

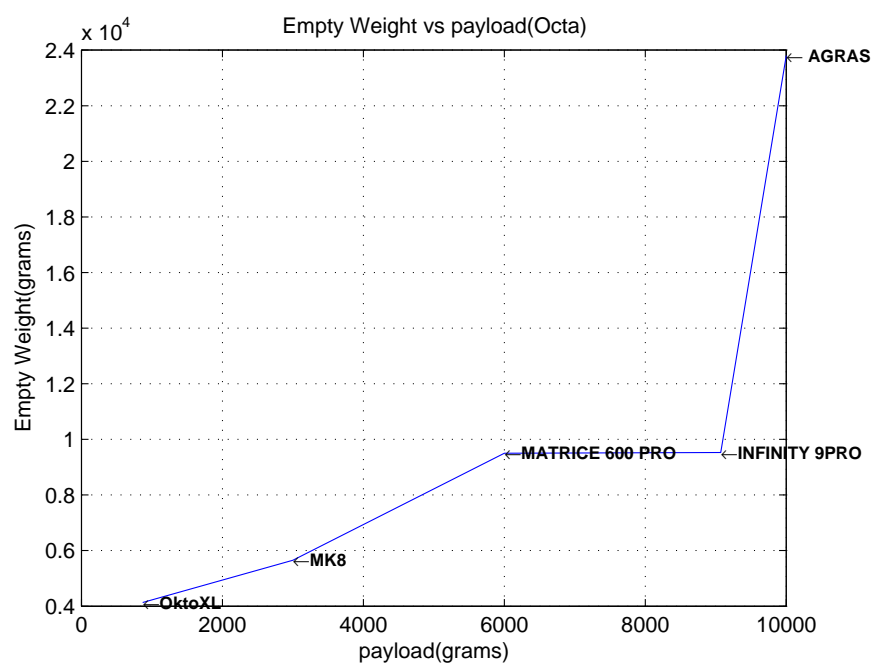


Figure 7.15.: Empty weight vs payload (octa copter)

7. Sizing

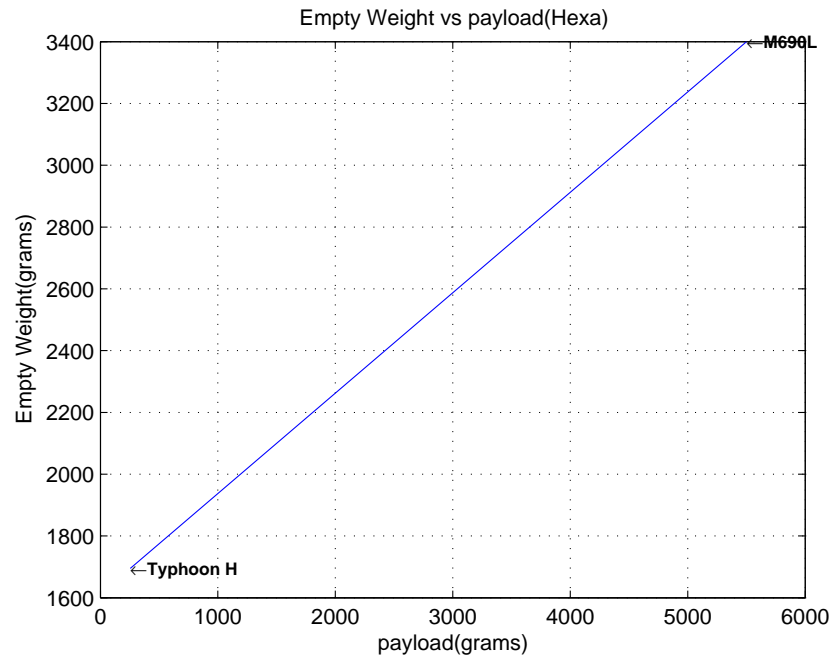


Figure 7.16.: Empty weight vs payload (hexa copter)

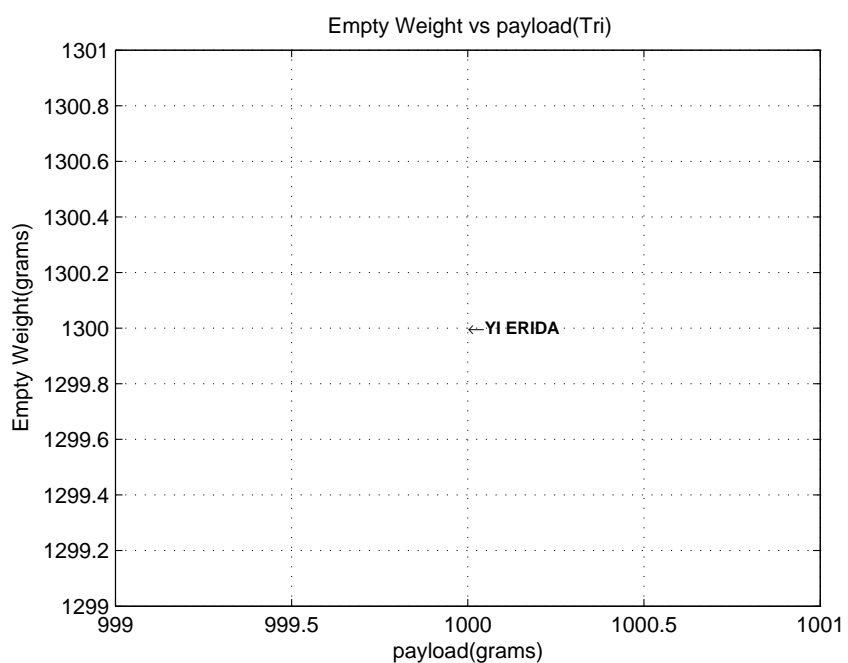


Figure 7.17.: Empty weight vs payload (tri copter)

7. Sizing

7.2. Coaxial vs Flat

Battery C required	3.00	(C)	Component weights: motors	648.86	(g, total)
Throttle / collective required	33.70	(%)	ESCs	202.10	(g, total)
Total drive current required	21.74	(A)	Batteries (drive)	1055.12	(g, total)
Motor electric power / motor	43.36	(W)	Payload	0.00	(g, total)
Motor mechanical power / motor	31.22	(W)	Structural	536.51	(g, total)
Efficiency: specific thrust	7.39	(g/W)	Wiring	127.01	(g, total)
Battery degradation coef V	100.00	(%)	Avionics	50.00	(g, total)
Battery degradation coef C	100.00	(%)	Propellers	58.47	(g, total)
Vehicle pitch angle	0.00	(deg)	GTOW	2540.11	(g, total)
Propeller speed	3623.42	(RPM)			
Motor speed	3623.42	(RPM)			
Tip speed	53.01	(m/s)			
Tip Mach number	0.16	(Mach)			
Motor torque / motor	0.03	(Nm)			
Disc loading	5.18	(kg/m^2)			
Power loading	59.11	(kg/kW)			
Max governor	0.00	(%)			
Blade pitch	4.70	(deg,")			
Mixed flight time	12.30	(min)	Hover time	20.51	(min)
			80	100	% throttle
Thrust/weight	5.68	8.88	(-)		
Specific thrust	0.60	0.49	(g/W)		
Current / motor	23.59	45.08	(A)		
Electric power / motor	376.44	719.55	(W)		
Total motor electric power	3011.49	5756.37	(W)		

(a) Flat #1

Battery C required	3.00	(C)	Component weights: motors	648.86	(g, total)
Throttle / collective required	33.70	(%)	ESCs	202.10	(g, total)
Total drive current required	23.89	(A)	Batteries (drive)	1055.12	(g, total)
Motor electric power / motor	47.67	(W)	Payload	0.00	(g, total)
Motor mechanical power / motor	34.32	(W)	Structural	536.51	(g, total)
Efficiency: specific thrust	6.72	(g/W)	Wiring	127.01	(g, total)
Battery degradation coef V	100.00	(%)	Avionics	50.00	(g, total)
Battery degradation coef C	100.00	(%)	Propellers	58.47	(g, total)
Vehicle pitch angle	0.00	(deg)	GTOW	2540.11	(g, total)
Propeller speed	3623.42	(RPM)			
Motor speed	3623.42	(RPM)			
Tip speed	53.01	(m/s)			
Tip Mach number	0.16	(Mach)			
Motor torque / motor	0.04	(Nm)			
Disc loading	5.18	(kg/m^2)			
Power loading	53.77	(kg/kW)			
Max governor	0.00	(%)			
Blade pitch	4.70	(deg,")			
Mixed flight time	11.22	(min)	Hover time		18.69 (min)
			80	100	% throttle
Thrust/weight	5.68	8.88	(-)		
Specific thrust	0.52	0.42	(g/W)		
Current / motor	27.20	52.13	(A)		
Electric power / motor	434.03	832.04	(W)		
Total motor electric power	3472.27	6656.32	(W)		

(b) Coaxial #1

Figure 7.18.: Coaxial vs Flat #1

Airspeed (m/s)	Pitch (deg)	Throttle/collective (%)	Drive current (A)	Flight time (min)	Range (km)
0.00	0.00	33.70	21.74	20.51	0.00
1.52	11.10	34.50	22.52	19.81	1.81
3.05	17.10	35.60	23.56	18.95	3.47
4.57	22.10	36.90	25.29	17.68	4.85
6.10	26.10	39.40	29.13	15.39	5.63
7.62	29.60	42.70	35.42	12.70	5.80
9.14	32.60	46.60	43.97	10.25	5.63
10.67	35.60	51.00	55.74	8.11	5.19
12.19	37.60	55.60	69.34	6.53	4.78
13.72	40.10	60.90	86.17	5.26	4.33
15.24	41.60	66.00	104.17	4.36	3.98

(a) Flat #2

Airspeed (m/s)	Pitch (deg)	Throttle/collective (%)	Drive current (A)	Flight time (min)	Range (km)
0.00	0.00	33.70	23.89	18.69	0.00
1.52	11.10	34.50	24.80	18.02	1.65
3.05	17.10	35.60	26.01	17.20	3.15
4.57	22.10	36.90	28.02	15.99	4.39
6.10	26.10	39.40	32.47	13.83	5.06
7.62	29.60	42.70	39.76	11.33	5.18
9.14	32.60	46.60	49.69	9.09	4.98
10.67	35.60	51.00	63.34	7.14	4.57
12.19	37.60	55.60	79.11	5.73	4.19
13.72	40.10	60.90	98.64	4.60	3.79
15.24	41.60	66.00	119.52	3.80	3.47

(b) Coaxial #2

Figure 7.19.: Coaxial vs Flat #2

7. Sizing

7.2.1. Experiment



Figure 7.20.: Experiment #1

7.2.1.1. Side by Side

7.2.1.2. Coaxial

7.3. Requirements

- Our mission is design and manufacture a VTOL system that will be able to carry 8 kg of payload
- Payload is our a NDVI camera that can capture a NIR images to know the quality & health of the plants

Payload	8000 grams
Height	50 meter
Velocity	max speed depend on the camera
Numbers of motor	depend on payload
Area of interest	1.5 feddan
Time in air	according to the area of interest

Table 7.1.: Mission requirements

7. Sizing

7.4. Sizing Procedure

In this section a common problem faced in every multi-copter design process which is the selection of the components (motors, propellers, batteries and ESC) and what combination gives you the ultimate performance for your endurance, payload and range requirements.

7.4.1. Data base

Collecting a data for this kind of a problem is hard to get without searching for the appropriate company which gives you Performance Testing Data Sheet, rare companies gives you such thing like KDE-Direct company gives you with each motor its testing data, the data will be like this figure

MOTOR VERSION	VOLTAGE LIHV [V]	PROPELLER SIZE	THROTTLE RANGE	AMPERAGE [A] (LOWER IS BETTER)	POWER INPUT [W] (LOWER IS BETTER)	[hp]	THRUST OUTPUT [g] (HIGHER IS BETTER)	[N]	[lb]	RPM [rev/min] (HIGHER IS BETTER)	EFFICIENCY [g/W] (HIGHER IS BETTER)	[lb/hp]		
KDE2814XF-515 (515KV) KDEXF-UAS35 S.R. ENABLED	15.4V (4S) 17.4V MAX	12.5" x 4.3 KDE-CF125-DP DUAL-BLADE	25.0%	0.5	7	0.01	120	1.18	0.26	2400	17.14	28.18		
			37.5%	1.1	16	0.02	130	2.26	0.51	3400	14.38	23.63		
			50.0%	2.0	30	0.04	170	3.63	0.82	4440	12.33	20.28		
			62.5%	3.2	49	0.07	550	5.39	1.21	5480	11.22	18.45		
			75.0%	5.0	77	0.10	750	7.35	1.65	6300	9.74	16.01		
			87.5%	7.1	109	0.15	980	9.61	2.16	7200	8.99	14.78		
			100.0%	9.5	146	0.20	1230	12.06	2.71	8040	8.42	13.85		
		12.5" x 4.3 KDE-CF125-TP TRIPLE-BLADE	25.0%	0.6	9	0.01	150	1.47	0.33	2380	16.67	27.40		
			37.5%	1.3	20	0.03	280	2.75	0.62	3400	14.00	23.02		
			50.0%	2.5	38	0.05	440	4.31	0.97	4280	11.58	19.04		
			62.5%	4.1	63	0.08	650	6.37	1.43	5200	10.32	16.96		
			75.0%	6.4	98	0.13	880	8.63	1.94	6040	8.98	14.76		
			87.5%	9.6	147	0.20	1140	11.18	2.51	6980	7.76	12.75		
			100.0%	12.2	187	0.25	1400	13.73	3.09	7600	7.49	12.31		
		15.5" x 5.3 KDE-CF155-DP DUAL-BLADE	25.0%	0.9	13	0.02	260	2.55	0.57	2180	20.00	32.88		
			37.5%	2.3	35	0.05	510	5.00	1.12	3000	14.57	23.96		
			50.0%	4.6	70	0.09	840	8.24	1.85	3780	12.00	19.73		
			62.5%	7.7	118	0.16	1190	11.67	2.62	4440	10.08	16.58		
			75.0%	11.4	175	0.23	1510	14.81	3.33	4980	8.63	14.19		
			87.5%	16.2	249	0.33	1840	18.04	4.06	5520	7.39	12.15		
			100.0%	20.2	311	0.42	2150	21.08	4.74	5880	6.91	11.37		
	23.1V (6S) 26.1V MAX	12.5" x 4.3 KDE-CF125-DP DUAL-BLADE	25.0%	0.9	20	0.03	270	2.65	0.60	3780	13.50	22.19		
			37.5%	1.9	43	0.06	480	4.71	1.06	5040	11.16	18.35		
			50.0%	3.6	83	0.11	760	7.45	1.68	6380	9.16	15.05		
			62.5%	5.8	133	0.18	1080	10.59	2.38	7620	8.12	13.35		
			75.0%	9.0	207	0.28	1460	14.32	3.22	8820	7.05	11.60		
			87.5%	13.1	302	0.40	1890	18.53	4.17	10020	6.26	10.29		
			100.0%	17.2	397	0.53	2360	23.14	5.20	10920	5.94	9.77		
		12.5" x 4.3 KDE-CF125-TP TRIPLE-BLADE	25.0%	1.0	23	0.03	320	3.14	0.71	3520	15.91	22.87		
			37.5%	2.3	53	0.07	570	5.59	1.26	4800	10.75	17.68		
			50.0%	4.2	97	0.13	900	8.83	1.98	6080	9.28	15.25		
			62.5%	7.5	173	0.23	1270	12.45	2.80	7280	7.34	12.07		
<small>Note : performance chart provided under the test conditions listed below. Measurements taken under alternate conditions will affect the final results.</small>														
<small>Location : KDE Direct HQ Dynamometer V2 (Bend, Oregon) Altitude : 3730 ft (1137 m) Pressure : 30.3 inHg (1026 hPa) Temperature : 72 °F (22°C) Humidity : 35% (Relative)</small>														

Figure 7.21.: Performance Testing Data Sheet for KDE2814XF-515

Calculating the efficiency at each test point by dividing thrust on power and choosing the higher one at each propeller with appropriate battery gives most efficient components for this motor and first selection in our data base, repeating this step for all available motors enlarges the data base to contain 30 motor to select .

7. Sizing

For example : the table provided shows one motor -according to higher efficiency- with its components (price,ESC,propeller,battery type)

motor	price	weight	ESC	price	weight	
KDE10218XF-105	815.95	1180.00	KDE-UAS125UVC	348.95	180.00	
KDE10218XF-105	815.95	1180.00	KDE-UAS125UVC	348.95	180.00	
KDE10218XF-105	815.95	1180.00	KDE-UAS125UVC	348.95	180.00	
KDE10218XF-105	815.95	1180.00	KDE-UAS125UVC	348.95	180.00	
KDE10218XF-105	815.95	1180.00	KDE-UAS125UVC	348.95	180.00	
KDE10218XF-105	815.95	1180.00	KDE-UAS125UVC	348.95	180.00	
KDE10218XF-105	815.95	1180.00	KDE-UAS125UVC	348.95	180.00	
KDE10218XF-105	815.95	1180.00	KDE-UAS125UVC	348.95	180.00	
prop	price	weight	battery	throttle range	power i/p	thrust o/p
30.5" X 9.7, DUAL	165	105	6.00	25.00	43.00	740.00
30.5" X 9.7, DUAL	165	105	6.00	37.50	87.00	1380.00
30.5" X 9.7, DUAL	165	105	6.00	50.00	147.00	2140.00
30.5" X 9.7, DUAL	165	105	6.00	62.50	233.00	3070.00
30.5" X 9.7, DUAL	165	105	6.00	75.00	351.00	4180.00
30.5" X 9.7, DUAL	165	105	6.00	87.50	485.00	5330.00
30.5" X 9.7, DUAL	165	105	6.00	100.00	600.00	6490.00

Table 7.2.: one of 30 motor in data base

Also the data base contains a variety of batteries capacity to combine with motors which gives the longest endurance.

battery	discharge	capacity	Voltage	BattPower	BattDischargePower
20000 / 14.8V / 4Cell/10C	10.00	20.00	14.80	296.00	2960.00
16000 / 14.8V / 4Cell/10C	10.00	16.00	14.80	236.80	2368.00
10000 / 14.8V / 4Cell/10C	10.00	10.00	14.80	148.00	1480.00
8000 / 14.8V / 4Cell/10C	10.00	8.00	14.80	118.40	1184.00
8400 / 11.1V/ 3 Cell/30C	30.00	8.40	11.10	93.24	2797.20
20000 / 22.2V / 6Cell/10C	10.00	20.00	22.20	444.00	4440.00

Table 7.3.: battery data collection

After collecting this data , we made a matlab-code to search for the optimum motor and battery that satisfies the payload and endurance required according to the following algorithm.

7. Sizing

7.4.2. Algorithm

7.4.2.1. Requirements

- According to multi rotor data provided previously to get pay load more than 1500 grams octa-copter is appropriate for this task
- Minimum take off weight = 7500 grams (including payload & batteries)
- Minimum Endurance (flight time) for the applied mission is 15 minutes

7.4.2.2. Motor selection

The criteria used in this part is checking that max of thrust of each motor (at 100% of throttle range) does not exceed thrust in each motor(Total take off weight*2/8) .If it exceeds the limit, the motor is not qualified for selection the other qualified one a polynomial fitting curve for Power and Thrust is made for further process.

Then we substitute in the curve fitting equation with required motor thrust (take off weight /8) multiplied by fraction 1.2 as there is losses in every motor thrust due to aerodynamics and frame design.

7.4.2.3. Battery selection

Choosing the battery is not hard at all as we first check battery discharge power whether it is sufficient for the power resulted from curve fitting or not (power resulted *8) then sorting every motor with its compatible battery cells.

After that we calculate the $ResultedEndurance = BatteryCapacity * 60 / (PowerResulted * 8)$ and check also the resulted endurance is enough for required flight time or not ,if not we multiply the number of batteries until it is be bigger than the required endurance.

7.4.2.4. Weight check

Calculating the base weight (take off weight without payload) which consists of the following parts:

- (Motor weight +ESC weight + propeller weight) * Number of motors
- Battery weight * Number of batteries
- Components weight (wires, electronic devices, sensors) = 400 grams
- Frame weight according to the following equation from practical experiment

$$FrameWeight = (22738/425) * PropellerDiameter - 88.801765;$$

Then we subtract the base weight calculated from the take off weight to get the pay load and if it is not satisfied, we change the endurance a bit or the total take off weight and iterate again with the algorithm.

7. Sizing

7.4.2.5. Flow chart

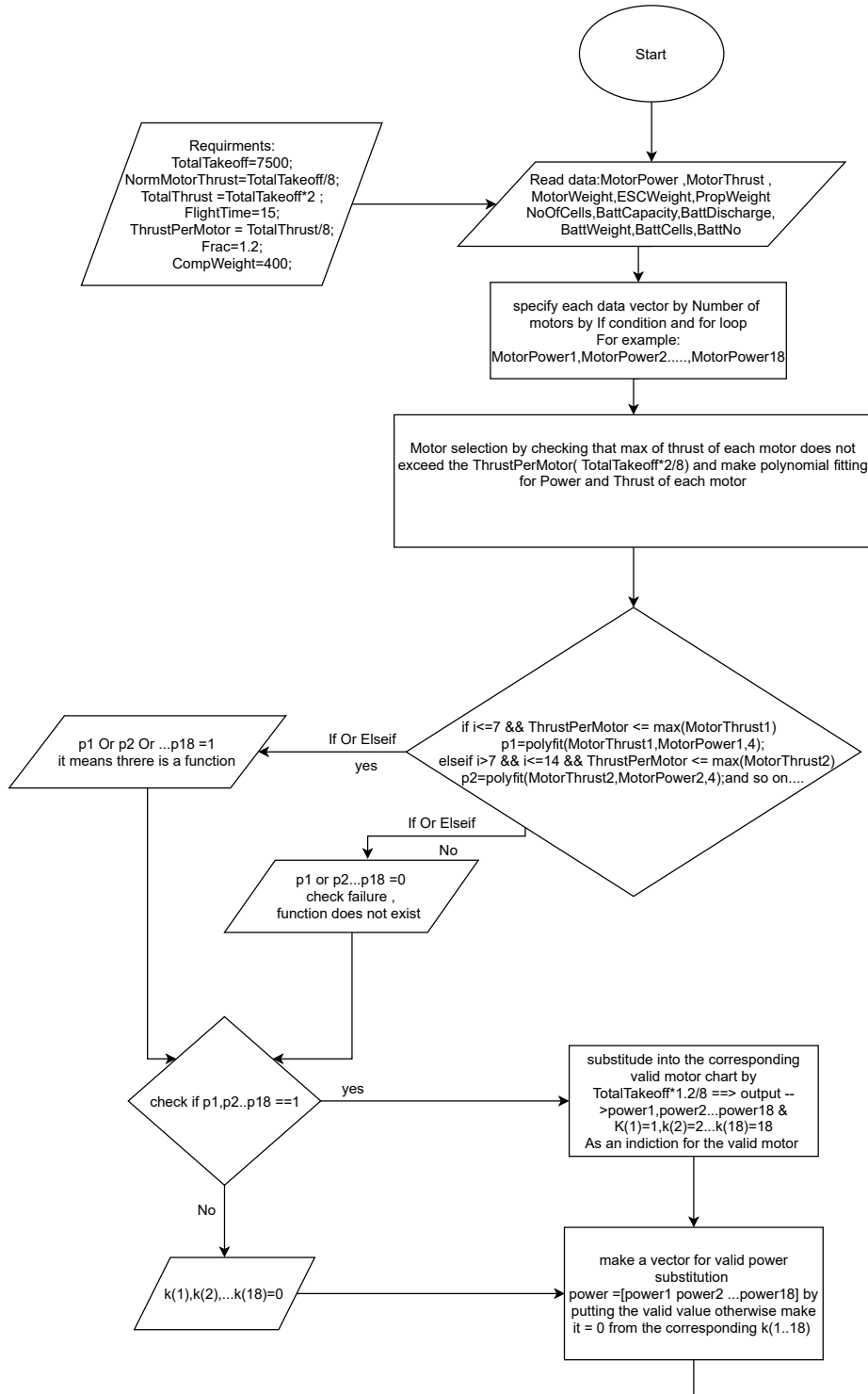


Figure 7.22.: flow chart part 1

7. Sizing

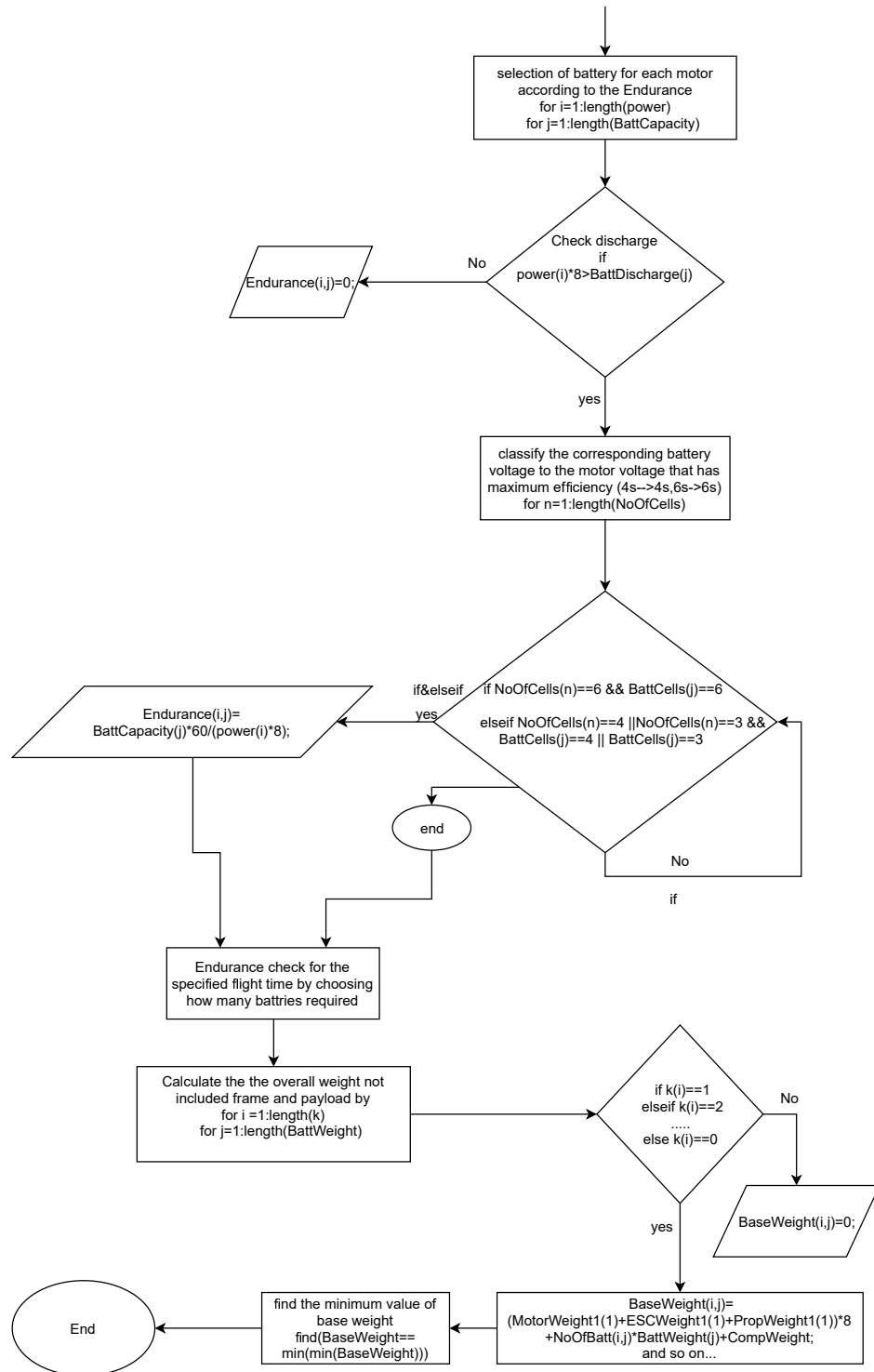


Figure 7.23.: flow chart part 2

7. Sizing

7.5. Sizing Algorithm

1. Collect data of all available motors according to their max efficiency
2. Specify your required total Take off Weight & Flight time
3. Specify your number of motors
4. Get required thrust per motor = $2 * \text{total take off weight} / \text{number of motors}$
5. Motor selection by checking that max of thrust of each motor does not exceed the thrust per motor and make polynomial fitting for power and thrust of each motor
6. Check thrust per motor \leq max thrust of that motor
 - a) if yes then take that motor
 - b) if no then ignore that motor
7. Substitute into the corresponding valid motor chart by total thrust per motor = $1.2 * \text{total take off weight} / \text{number of motors}$
8. Get power at that thrust
9. Select a battery for each motor according to your required endurance & motor voltage
10. Check discharge for each battery, $\text{power} * \text{number of motors} > \text{battery power}$
11. Get endurance = $\text{battery capacity} * 60 / \text{Power when} / 8$
12. Assume no of batteries is 1 to 8
13. Get the least number of batteries to satisfy your required endurance
14. Get weight of selected motors & ESC &batteries
15. Choose the motors , ESC's and Batteries min base weight with the max endurance

Results:

7. Sizing

Total take off weight =4000 kg FlightTime=15 min	Minimum base Weight = 2756.7088 grams Payload = 1243.2912 grams Selected motor = KDE2315XF-885 Selected ESC = KDEXF-UAS35 Selected prop = 9" X 3.0 Selected Battery is 10000 / 14.8V / 4Cell/10C Selected Battery No of cells = 4S NO of batteries = 1 NewEndurance = 15.0629min
Total take off weight =4000 kg FlightTime=20 min	Minimum base Weight = 3238.7088 grams Payload = 761.2912 grams Selected motor = KDE2315XF-885 Selected ESC = KDEXF-UAS35 Selected prop = 9" X 3.0 Selected Battery is 8000 / 14.8V / 4Cell/10C Selected Battery No of cells = 4S NO of batteries = 2 NewEndurance = 24.1006min
Total take off weight =5000 kg FlightTime=20 min	Minimum base Weight = 3268.21 grams Payload = 1731.79 grams Selected motor = KDE2315XF-965 Selected ESC = KDEXF-UAS35 Selected prop = 10" X3.3 Selected Battery is 8000 / 14.8V / 4Cell/10C Selected Battery No of cells = 4S NO of batteries = 2 NewEndurance = 20.4799min
Total take off weight =7500 kg FlightTime=15 min	Minimum base Weight = 4017.5112 grams Payload = 3482.4888 grams Selected motor = KDE2315XF-965 Selected ESC = KDEXF-UAS35 Selected prop = 11" X3.7 Selected Battery is 8000 / 14.8V / 4Cell/10C Selected Battery No of cells = 4S NO of batteries = 3 NewEndurance = 15.8992 min

Table 7.4.: Sizing's results

8. Control and Simulation

8.1. Open loop test

8.1.1. Rig configuration

Iteration 1

We used a bar and inserted it through the quad to measure the open loop response but it only offered one degree of freedom at a time.

if there was any coupling between states we wouldn't be able to measure it.

Iteration 2

We connected four robes to the quad and four people should hold their ends then we apply input and the four people must free some of the robes and we begin to record the response.

this method had much work and it needed a large place to do it.

Iteration 3

We settled on using the test jig to provide three degrees of freedom with the lowest possible resistance.



Figure 8.1.: 3DOF Test Jig

system' inputs

Excite the system with appropriate input so as for not damaging the vehicle and also to get the actual response is difficult to define in the first time without making mistakes, so after a couple of practical experiments on the vehicle and solving the facing problems, a step input with 10 seconds period was enough to get response to study.

8. Control and Simulation

Enter the input to the system is also a problem as it must wait 10 seconds before and after the start of step input to make the quad copter in hovering position without any oscillations which can disturb the required response.

To make the step input in the quad copter according to roll, pitch and yaw which we want to get their responses, a specified quantity of change in the motor thrust must be added or subtracted from each motor for example to make input for pitch or roll the change is added to one motor and subtracted from the opposite one and for yaw' input the change is added for two motors facing each other and subtracted from the other ones.

Also, for the non linearity of the system the test is made for different nominal thrust and positive & negative inputs are used too.

8.1.2. Actual System Response in case of Δ_{Roll}

Roll' input Delta thrust = 10, Nominal thrust = 1650

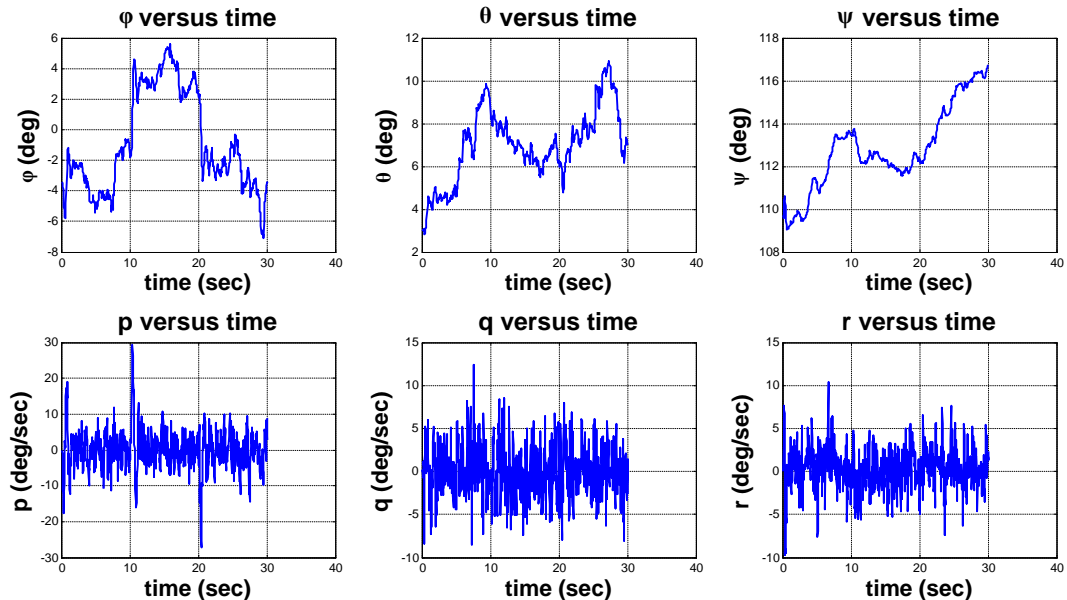


Figure 8.2.: Nominal thrust = 1650 , $\Delta_{Roll} = 10$

8. Control and Simulation

Roll' input Delta thrust = 10, Nominal thrust = 1700

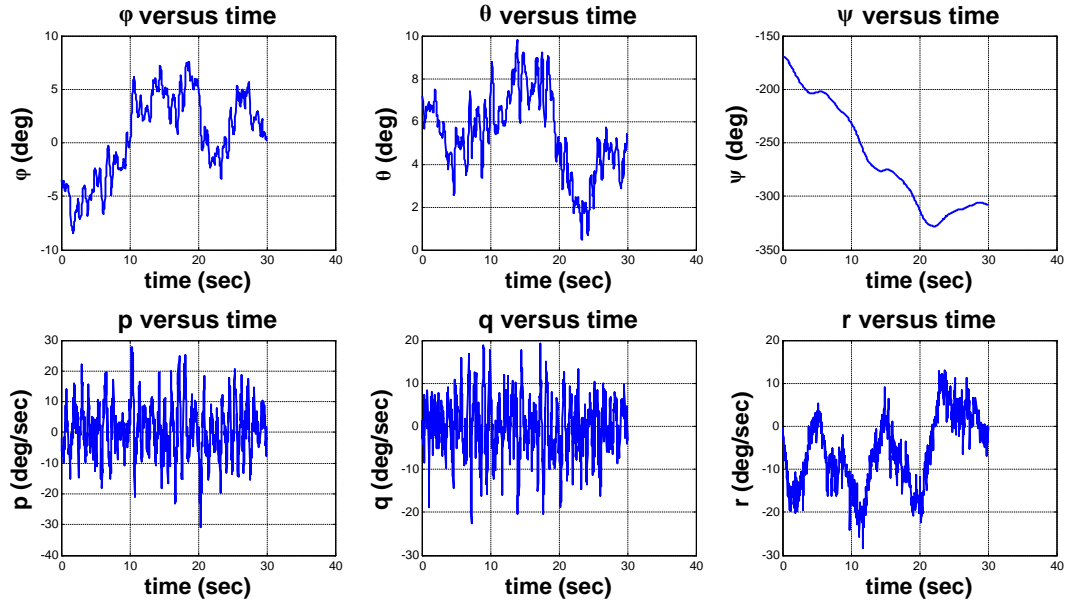


Figure 8.3.: Nominal thrust = 1700 , $\Delta_{Roll} = 10$

Roll' input Delta thrust = -10, Nominal thrust = 1650

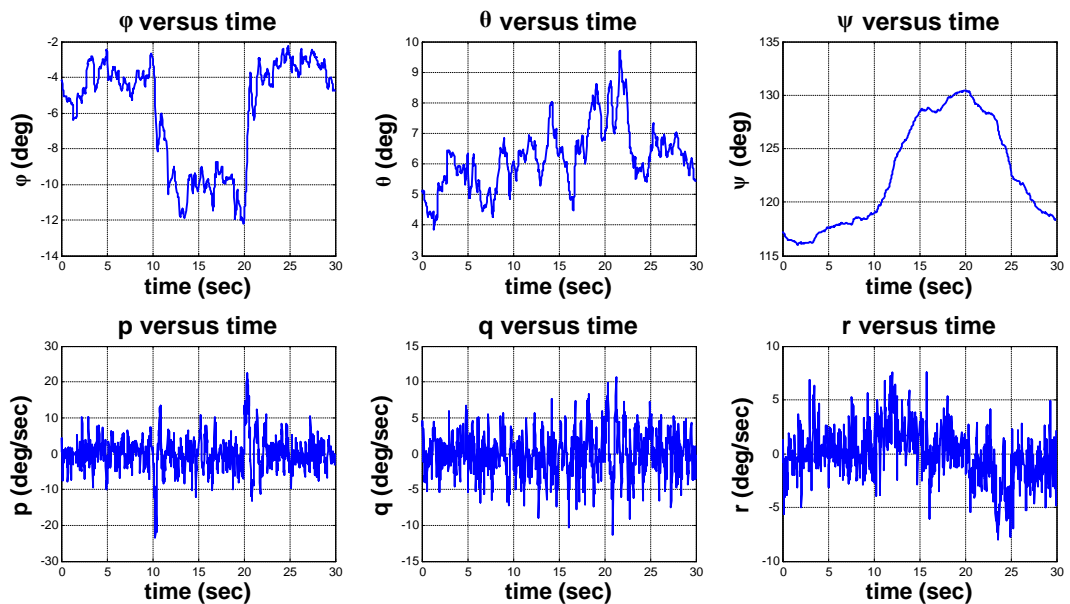


Figure 8.4.: Nominal thrust = 1650 , $\Delta_{Roll} = -10$

8. Control and Simulation

Roll' input Delta thrust = -10, Nominal thrust = 1700

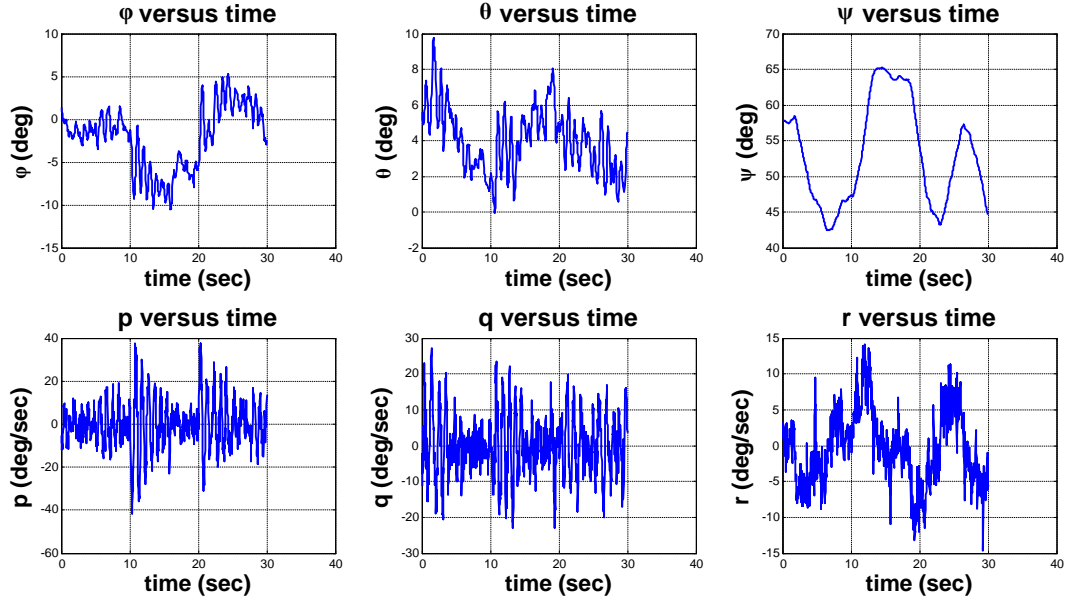


Figure 8.5.: Nominal thrust = 1700 , $\Delta_{Roll} = -10$

Roll' input Delta thrust = 20, Nominal thrust = 1650

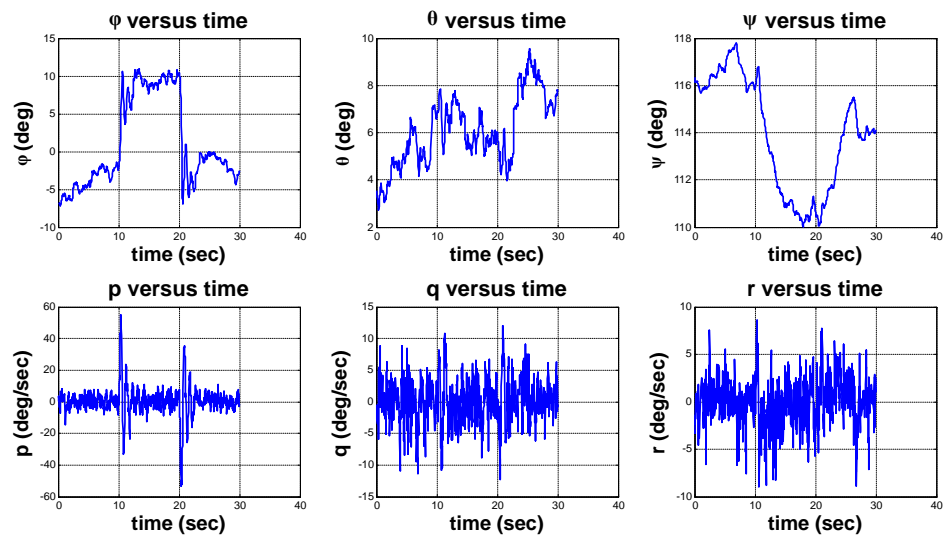


Figure 8.6.: Nominal thrust = 1650 , $\Delta_{Roll} = 20$

8. Control and Simulation

Roll' input Delta thrust = 20, Nominal thrust = 1700

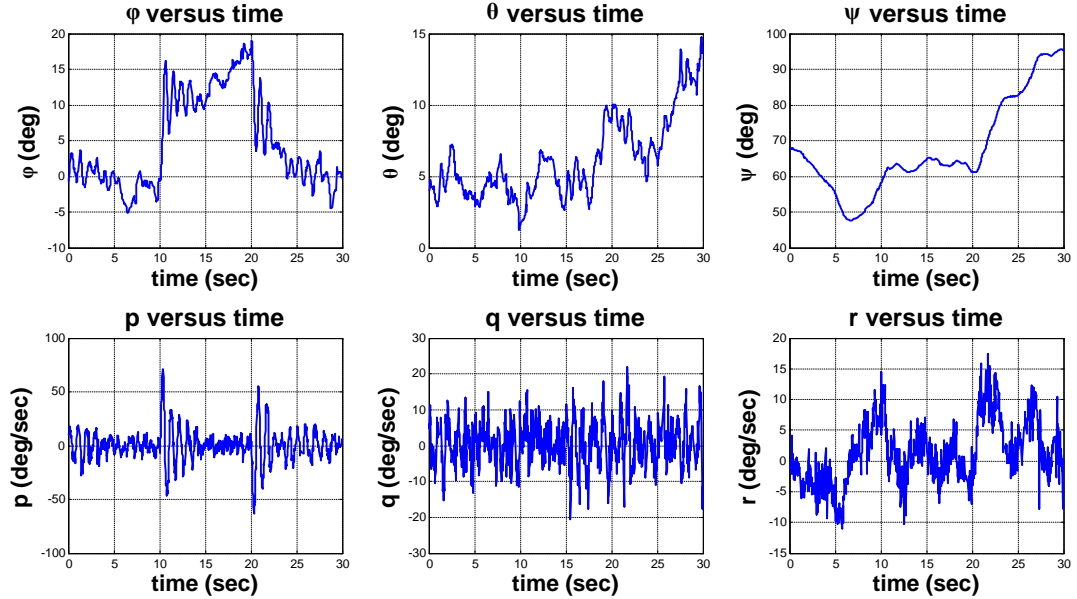


Figure 8.7.: Nominal thrust = 1700 , $\Delta_{Roll} = 20$

Roll' input Delta thrust = -20, Nominal thrust = 1650

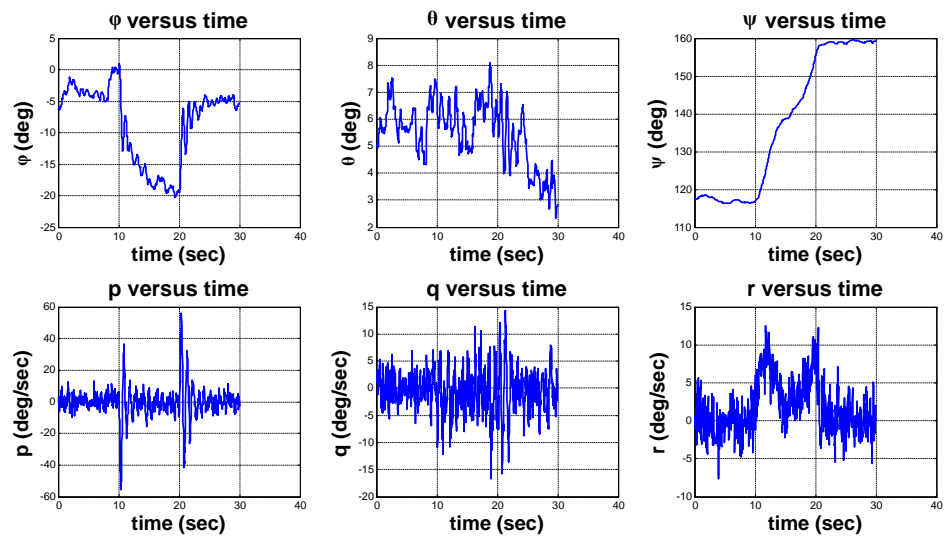


Figure 8.8.: Nominal thrust = 1650 , $\Delta_{Roll} = -20$

8. Control and Simulation

Roll' input Delta thrust = -20, Nominal thrust = 1700

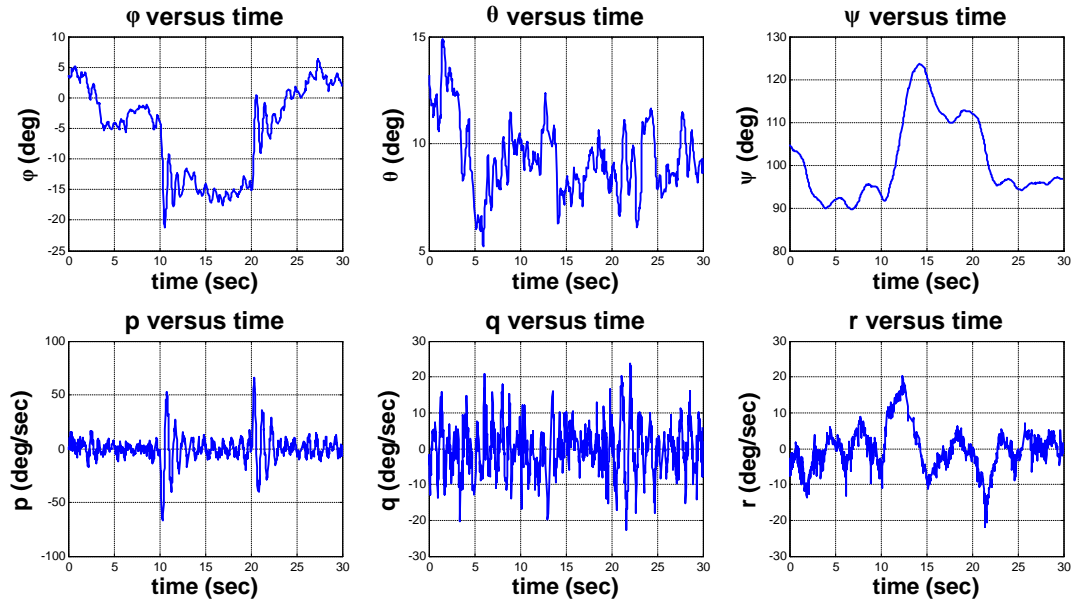


Figure 8.9.: Nominal thrust = 1700 , $\Delta_{Roll} = -20$

8. Control and Simulation

Roll' input Delta thrust = 30, Nominal thrust = 1650

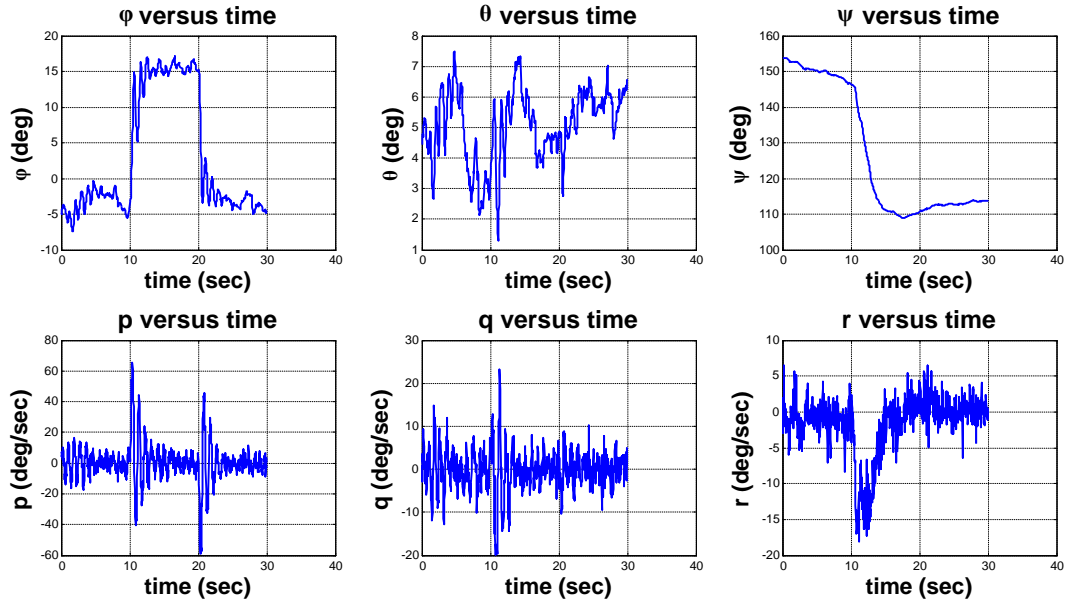


Figure 8.10.: Nominal thrust = 1650 , $\triangle_{Roll} = 30$

Roll' input Delta thrust = 30, Nominal thrust = 1700

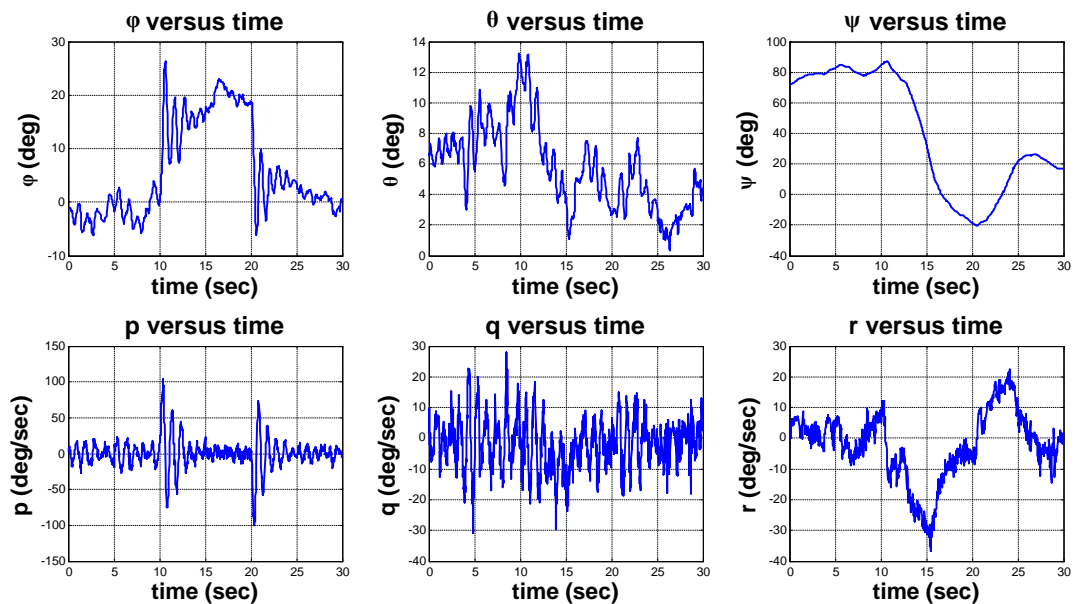


Figure 8.11.: Nominal thrust = 1700 , $\triangle_{Roll} = 30$

8. Control and Simulation

Roll' input Delta thrust = -30, Nominal thrust = 1650

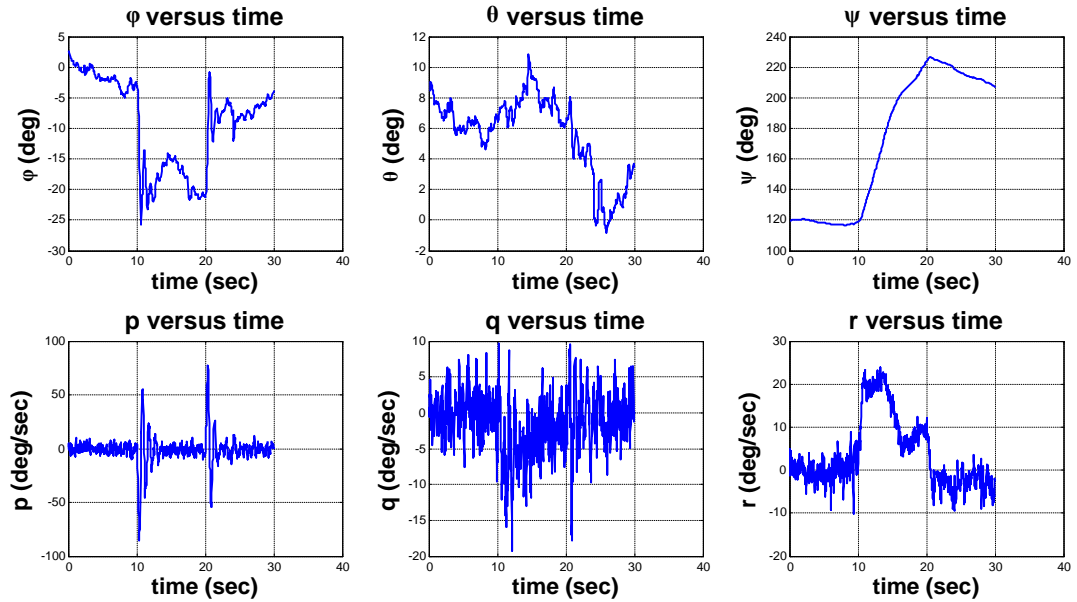


Figure 8.12.: Nominal thrust = 1650 , $\triangle_{Roll} = -30$

8. Control and Simulation

Roll' input Delta thrust = -30, Nominal thrust = 1700

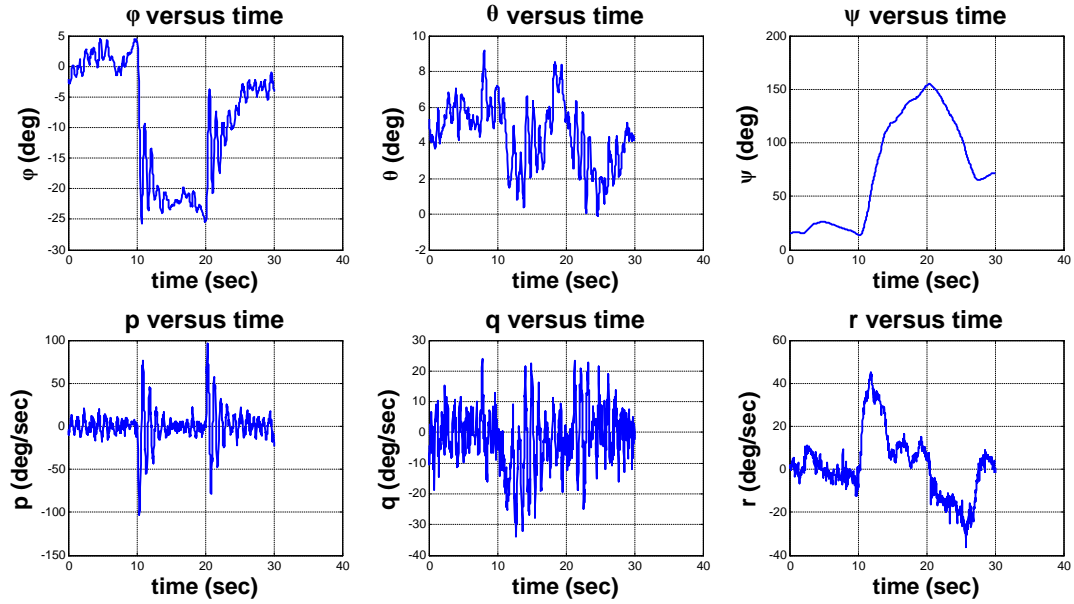


Figure 8.13.: Nominal thrust = 1700 , $\Delta_{Roll} = -30$

Equivalent response in Laplace domain

The step input has two sides which one goes up and the other goes down so the extracted data for this process uses only going up step side not for a specific reason but to display it in a convenient way, so when the time begins from 10 second to 20 seconds it means it is positive step in the other side when the time begins from 20 second to 30 seconds it means it is negative step.

The criteria used to get the response is to get both peak time and settling time of any test for the angle or the rate angle graphically by hand and fin tune to make all test' responses look the same.

Also, every test in positive step has its on dc gain value whatever the angle or the rate angle.

Whatever the angle response or the rate angle you study you can get the other by putting (s) in transfer function at the nominator for convert from angle to rate angle and the opposite state is correct.

Another problem faced is the initial condition of the angle response when transferring to Laplace domain, do we need to add it or not, there are the two conditions in the next graphs.

8. Control and Simulation

Positive step response for roll rate

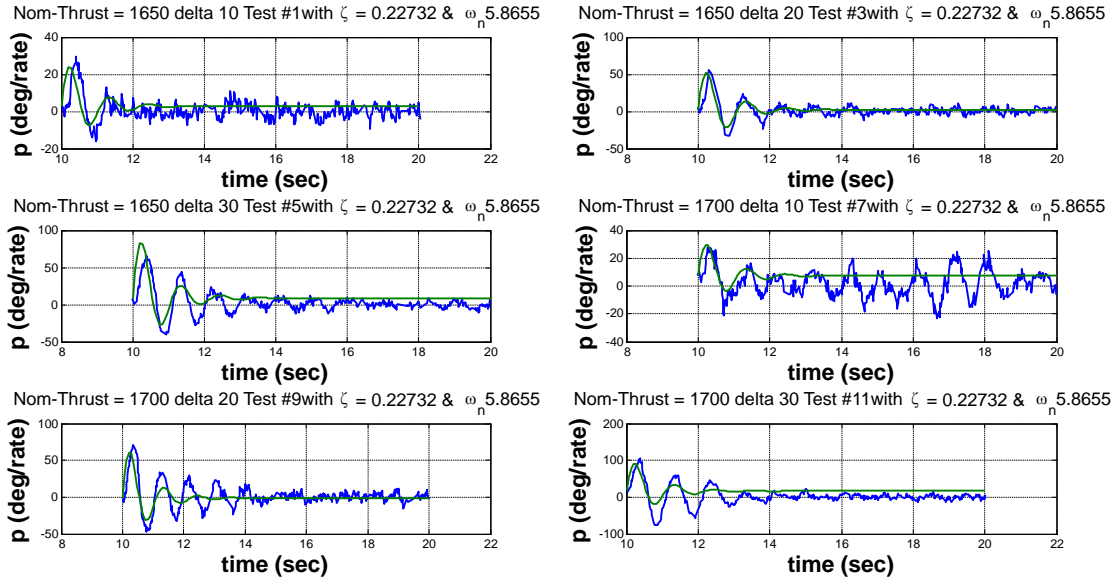


Figure 8.14.: Positive step response for roll rate

Negative step response for roll rate

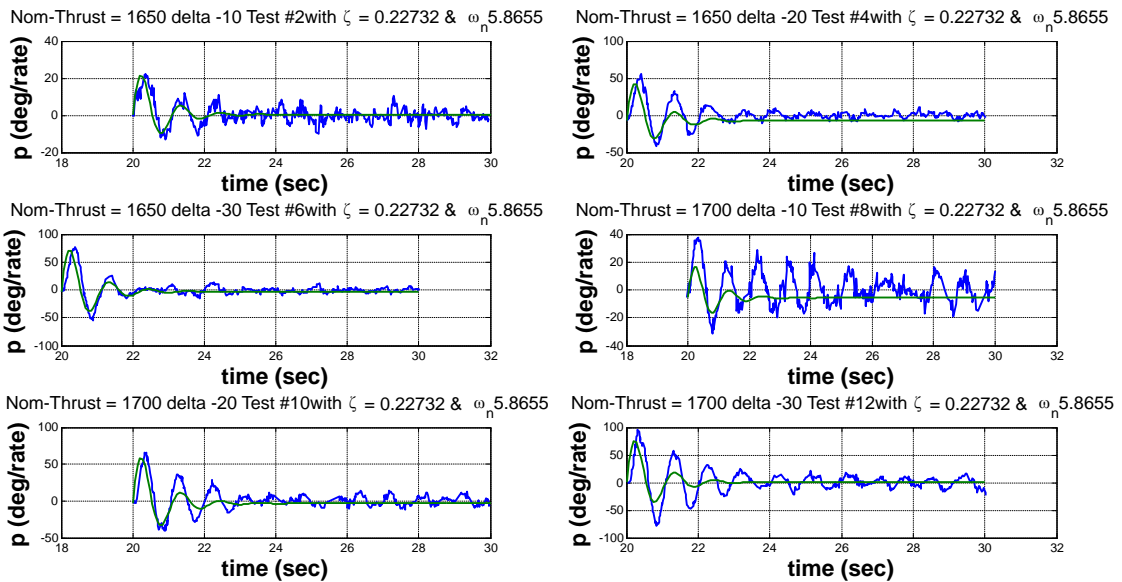


Figure 8.15.: Negative step response for roll rate

8. Control and Simulation

Positive step response for roll angle

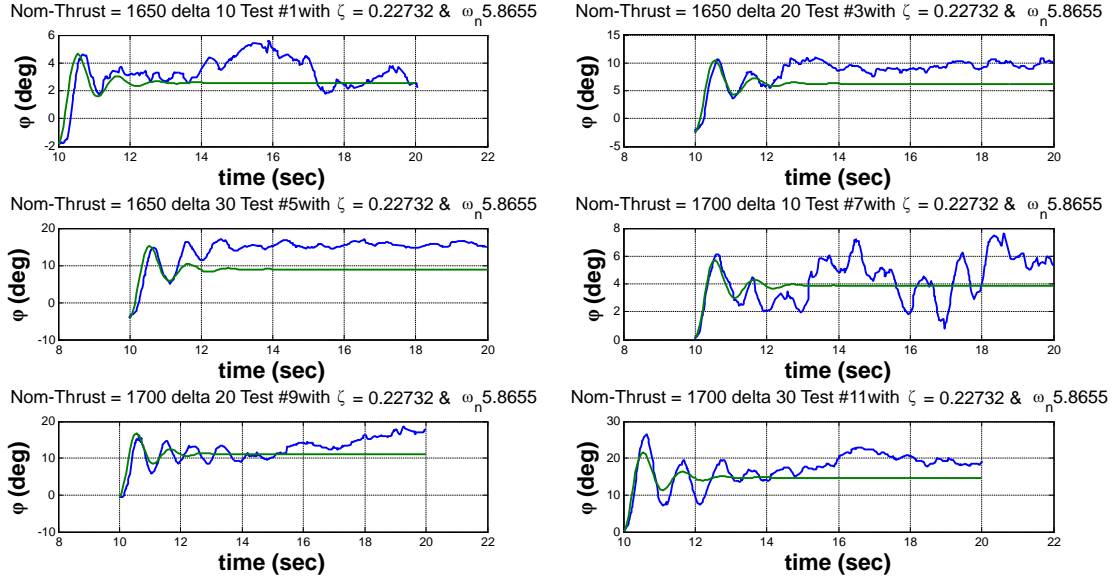


Figure 8.16.: Positive step response for roll angle

8. Control and Simulation

Negative step response for roll angle

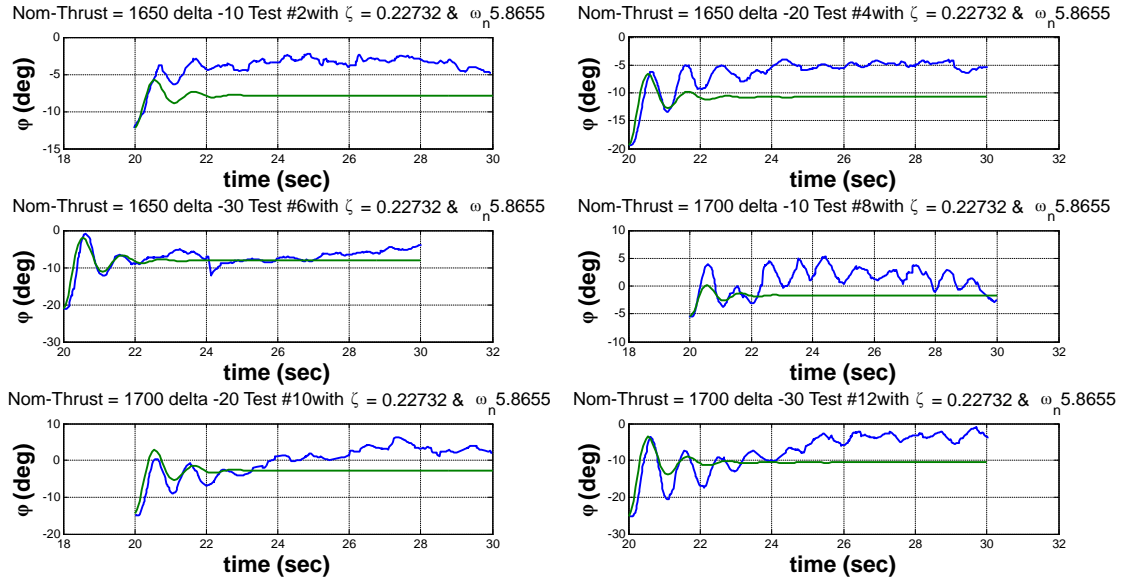


Figure 8.17.: Negative step response for roll angle

Equivalent transfer function for every test for roll rate

$$T_{peak} = 0.55 \text{ sec} \quad T_{settling} = 3 \text{ sec}$$

	Nominal thrust = 1650	Nominal thrust = 1700
Delta thrust = 10	170 s ----- $s^2 + 2.667 s + 34.4$	180 s ----- $s^2 + 2.667 s + 34.4$
Delta thrust = 20	400 s ----- $s^2 + 2.667 s + 34.4$	500 s ----- $s^2 + 2.667 s + 34.4$
Delta thrust = 30	600 s ----- $s^2 + 2.667 s + 34.4$	600 s ----- $s^2 + 2.667 s + 34.4$

Table 8.1.: Equivalent transfer function for every test for roll rate

Note: Positive & negative step angle has the same transfer function.

8. Control and Simulation

Equivalent transfer function for every test for roll angle

$$T_{peak} = 0.55 \text{ sec} \quad T_{settling} = 3 \text{ sec}$$

	Nominal thrust = 1650	Nominal thrust = 1700
Delta thrust = 10	150 ----- $s^2 + 2.667 s + 34.4$	130 ----- $s^2 + 2.667 s + 34.4$
Delta thrust = 20	300 ----- $s^2 + 2.667 s + 34.4$	400 ----- $s^2 + 2.667 s + 34.4$
Delta thrust = 30	450 ----- $s^2 + 2.667 s + 34.4$	500 ----- $s^2 + 2.667 s + 34.4$

Table 8.2.: Equivalent transfer function for every test for roll angle

Note: Positive & negative step angle has the same transfer function.

8. Control and Simulation

8.1.3. Actual System Response in case of Δ_{Pitch}

Theta' input Delta thrust = 10, Nominal thrust = 1650

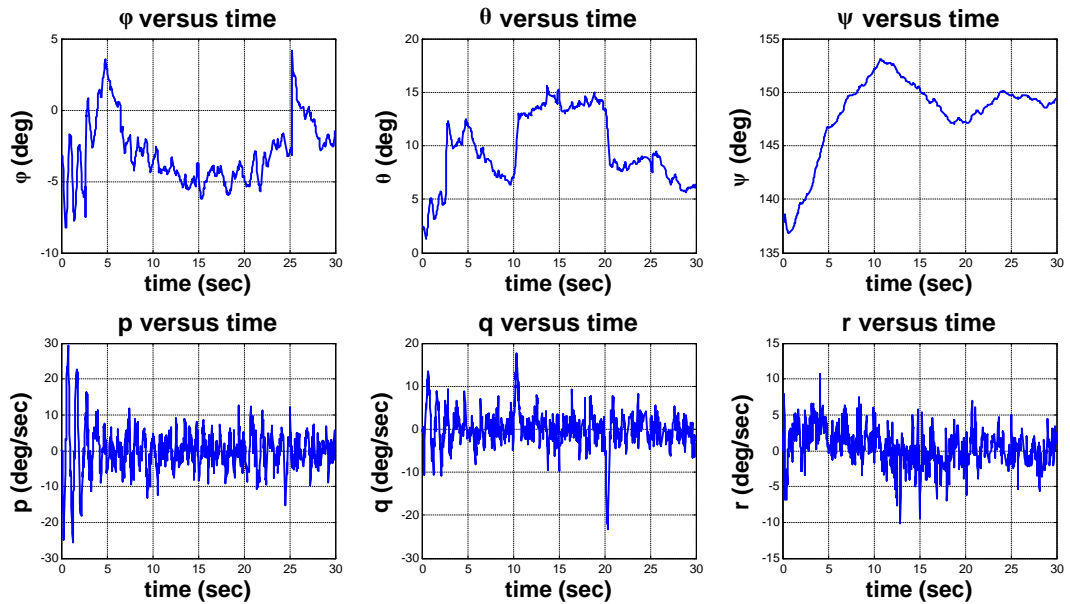


Figure 8.18.: Nominal thrust = 1650 , $\Delta_{Pitch} = 10$

Theta' input Delta thrust = 10, Nominal thrust = 1700

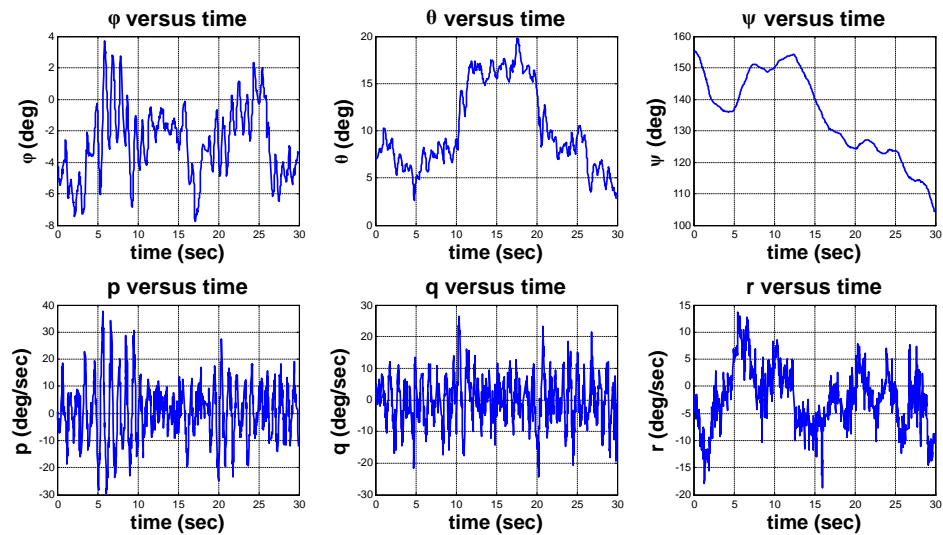


Figure 8.19.: Nominal thrust = 1700 , $\Delta_{Pitch} = 10$

8. Control and Simulation

Theta' input Delta thrust = -10, Nominal thrust = 1650

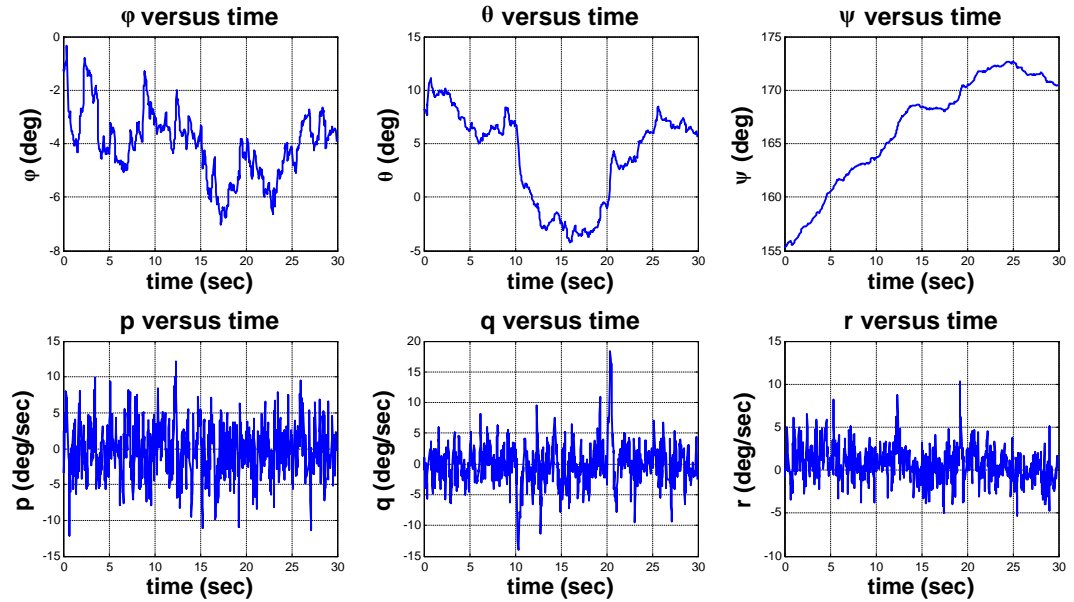


Figure 8.20.: Nominal thrust = 1650 , $\Delta_{Pitch} = -10$

8. Control and Simulation

Theta' input Delta thrust = -10, Nominal thrust = 1700

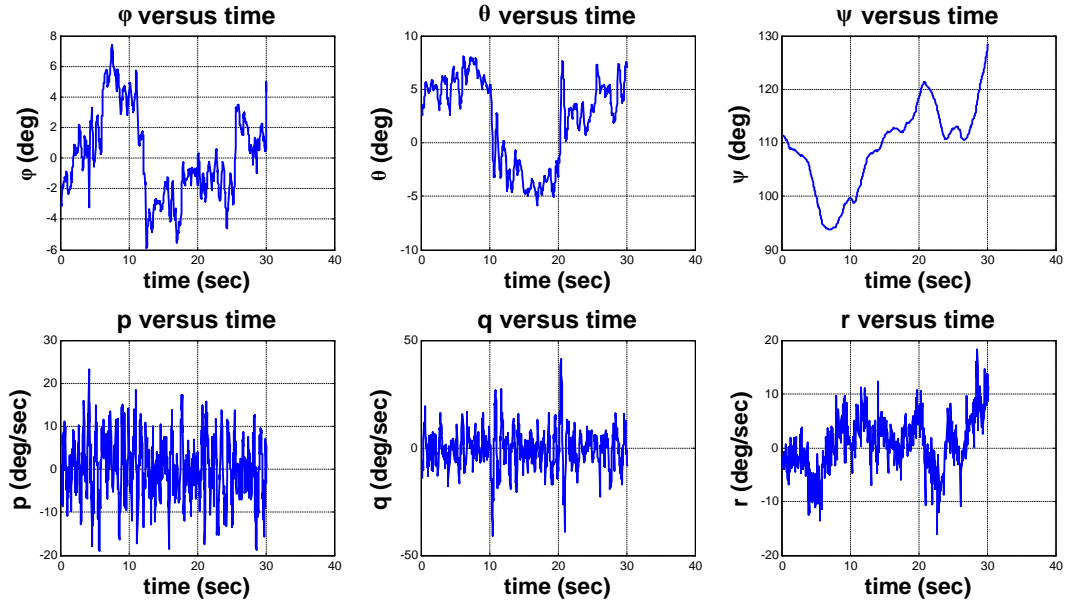


Figure 8.21.: Nominal thrust = 1700 , $\Delta_{Pitch} = -10$

Theta' input Delta thrust = 20, Nominal thrust = 1650

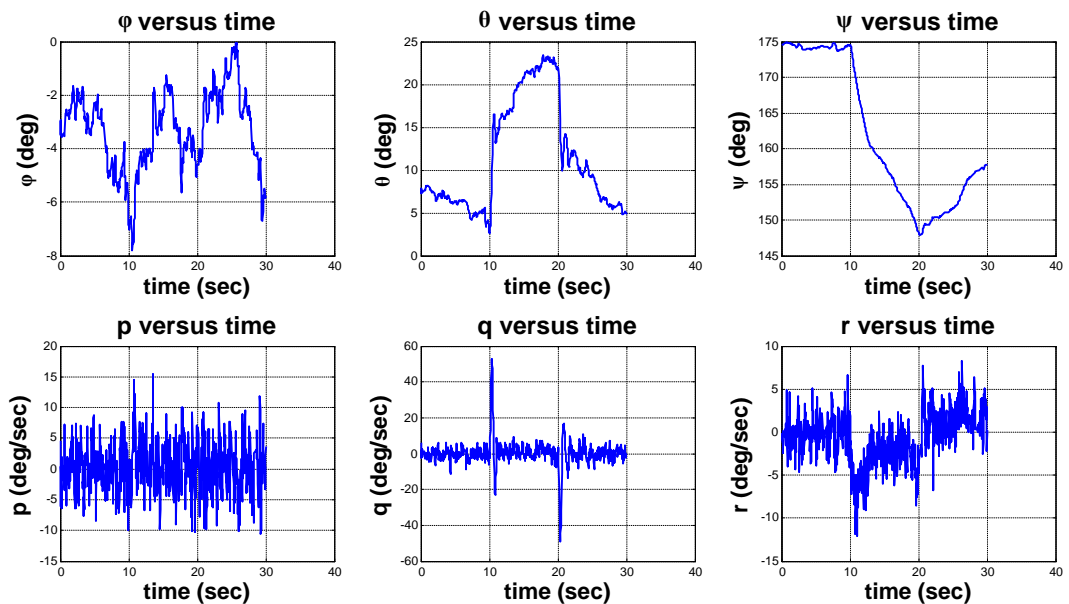


Figure 8.22.: Nominal thrust = 1650 , $\Delta_{Pitch} = 20$

8. Control and Simulation

Theta' input Delta thrust = 20, Nominal thrust = 1700

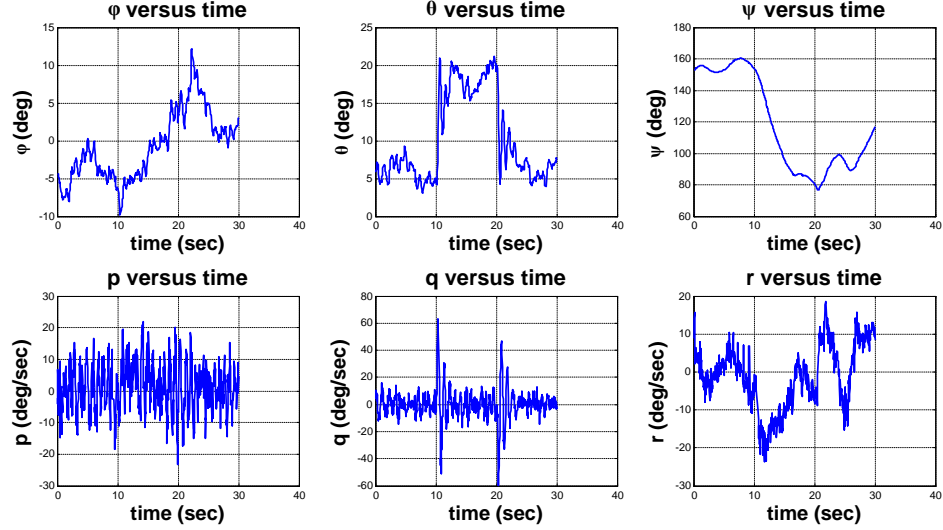


Figure 8.23.: Nominal thrust = 1700 , $\Delta_{Pitch} = 20$

Theta' input Delta thrust = -20, Nominal thrust = 1650

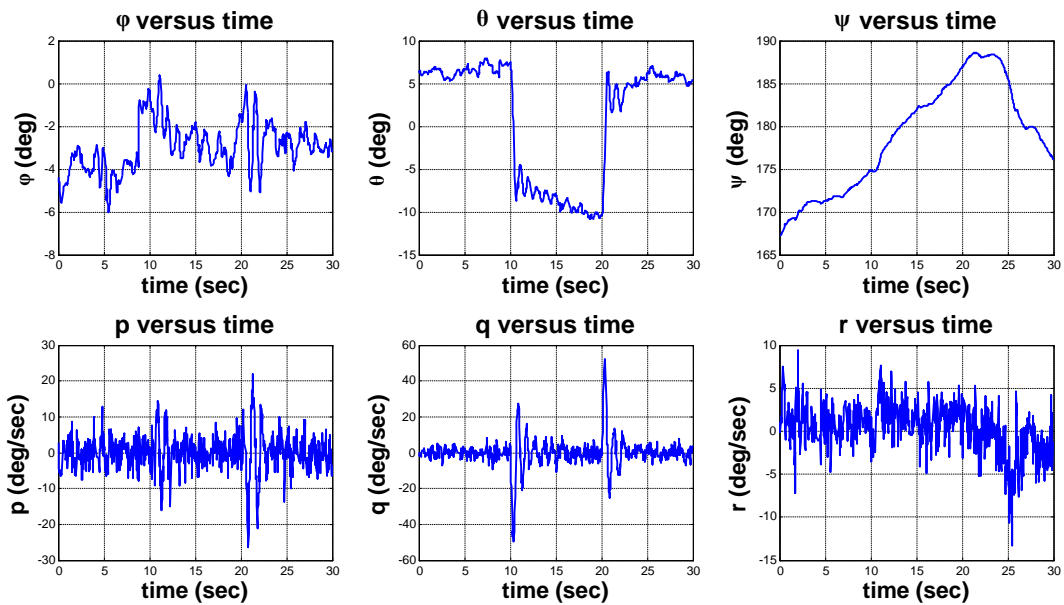


Figure 8.24.: Nominal thrust = 1650 , $\Delta_{Pitch} = -20$

8. Control and Simulation

Theta' input Delta thrust = -20, Nominal thrust = 1700

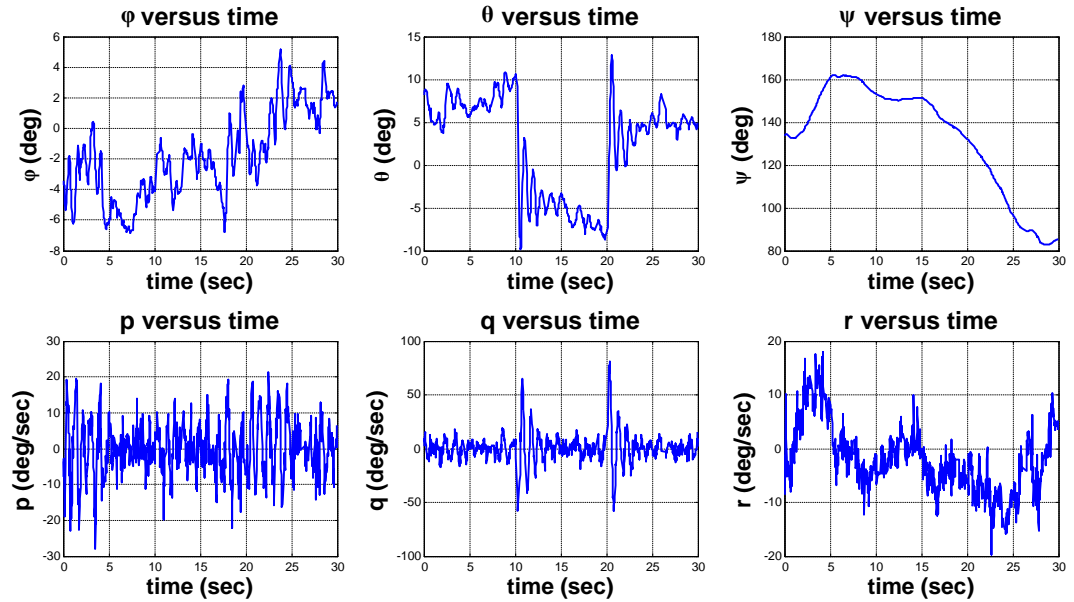


Figure 8.25.: Nominal thrust = 1700 , $\Delta_{Pitch} = -20$

8. Control and Simulation

Theta' input Delta thrust = 30, Nominal thrust = 1650

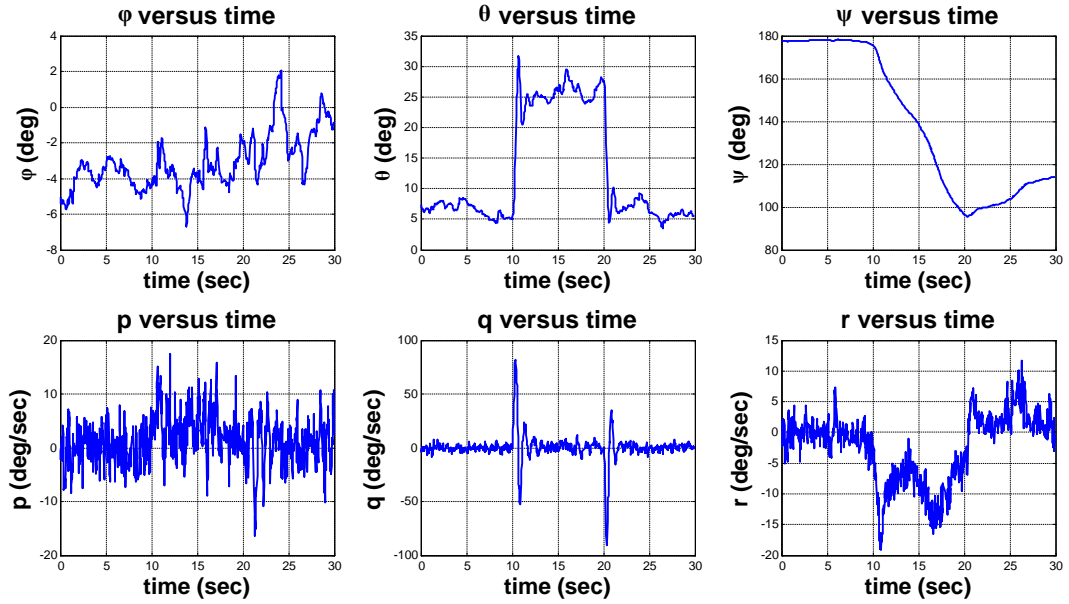


Figure 8.26.: Nominal thrust = 1650 , $\Delta_{Pitch} = 30$

Theta' input Delta thrust = 30, Nominal thrust = 1700

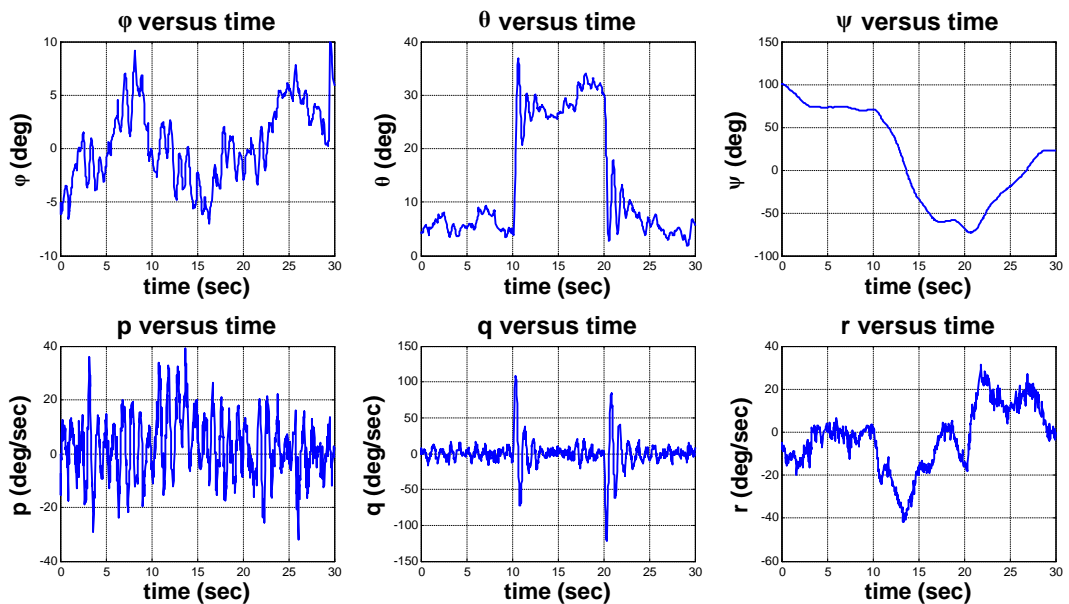


Figure 8.27.: Nominal thrust = 1700 , $\Delta_{Pitch} = 30$

8. Control and Simulation

Theta' input Delta thrust = -30, Nominal thrust = 1650

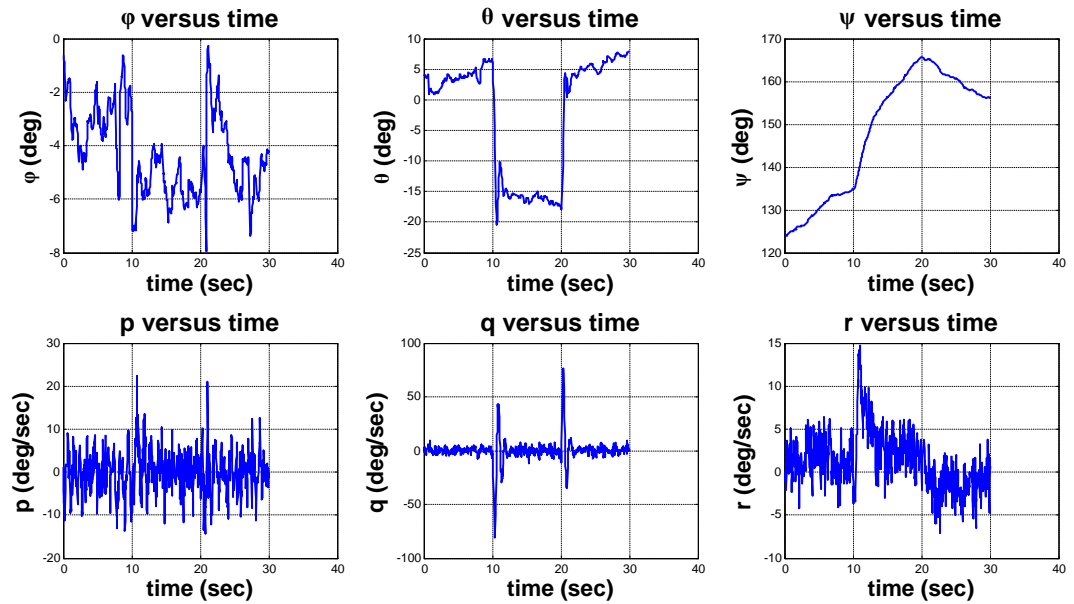


Figure 8.28.: Nominal thrust = 1650 , $\Delta_{Pitch} = -30$

8. Control and Simulation

Theta' input Delta thrust = -30, Nominal thrust = 1700

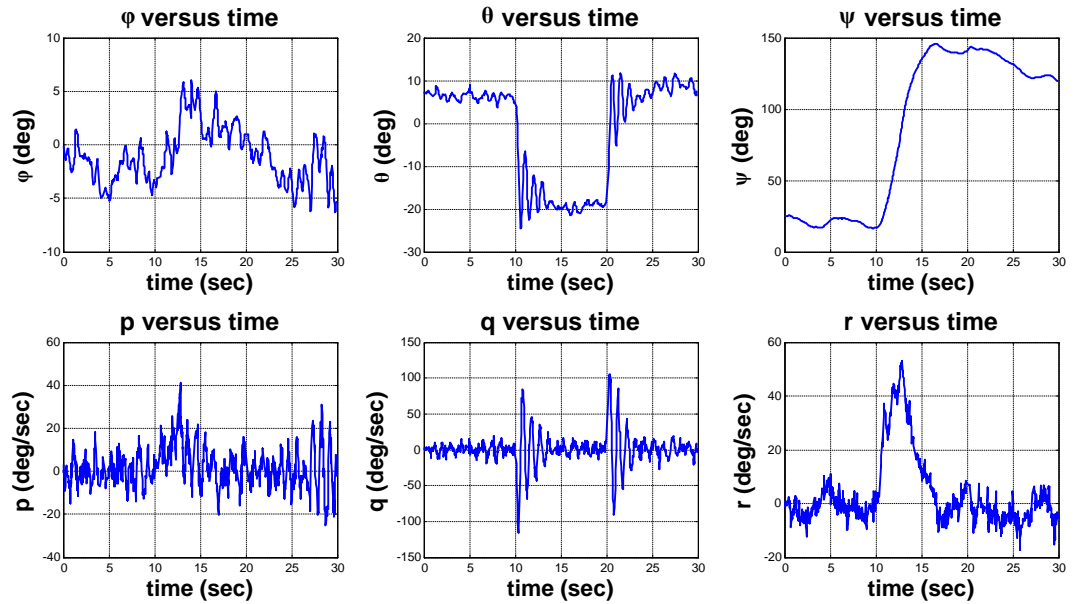


Figure 8.29.: Nominal thrust = 1700 , $\Delta_{Pitch} = -30$

8. Control and Simulation

Equivalent response in Laplace domain

Positive step response for pitch rate

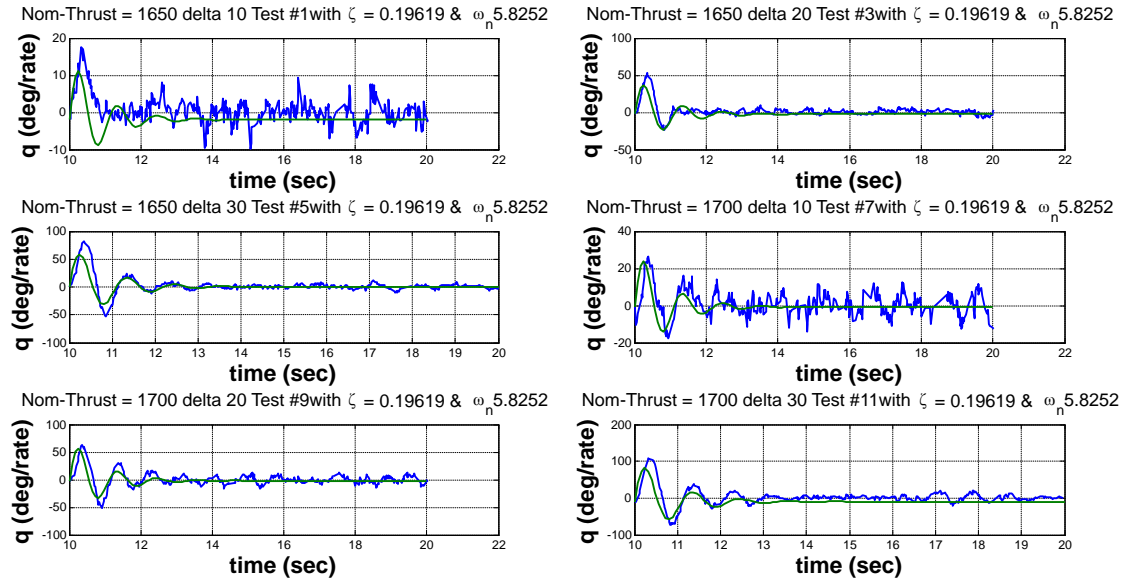


Figure 8.30.: Positive step response for pitch rate

8. Control and Simulation

Negative step response for pitch rate

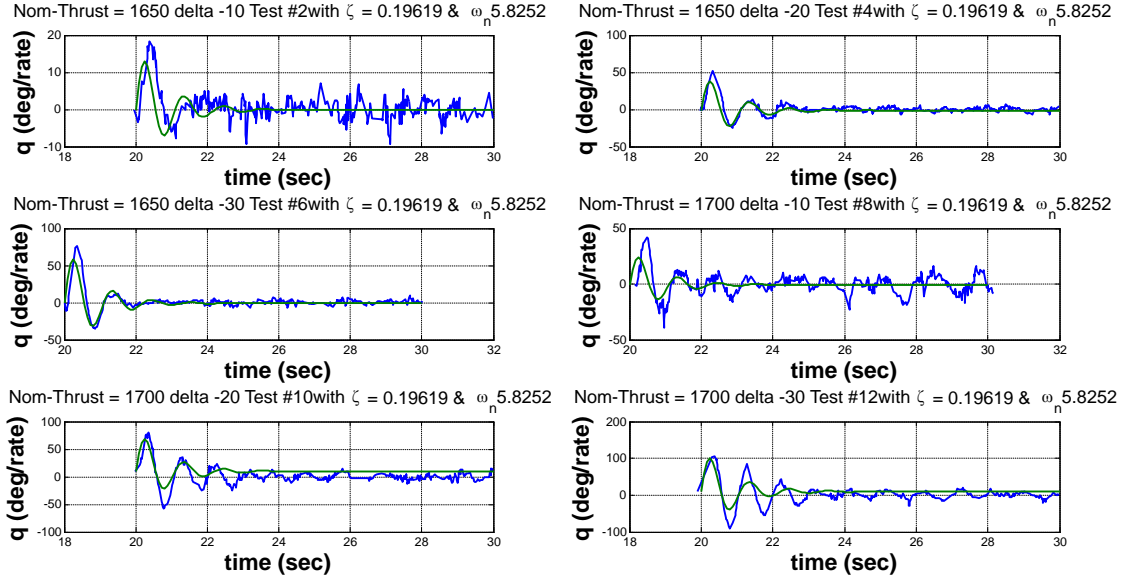


Figure 8.31.: Negative step response for pitch rate

Positive step response for pitch angle

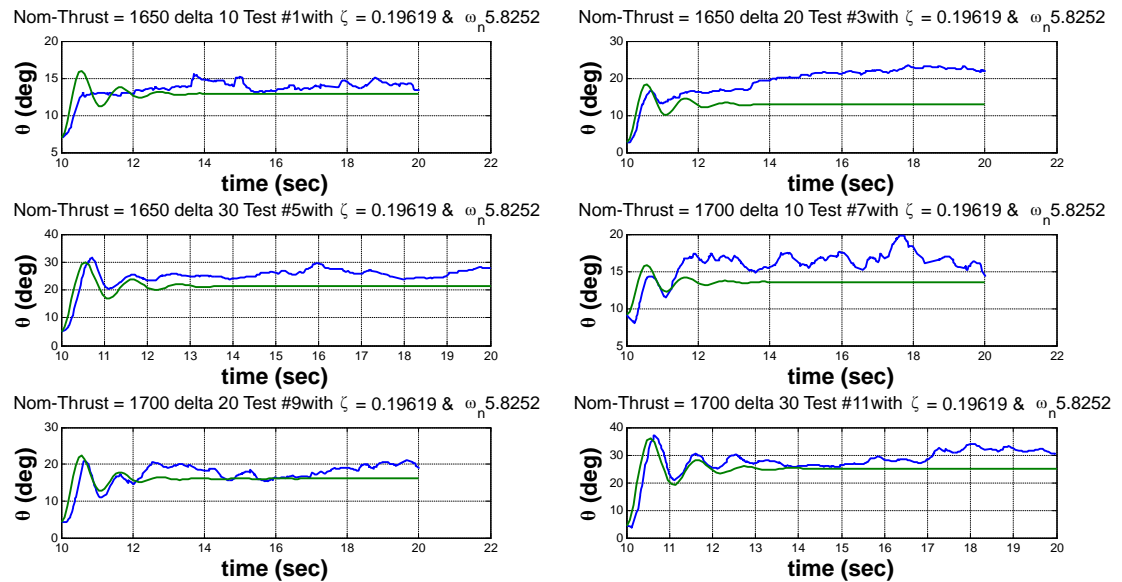


Figure 8.32.: Positive step response for pitch angle

8. Control and Simulation

Negative step response for pitch angle

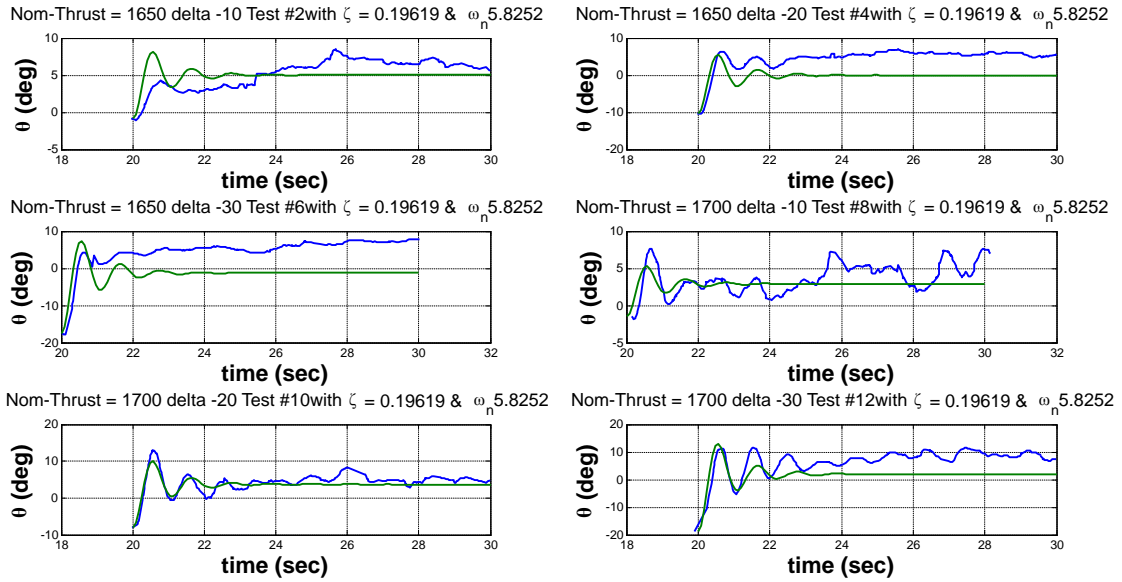


Figure 8.33.: Negative step response for pitch angle

Equivalent transfer function for every test for pitch rate

$T_{peak} = 0.55$ sec	$T_{settling} = 3.5$ sec
-----------------------	--------------------------

	Nominal thrust = 1650	Nominal thrust = 1700
Delta thrust = 10	100 s ----- $s^2 + 2.286 s + 33.93$	190 s ----- $s^2 + 2.286 s + 33.93$
Delta thrust = 20	300 s ----- $s^2 + 2.286 s + 33.93$	450 s ----- $s^2 + 2.286 s + 33.93$
Delta thrust = 30	450 s ----- $s^2 + 2.286 s + 33.93$	700 s ----- $s^2 + 2.286 s + 33.93$

Table 8.3.: Equivalent transfer function for every test for pitch rate

Note: Positive & negative step angle has the same transfer function.

8. Control and Simulation

Equivalent transfer function for every test for pitch angle

$$\boxed{T_{peak} = 0.55 \text{ sec} \quad T_{settling} = 3.5 \text{ sec}}$$

	Nominal thrust = 1650	Nominal thrust = 1700
Delta thrust = 10	200 ----- $s^2 + 2.286 s + 33.93$	150 ----- $s^2 + 2.286 s + 33.93$
Delta thrust = 20	350 ----- $s^2 + 2.286 s + 33.93$	400 ----- $s^2 + 2.286 s + 33.93$
Delta thrust = 30	550 ----- $s^2 + 2.286 s + 33.93$	700 ----- $s^2 + 2.286 s + 33.93$

Table 8.4.: Equivalent transfer function for every test for pitch angle

Note: Positive & negative step angle has the same transfer function.

8. Control and Simulation

8.1.4. Actual System Response in case of ΔY_{aw}

Yaw' input Delta thrust = 10, Nominal thrust = 1650

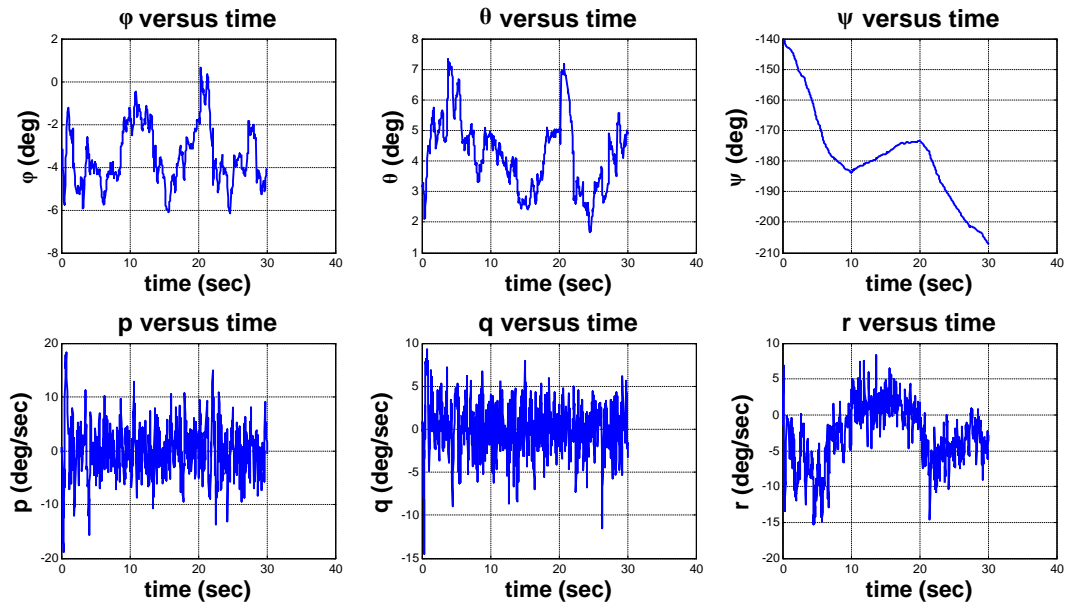


Figure 8.34.: Nominal thrust = 1650 , $\Delta Y_{aw} = 10$

8. Control and Simulation

Yaw' input Delta thrust = 10, Nominal thrust = 1700

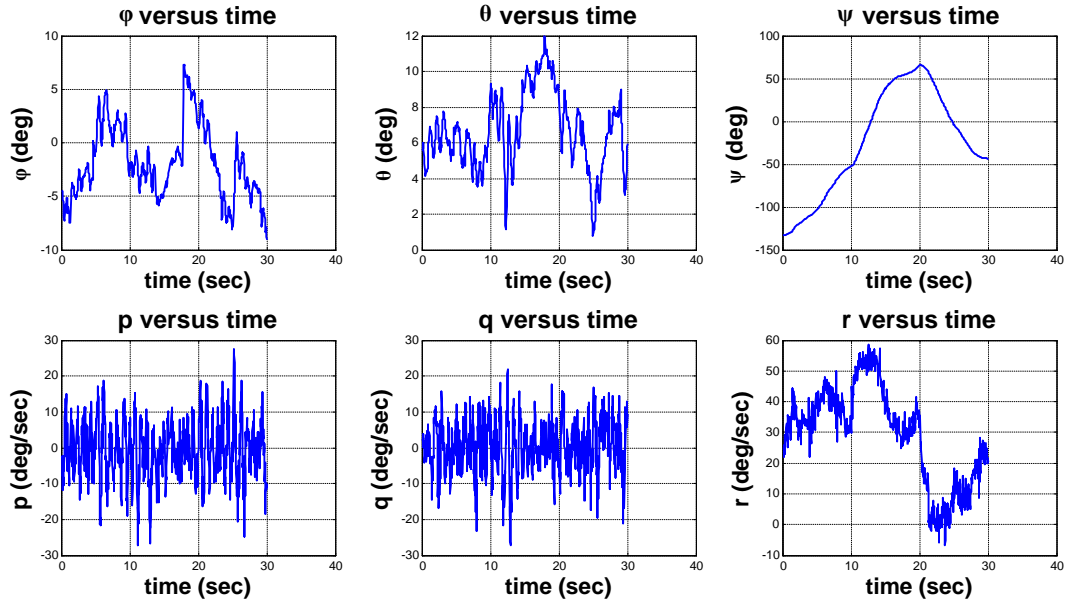


Figure 8.35.: Nominal thrust = 1700 , $\Delta_{Yaw} = 10$

Yaw' input Delta thrust = -10, Nominal thrust = 1650

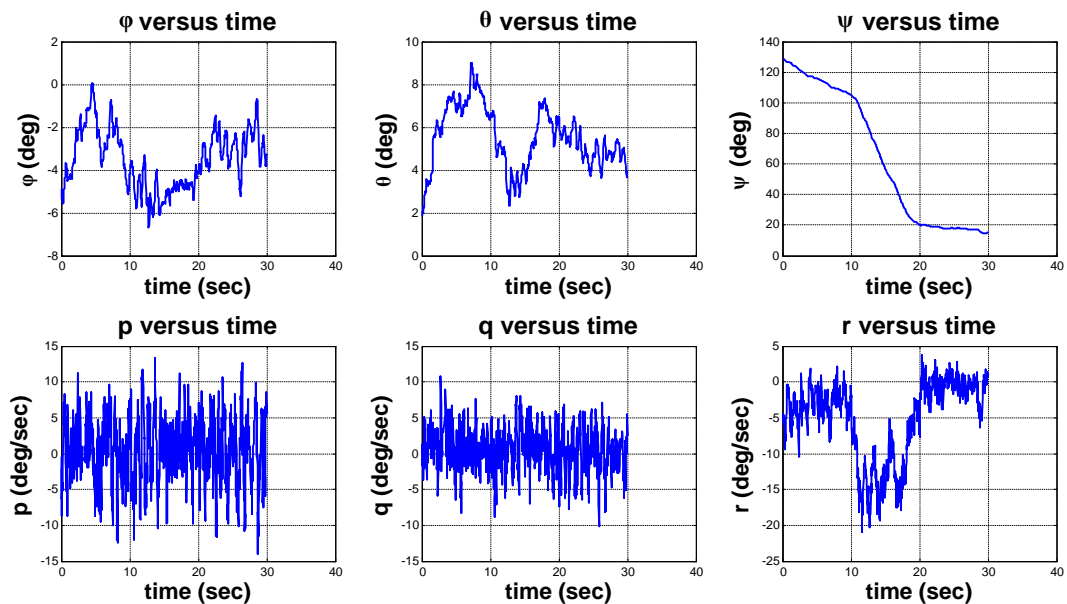


Figure 8.36.: Nominal thrust = 1650 , $\Delta_{Yaw} = -10$

8. Control and Simulation

Yaw' input Delta thrust = -10, Nominal thrust = 1700

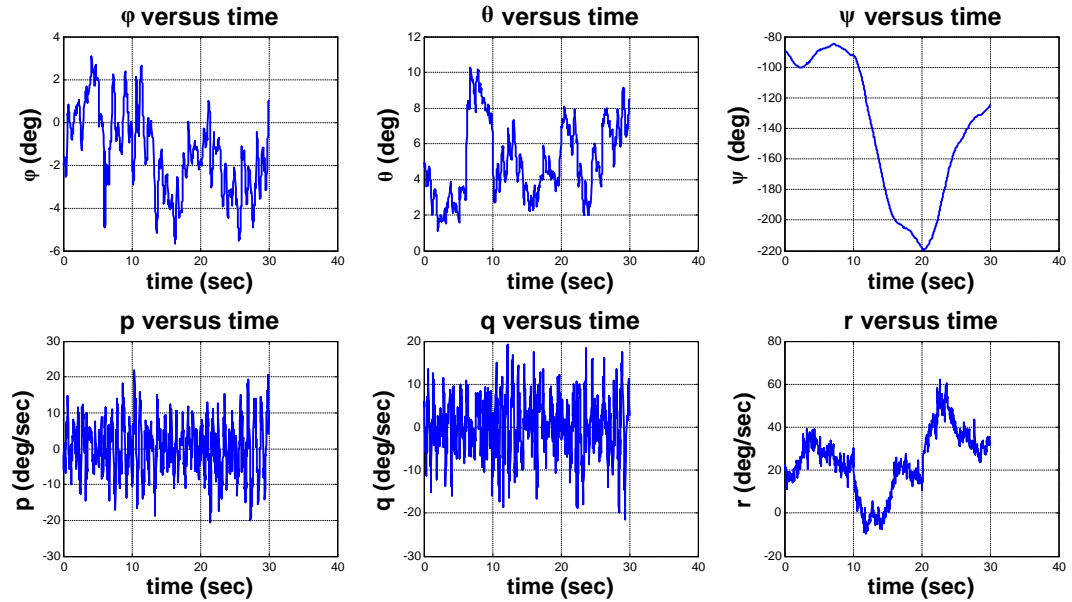


Figure 8.37.: Nominal thrust = 1700 , $\Delta_{Yaw} = -10$

8. Control and Simulation

Yaw' input Delta thrust = 20, Nominal thrust = 1650

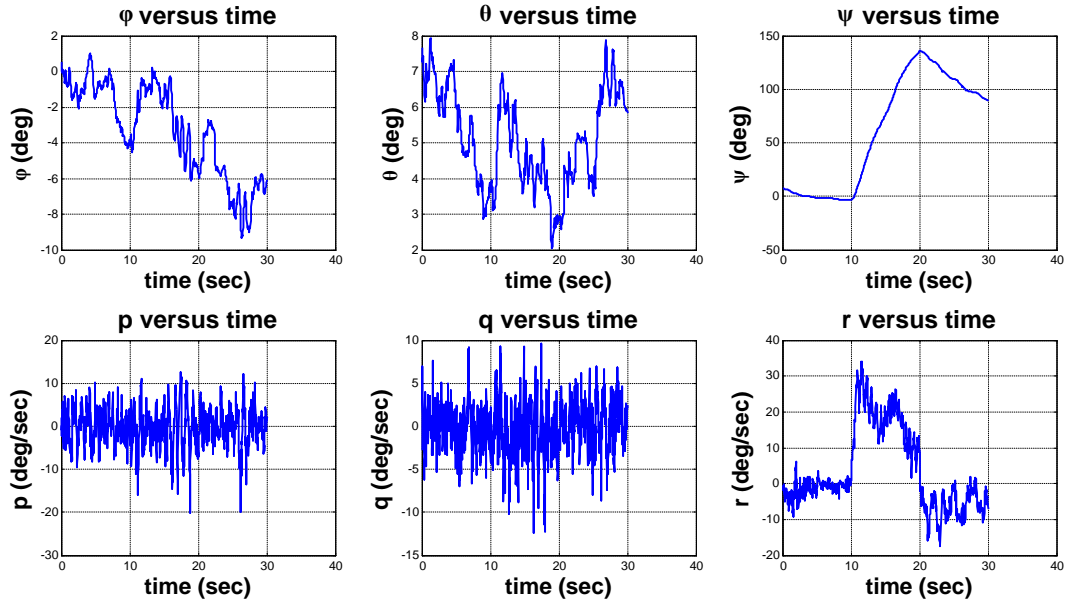


Figure 8.38.: Nominal thrust = 1650 , $\Delta_{Yaw} = 20$

Yaw' input Delta thrust = 20, Nominal thrust = 1700

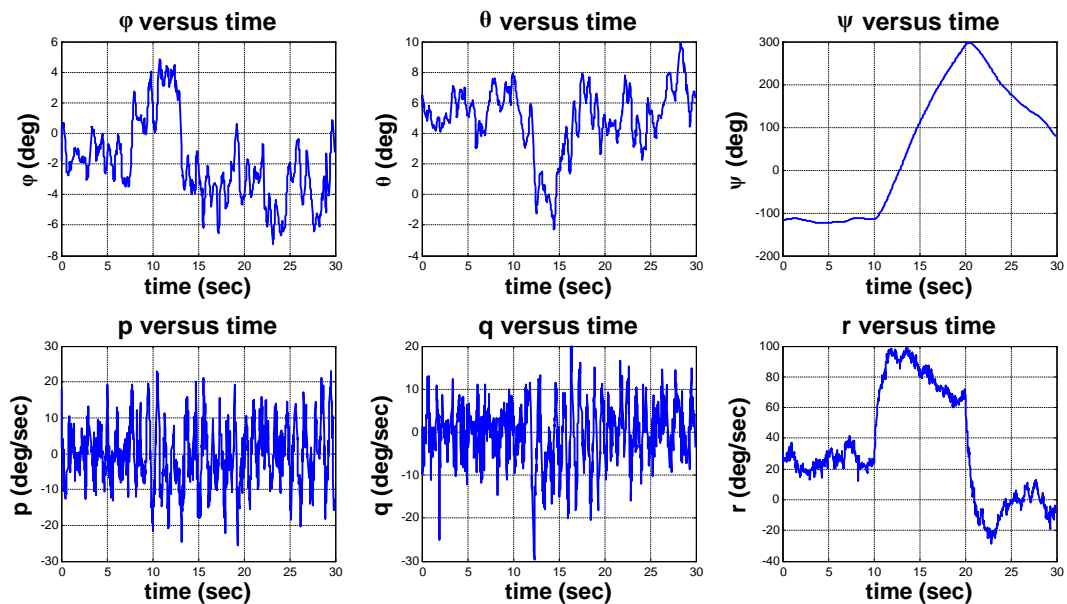


Figure 8.39.: Nominal thrust = 1700 , $\Delta_{Yaw} = 20$

8. Control and Simulation

Yaw' input Delta thrust = -20, Nominal thrust = 1650

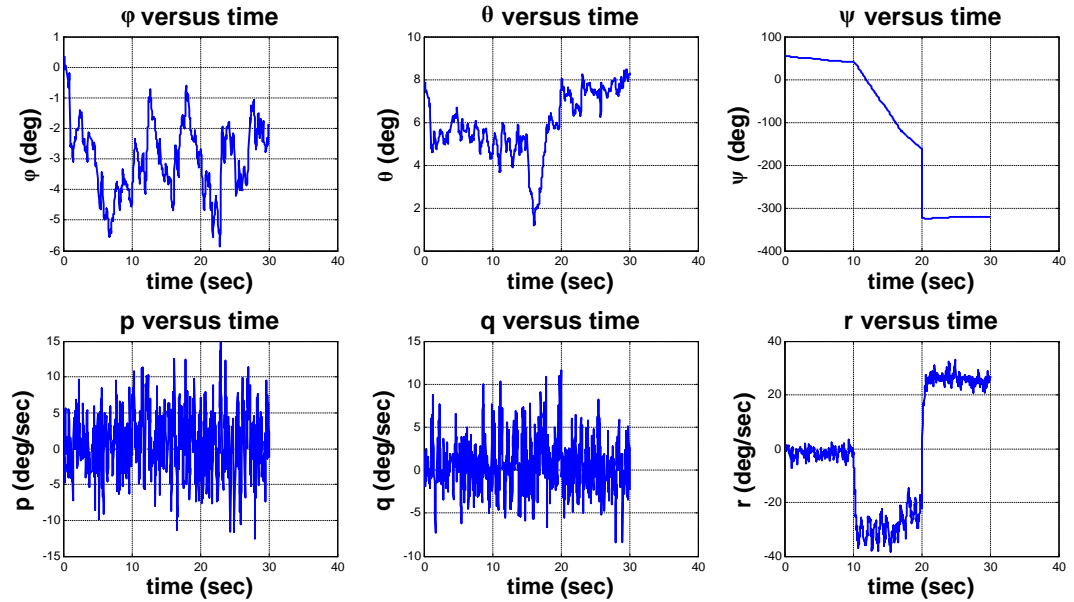


Figure 8.40.: Nominal thrust = 1650 , $\Delta_{Yaw} = -20$

8. Control and Simulation

Yaw' input Delta thrust = -20, Nominal thrust = 1700

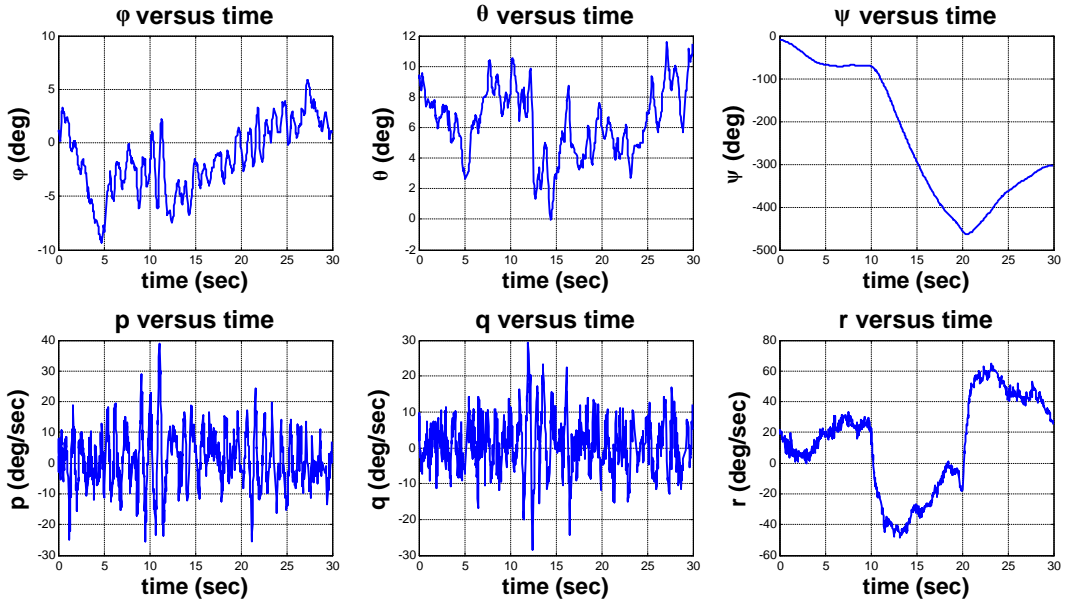


Figure 8.41.: Nominal thrust = 1700 , $\Delta_{Yaw} = -20$

Yaw' input Delta thrust = 30, Nominal thrust = 1650

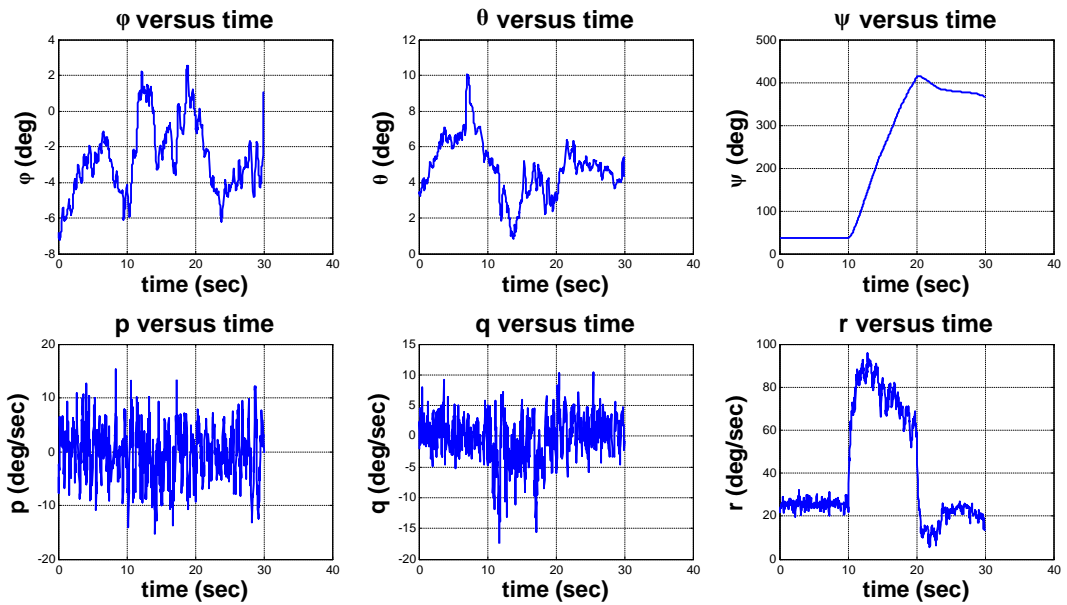


Figure 8.42.: Nominal thrust = 1650 , $\Delta_{Yaw} = 30$

8. Control and Simulation

Yaw' input Delta thrust = 30, Nominal thrust = 1700

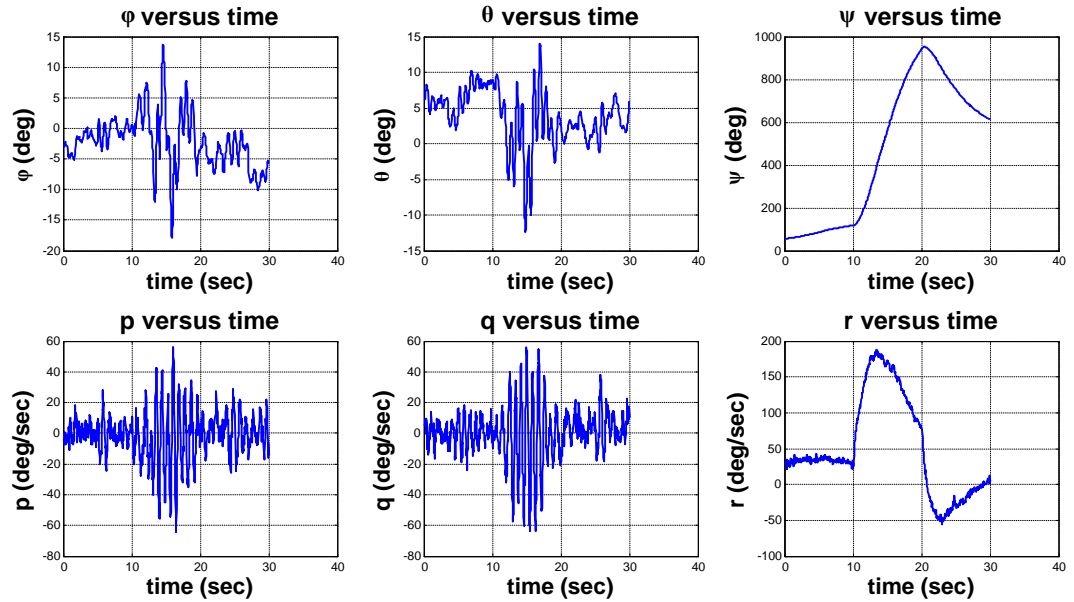


Figure 8.43.: Nominal thrust = 1700 , $\Delta_{Yaw} = 30$

8. Control and Simulation

Yaw' input Delta thrust = -30, Nominal thrust = 1650

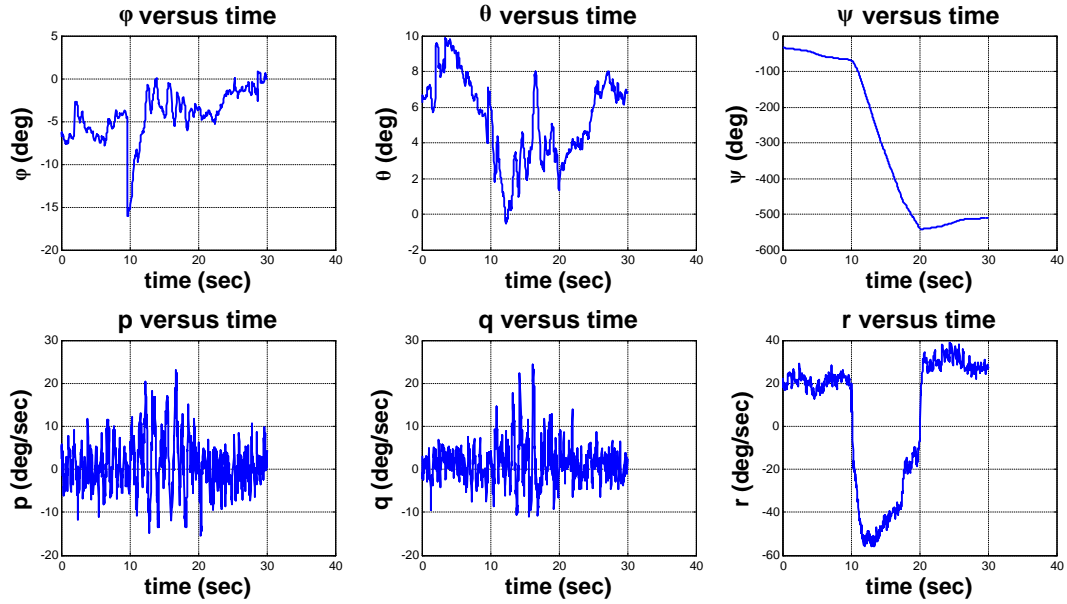


Figure 8.44.: Nominal thrust = 1650 , $\Delta_{Yaw} = -30$

Yaw' input Delta thrust = -30, Nominal thrust = 1700

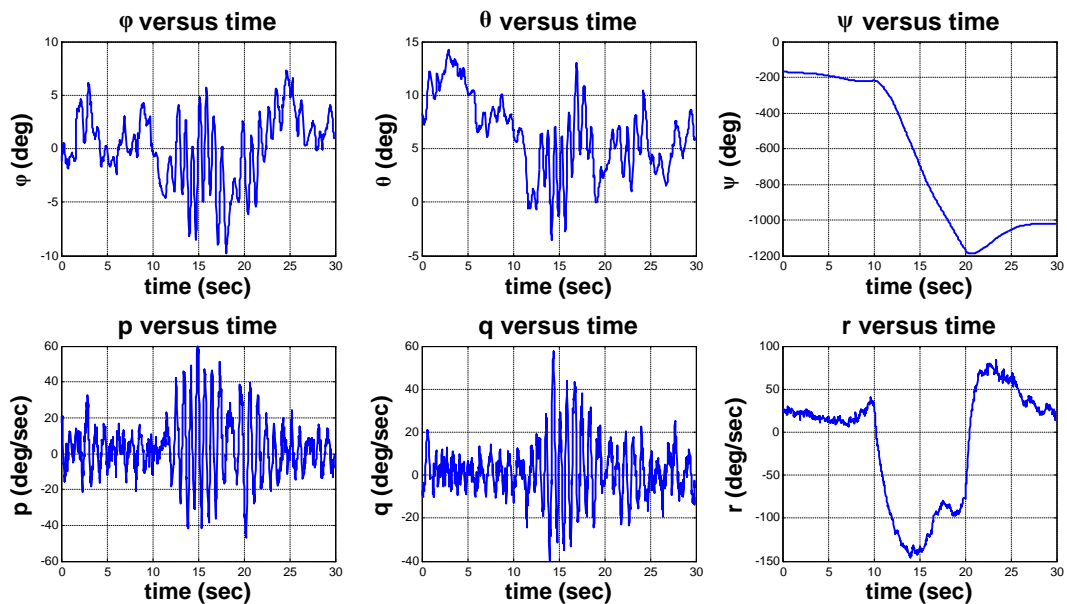


Figure 8.45.: Nominal thrust = 1700 , $\Delta_{Yaw} = -30$

8. Control and Simulation

Equivalent response in Laplace domain

Positive step response for yaw rate

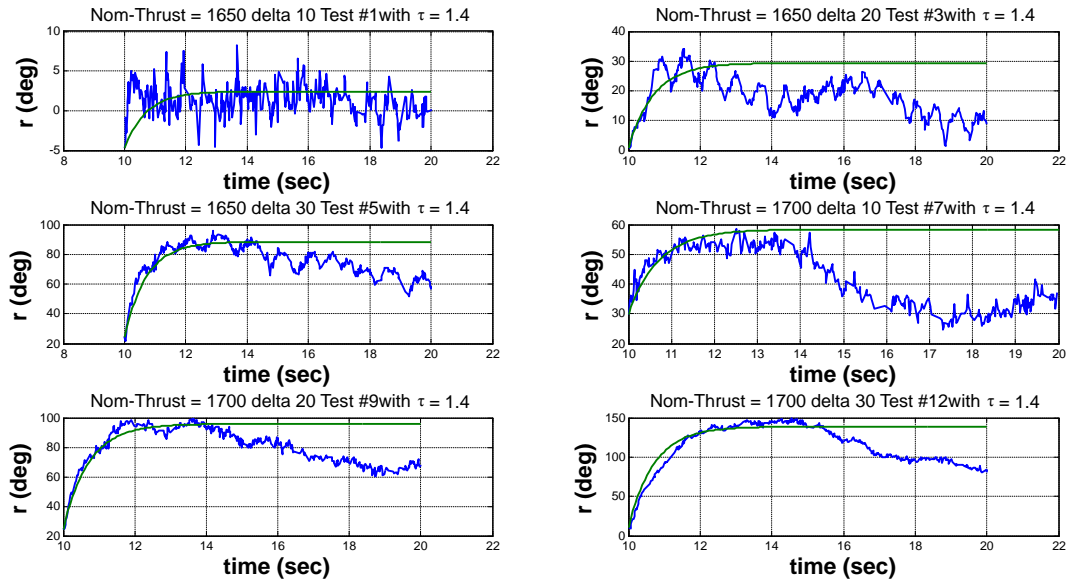


Figure 8.46.: Positive step response for yaw rate

8. Control and Simulation

Negative step response for yaw rate

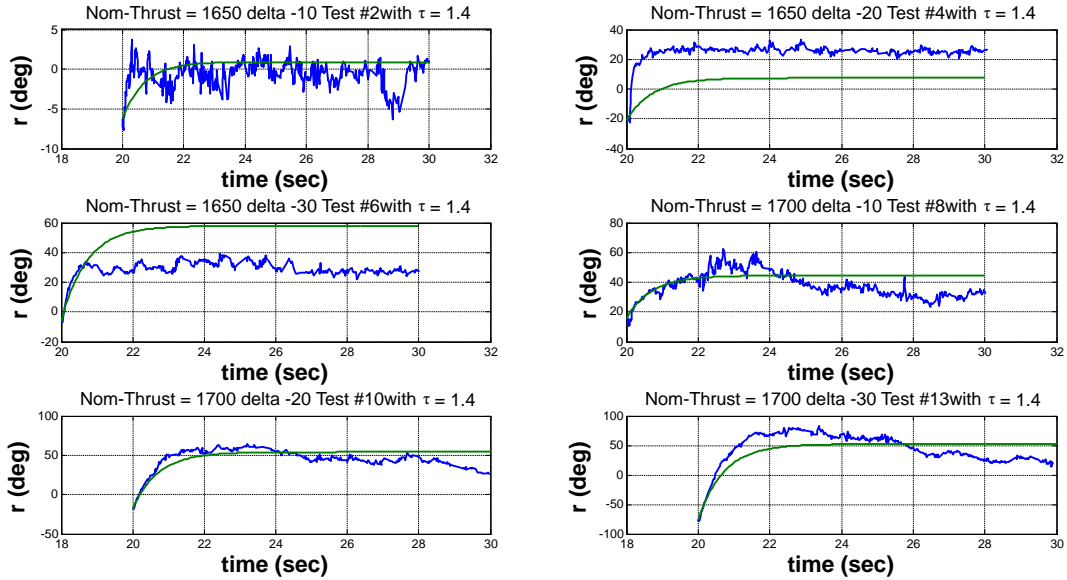


Figure 8.47.: Negative step response for yaw rate

Positive step response for yaw angle

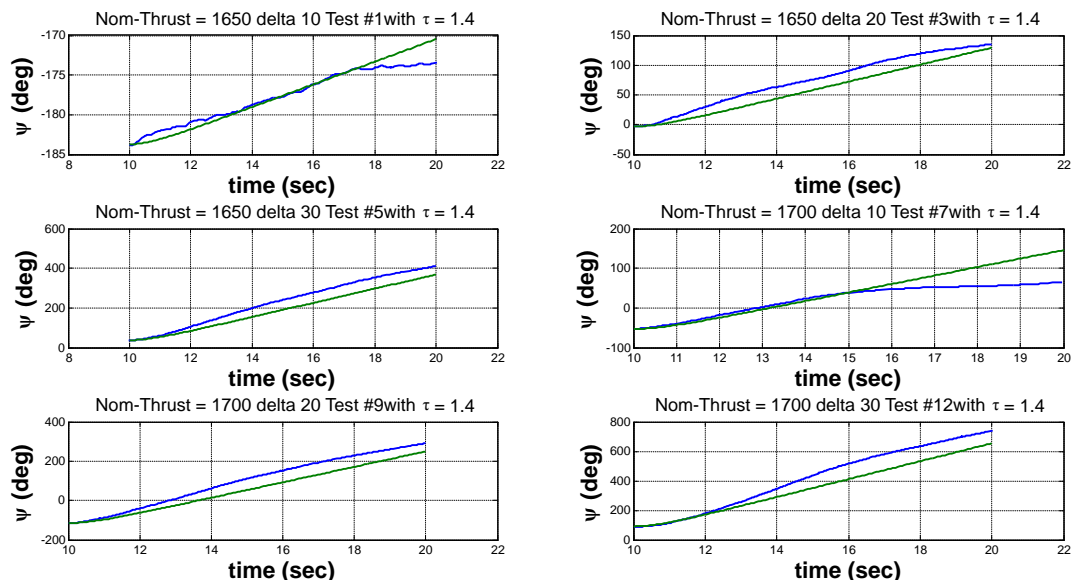


Figure 8.48.: Positive step response for yaw angle

8. Control and Simulation

Negative step response for yaw angle

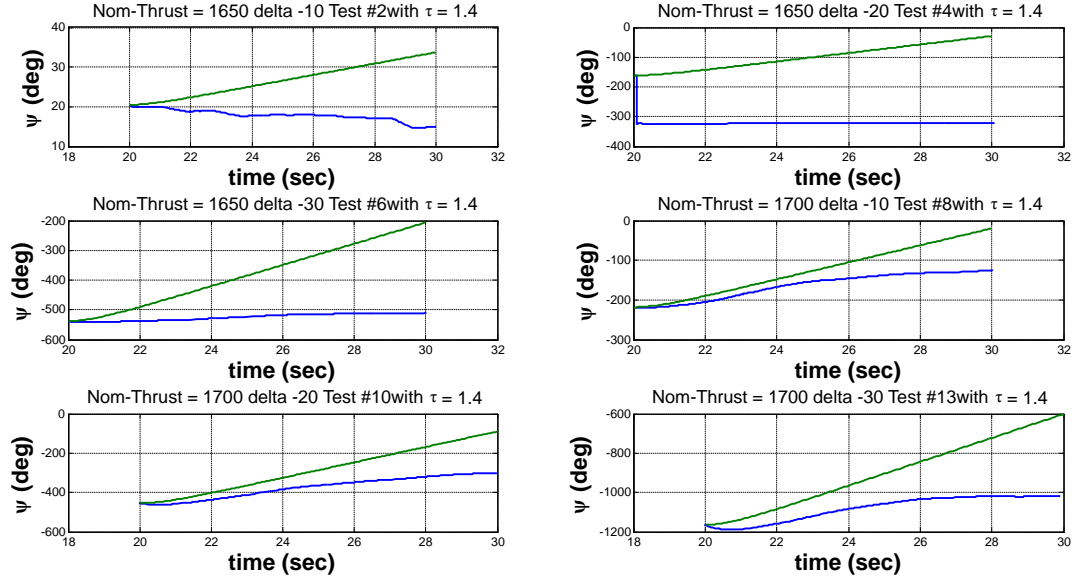


Figure 8.49.: Negative step response for yaw angle

Equivalent transfer function for every test for yaw rate

$$\tau = 1.4 \text{ sec}$$

	Nominal thrust = 1650	Nominal thrust = 1700
Delta thrust = 10	10 ----- $s+1.4$	40 ----- $s+1.4$
Delta thrust = 20	40 ----- $s+1.4$	100 ----- $s+1.4$
Delta thrust = 30	90 ----- $s+1.4$	180 ----- $s+1.4$

Table 8.5.: Equivalent transfer function for every test for yaw rate

Note: Positive & negative step angle has the same transfer function.

8. Control and Simulation

Equivalent transfer function for every test for yaw angle

$$\boxed{\tau = 1.4 \text{ sec}}$$

	Nominal thrust = 1650	Nominal thrust = 1700
Delta thrust = 10	$\frac{10}{s^2 + 1.4 s}$	$\frac{40}{s^2 + 1.4 s}$
Delta thrust = 20	$\frac{40}{s^2 + 1.4 s}$	$\frac{100}{s^2 + 1.4 s}$
Delta thrust = 30	$\frac{90}{s^2 + 1.4 s}$	$\frac{180}{s^2 + 1.4 s}$

Figure 8.50.: Equivalent transfer function for every test for yaw angle

Note: Positive & negative step angle has the same transfer function.

8.2. Non linear Simulation

8.2.1. Airplane Equations of Motion

Summary of kinematic and dynamic equations [24]

$$X - mgS_\theta = m(\dot{u} + qw - rv)$$

$$Y + mgC_\theta S_\Phi = m(\dot{v} + ru - pw) \quad \text{Force equations}$$

$$Z + mgC_\theta C_\Phi = m(\dot{w} + pv - qu)$$

$$L = I_x\dot{p} - I_{xz}\dot{r} + qr(I_z - I_y) - I_{xz}pq$$

$$M = I_y\dot{q} + rp(I_x - I_z) + I_{xz}(p^2 - r^2) \quad \text{Moment equations}$$

$$N = -I_{xz}\dot{p} + I_z\dot{r} + pq(I_y - I_x) + I_{xz}qr$$

$$p = \dot{\Phi} - \dot{\psi}S_\theta$$

$$q = \dot{\theta}C_\Phi - \dot{\psi}C_\theta S_\Phi$$

$$r = \dot{\psi}C_\theta C_\Phi - \dot{\theta}S_\Phi$$

Body angular velocities
in terms of Euler angles
and Euler rates

$$\dot{\theta} = qC_\Phi - rS_\Phi$$

$$\dot{\Phi} = p + qS_\Phi T_\theta + rC_\Phi T_\theta$$

$$\dot{\psi} = (qS_\Phi - rC_\Phi) \sec \theta$$

Euler rates in terms of
Euler angles and body
angular velocities

where

$$S_\theta = \sin(\theta)$$

$$C_\theta = \cos(\theta)$$

$$T_\theta = \tan(\theta)$$

$$S_\Phi = \sin(\Phi)$$

$$C_\Phi = \cos(\Phi)$$

$$T_\Phi = \tan(\Phi)$$

8. Control and Simulation

Velocity of aircraft in the fixed frame in terms of Euler angles and body velocity components

$$\begin{bmatrix} \frac{dx}{dt} \\ \frac{dy}{dt} \\ \frac{dz}{dt} \end{bmatrix} = \begin{bmatrix} C_\theta C_\psi & S_\Phi S_\theta C_\psi - C_\Phi S_\psi & C_\Phi S_\theta C_\psi + S_\phi S_\psi \\ C_\theta S_\psi & S_\Phi S_\theta S_\psi + C_\Phi C_\psi & C_\Phi S_\theta S_\psi - S_\phi C_\psi \\ -S_\theta & S_\Phi C_\theta & C_\Phi C_\theta \end{bmatrix} \begin{bmatrix} u \\ v \\ w \end{bmatrix}$$

Using small disturbance theory all the variables in the equations of motion are replaced by a reference value plus a perturbation or disturbance:

$$\begin{aligned} X &= X_0 + \Delta X & Y &= Y_0 + \Delta Y & Z &= Z_0 + \Delta Z \\ L &= L_0 + \Delta L & M &= M_0 + \Delta M & N &= N_0 + \Delta N \end{aligned}$$

For multi-copters, Basic assumptions :

- X direction is in the same direction of motor 1
- Motor 1 rotates CW
- + ve rotating of A/C is counter-clockwise
- We assumed that center of rotation (COR) and center of gravity (COG) are not the same.
- We assumed that jig has damping constant in the 3 directions

Therefore we can represent the forces and moments in the following manner

$$\begin{aligned} X_0 &= mgS_\theta & \Delta X &= 0 \\ Y_0 &= -mgC_\theta S_\Phi & \Delta Y &= 0 \\ Z_0 &= -mgC_\theta C_\Phi & \Delta Z &= \sum_{i=1}^n K_i \text{ PWM}_i \end{aligned}$$

Table 8.6.: Forces

Where :

K is the motor thrust constant (N/PWM), we measured it for each motor (see [appendix E](#))
 n is the number of motors

8. Control and Simulation

$$\begin{aligned}
 L_0 &= -m * g * Length_{RG} * \cos(\theta) * \sin(\phi) - \nu * p - \kappa * \phi \\
 M_0 &= -m * g * Length_{RG} * \sin(\theta) - \nu * q - \kappa * \theta \\
 N_0 &= -\nu * r \\
 \Delta L &= d * \sum_{i=1}^{n/2} (-1)^{i+1} K_{2i} PWM_{2i} \\
 \Delta M &= d * \sum_{i=1}^{n/2+1} (-1)^{i+1} K_{2i-1} PWM_{2i-1} \\
 \Delta N &= \sum_{i=1}^{n/2+1} B_{2i-1} * PWM_{2i-1} - \sum_{i=1}^{n/2} B_{2i} * PWM_{2i}
 \end{aligned}$$

Table 8.7.: Moments

Where :

d is the length between any motor and COG (in meter)

m is the multi copter mass (in kg)

g is the gravitational acceleration (in meter / sec²)

$Length_{RG}$ is the distance between the COR and COG (in meter)

ν is the damping constant of the jig (in N.m * sec / rad)

κ is the spring constant of the jig (in N.m / rad)

p is the rate of angle ϕ (in rad / sec)

q is the rate of angle θ (in rad / sec)

r is the rate of angle ψ (in rad / sec)

B is the motor torque constant (N.m / PWM), we measured it for each motor (see [appendix E](#))

So the following parameter are unknown

jig	κ, ν
-----	---------------

But we already recorded the actual response so we can assume these parameters until the non linear response closely matches the actual response

We used Rounge-kutta to integrate the above equations (see [appendix C](#))

Our vehicle had the following parameters :

mass (m)	1.66 Kg
d	0.23 m
$Length_{RG}$	0.04 m
I_{xx}	0.0181 Kg.m ²
I_{yy}	0.0181 Kg.m ²
I_{zz}	0.0359 Kg.m ²
I_{xz}	0 Kg.m ²

The moment of inertia was measured using bifilar pendulum method (see [appendix D](#))

The following equations are used to calculate PWM of each motor

$$\begin{aligned}
 PWM_1 &= -\Delta_{Pitch} + \Delta_{Yaw} \\
 PWM_2 &= +\Delta_{Roll} - \Delta_{Yaw} \\
 PWM_3 &= +\Delta_{Pitch} + \Delta_{Yaw} \\
 PWM_4 &= -\Delta_{Roll} - \Delta_{Yaw}
 \end{aligned}$$

8. Control and Simulation

8.2.2. Results for Nominal Thrust is 1650

We assumed the following parameters

κ (N.m / rad)	1.2
ν (N.m * sec / rad)	0.09

8. Control and Simulation

8.2.2.1. Roll

$$\Delta_{Roll} = 10$$

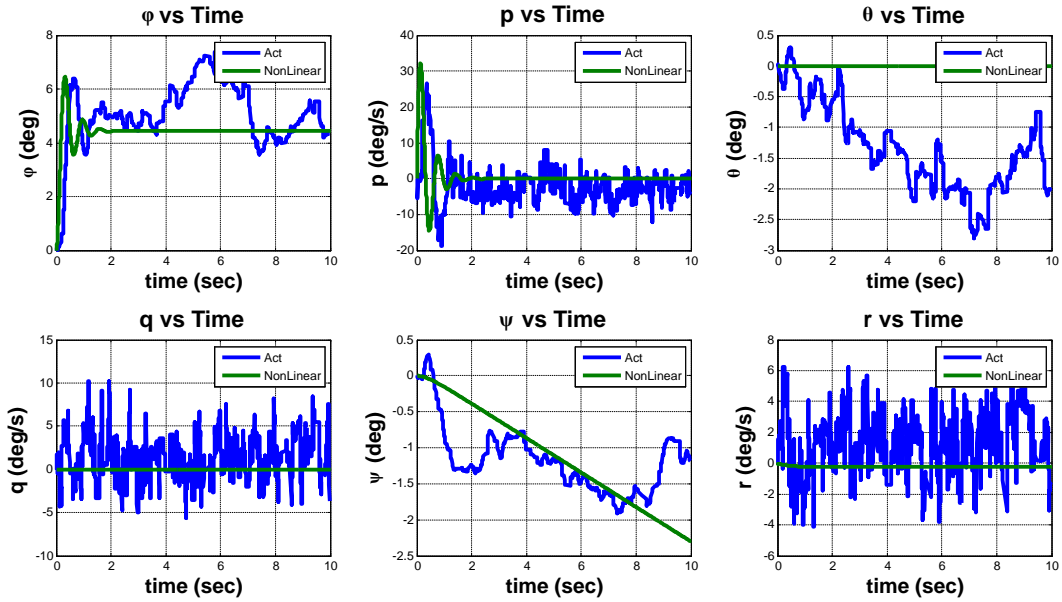


Figure 8.51.: Nominal thrust = 1650 , $\Delta_{Roll} = 10$

$$\Delta_{Roll} = -10$$

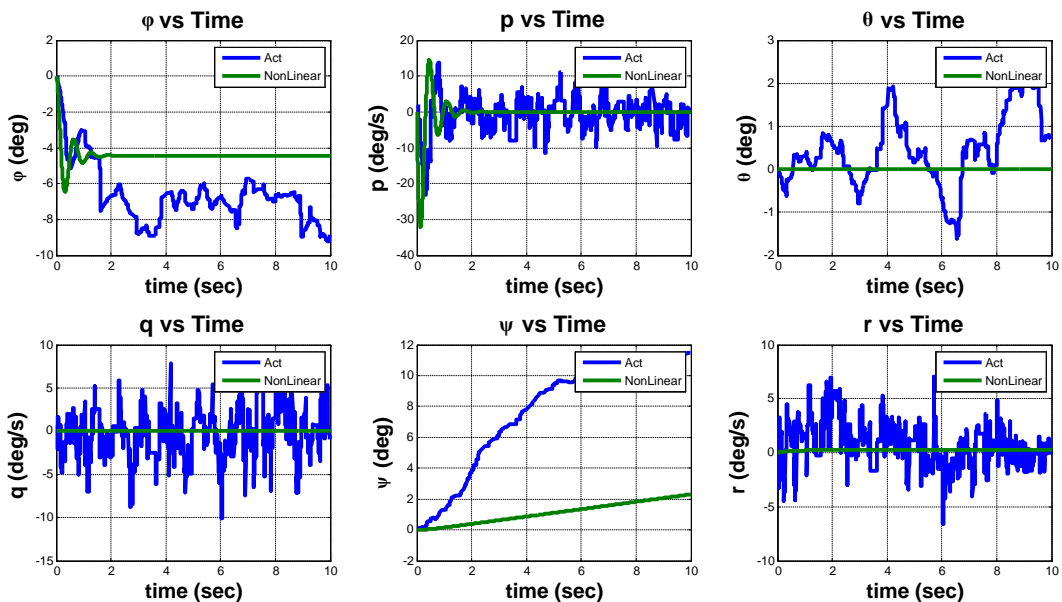


Figure 8.52.: Nominal thrust = 1650 , $\Delta_{Roll} = -10$

8. Control and Simulation

$$\Delta_{Roll} = 20$$

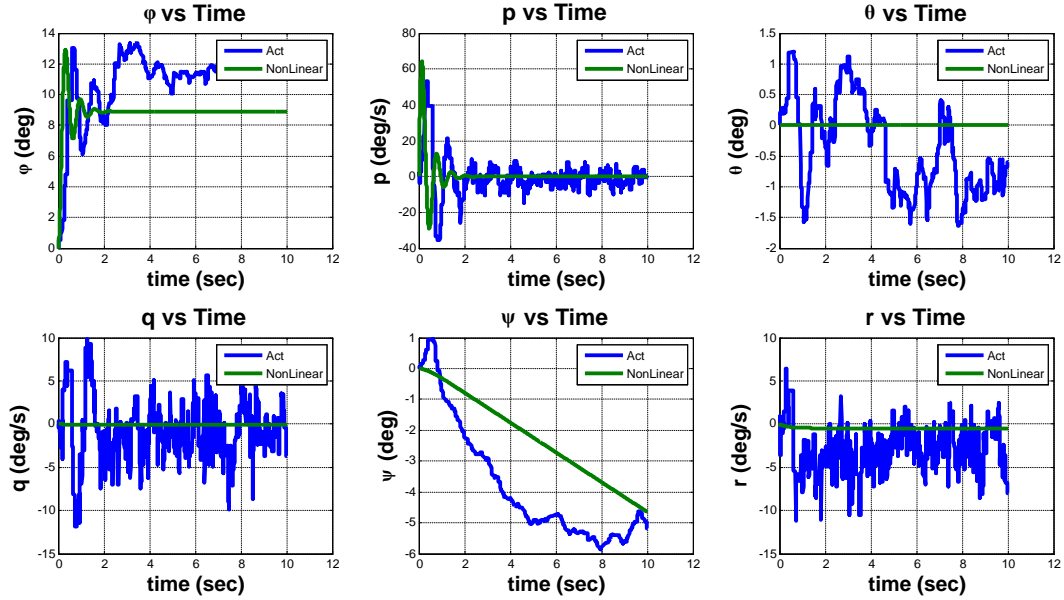


Figure 8.53.: Nominal thrust = 1650 , $\Delta_{Roll} = 20$

$$\Delta_{Roll} = -20$$

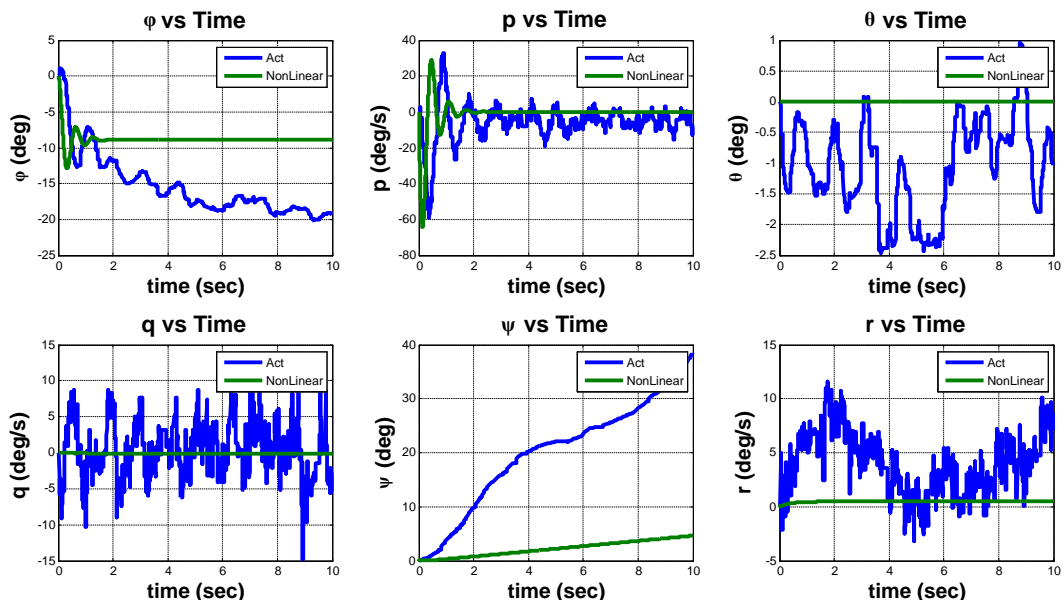


Figure 8.54.: Nominal thrust = 1650 , $\Delta_{Roll} = -20$

8. Control and Simulation

$$\Delta_{Roll} = 30$$

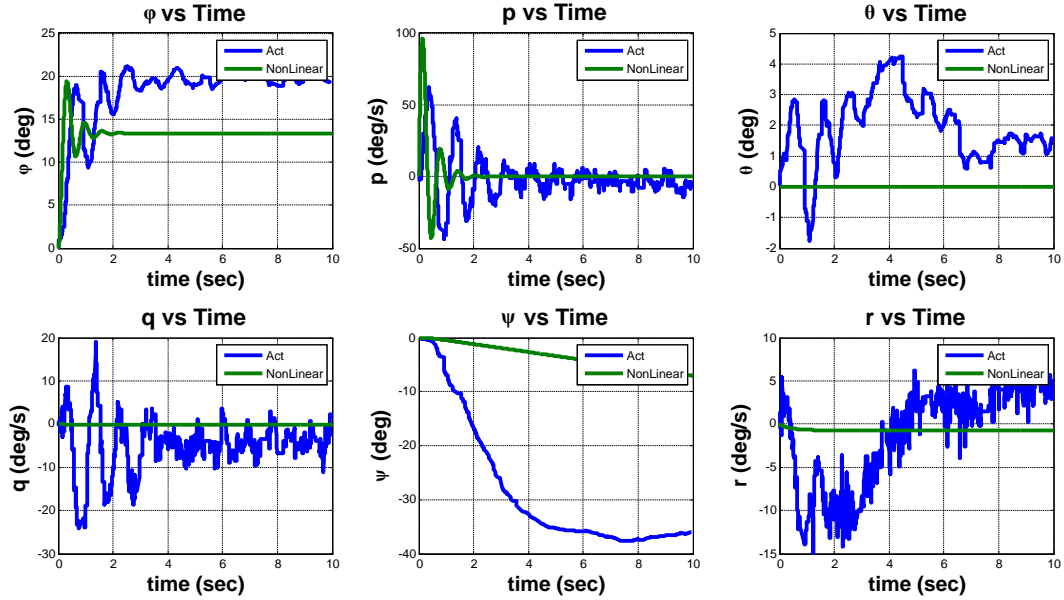


Figure 8.55.: Nominal thrust = 1650 , $\Delta_{Roll} = 30$

$$\Delta_{Roll} = -30$$

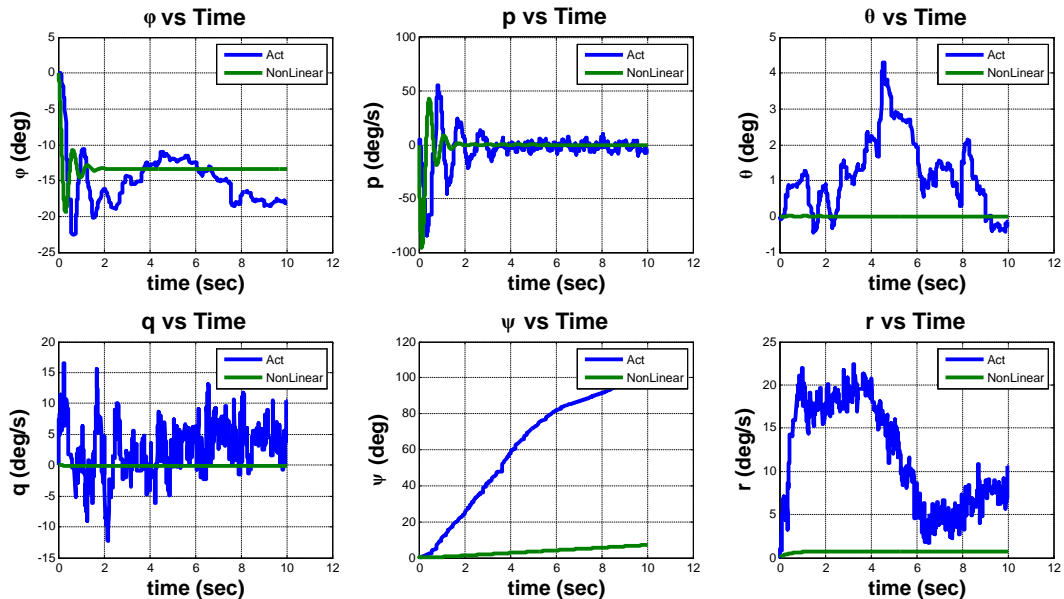


Figure 8.56.: Nominal thrust = 1650 , $\Delta_{Roll} = -30$

8. Control and Simulation

8.2.2.2. Pitch

$$\Delta_{Pitch} = 10$$

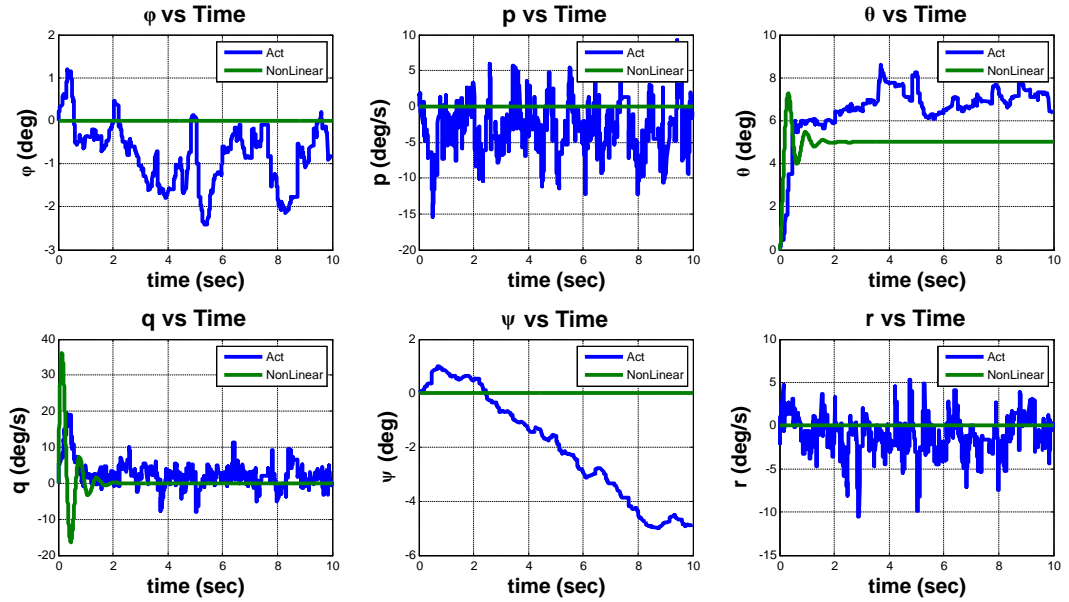


Figure 8.57.: Nominal thrust = 1650 , $\Delta_{Pitch} = 10$

$$\Delta_{Pitch} = -10$$

8. Control and Simulation

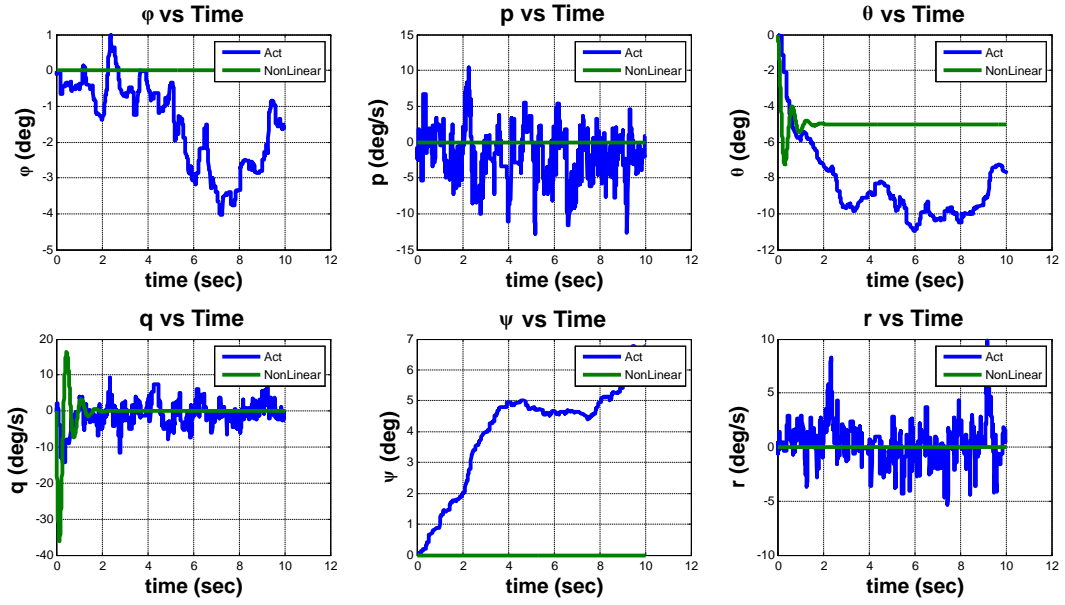


Figure 8.58.: Nominal thrust = 1650 , $\Delta_{Pitch} = -10$

$$\Delta_{Pitch} = 20$$

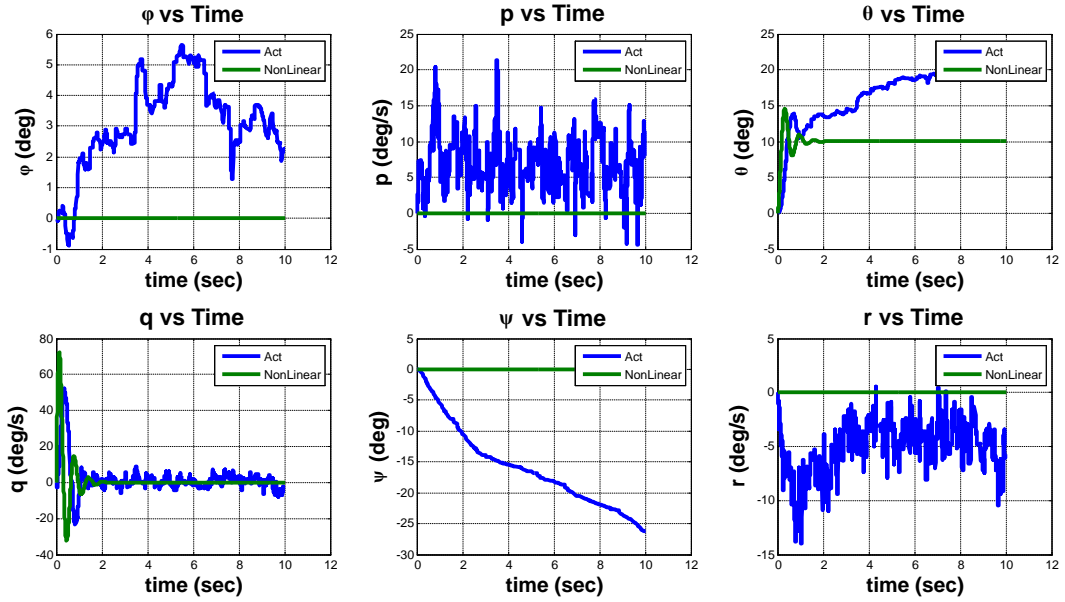


Figure 8.59.: Nominal thrust = 1650 , $\Delta_{Pitch} = 20$

$$\Delta_{Pitch} = -20$$

8. Control and Simulation

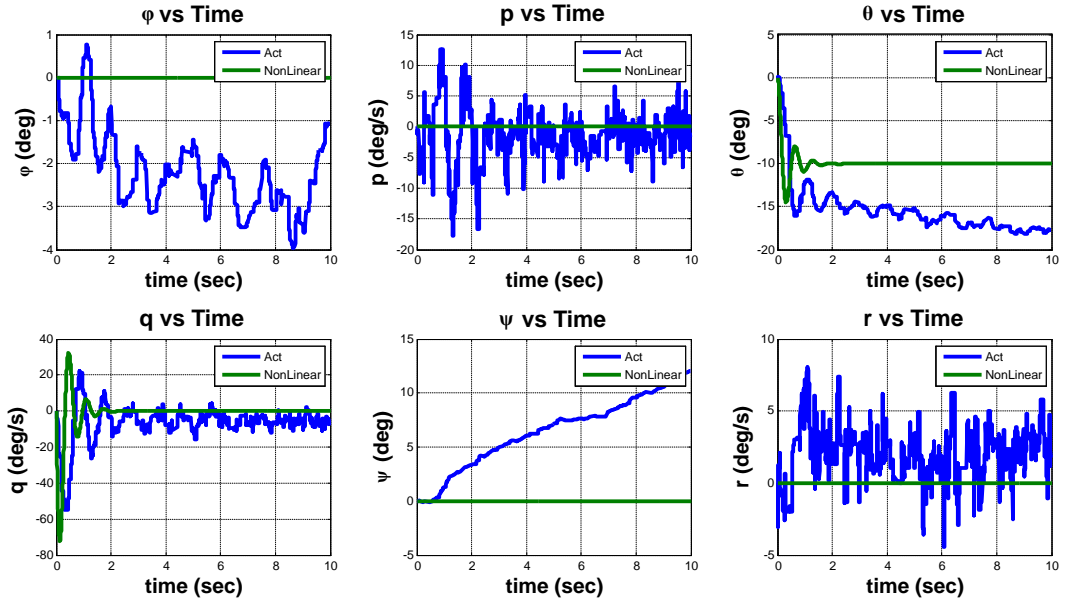


Figure 8.60.: Nominal thrust = 1650 , $\Delta_{Pitch} = -20$

$$\Delta_{Pitch} = 30$$

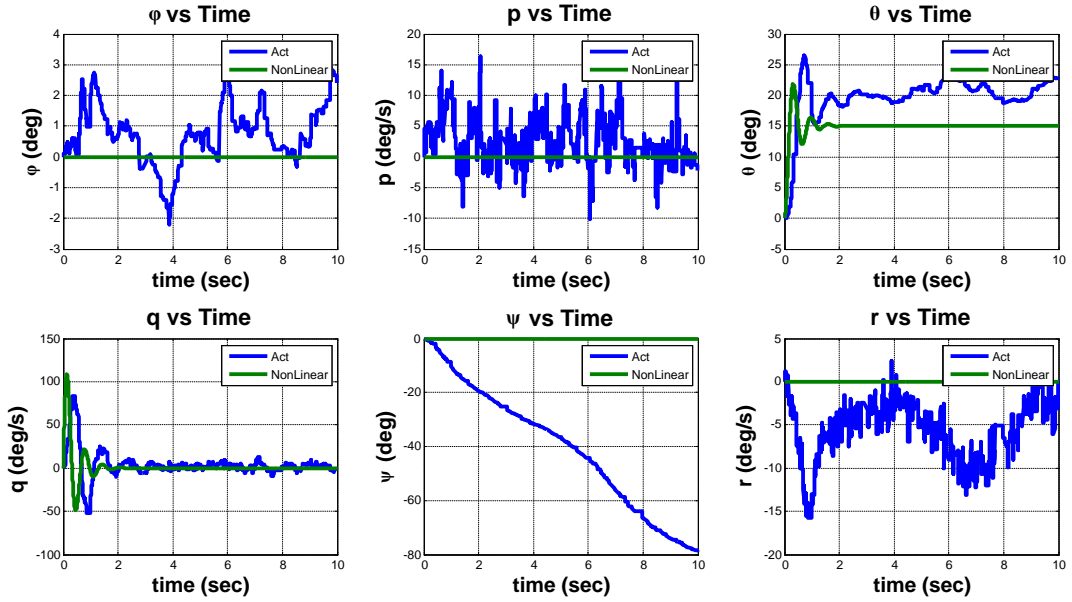


Figure 8.61.: Nominal thrust = 1650 , $\Delta_{Pitch} = 30$

$$\Delta_{Pitch} = -30$$

8. Control and Simulation

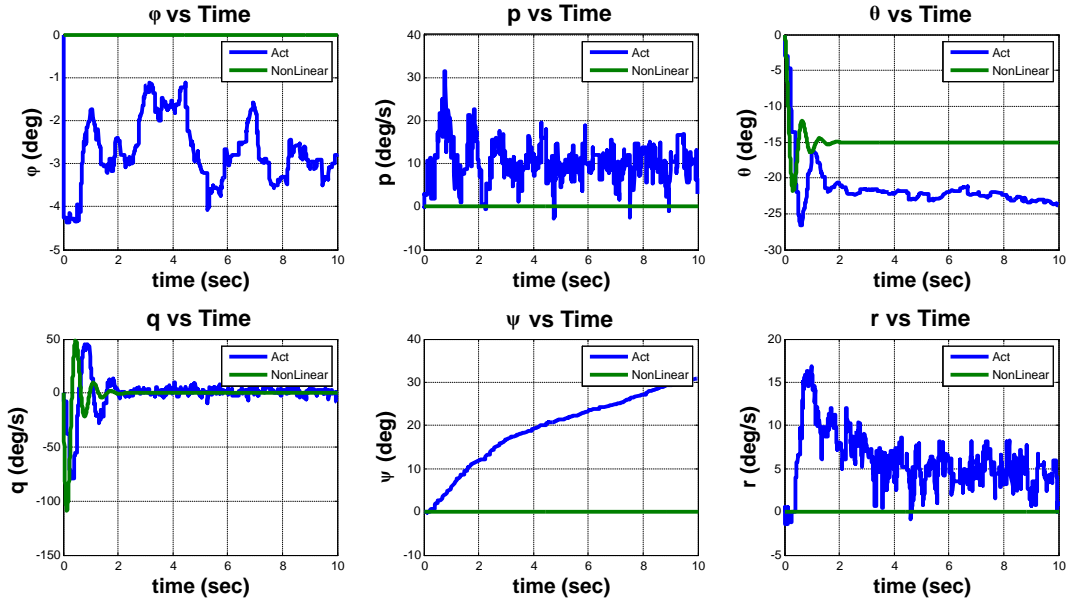


Figure 8.62.: Nominal thrust = 1650 , $\Delta_{Pitch} = -30$

8.2.2.3. Yaw

$$\Delta_{Yaw} = 10$$

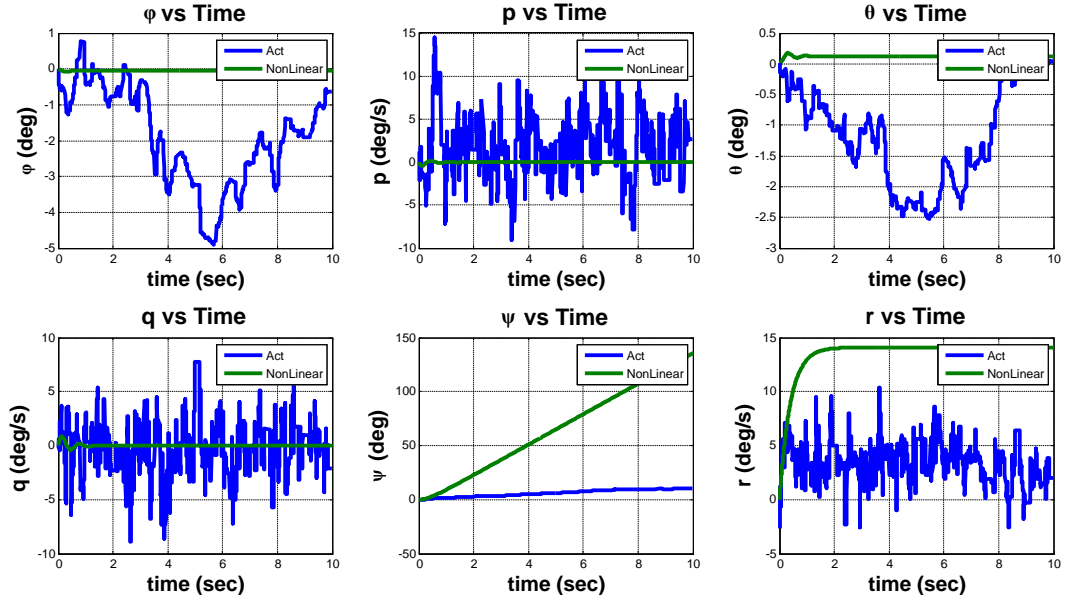


Figure 8.63.: Nominal thrust = 1650 , $\Delta_{Yaw} = 10$

8. Control and Simulation

$$\Delta Y_{aw} = -10$$

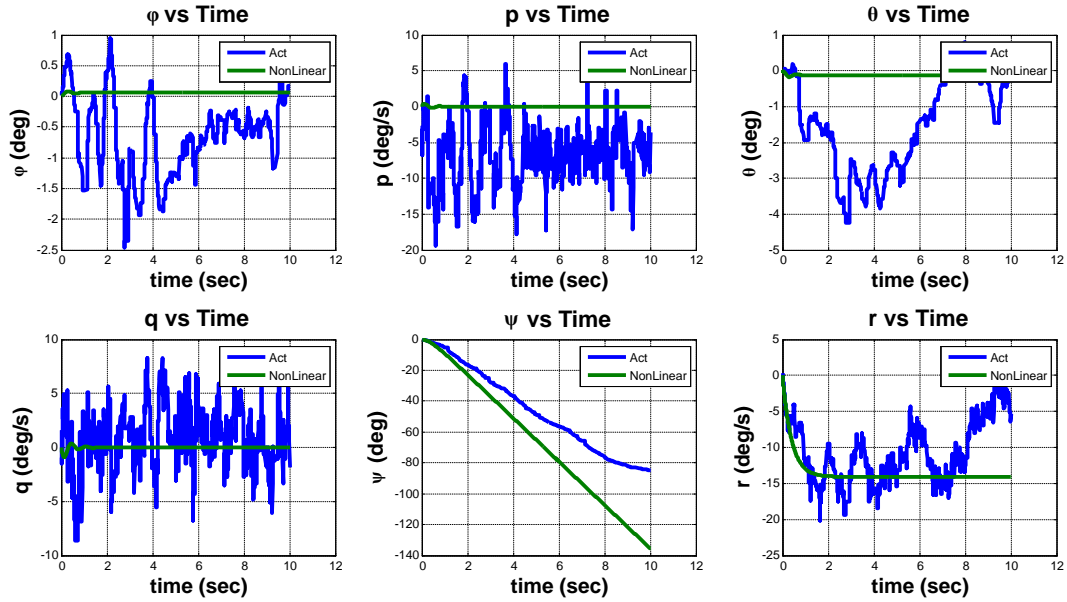


Figure 8.64.: Nominal thrust = 1650 , $\Delta Y_{aw} = -10$

$$\Delta Y_{aw} = 20$$

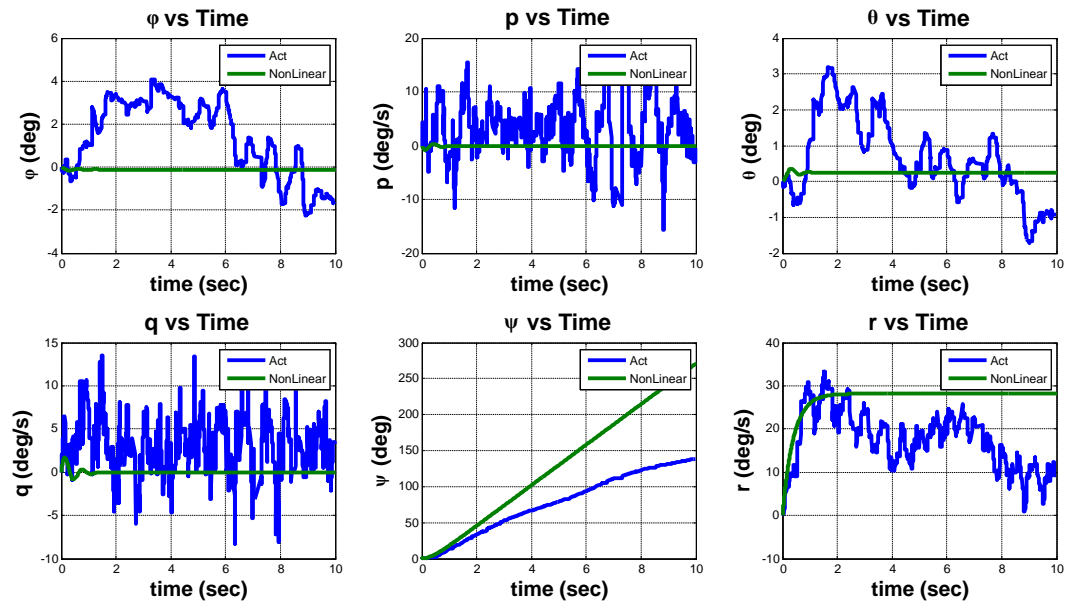


Figure 8.65.: Nominal thrust = 1650 , $\Delta Y_{aw} = 20$

8. Control and Simulation

$$\Delta Y_{aw} = -20$$

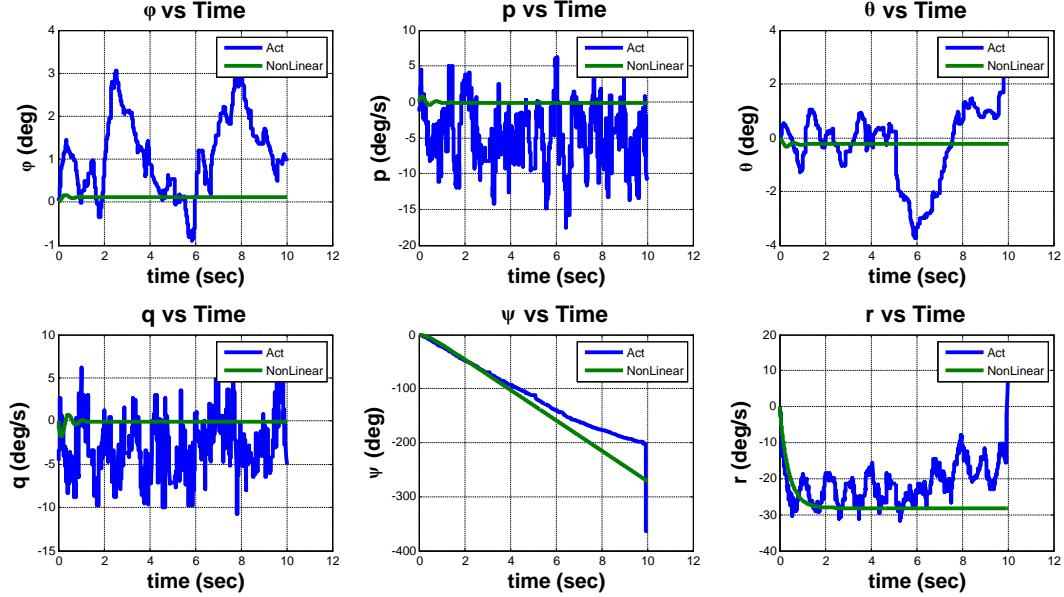


Figure 8.66.: Nominal thrust = 1650 , $\Delta Y_{aw} = -20$

$$\Delta Y_{aw} = 30$$

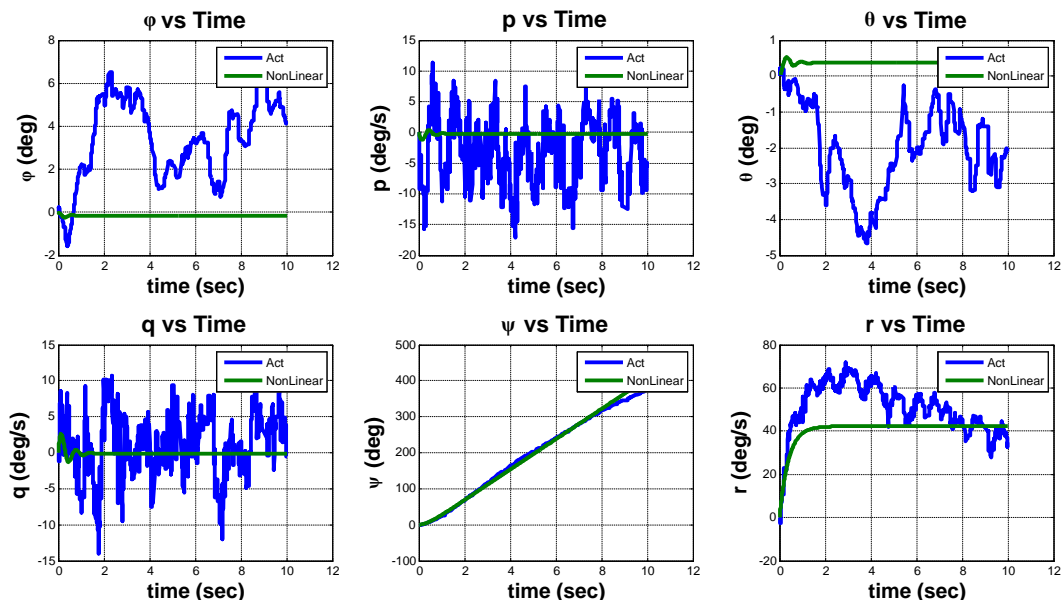


Figure 8.67.: Nominal thrust = 1650 , $\Delta Y_{aw} = 30$

8. Control and Simulation

$$\Delta Y_{aw} = -30$$

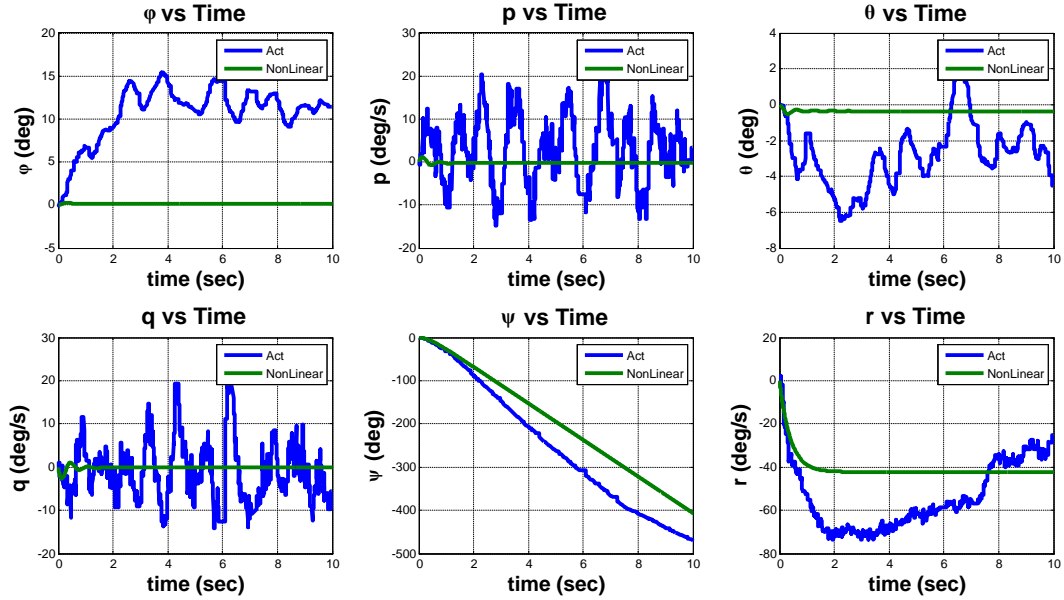


Figure 8.68.: Nominal thrust = 1650 , $\Delta Y_{aw} = -30$

8.2.3. Results for Nominal Thrust is 1700

κ (N.m / rad)	0.8
ν (N.m * sec / rad)	0.04

8.2.3.1. Roll

$$\Delta_{Roll} = 10$$

8. Control and Simulation

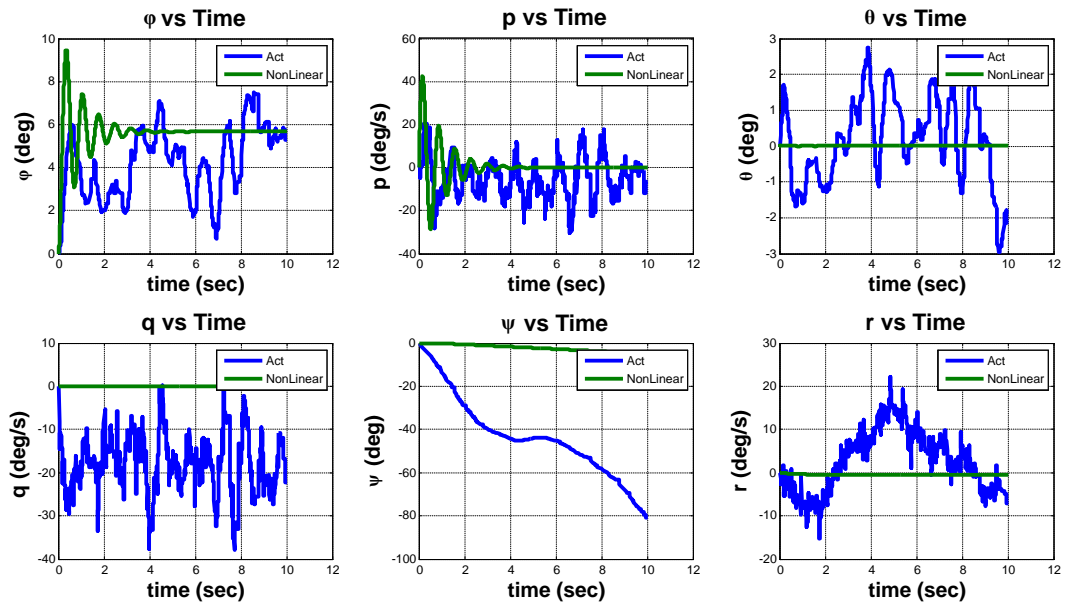


Figure 8.69.: Nominal thrust = 1700 , $\triangle_{Roll} = 10$

8. Control and Simulation

$$\Delta_{Roll} = -10$$

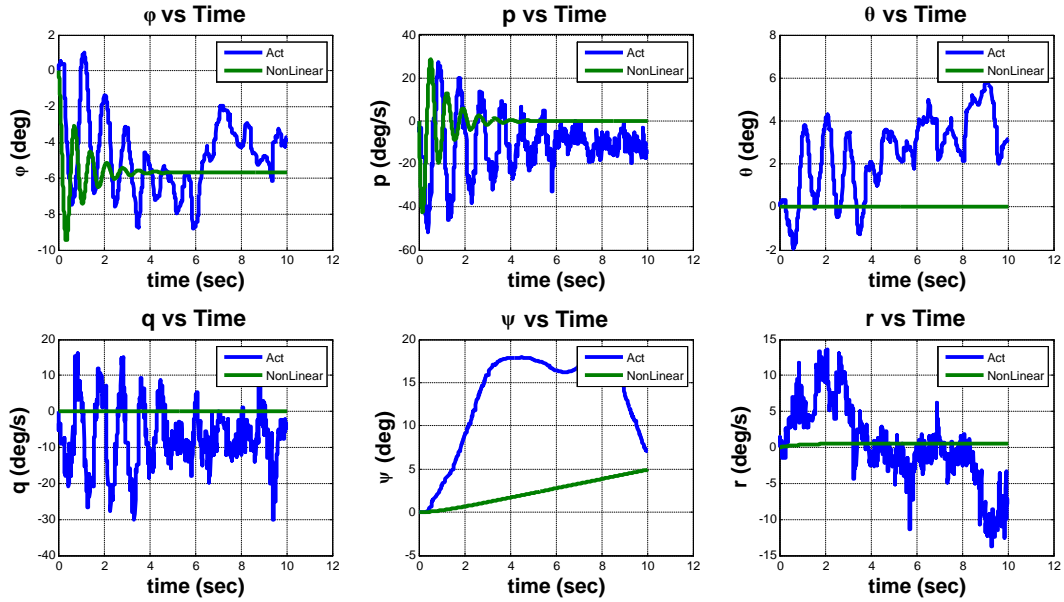


Figure 8.70.: Nominal thrust = 1700 , $\Delta_{Roll} = -10$

$$\Delta_{Roll} = 20$$

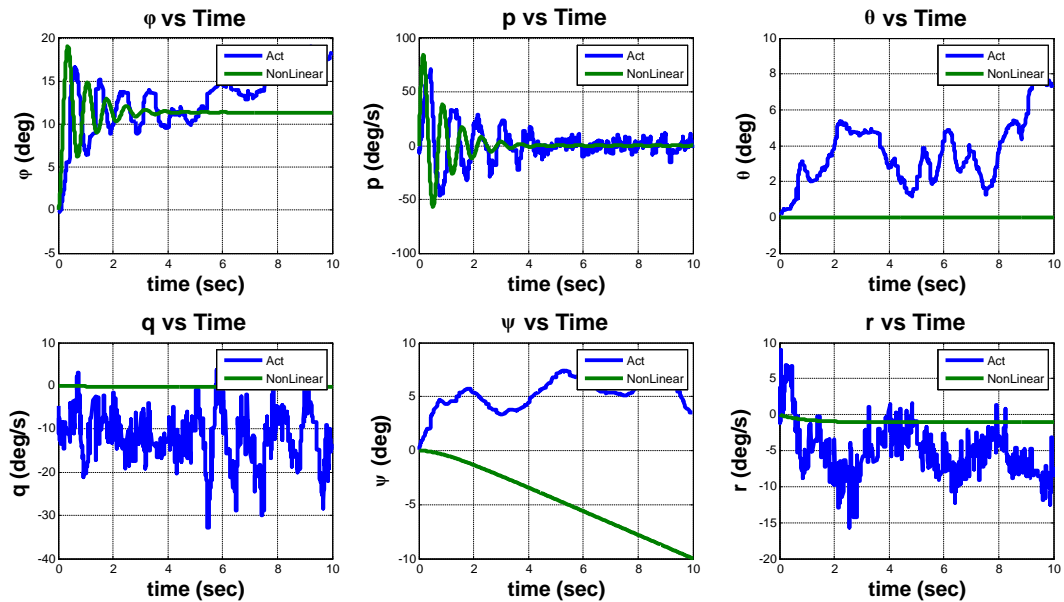


Figure 8.71.: Nominal thrust = 1700 , $\Delta_{Roll} = 20$

8. Control and Simulation

$$\Delta_{Roll} = -20$$

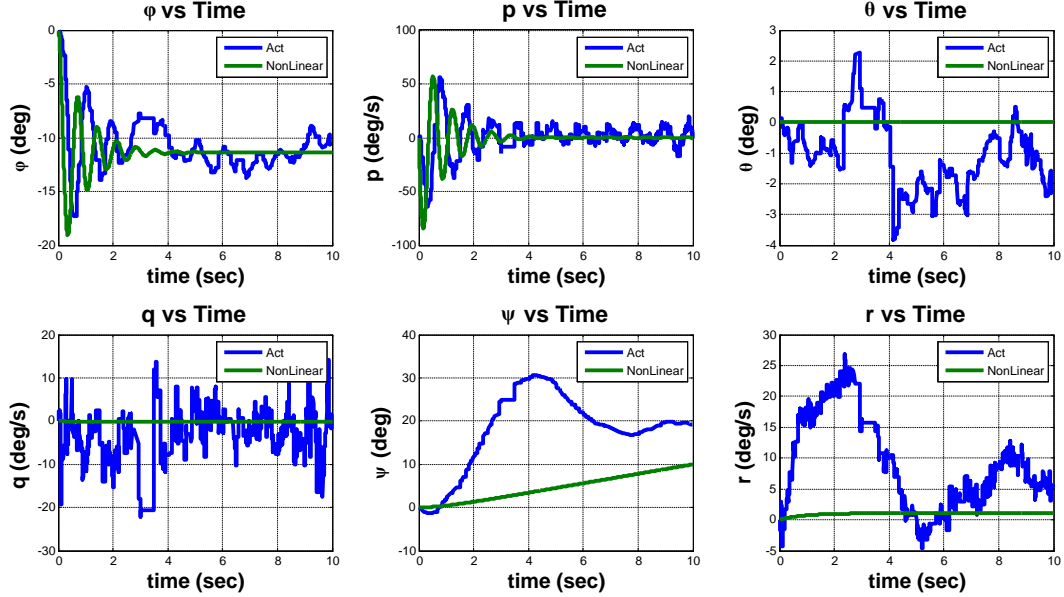


Figure 8.72.: Nominal thrust = 1700 , $\Delta_{Roll} = -20$

$$\Delta_{Roll} = 30$$

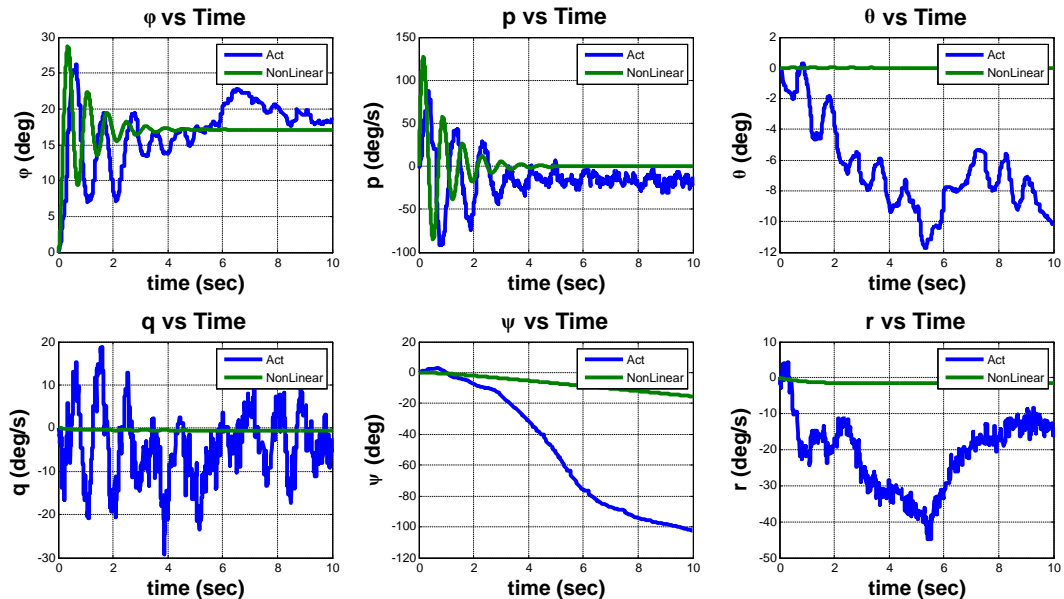


Figure 8.73.: Nominal thrust = 1700 , $\Delta_{Roll} = 30$

8. Control and Simulation

$$\Delta_{Roll} = -30$$

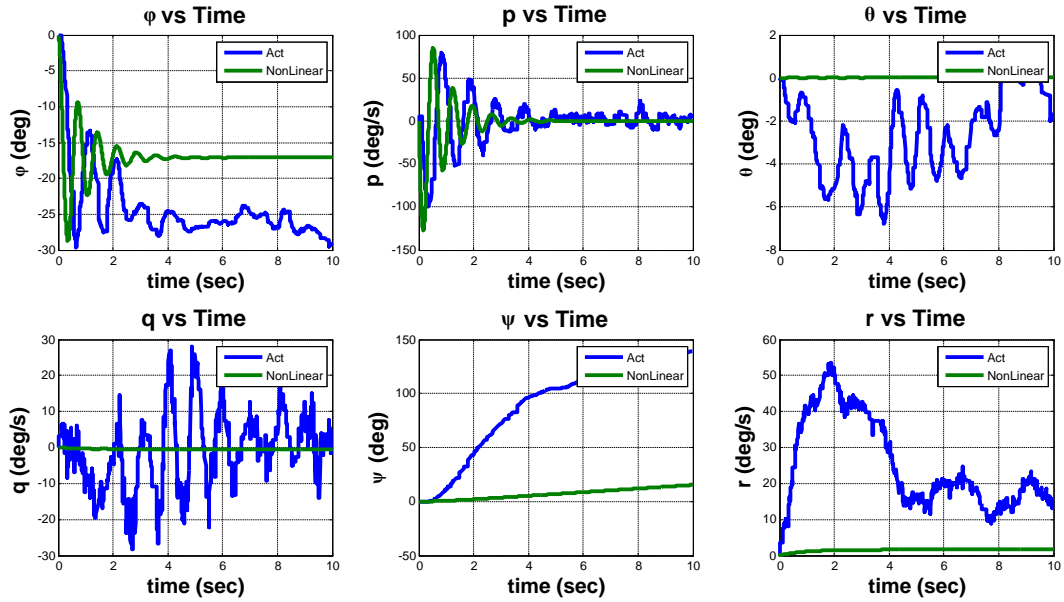


Figure 8.74.: Nominal thrust = 1700 , $\Delta_{Roll} = -30$

8. Control and Simulation

8.2.3.2. Pitch

$$\Delta_{Pitch} = 10$$

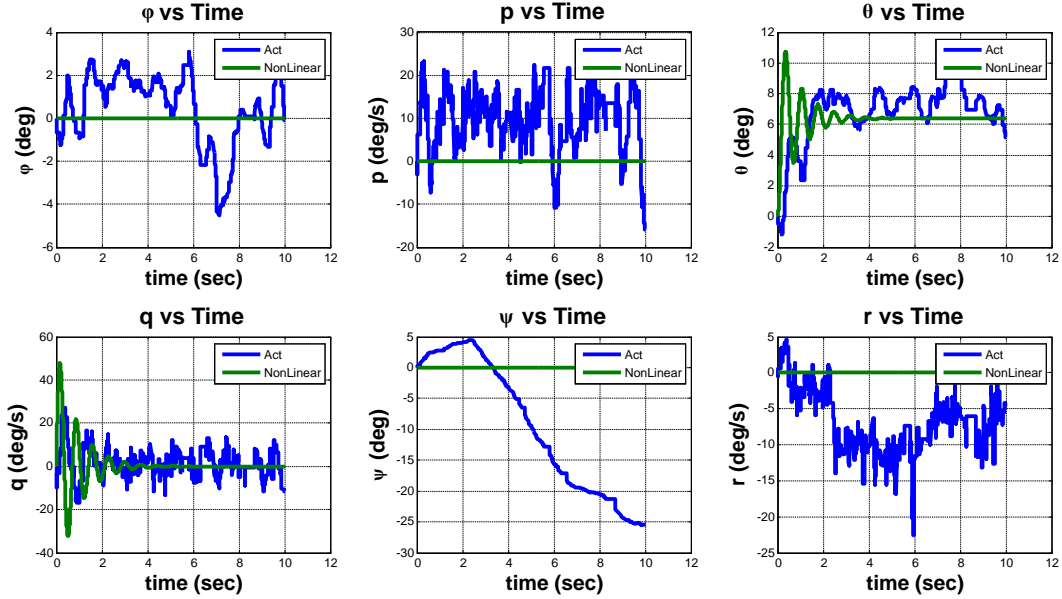


Figure 8.75.: Nominal thrust = 1700 , $\Delta_{Pitch} = 10$

$$\Delta_{Pitch} = -10$$

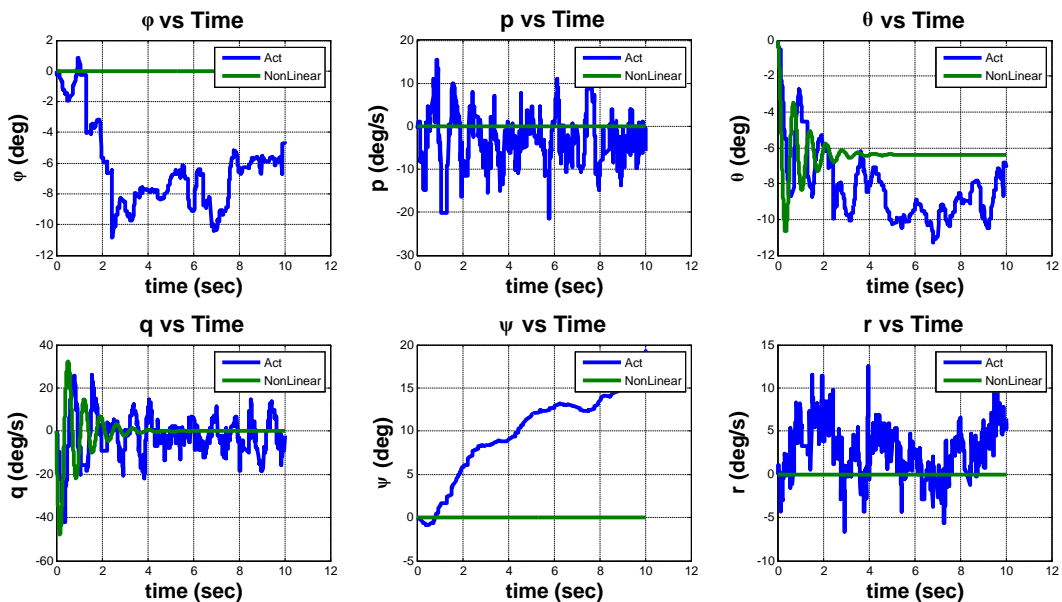


Figure 8.76.: Nominal thrust = 1700 , $\Delta_{Pitch} = -10$

8. Control and Simulation

$$\Delta_{Pitch} = 20$$

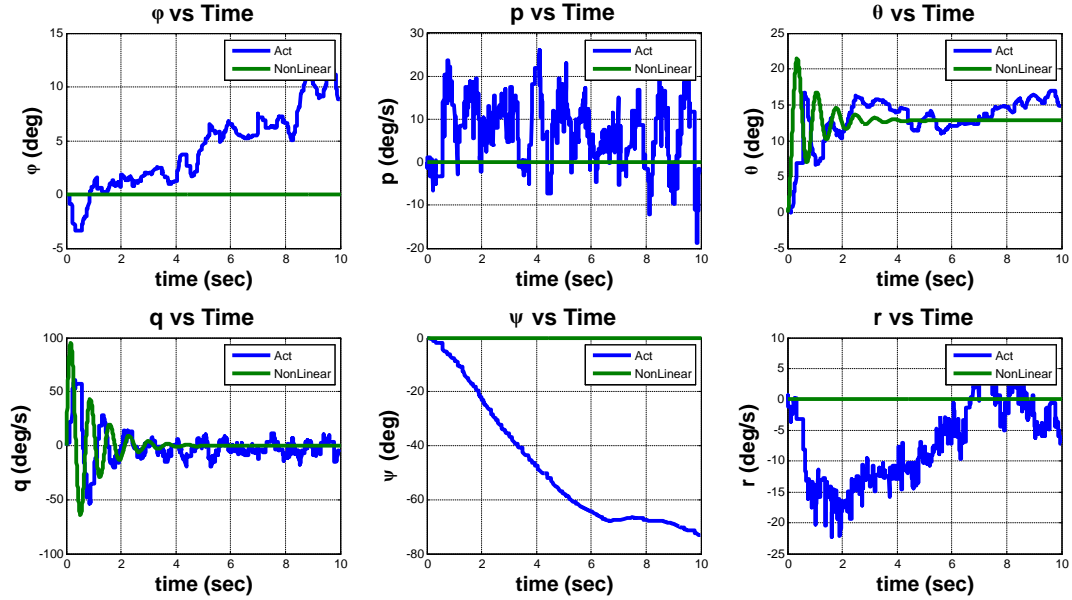


Figure 8.77.: Nominal thrust = 1700 , $\Delta_{Pitch} = 20$

$$\Delta_{Pitch} = -20$$

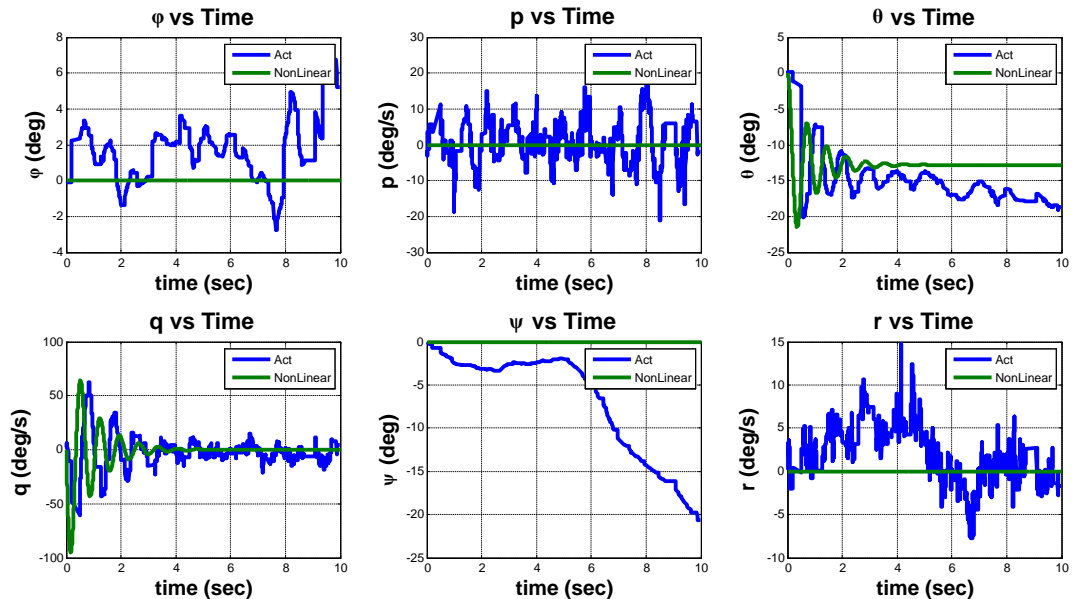


Figure 8.78.: Nominal thrust = 1700 , $\Delta_{Pitch} = -20$

8. Control and Simulation

$$\Delta_{Pitch} = 30$$

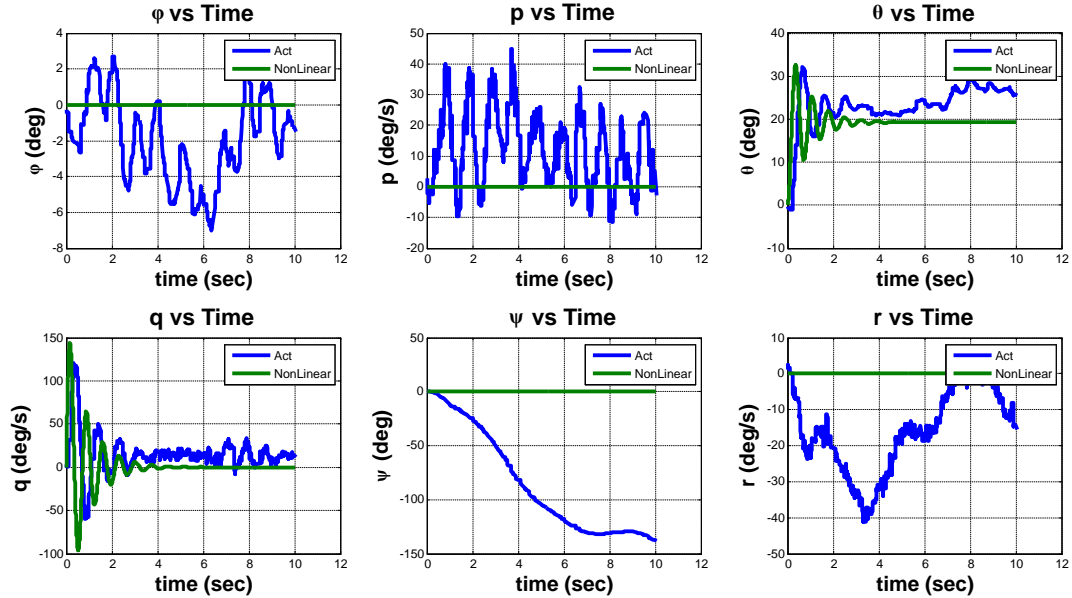


Figure 8.79.: Nominal thrust = 1700 , $\Delta_{Pitch} = 30$

$$\Delta_{Pitch} = -30$$

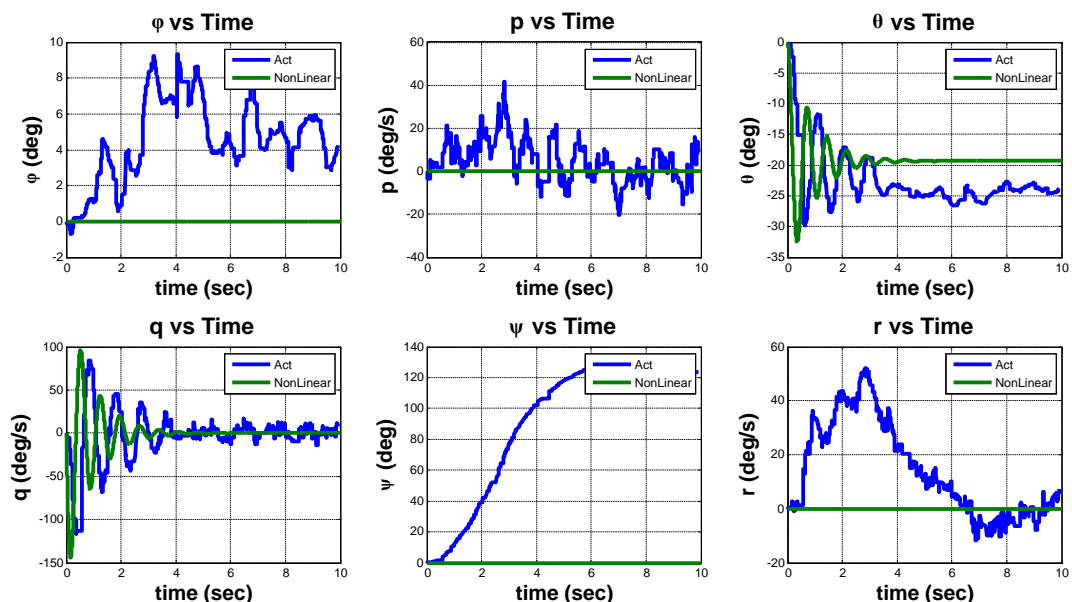


Figure 8.80.: Nominal thrust = 1700 , $\Delta_{Pitch} = -30$

8. Control and Simulation

8.2.3.3. Yaw

$$\Delta Y_{aw} = 10$$

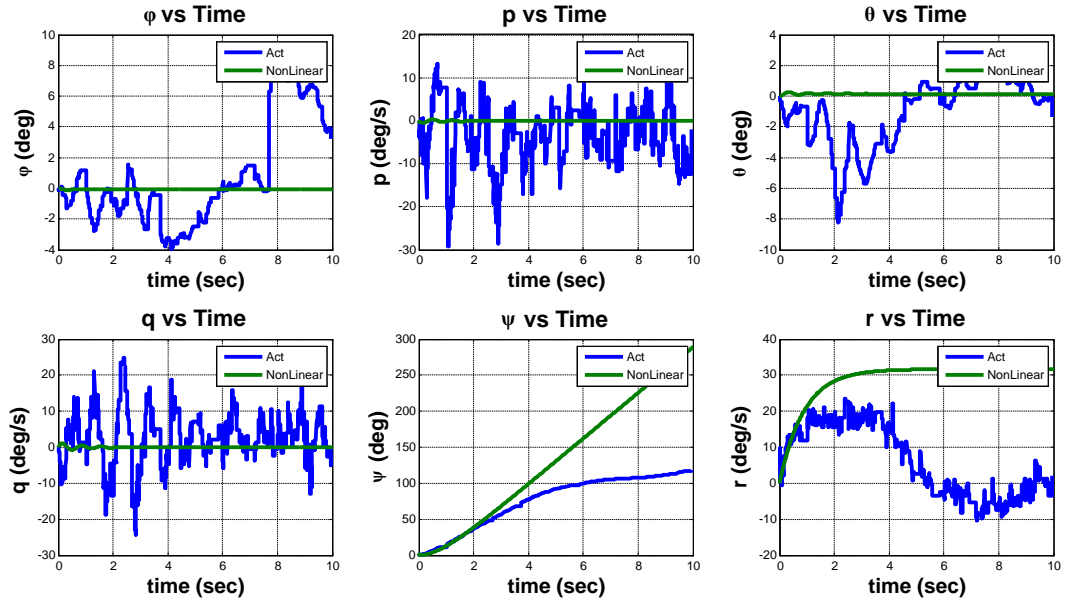


Figure 8.81.: Nominal thrust = 1700 , $\Delta Y_{aw} = 10$

$$\Delta Y_{aw} = -10$$

8. Control and Simulation

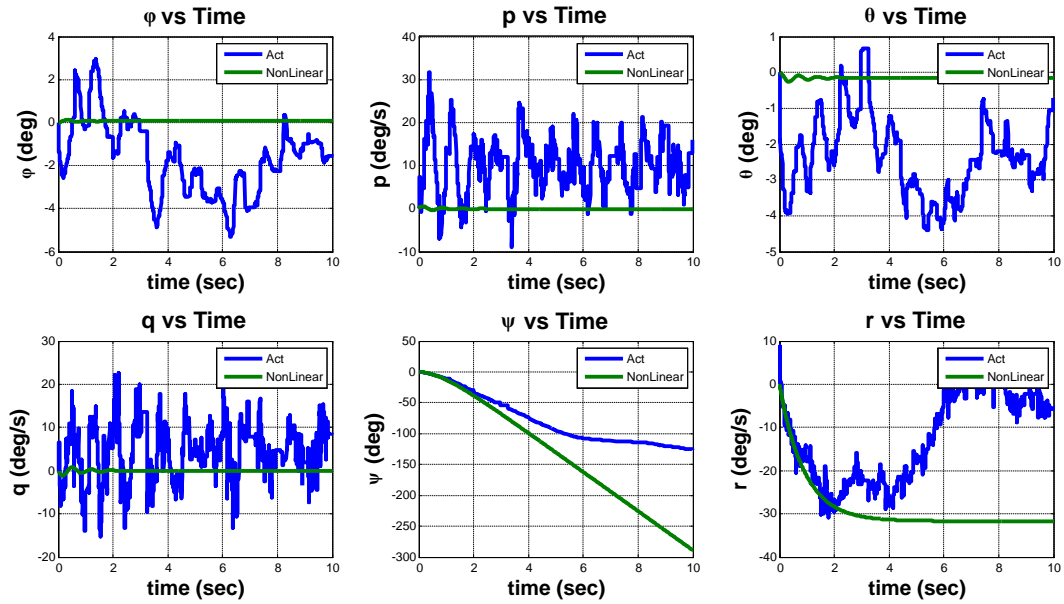


Figure 8.82.: Nominal thrust = 1700 , $\triangle Y_{aw} = -10$

$$\triangle Y_{aw} = 20$$

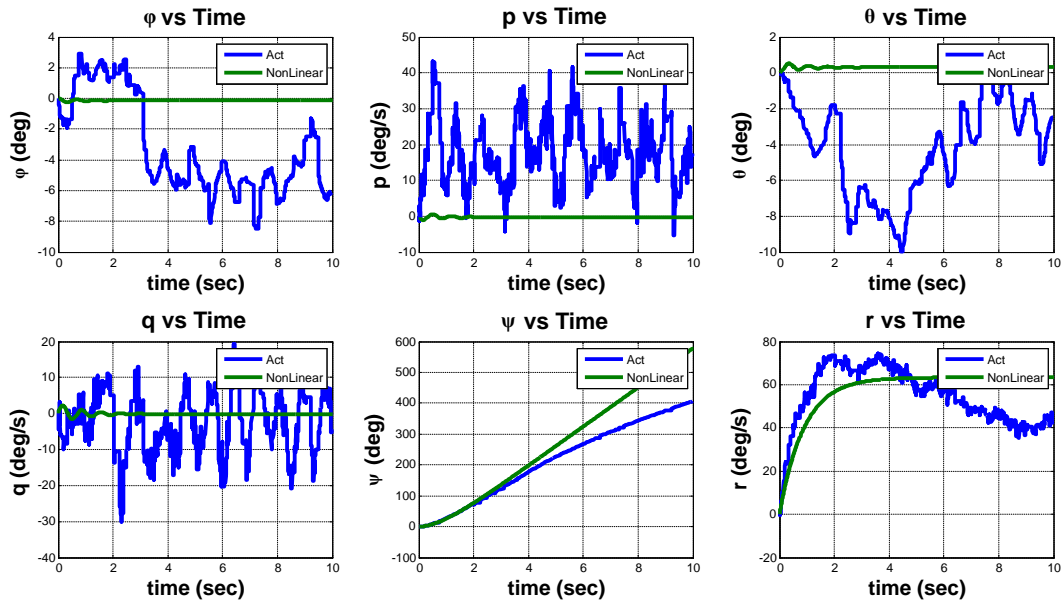


Figure 8.83.: Nominal thrust = 1700 , $\triangle Y_{aw} = 20$

$$\triangle Y_{aw} = -20$$

8. Control and Simulation

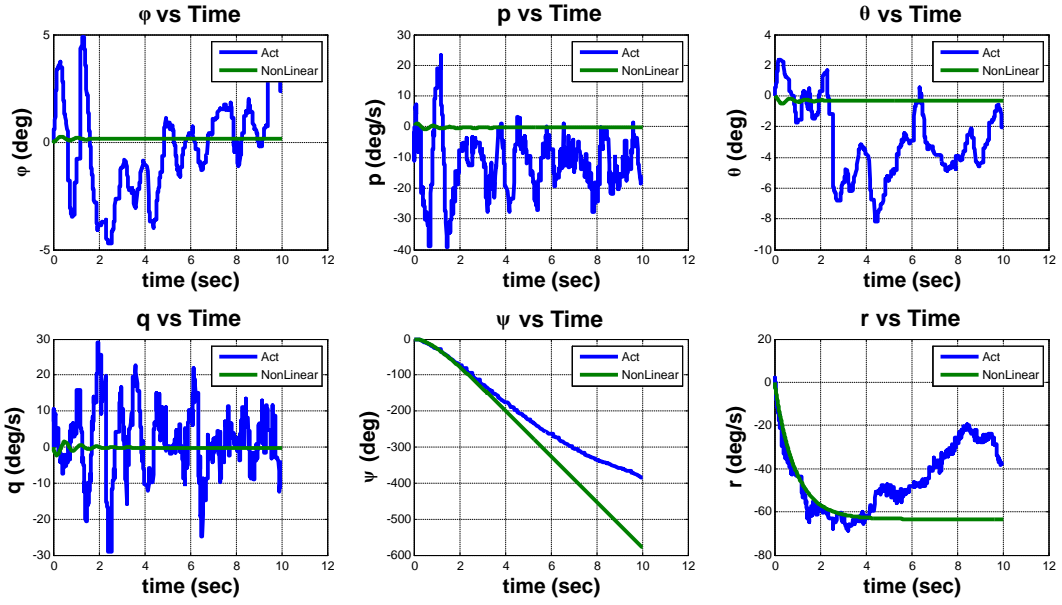


Figure 8.84.: Nominal thrust = 1700 , $\Delta Y_{aw} = -20$

$\Delta Y_{aw} = 30$ test #1

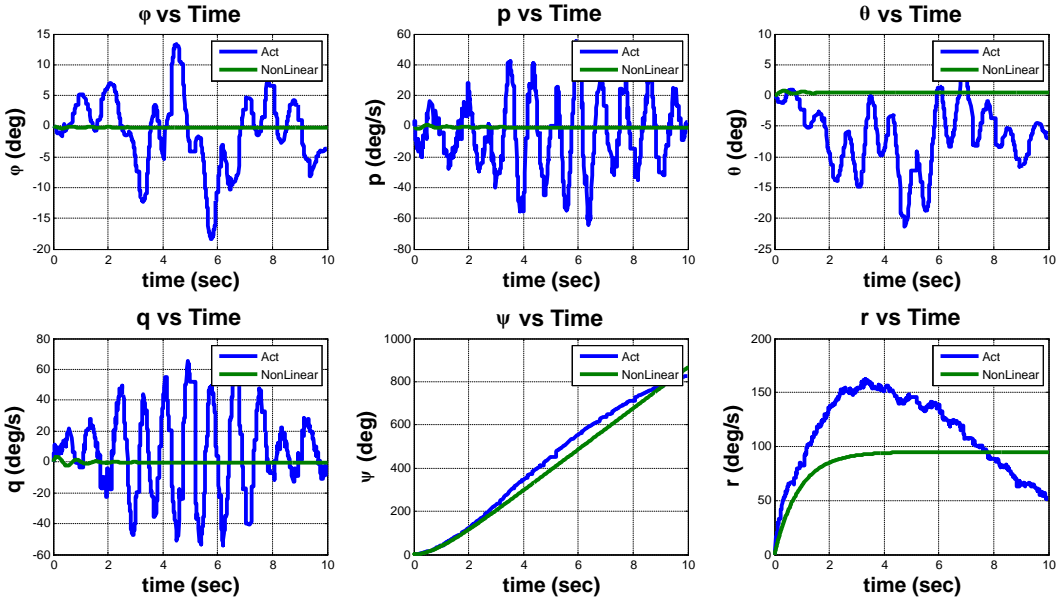


Figure 8.85.: Nominal thrust = 1700 , $\Delta Y_{aw} = 30$ test #1

$\Delta Y_{aw} = 30$ test #2

8. Control and Simulation

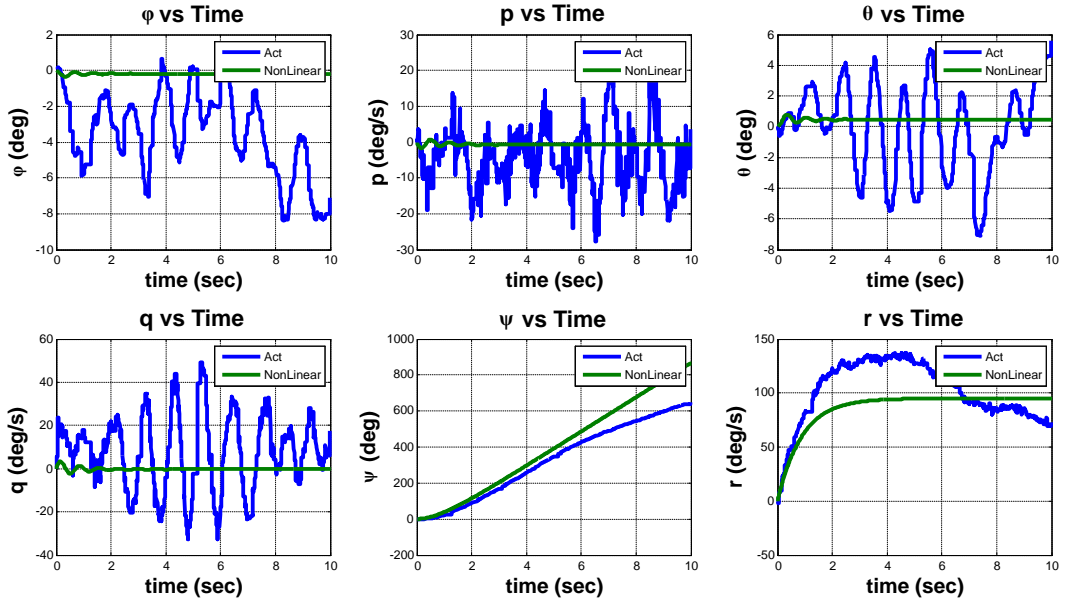


Figure 8.86.: Nominal thrust = 1700 , $\Delta Y_{aw} = 30$ test #2

$$\Delta Y_{aw} = -30$$

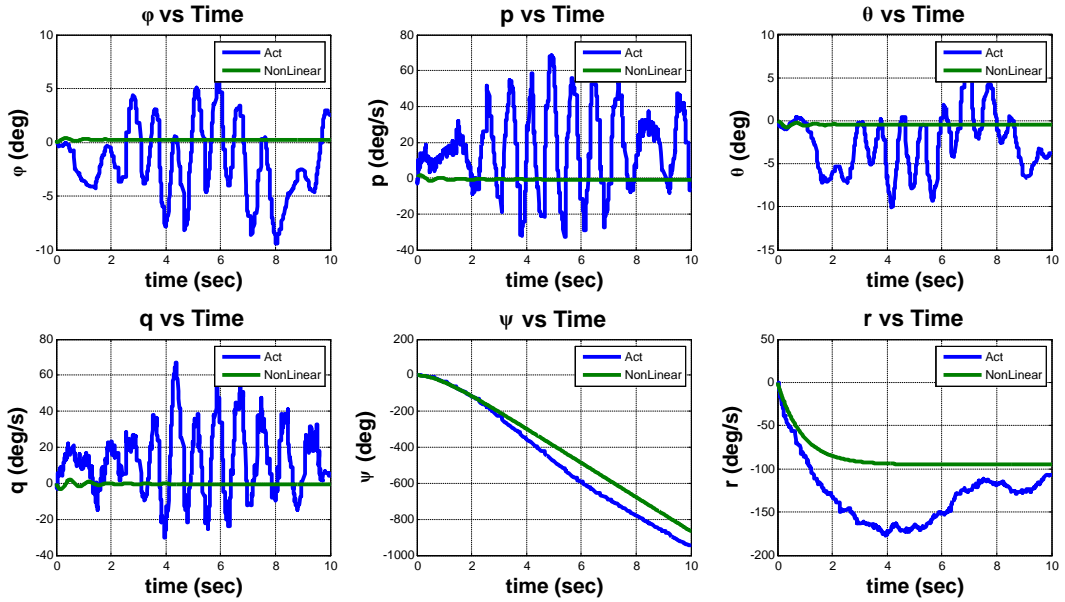


Figure 8.87.: Nominal thrust = 1700 , $\Delta Y_{aw} = -30$

8.3. Linearization

Assume

- Zero initial conditions
- Small angle approximation
 - $C_\theta \approx 1$
 - $S_\theta \approx \Delta\theta$
 - $T_\theta \approx \Delta\theta$
- Thrust and torque constants are equal to

$$\bar{K} = \frac{\sum_{i=1}^n K_i}{n}, \quad \bar{B} = \frac{\sum_{i=1}^n B_i}{n}$$

Force equation in Z direction

$$\therefore Z + mgC_\theta C_\Phi = m(\dot{w} + pv - qu)$$

$$\therefore Z = Z_0 + \Delta Z$$

$$\begin{aligned}\therefore Z &= -mgC_\theta C_\Phi + \sum_{i=1}^n K_i PWM_i \\ \bar{K} \sum_{i=1}^n PWM_i &= m(\dot{w} + pv - qu)\end{aligned}$$

Using Small disturbance theory[24] and checking our previous assumptions (Zero initial conditions)
 $pv = (p_0 + \Delta p)(v_0 + \Delta v) = p_0 * v_0 + v_0 * \Delta p + p_0 * \Delta v = 0$

likewise $qu = 0$

$$\sum_{i=1}^n K_i PWM_i = \bar{K} * \sum_{i=1}^n PWM_i$$

$$\text{Let } \delta_{Col} = \sum_{i=1}^n PWM_i$$

$$\dot{w} = \frac{\bar{K}}{m} \delta_{Col}$$

$$\therefore a_z = \dot{w} + pv - qu = \dot{w}$$

$$\therefore \ddot{z} = \dot{w} = \frac{\bar{K}}{m} \delta_{Col}$$

By taking laplace transform

$$\frac{Z(s)}{\delta_{Col}(s)} = \frac{\bar{K}}{mS^2}$$

8. Control and Simulation

Moment equation in X direction

$$\therefore L = I_x \dot{p} - I_{xz} \dot{r} + qr(I_z - I_y) - I_{xz} pq$$

$$\therefore L = L_0 + \Delta L$$

$$L = -m * g * Length_{RG} * \cos(\theta) * \sin(\phi) - \nu * p - \kappa * \phi + d * \sum_{i=1}^{n/2} (-1)^{i+1} K_{2i} PWM_{2i}$$

$$\text{Let } \delta_{Lat} = \sum_{i=1}^{n/2} (-1)^{i+1} PWM_{2i}$$

Like the previous example, we can simplify it to

$$L = -(m * g * Length_{RG} + \kappa) \Delta\phi - \nu * \Delta p + d * \bar{K} * \delta_{Lat}$$

$$qr = 0 \text{ and } I_{xz} = 0$$

for simplicity let $\Delta\phi = \phi$, $\Delta p = p$ and we know that these quantities are deltas of the original values

$$\therefore I_x \dot{p} = -(m * g * Length_{RG} + \kappa) \phi - \nu * p + d * \bar{K} * \delta_{Lat}$$

$$\therefore \ddot{\phi} = \dot{p}$$

$$\therefore I_x \ddot{\phi} = -(m * g * Length_{RG} + \kappa) \phi - \nu * \dot{\phi} + d * \bar{K} * \delta_{Lat}$$

$$\therefore I_x \ddot{\phi} + \nu * \dot{\phi} + (m * g * Length_{RG} + \kappa) \phi = d * \bar{K} * \delta_{Lat}$$

By taking laplace transform

$$\frac{\phi(s)}{\delta_{Lat}(s)} = \frac{d * \bar{K}}{I_x S^2 + \nu * S + (m * g * Length_{RG} + \kappa)}$$

Moment equation in Y direction

As the system is symmetric in both structure and load, the transfer function is the same.

$$\frac{\theta(s)}{\delta_{Long}(s)} = \frac{d * \bar{K}}{I_y S^2 + \nu * S + (m * g * Length_{RG} + \kappa)}$$

$$\text{Let } \delta_{Long} = \sum_{i=1}^{n/2+1} (-1)^{i+1} PWM_{2i-1}$$

Moment equation in Z direction

$$\therefore N = -I_{xz} \dot{p} + I_z \dot{r} + pq(I_y - I_x) + I_{xz} qr$$

$$\therefore N = N_0 + \Delta N$$

$$N = -\nu * r + \sum_{i=1}^{n/2} B_{2i} * PWM_{2i} - \sum_{i=1}^{n/2+1} B_{2i-1} * PWM_{2i-1}$$

$$\text{Let } \delta_{Pend} = \sum_{i=1}^{n/2+1} PWM_{2i-1} - \sum_{i=1}^{n/2} PWM_{2i}$$

8. Control and Simulation

Like the previous example, we can simplify it to

$$N = -\nu * \Delta r + \bar{B} * \delta_{Pend}$$

$$pq = 0 \text{ and } I_{xz} = 0$$

for simplicity let $\Delta\psi = \psi$, $\Delta r = r$ and we know that these quantities are deltas of the original values

$$\therefore I_z \dot{r} = -\nu * r + \bar{B} * \delta_{Pend}$$

$$\therefore \ddot{\psi} = \dot{r}$$

$$\therefore I_z \ddot{\psi} = -\nu * \dot{\psi} + \bar{B} * \delta_{Pend}$$

$$\therefore I_z \ddot{\psi} + \nu * \dot{\psi} = \bar{B} * \delta_{Pend}$$

By taking laplace transform

$$\frac{\psi(s)}{\delta_{Pend}(s)} = \frac{\bar{B}}{I_z S^2 + \nu * S}$$

8.4. Comparing with Nonlinear Response

This step is made to make sure that our linear model's response is close to the nonlinear model, We simulate different inputs.

Nom.Thrust = 1650	PWM1 = 0	PWM2 = 10	PWM3 = 0	PWM4 = 10
-------------------	----------	-----------	----------	-----------

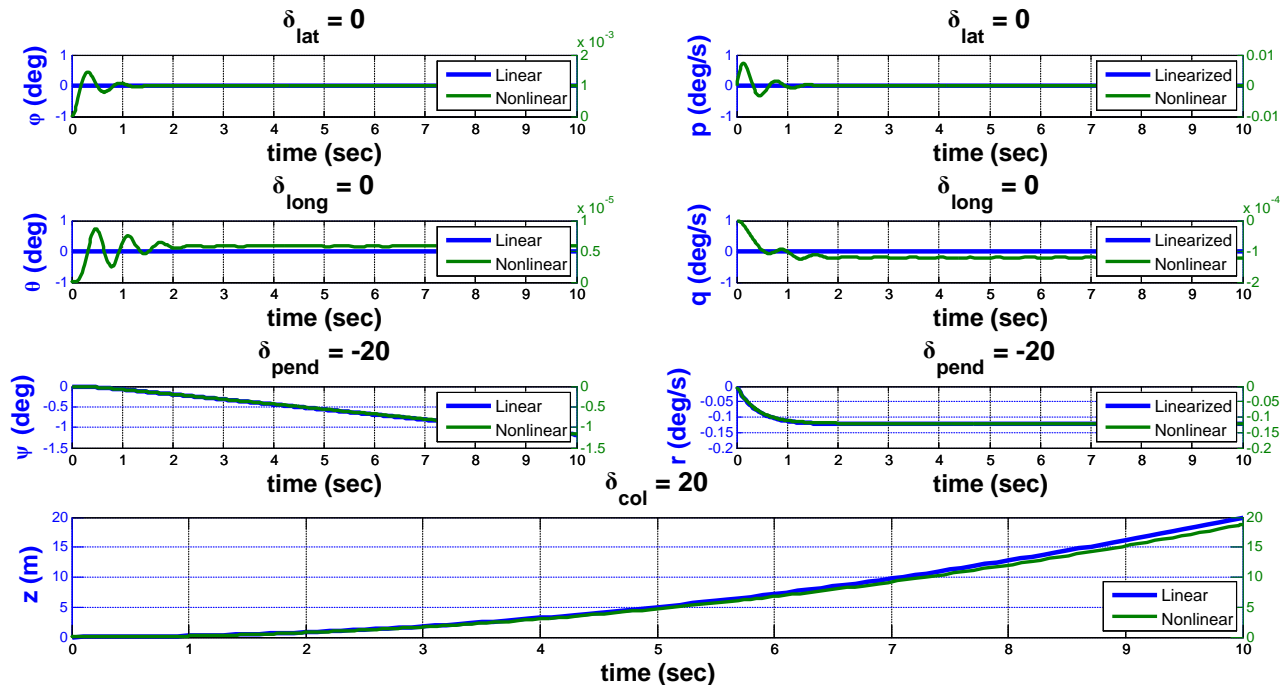


Figure 8.88.: Response #!

8. Control and Simulation

Nom.Thrust = 1650	PWM1 = 9	PWM2 = 10	PWM3 = 10	PWM4 = 10
-------------------	----------	-----------	-----------	-----------

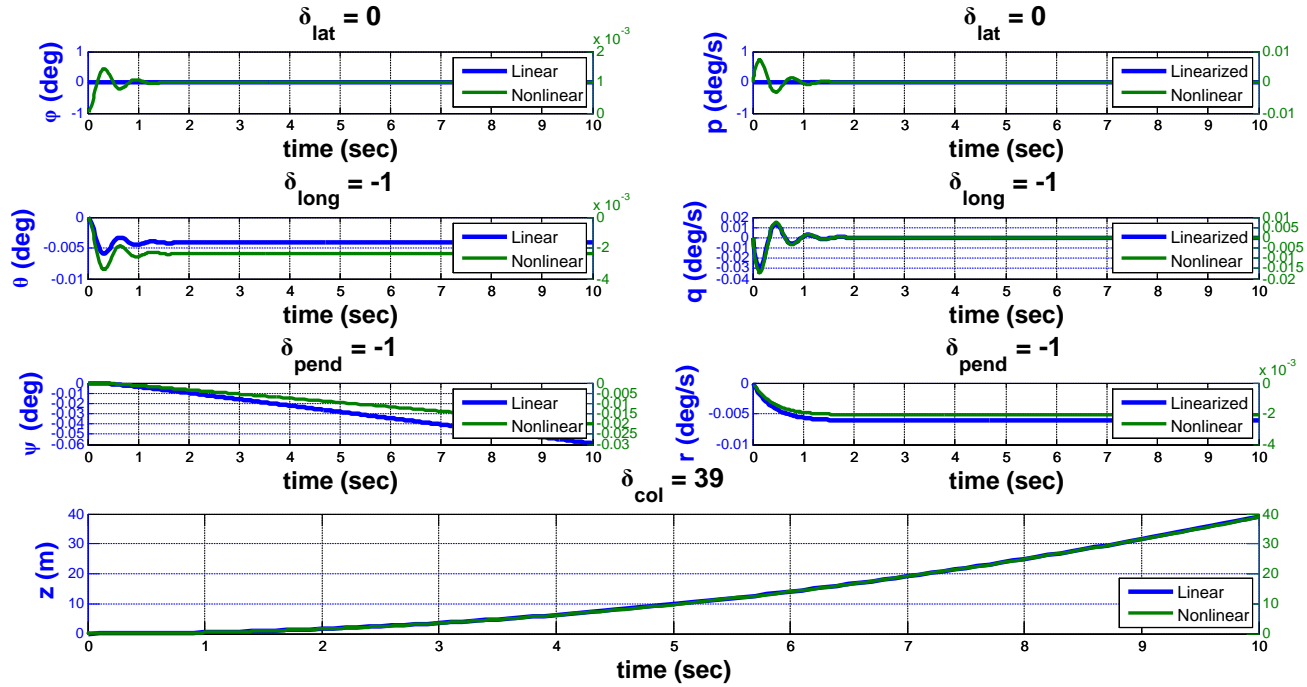


Figure 8.89.: Response #2

Nom.Thrust = 1650	PWM1 = 10	PWM2 = 0	PWM3 = 10	PWM4 = 0
-------------------	-----------	----------	-----------	----------

8. Control and Simulation

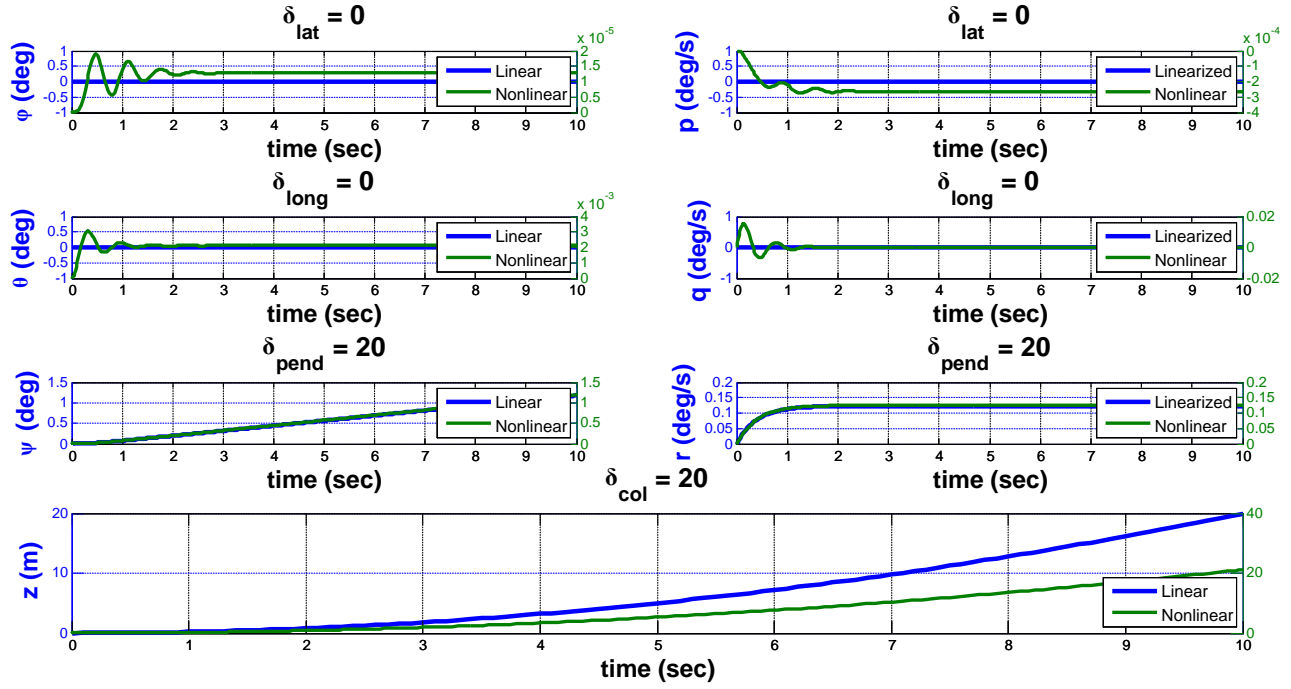


Figure 8.90.: Response #3

Nom.Thrust = 1650	PWM1 = 10	PWM2 = 9	PWM3 = 10	PWM4 = 10
-------------------	-----------	----------	-----------	-----------

8. Control and Simulation

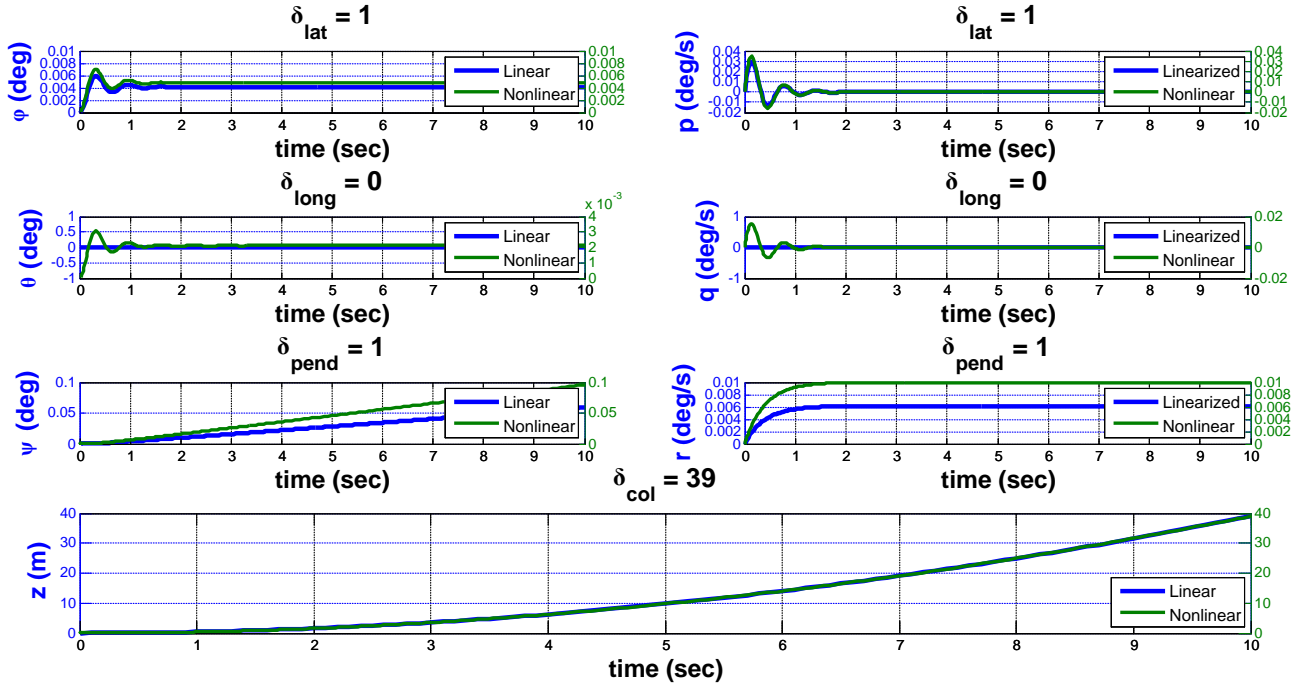


Figure 8.91.: Response #4

Nom.Thrust = 1700	PWM1 = 0	PWM2 = 10	PWM3 = 0	PWM4 = 10
-------------------	----------	-----------	----------	-----------

8. Control and Simulation

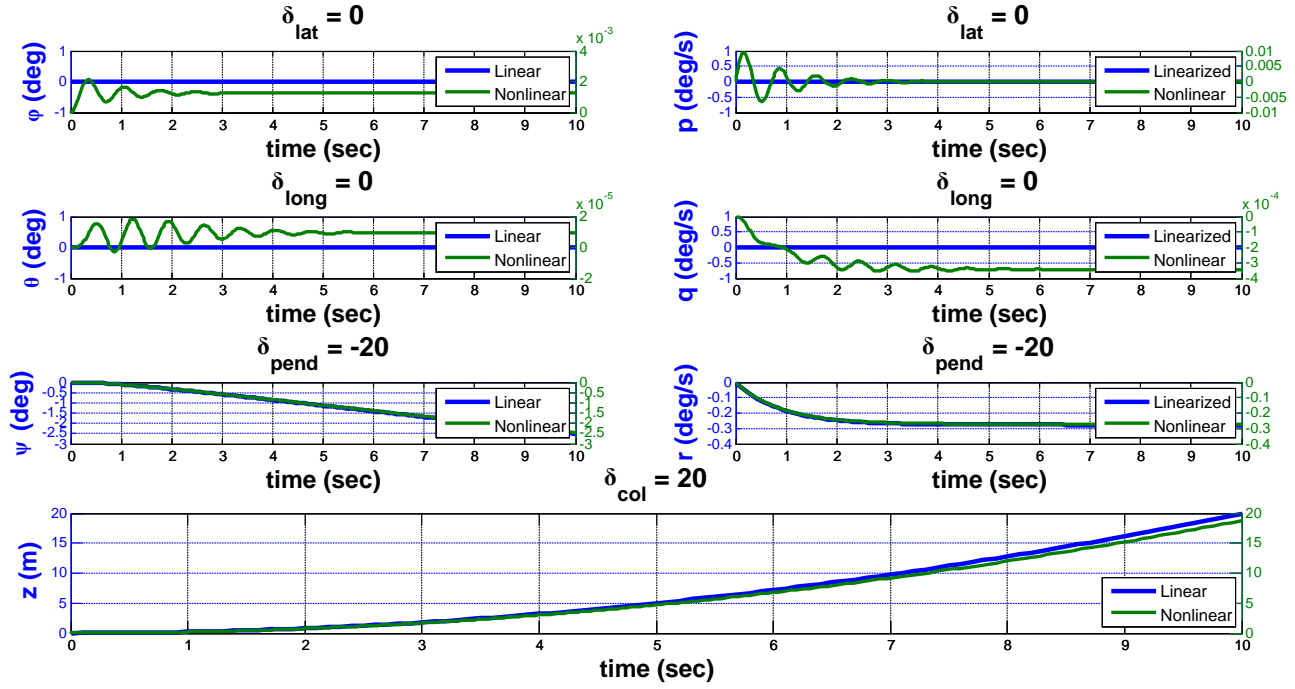


Figure 8.92.: Response #5

Nom.Thrust = 1700	PWM1 = 9	PWM2 = 10	PWM3 = 10	PWM4 = 10
-------------------	----------	-----------	-----------	-----------

8. Control and Simulation

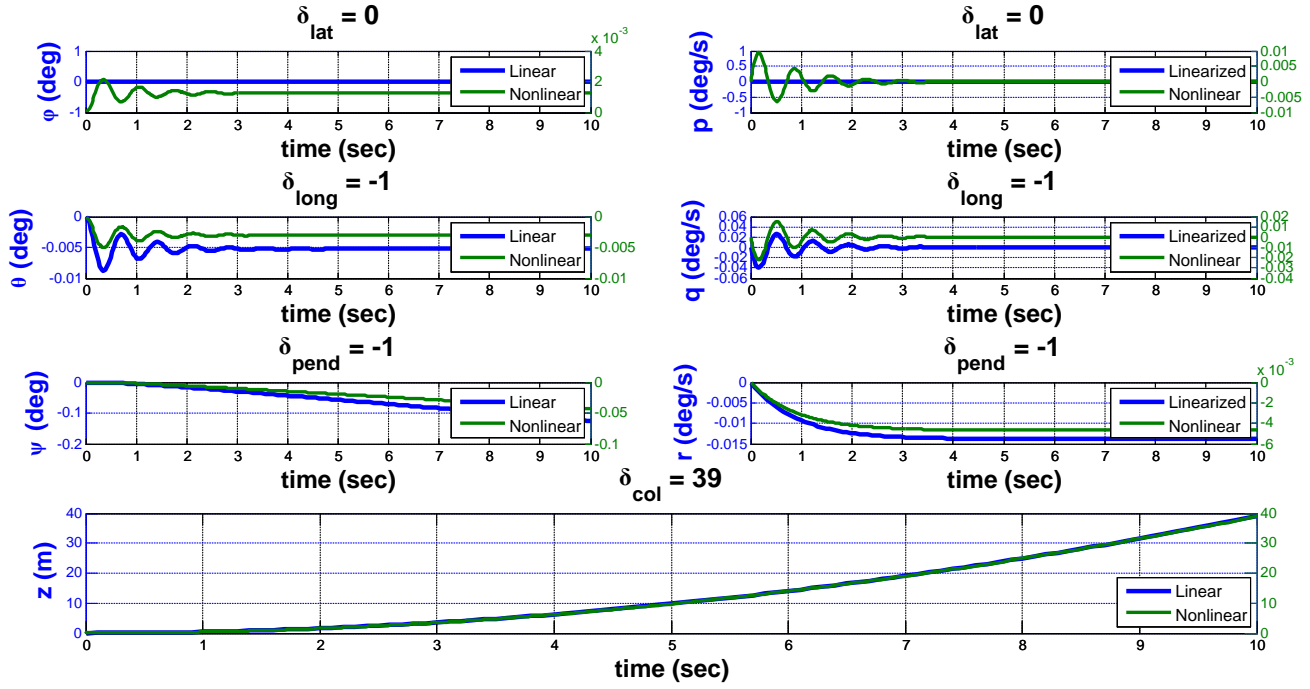


Figure 8.93.: Response #6

Nom.Thrust = 1700	PWM1 = 10	PWM2 = 0	PWM3 = 10	PWM4 = 0
-------------------	-----------	----------	-----------	----------

8. Control and Simulation

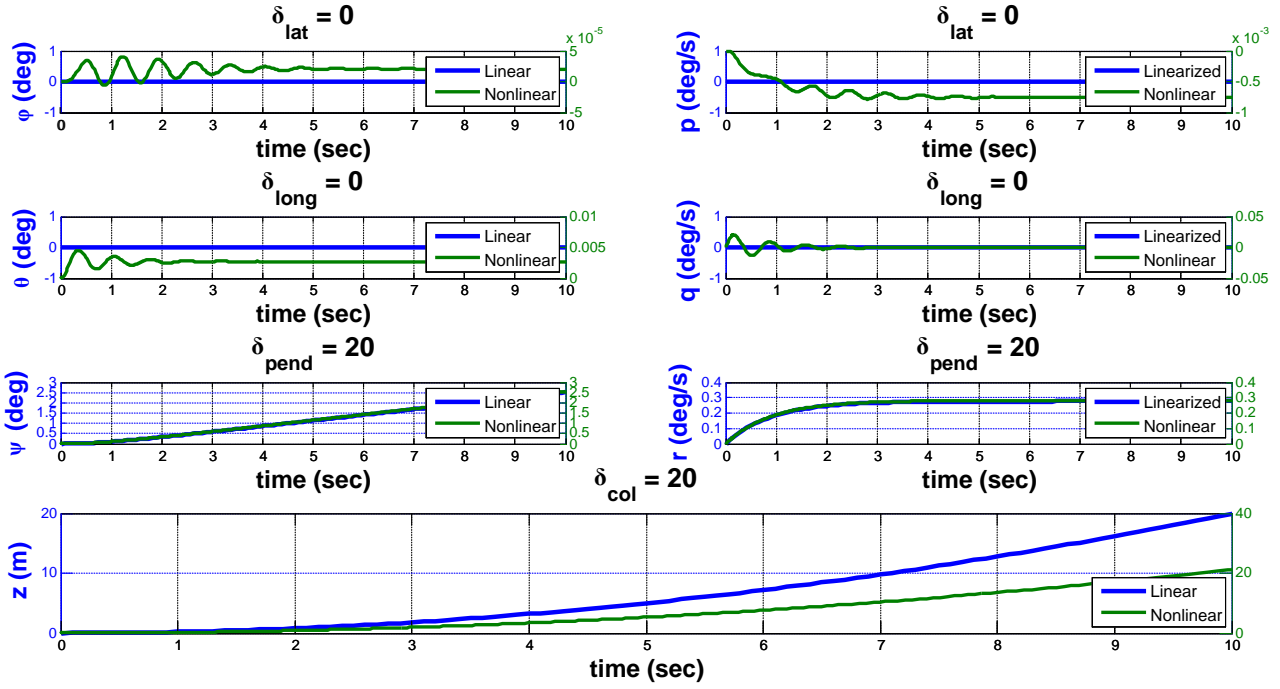


Figure 8.94.: Response #7

Nom.Thrust = 1700	PWM1 = 10	PWM2 = 9	PWM3 = 10	PWM4 = 10
-------------------	-----------	----------	-----------	-----------

8. Control and Simulation

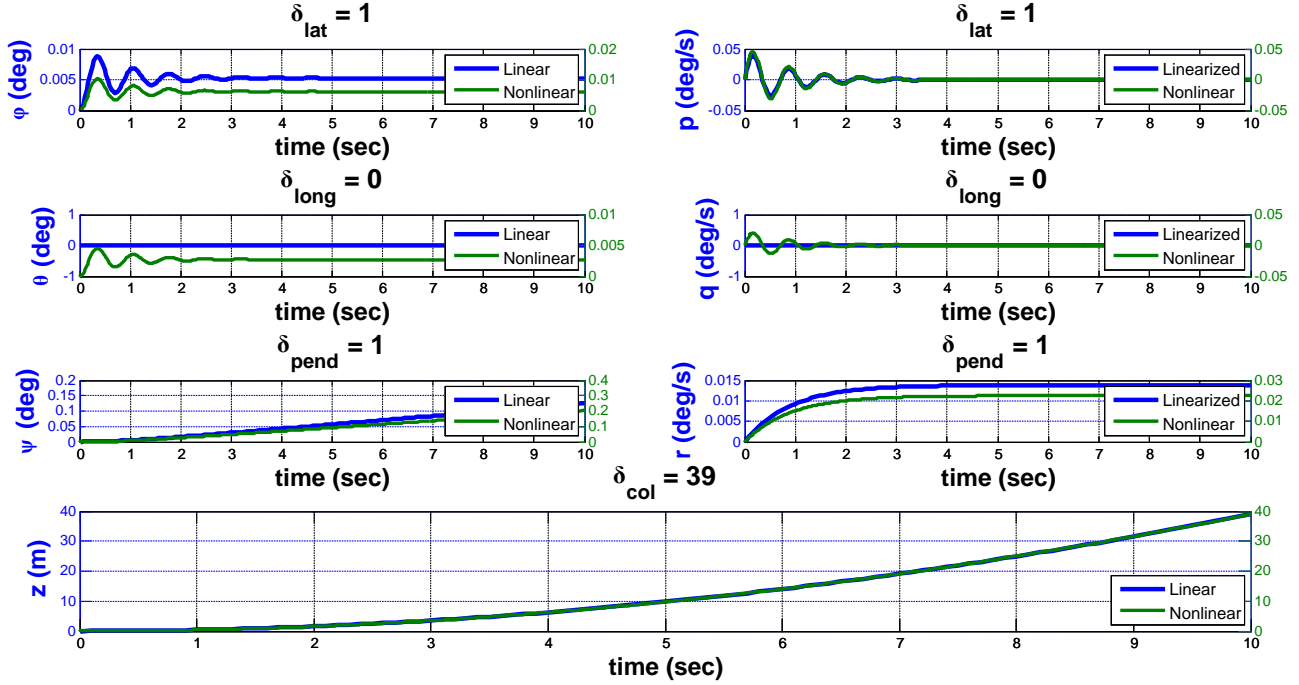


Figure 8.95.: Response #8

8.5. Control

We followed design procedure mentioned in 2.5.

We designed two times at PWM = 1650 and 1700

Design criteria

For z transfer function

settling time = 4 sec	OS = 0.01
-----------------------	-----------

For p,q transfer function

settling time = 2 sec	OS = 0.01
-----------------------	-----------

For r transfer function

settling time = 1 sec	OS = 0.01
-----------------------	-----------

For ϕ, θ transfer function

settling time = 3 sec	OS = 0.05
-----------------------	-----------

For ψ transfer function

settling time = 3 sec	OS = 0.01
-----------------------	-----------

8. Control and Simulation

Response

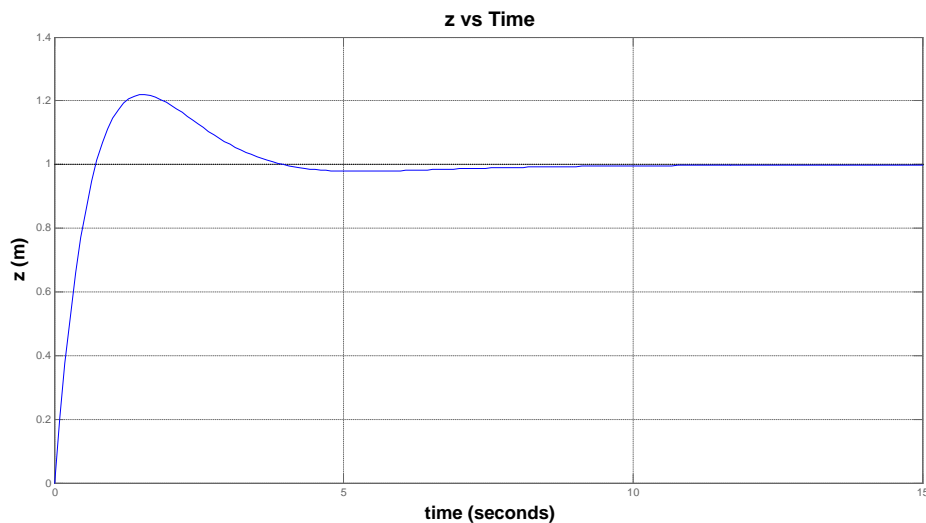


Figure 8.96.: Z vs time

At Nom. Thrust = 1650

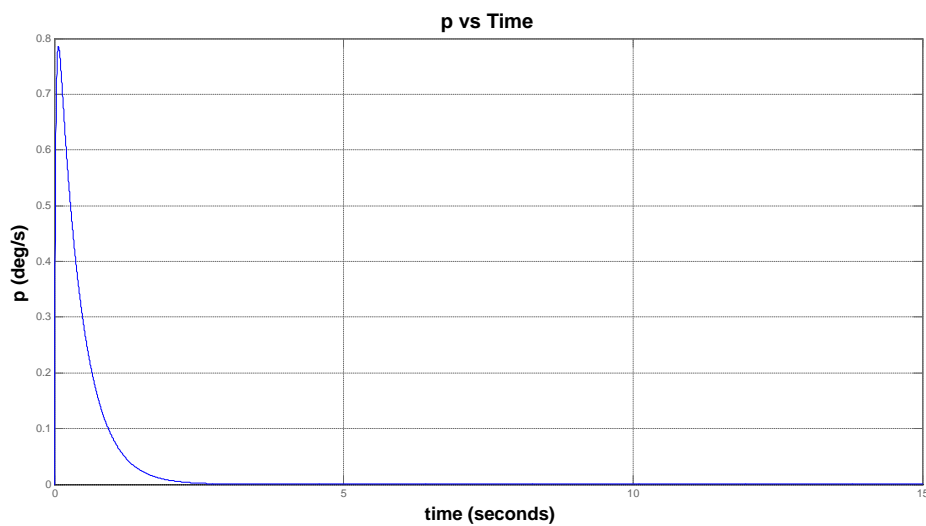


Figure 8.97.: p vs time

8. Control and Simulation

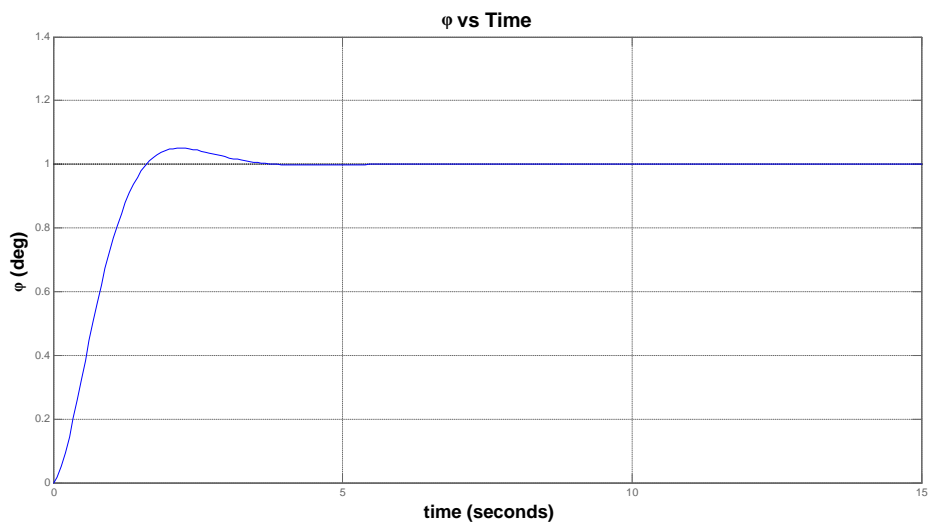


Figure 8.98.: ϕ vs time

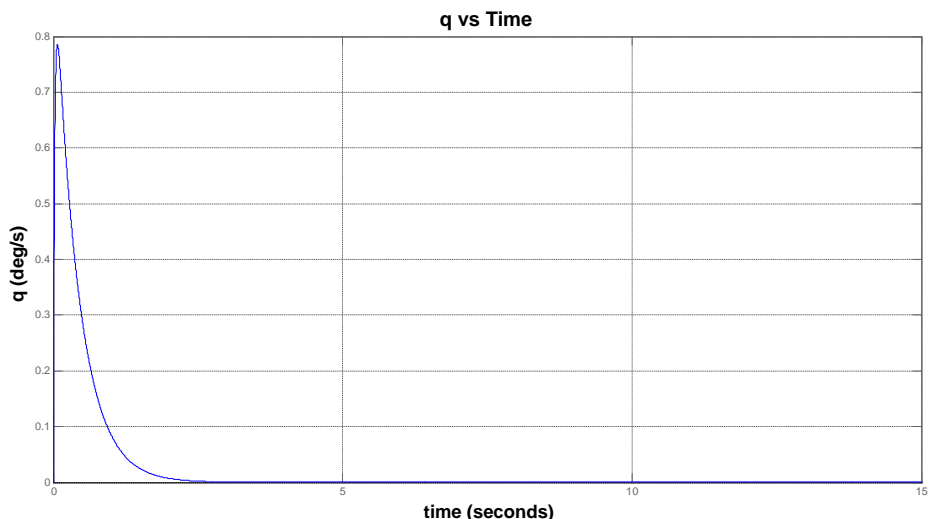


Figure 8.99.: q vs time

8. Control and Simulation

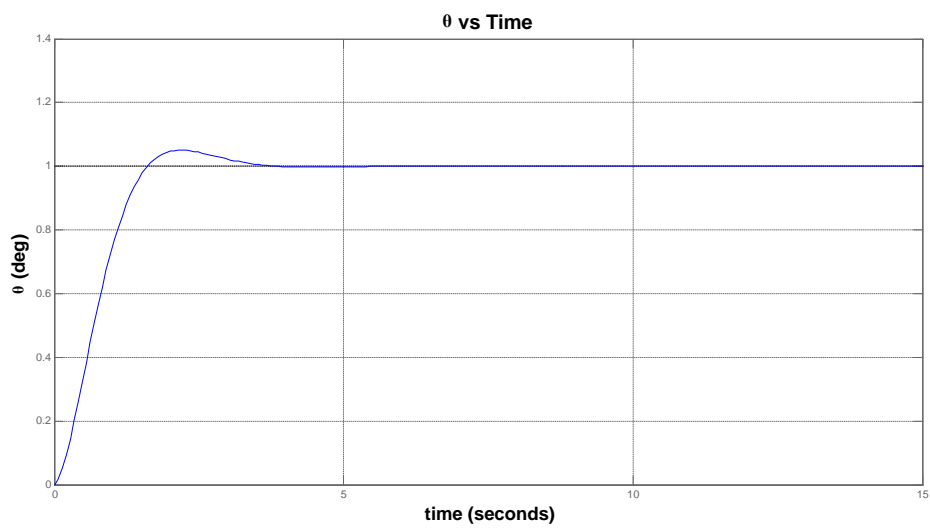


Figure 8.100.: θ vs time

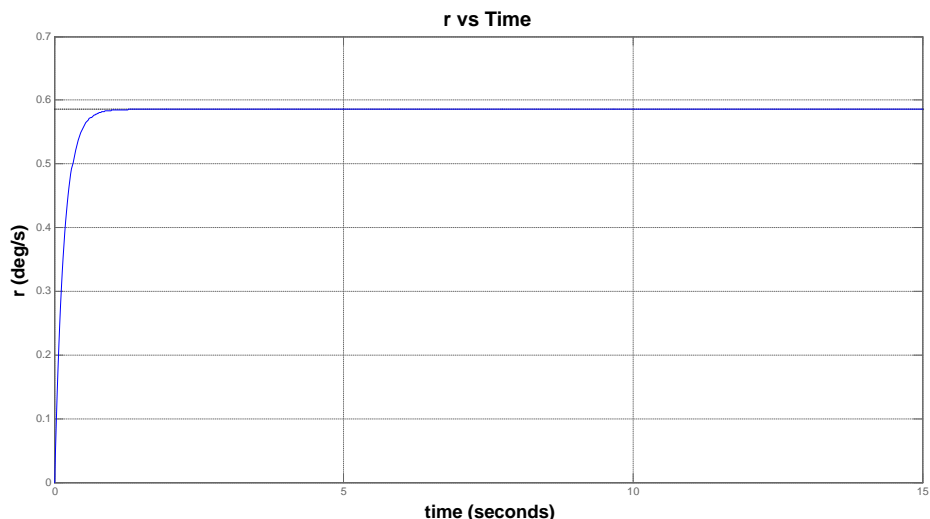


Figure 8.101.: r vs time

8. Control and Simulation

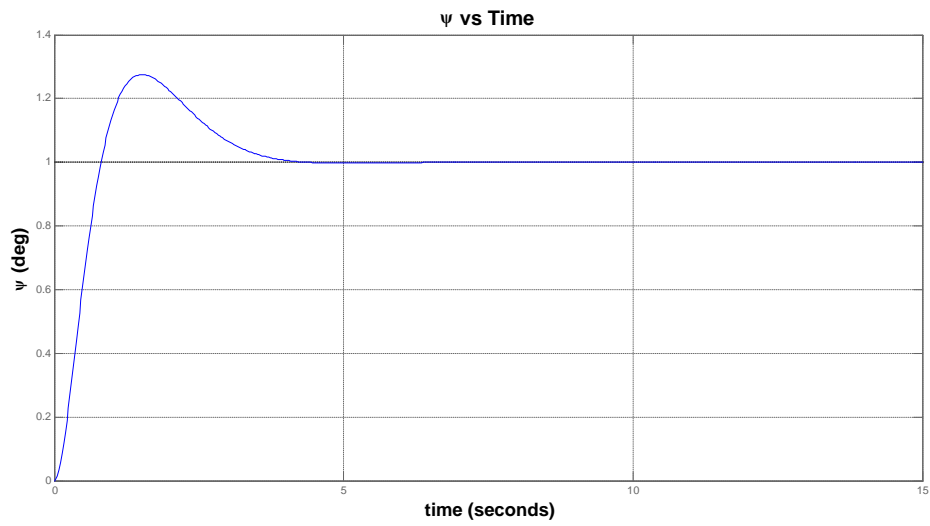


Figure 8.102.: ψ vs time

At Nom. Thrust = 1700

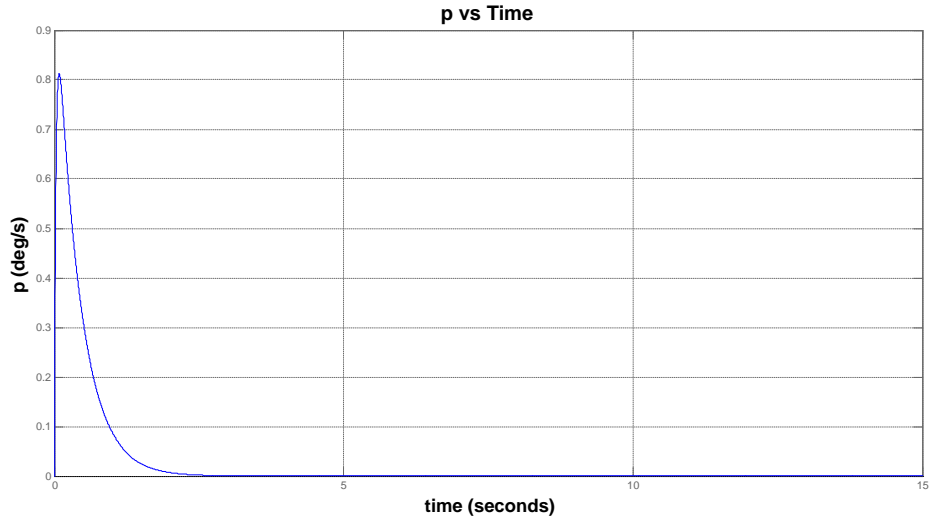


Figure 8.103.: p vs time

8. Control and Simulation

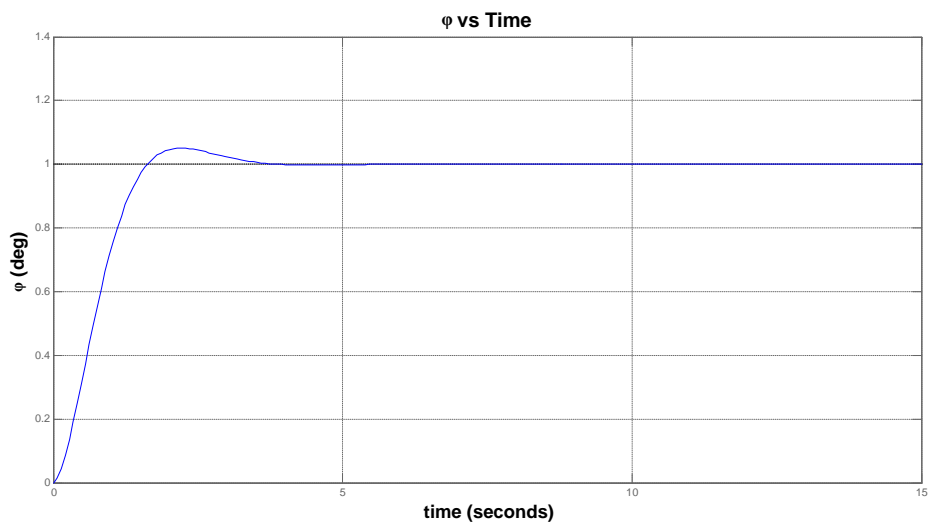


Figure 8.104.: ϕ vs time

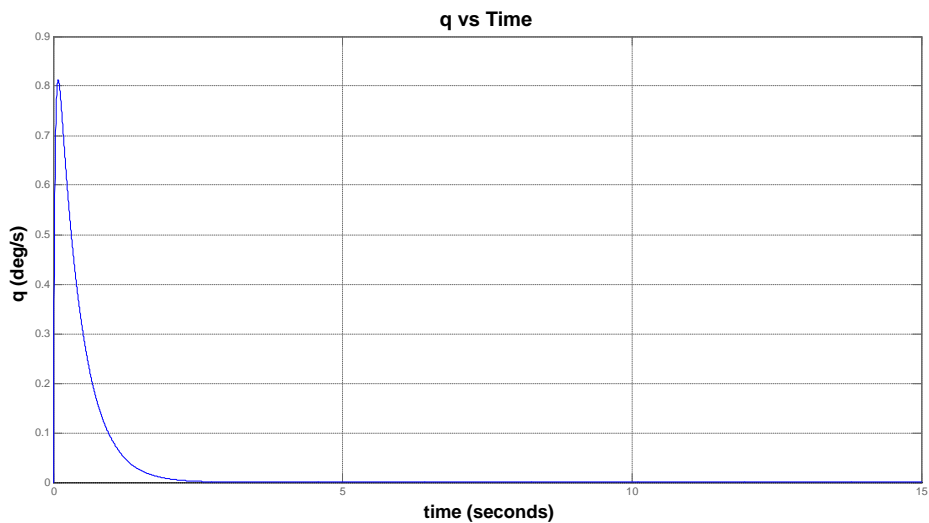


Figure 8.105.: q vs time

8. Control and Simulation

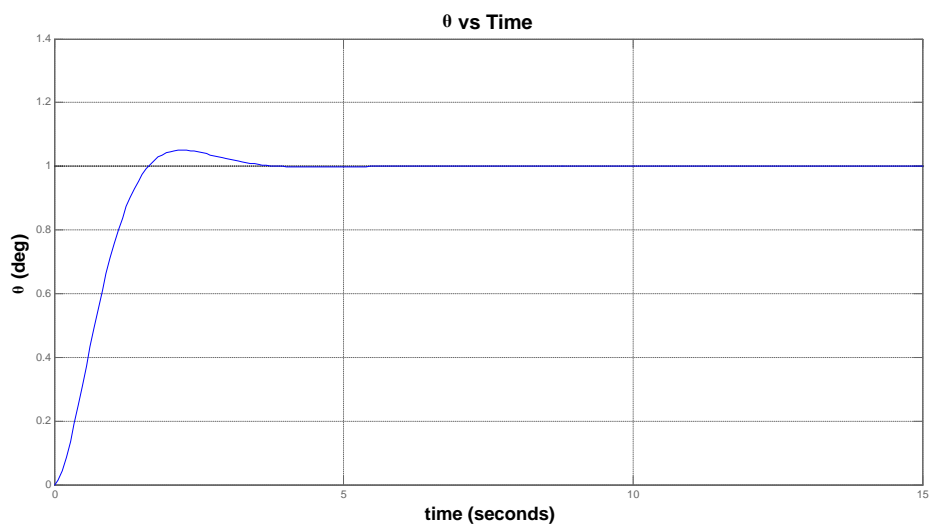


Figure 8.106.: θ vs time

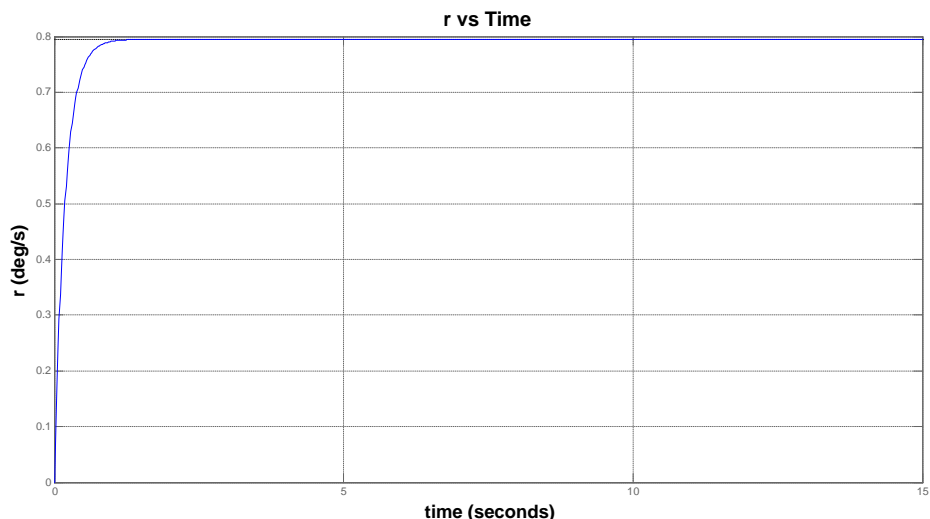


Figure 8.107.: r vs time

8. Control and Simulation

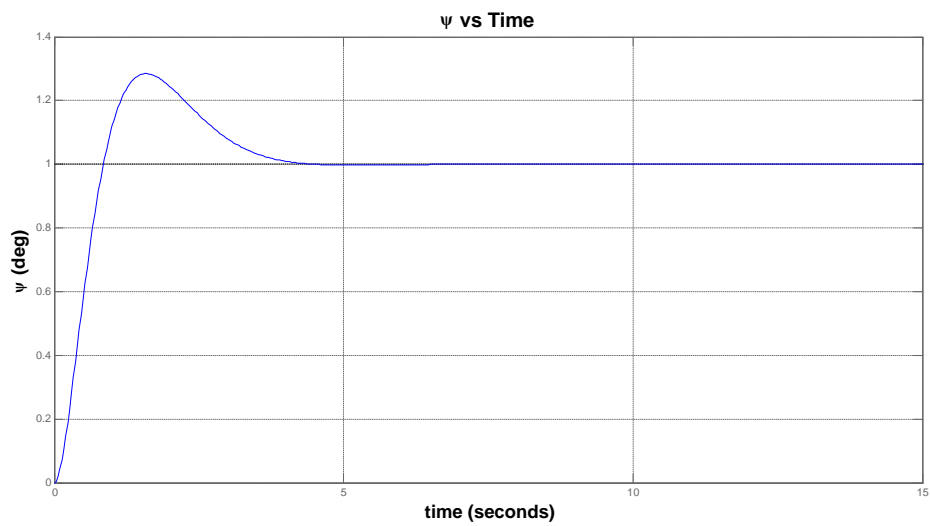


Figure 8.108.: ψ vs time

8. Control and Simulation

8.6. Applying Controller on The Non Linear model

Required Z = 1 m

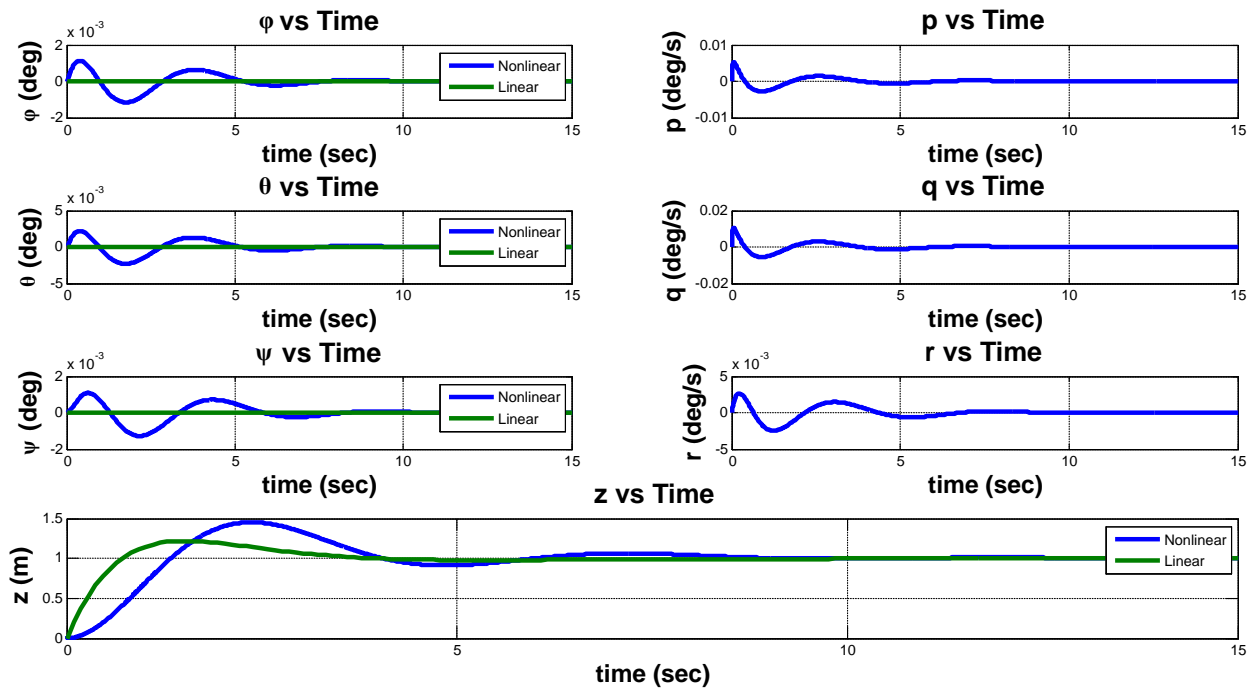


Figure 8.109.: Response at Nom. Thrust = 1650

8. Control and Simulation

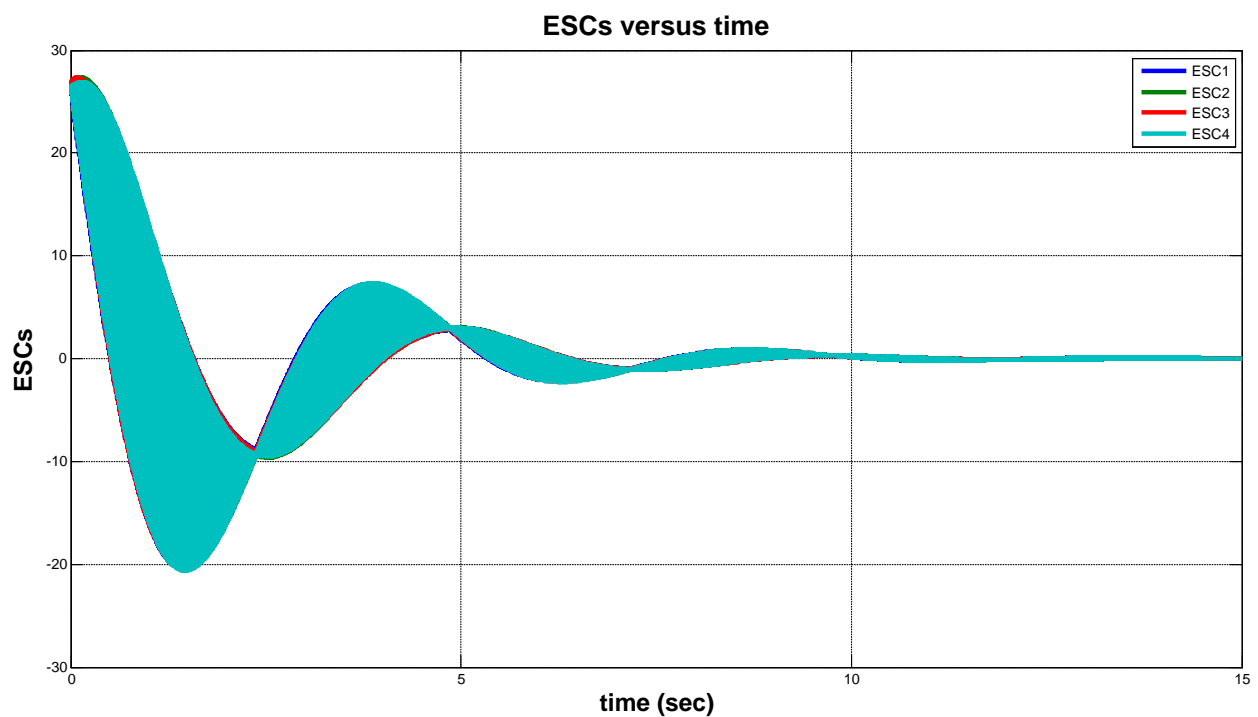


Figure 8.110.: Control actions at Nom. Thrust = 1650

8. Control and Simulation

At Nom. Thrust = 1650

Required $\phi = \theta = \psi = 0.1$ rad

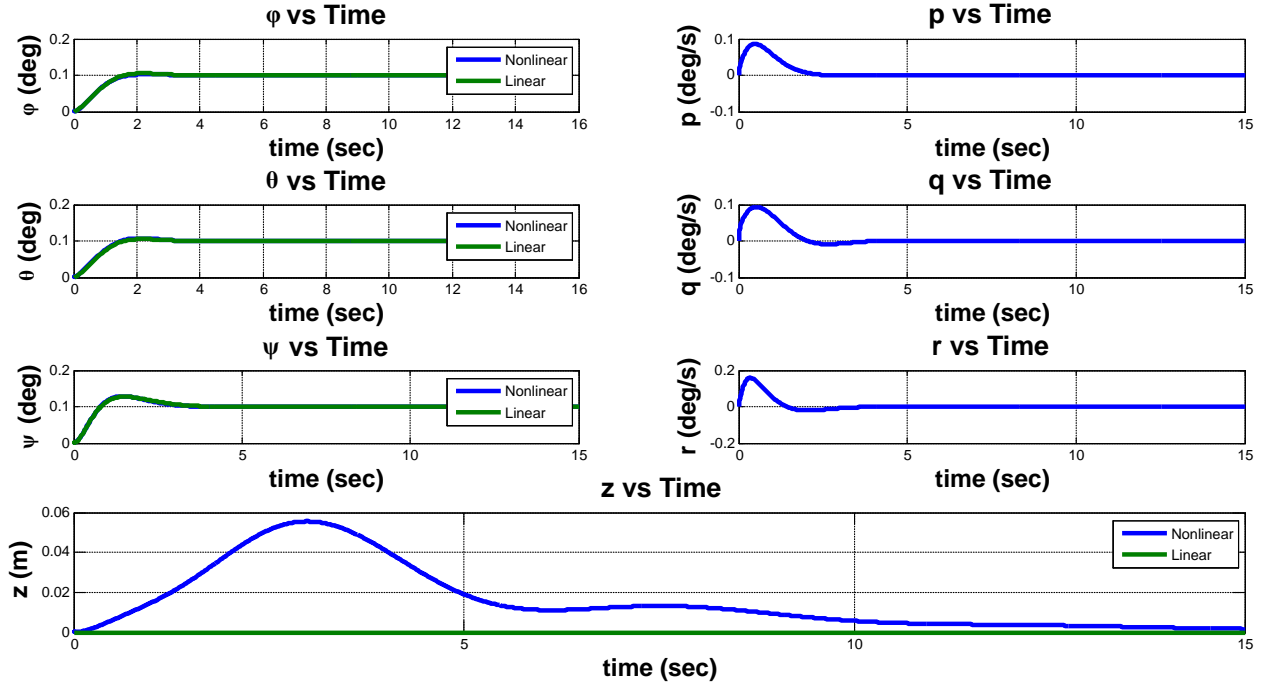


Figure 8.111.: Response at Nom. Thrust = 1650

8. Control and Simulation

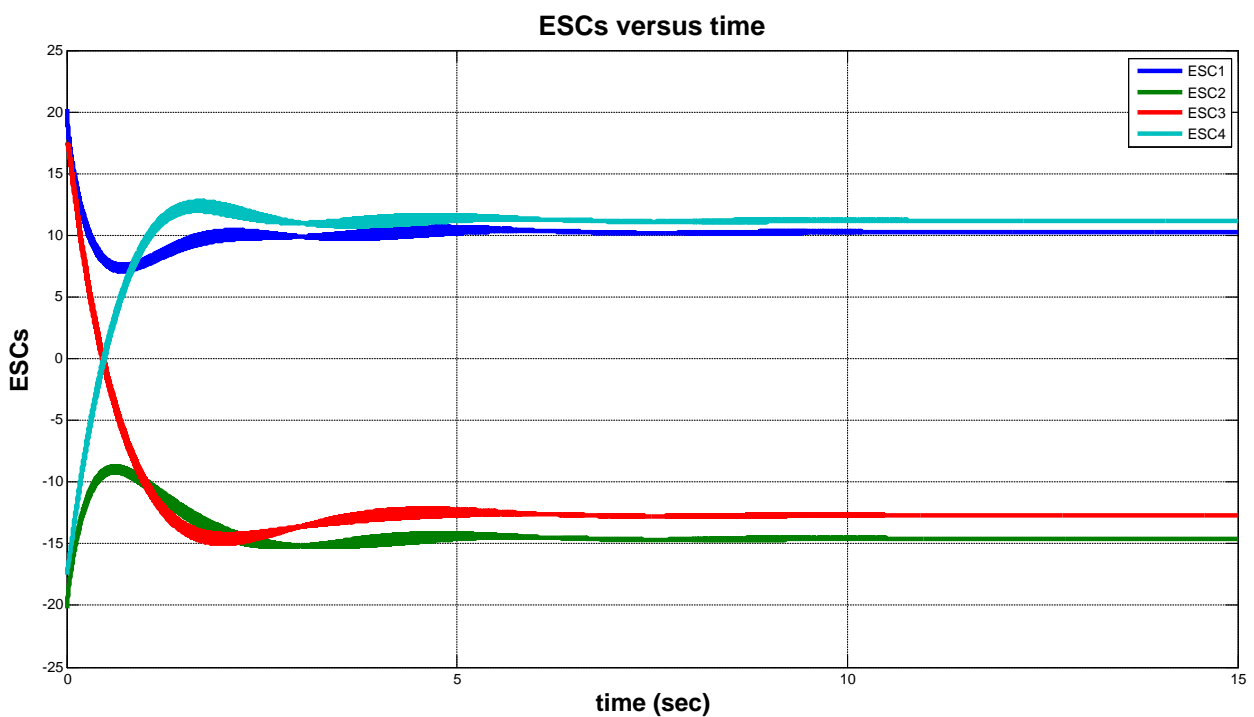


Figure 8.112.: Control actions at Nom. Thrust = 1650

8. Control and Simulation

Required $\phi = \theta = \psi = -0.1$ rad

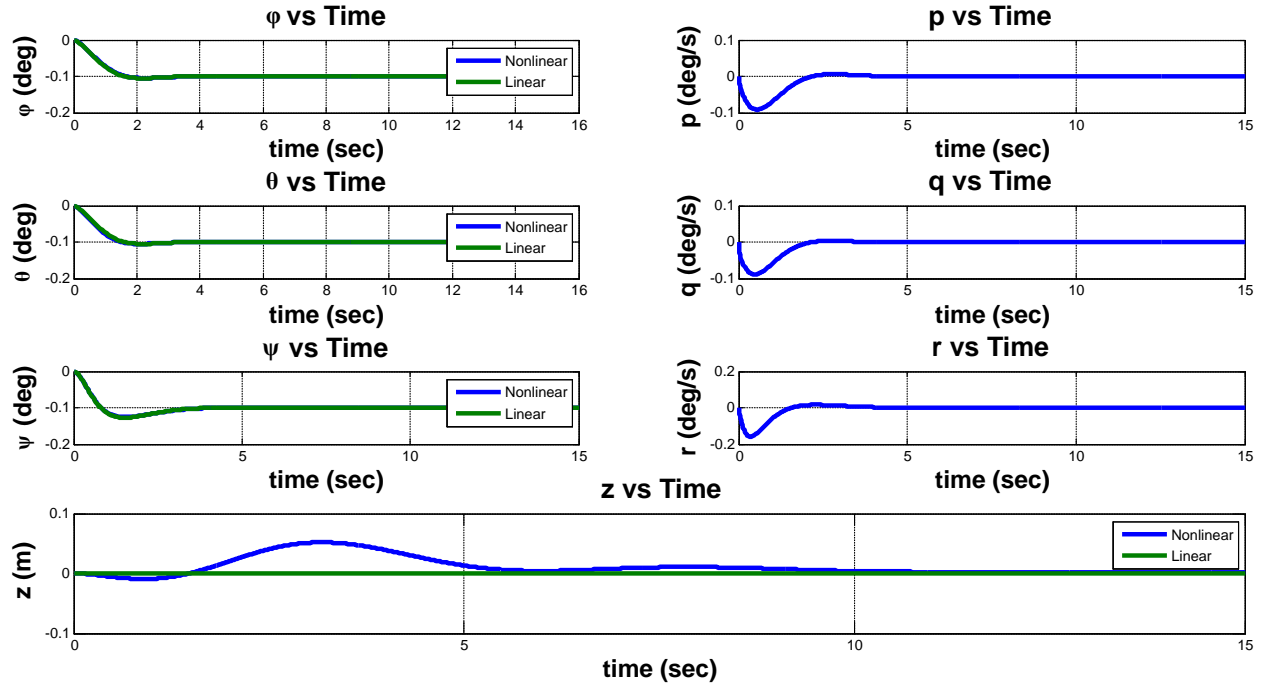


Figure 8.113.: Response at Nom. Thrust = 1650

8. Control and Simulation

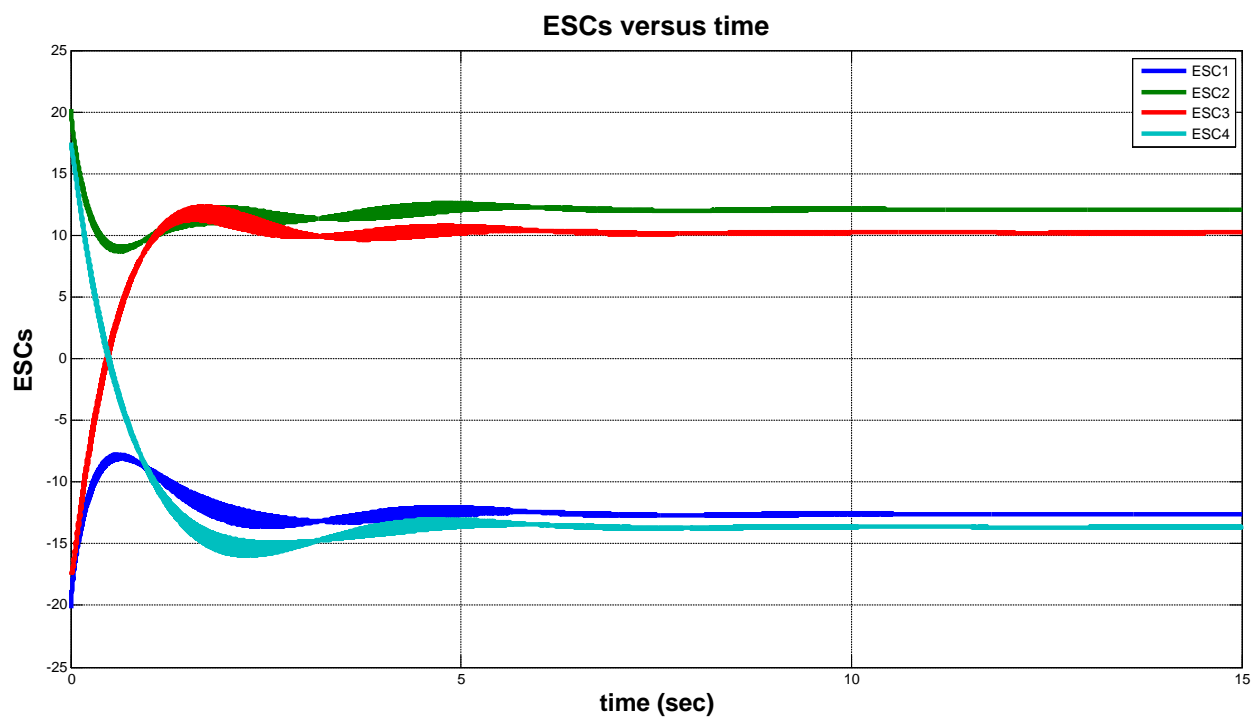


Figure 8.114.: Control actions at Nom. Thrust = 1650

8. Control and Simulation

At Nom. Thrust = 1700

Required $\phi = \theta = \psi = 0.1$ rad

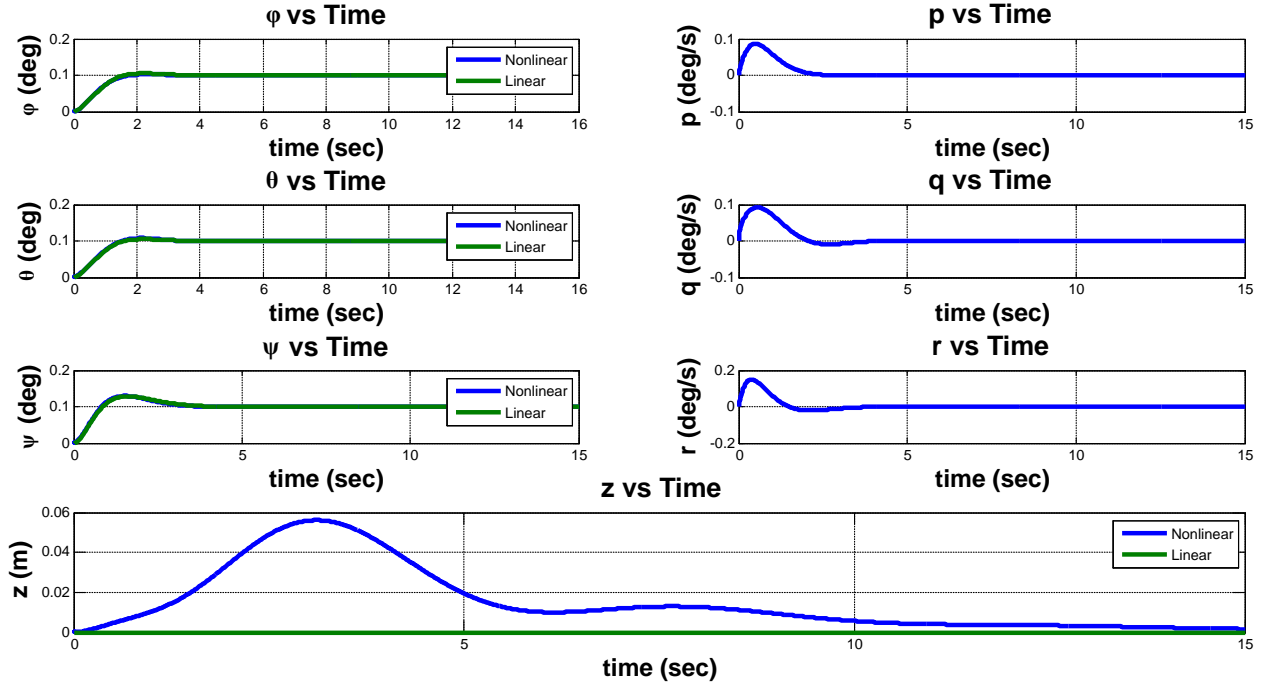


Figure 8.115.: Response at Nom. Thrust = 1650

8. Control and Simulation

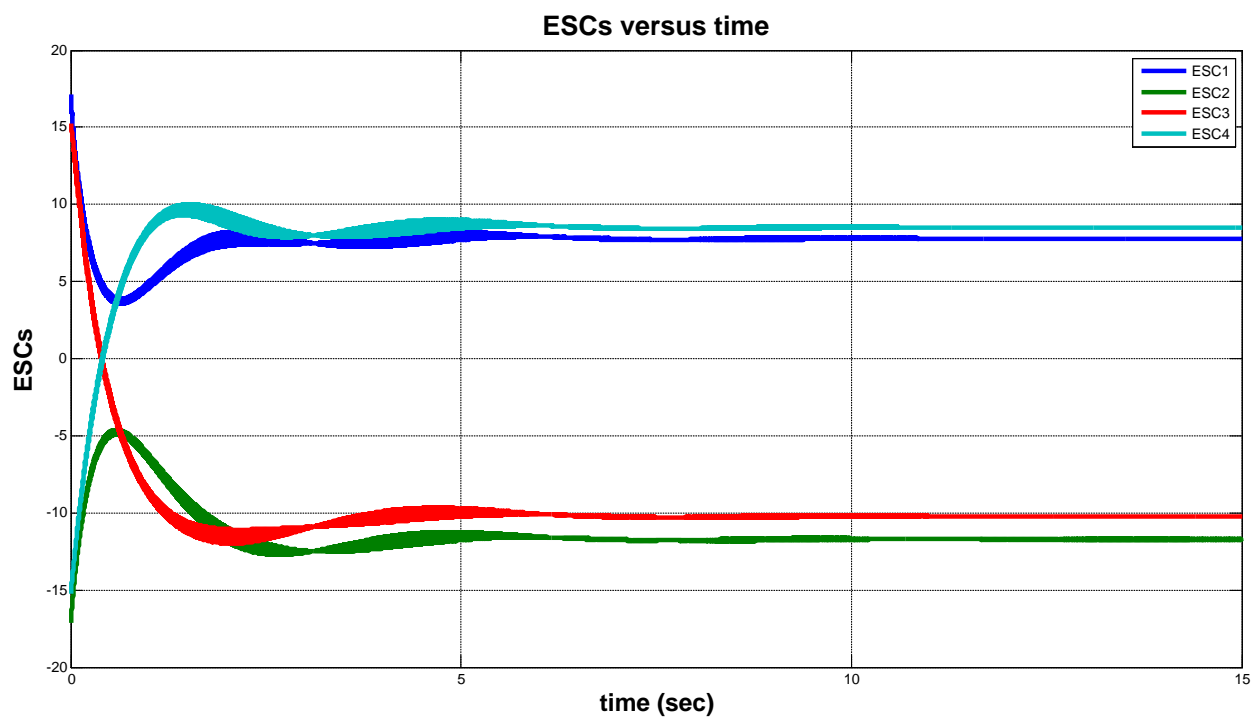


Figure 8.116.: Control actions at Nom. Thrust = 1650

8. Control and Simulation

Required $\phi = \theta = \psi = -0.1$ rad

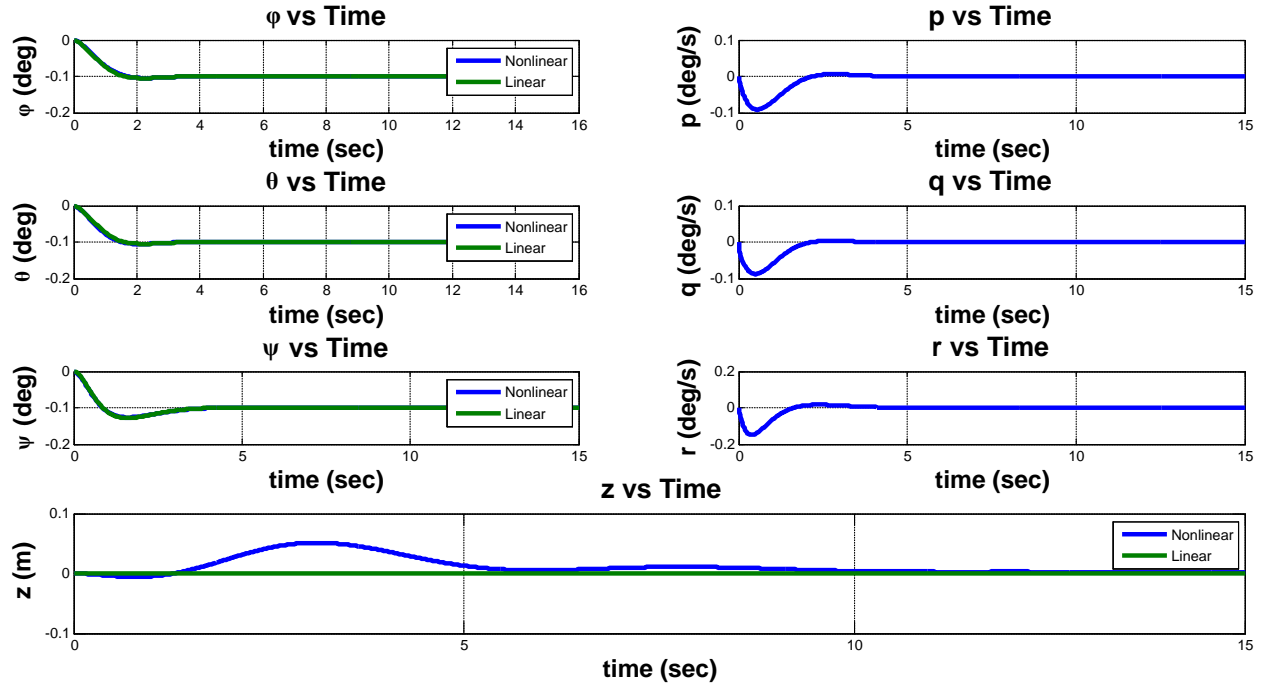


Figure 8.117.: Response at Nom. Thrust = 1650

8. Control and Simulation

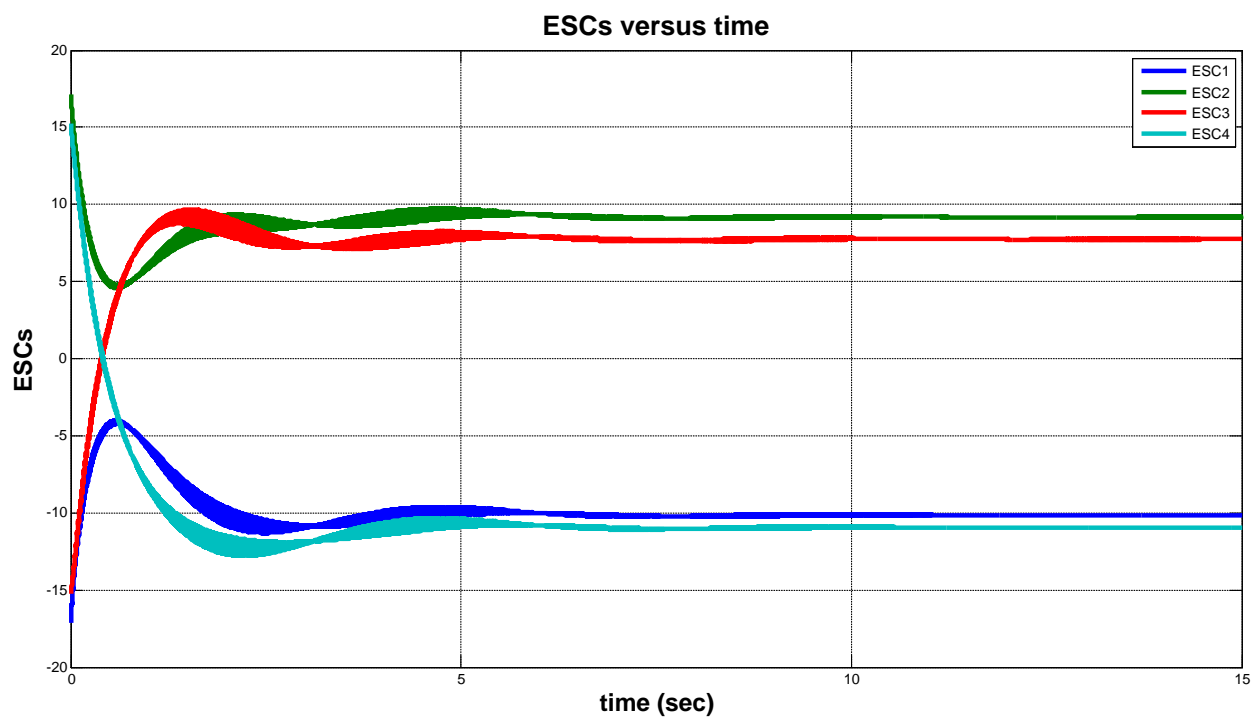


Figure 8.118.: Control actions at Nom. Thrust = 1650

8.7. Testing on Actual System and Results

9. Mechanical Design

In this chapter mechanical design, main parameters, hardware manufacturing and assembly are discussed .Vehicle's CAD drawings are presented highlighting different parts assembly using SOLIDWORKS software.

9.1. Design Specifications

Quadcopters utilize two sets of identical propellers in fixed locations. Two of the propellers will spin clockwise, and the other two will spin counter-clockwise to negate the torque generated by the opposing rotors.

The Quadcopter has obtained quite a reputation as a UAV system in the engineering field mainly because of system's simplicity in terms of function and set up, which makes it a desirable platform to work on. This particular design will perform different tasks; one of which is inspection for crop health and checking the availability of the main elements necessary for a healthy growing crops, where it will utilize an onboard camera system to send feedback to the operator as it flies over the fields to capture photos with infrared technology to be later analyzed, so we can collect data about the crop and the soil health.

The Quadcopter is also known for its ability to carry a relatively small payload, an ability which will be utilized to carry a small spray system, which will spray pesticides on the fields.



Figure 9.1.: Matrice

9.2. Constraints and Other Considerations

- Payload = 8 kg.
- The camera constraints (angle of view $\alpha = 85.22$ deg).
- The system is subjected to very high vibration, because of the brushless motors, which makes it a must to have a well-fixed frame, well-fixed motors and well connected components and sensors.

9. Mechanical Design

- The landing gear should be strong enough to withstand ground impact, and don't forget to make the landing gear long enough to protect the Quadrotor from landing on its components (e.g. camera).
- It is a must to prepare a suitable plate at the c.g. of the Quadrotor to hold the sensors and the processors.
 - The IMU is placed in the middle of the quadrotor at the closest position to the quadrotor's C.G.
- Make the weight distribution of components symmetrical from all sides and close as possible from the quadrotor C.G.
- When flying above the fields, the Quadcopter runs the risk of flying through trees and among workers, which can increase the chances of it colliding with the branches, workers or losing control; therefore, a safety frame is to be designed as a protection for both human and Quadcopter components . Also, operators must be well trained when in operation of the quadcopter and good calibration of the altitude as well as the proximity sensors will reduce the chance of collisions; therefore enabling more accurate acquisition of measurements and observations in an easier fashion.

9.3. Major Components

Multi-RotorFrame - This is the structure that holds all of the components together; not only does it need to be designed with strength in mind, but also to be light weight.

Motors/SpeedController - The KDE motors are brushless motors that can provide the necessary thrust to propel the craft. Each rotor needs to be controlled separately by a speed controller.

Propellers - All multi-rotor RC aircrafts use propellers (not to be confused with helicopter blades) to achieve lift. Propellers attach to the drone's motors. When the motor spins, so do the propellers. Similar to drone frames, propellers can be made from a wide variety of materials, as well as exist in many different sizes.

PowerSource

Controller - National Instrument real-time input output system (NImyRIO)

GPS

PressureSensor

IMU

Transmitter&Receiver

Camera

SafetyFrame

9. Mechanical Design

9.3.1. Common Types of Materials Used For Drone Frames

- Wood: If you're trying to build a drone as cheaply as possible, then consider using a wooden frame. It's certainly one of the most inexpensive. One reason why I love wooden frames is because if something breaks, you can quickly and easily replace it. If you're going to use wood for your drone's frame, then make sure that it doesn't have any areas that are warped or twisted.
- Carbon Fiber: carbon fiber is very tough and extremely lightweight. It's this combination that will make your RC drone fly better and consume less energy. Remember that carbon fiber impedes RF signals, so make sure that you keep this in mind when you're mounting important electronic components (like an antenna for example).
- Plastic: Most commercial RC drones that you buy today come with plastic frames. 3D printed molded plastic frames have become an incredibly popular amongst DIY drone enthusiasts. Generally, using a 3D printer to create a perfectly shaped plastic frame is something that only works on smaller drones. When using plastic sheets (not 3D printed shapes or objects), you can strategically use them on your landing gear or for the cover of your drone.
- Aluminum: Aluminum can also be used when building your frame. It's lightweight (though not as lightweight as carbon fiber), flexible, and is relatively easy to work with. You can use aluminum to build the entire frame, or simply use the material to supplement certain parts of the frame (arms, landing gear, etc.). Another benefit to aluminum frames is that this type of material is both inexpensive as well as readily accessible.



Figure 9.2.: Wooden frame



Figure 9.3.: Carbon Fiber frame



Figure 9.4.: Metal Frame

9. Mechanical Design



Figure 9.5.: Plastic frame

9.3.2. Airframe Configuration

9.3.2.1. Quad , Hexa & Octa

	Pros	Cons
Quadcopter	One of the biggest benefit to using a quadcopter frame is that nearly all of the flight controllers on the market today can work with this type of design. It's also one of the simplest designs you can use, which is perfect if you're learning how to build a drone for the first time.	No frame design is perfect – not even the quadcopter. A drawback to using this frame type is that if one motor or propeller fails, the remaining motors/propellers won't be able to compensate, resulting in a crash.
Hexacopter	One of the main benefits to a hexacopter frame is that you'll be able to deliver more thrust. This comes in handy for lifting heavier payloads. Also, if one motor fails, then there's still a chance that the drone can land safely rather than crashing. Another great advantage to this design is that nearly all flight controllers support this type of frame setup	In general, building a hexacopter is going to be more expensive than building say, a triocopter or quadcopter. This is due to the larger number of parts required to make it fly. Also keep in mind that more parts equals more weight, so in order to achieve the type of thrust you'll need to get a hexacopter in the air, a larger battery will be required.
Octocopter	The high amount of motors present means more thrust, which subsequently means it can lift heavier things. Another great advantage to this type of design is that if one motor fails, the drone can probably still make it to the ground safely rather than crashing.	As you've probably guessed, more motors equals a more expensive build, as well as a larger battery pack. For the most part, people who build larger octocopters are interested in serious aerial photography and/or videography.

Table 9.1.: Pros & Cons of different airframes configurations

9. Mechanical Design

9.3.2.2. Octoquad

In our research concerning development of drones, we focus on few multi rotor designs, with so called x8 quadrotor or octoquad among them. This configuration of multi rotor extends original quadcopter concept by increasing the total thrust output of platform thanks to additional set of motors. On each side, there are two identical rotors installed, one above another. The propellers rotate in opposite directions, which equalizes the momentum of platform. The upper propeller works as a tractor, while the lower unit is a pusher. As a result, the total thrust of propulsion unit is increased with similar physical volume in comparison to single propeller. However, considering that a lower propeller operates in a prop wash of upper unit, the total thrust performance of coaxial propulsion is lower comparing to two separated propellers. The average loss of total thrust outcome of coaxial propulsion unit in comparison to design with 8 isolated propellers was estimated at about 14 %, with equal rotational speeds of both motors.



Figure 9.6.: Octoquad

9.3.2.3. Conclusion

- Introducing octoquad configuration allows to increase lift capabilities by about 40 %, considering weight of additional motor unit and slight rise in vehicle's volume, comparing to classic quadrotor design.
- Coaxial propulsion does not operate on maximum motor's power, probably because of the lower propeller operating in prop wash of upper unit.
- The loss in efficiency for coaxial propulsion is not that significant, because lower than double thrust gain comes with less power consumption. Considering grams per watt ratio, coaxial propulsion units needs about 17 to 29 % of more power to produce the same thrust. However, this values vary for different rotational speeds. In addition, different sizes of propellers have different loss in efficiency, with best results for smaller, high-speed propellers.

9.3.3. Types of Motors

- Brushed Motors: Like all RC motors, brushed motors contain windings (coil) and magnets. With this particular type of RC motor, the magnets remain FIXED while the coils SPIN. Generally speaking, brushed motors are quite popular amongst smaller, inexpensive model quadcopters (like the Syma X5C or Cheerson CX-10). One potential downside to this type of motor is that the brushes can wear out rather quickly, so their lifespans tend to be less than that of a brushless motor. Obviously, there are exceptions, but this tends to be the general rule.

9. Mechanical Design

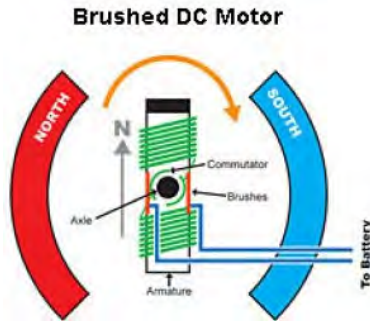


Figure 9.7.: Brushed DC Motors

- Brushless Motors: Brushless motors act in the exact opposite manner: their COILS remain fixed while their MAGNETS are spun. As its name implies, a brushless motor does not contain any brushes, which can actually lead to the longevity of the RC motor. Here are a very common types of brushless DC motors that you'll encounter:

- Inrunner: These types of brushless motors have coils that are fixed on the outer casing, while the mobile magnets spin on the inside of the casing.
- Outrunner: As you can probably guess, these types of brushless motors have their magnets on the outer casing, and are spun around the fixed coils that are located within the middle of the motor casing.

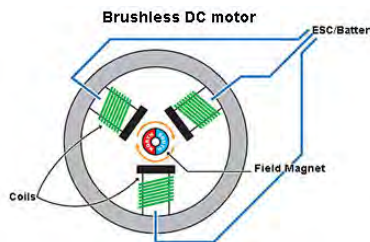


Figure 9.8.: Brushless Motors

9.3.4. Propellers Types and Materials

The majority of RC drones come with three-bladed or two-bladed propellers, with the most common setup being two. Smaller blades (those with smaller diameters) tend to be easier to slow down and speed up, which comes in handy if you're interested in doing acrobatic flights. Larger blades, or those with larger diameters, are better-suited for more stable flights since it's harder to speed up or slow down the blades. All propellers that you use to build a drone come designed to spin in one of two ways:

- Clockwise (CW)
- Counterclockwise (CCW)

Obviously, it's important that you be able to tell which part of the propeller is supposed to face upwards and which part of the propeller is supposed to face downwards.

Materials Used to Make Propellers:

9. Mechanical Design

- Plastic: Plastic is by far the most popular choice for propellers in the multi-rotor industry. This is mainly due to their low cost and respectable durability. Unfortunately, plastic propellers do have their downsides. For example, when you crash, it's very likely that, without a prop guard, you'll damage your propellers (even with prop guards there's a chance you can damage them). The good news is that plastic propellers are dispensable, so you can break the again and again without worrying about spending a lot on new ones.
- Wood: Due to the intricate machining required to produce wooden propellers, they will cost much more than plastic. On a good note, wooden propellers tend to be very durable. They won't bend, and tend to remain in pretty good condition after light crashes. While they're not common in the RC drone industry, you can still find them in various RC planes.
- Carbon Fiber: If you're looking for something that's super-high quality and that won't break, then consider using carbon fiber propellers when building a drone. Just note that you will be paying top dollar for these propellers. What I love about carbon fiber propellers is that they are very hard to break, and offer much more flex than a standard plastic propeller.



Figure 9.9.: Carbon Fiber propellers



Figure 9.10.: Wooden propellers



Figure 9.11.: Plastic propellers

9. Mechanical Design

9.3.5. Propeller Guards

A “prop guard” is the thing that surrounds the propeller and prevents it from coming in contact with anything from the outside environment. When learning how to build a drone, I would definitely keep prop guards in mind. If you’ve never flown before, chances are good that you’re going to crash... a lot. And the best way I can think of to protect your props is to use a prop guard. RC quadcopters like the UDI U818A or FQ777-124 Pocket Drone come with removable plastic prop guards. Just keep in mind that they’re not perfect, and do come with their own set of drawbacks:



Figure 9.12.: Phantom drone with prop guards

- They add weight to your drone, which can decrease overall flight time.
- They only work for “light” crashes.
- They can contribute vibration of your RC aircraft.

9.3.6. Collision Tolerant

Carrying its own protective frame, the drone is collision-tolerant. This means you can access the tightest spaces without any risk of crashing. No need to focus on avoiding obstacles, the drone bounces off and roll on them to find its way. You can fly close or even in direct contact with humans without any risks of injuries.



Figure 9.13.: Elios Inspection Drone

9.4. Design Layout

9.4.1. Structural Design

One of the most important structural considerations for this quadcopter is to maintain an even weight distribution when designing the structural framework and placement of major components. The main control components will be centered above the central, circular plates to maintain minimal moments about the central axis of the quadcopter. The arms are also evenly placed about the central plate arrangement and made to be even lengths in order to cancel out any moment obtained when the motors are running. To compensate for the torque incurred by the running motors, opposing motors are given the same rotation while adjacent motors are given opposing rotations with corresponding propellers. Doing this will help to cancel out the torque of the running motors and resulting lift of the motors and propellers.

9.4.2. Material Selection

The main consideration when discussing material selection for this project is the weight limitation. Because the quadcopter has to carry a relatively significant amount of weight between the onboard control components, camera and batteries, the structural framework, the safety frame, and a spray system, a light weight was chosen for the main structural framework: foam and propellers of the quadcopter: ABS. The light weight properties of foam will help to minimize the overall weight of it while maintaining enough strength through the structure to ensure that the quadcopter will be able to structurally survive and crashes. Foam was chosen as the material due to its ease of fabrication, light weight properties and strength for the task at hand. If a crash were to occur where the safety frame is damaged, spare parts or a completely new safety frame can be fabricated relatively quickly or be on hand for fast replacement. Apart from the structural framework and safety frame, the rest of the quadcopter consists of components where material selection does not apply.

9.4.2.1. Why Foam?

- ***They are lightweight.*** Over time the density of polyurethanes has been reduced by 30 to 40% while still maintaining the same mechanical properties.
- ***They are durable:*** Polyurethane is not prone to corrosion, throughout their life they ensure stability even under severe conditions.
- ***They are versatile and offer freedom of design:*** Drone frames have widely evolved over time together with knowledge of ergonomics. And they keep doing so, because polyurethanes offer a wide choice of performance and processing characteristics, allowing applications to be tailored for advanced shapes and forms using the same basic chemicals.
- ***They can be recycled*** through a range of approved technologies and offer the potential for mono-material solutions, which facilitate dismantling and recycling.

9.4.3. Landing Leg Configuration

9.4.3.1. 1st Iteration



Figure 9.14.: Landing leg first iteration

9.4.3.2. 2nd Iteration

9.4.4. Safety Frame

Through the design, manufacturing and testing process various configurations of safety frames were used till the optimal one was reached as it will be discussed below

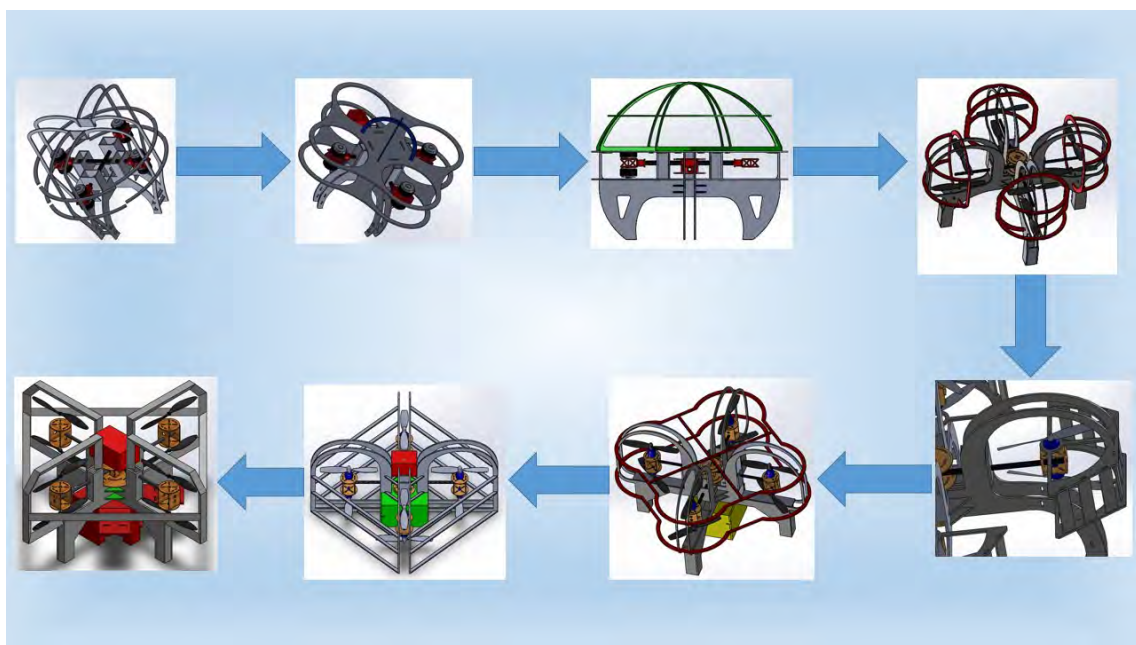


Figure 9.15.: Safety frame progress

9. Mechanical Design

9.4.5. Motor Propellers Mounted

In order to increase the loading capacity (by increasing the number of propellers) without increasing the size of the multi-copter, we would mount two propellers at the end of one arm (one at the top and the other at the bottom), which is called the co-axis form, as shown in Fig. However, due to the interference in air flow, adopting this form will reduce the efficiency of the single propeller. The two propellers of the co-axis form are approximately equivalent to 1.6 propellers as the common form. In order to improve efficiency, it is necessary to further optimize the co-axis system. When combining with different motors and propellers, the co-axis efficiency can be improved to some extent.

Experiments have also indicated that the space between two propellers will affect the efficiency of the co-axis propeller system as well. It is recommended that $h/r_p > 0.357$, where the definitions of h and r_p are shown in Fig.

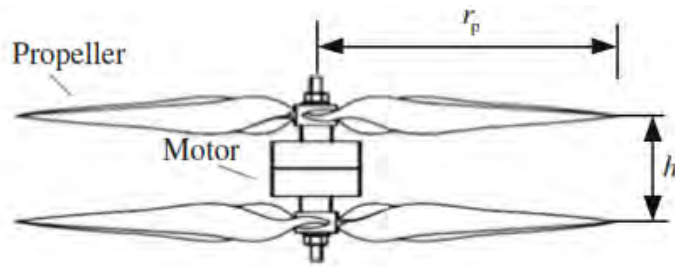


Figure 9.16.: A simple connection and its geometry parameters of a co-axis form with two propellers

9.4.6. Design Alternatives

9.4.6.1. Overview of Conceptual Design Alternative

In order to accomplish the necessary functions that the quadcopter will execute, four main designs were chosen. These designs involve the quadcopter's main components that will be optimized, which are the safety frame and camera. The safety frame designs were designed in order to avoid human injuries and protect the components from crashes. Additionally, a camera is to be installed on the bottom of the quadcopter that will be utilized for recording, photographing, and inspecting purposes. The camera will be predominantly used to inspect for crop health and checking the availability of the main elements necessary for a healthy growing crops. These two key characteristics of the quadcopter are the focal points to the designs demonstrated in the subsequent sections.

9. Mechanical Design

9.4.6.2. Design Alternative 1

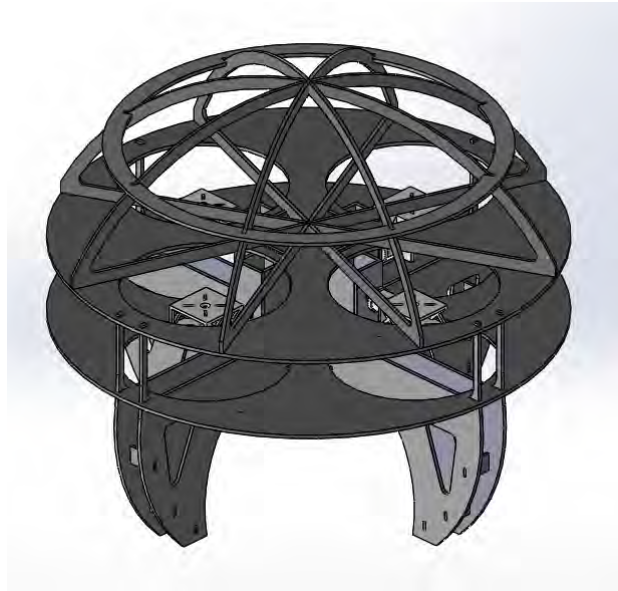


Figure 9.17.: Design alternative (1) SOLIDWORKS model



Figure 9.18.: Design alternative (1) prototype

The first design illustrates the concept of safety that we are looking for. This frame is designed to protect the people around the rotor using plates and a structural dome that surround the propellers. The camera location is at the bottom centered between the landing legs. On top under the dome, there

9. Mechanical Design

would be the system box that contains the controller and sensors. The safety frame will be composed of foam because it is lightweight and ease of manufacturing & assembly. One of the main disadvantages of this design is its dimensions and relative heavy weight in comparison with other designs. Another disadvantage is that the landing legs are not solid enough.

9.4.6.3. Design Alternative 2

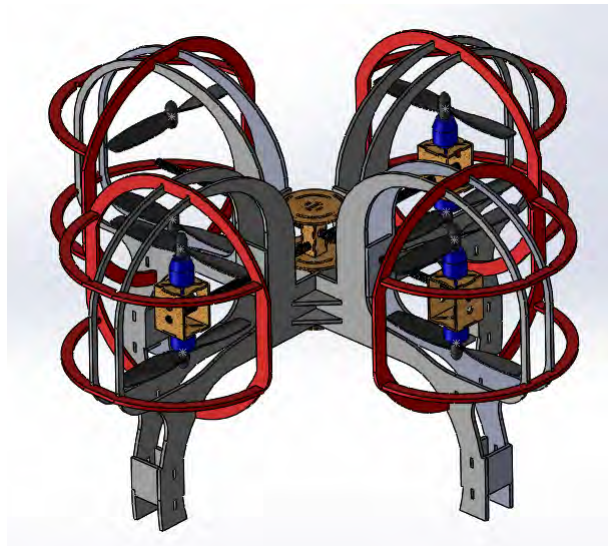


Figure 9.19.: Design alternative(2) SOLIDWORKS model



Figure 9.20.: Design alternative(2) prototype

9. Mechanical Design

This frame is designed to protect the people around the rotor using half round plates around each propeller. It is distinctive with its light weight as it weighs 1535 grams with the control system and motors onboard. The camera location is at the bottom centered between the landing legs. On top, there would be the system box that contains the controller and sensors. The safety frame will be composed of foam because it is lightweight and ease of manufacturing & assembly. Problems with this design aroused during the assembly process as the propeller safety are easily broken due to the small thickness. During the tests the landing legs suffered severe cracks at the moment of impact with the ground specially at the curves below the propellers.

9.4.6.4. Design Alternative 3

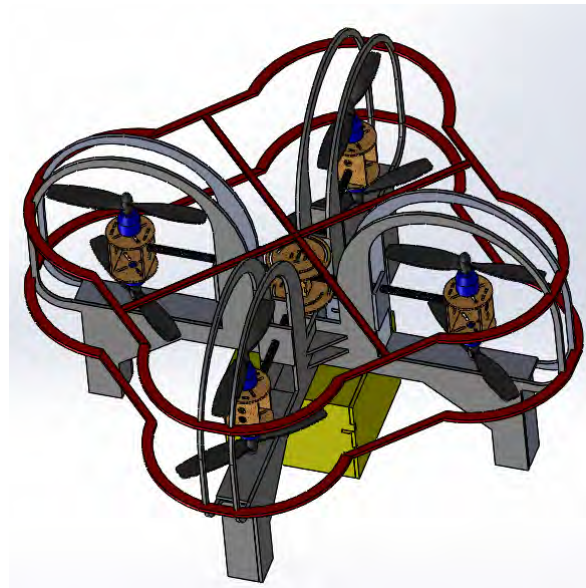


Figure 9.21.: Design alternative(3) SOLIDWORKS model

This frame is designed to deal with the lack of stiffness in the landing legs that the previous designs had. The Landing legs are designed as square closed sections to withstand the impact with ground during landing. The bottom box is the same height as the landing legs to share the impact load as well. This box is to carry the batteries and the camera. With such a load at the bottom the C.G. is lowered down further than the previous designs. On top, there would be the system box that contains the controller and sensors. The safety frame will be composed of foam because it is lightweight and ease of manufacturing & assembly. The main problem with this design is that the propeller safety are still easily broken during assembly due to the small thickness.

9. Mechanical Design

9.4.6.5. Design Alternative 4

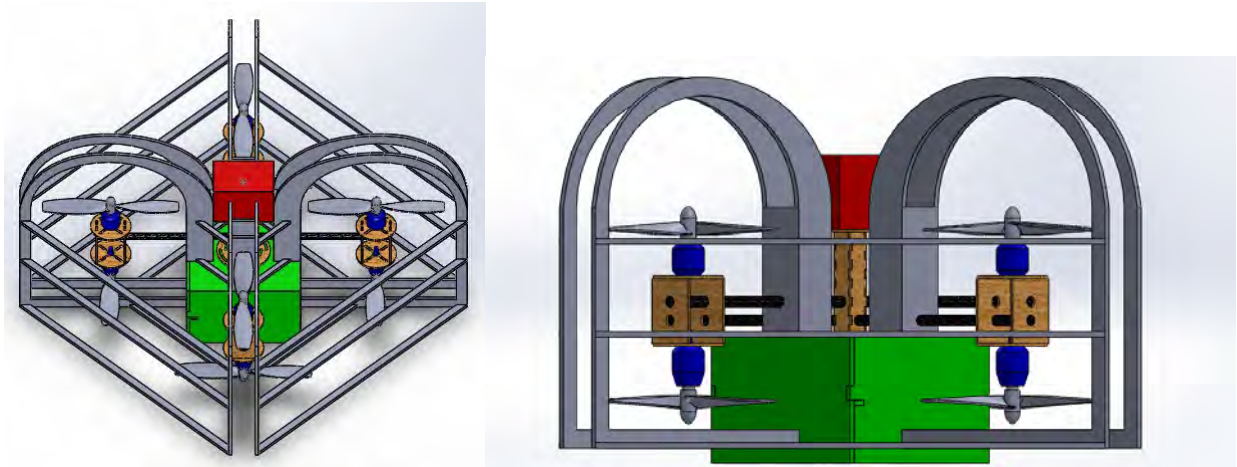


Figure 9.22.: Design alternative(4) SOLIDWORKS model

This frame is designed to deal with the lack of stiffness in the landing legs that the earlier designs had and the propeller safety are designed more stiff as well. The bottom box is to replace the landing legs. This box is to carry the batteries and the camera. With such a load at the bottom the C.G. is lowered down further than the previous designs. On top, there would be the system box that contains the controller and sensors. The propeller protection is designed as C sections to be more stiff without affecting the weight much. The safety frame will be composed of foam because it is lightweight and ease of manufacturing & assembly. The main disadvantage of this design is that it makes both the camera and the batteries are exposed to damage during landing impact.

9. Mechanical Design

9.4.6.6. Design Alternative 5

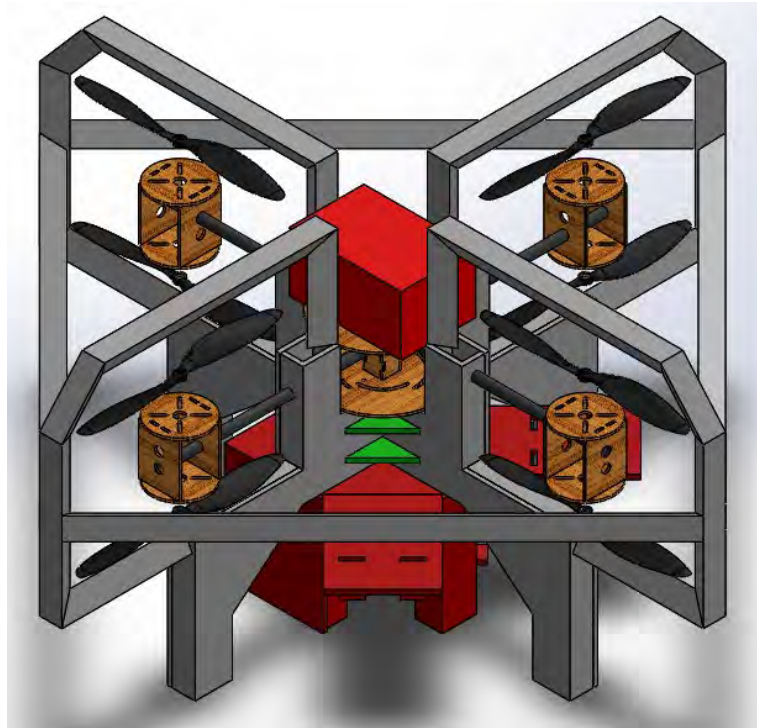


Figure 9.23.: Design alternative (5) SOLIDWORKS model

This frame is designed to merge both alternative design (3) and alternative design (4) using both the bottom box and the landing legs. This box is to carry the batteries and the camera. With such a load at the bottom the C.G. is lowered down like the previous designs. On top, there would be the system box that contains the controller and sensors. The propeller protection is designed as triangular closed sections to be more stiff without affecting the weight much. The safety frame will be composed of foam because it is lightweight and ease of manufacturing & assembly. The main disadvantage of this design is

9.4.6.7. Comparing Weights

The Weight includes The Foam Frame, Metal rods & Motor mounts.

All Designs are used with 11" propellers.

9. Mechanical Design

Design	Weight (in grams)	Dimensions	Notes
1	1389.2	800 mm x 800 mm x 683.21 mm	Motor Mounts are made of Artylon. Metal rods diameter is 20mm.
2	1335	891 mm x 891 mm x 521.26 mm	Motor Mounts are made of Wood. Metal rods diameter is 12mm.
3	1409	858 mm x 858 mm x 533 mm	Motor Mounts are made of Wood. Metal rods diameter is 12mm.
4	1436	750 mm x 750 mm x 400 mm	Motor Mounts are made of Wood. Metal rods diameter is 12mm.
5	725(needs to be checked)	890.53 mm x 890.53 mm x 449.98 mm	Motor Mounts are made of Wood. Metal rods diameter is 12mm.

9.5. Final Design

9.6. Manufacturing Process

The section's aim is not discussing in detail manufacturing techniques and process used, as this is not the main concern for the text. Rather it is only highlighting engineering ideas and concepts used for achieving the best implementation.

9.7. Assembly Process

9.7.1. Jigs

9.7.2. Steps for Assembly

9.8. Stress Analysis

9.9. Strain Analysis

9.10. Vibrations Frequency Analysis

9.11. Suggestions to Enhance The Design

10. Numerical Analysis of The Drone

10.1. Introduction

Small multi-rotor vehicles have often been designed using an approach that consists of the steps “sketch, build, fly, and iterate”.

In that approach, there is no systematic way to explore trade-offs or determine logical next steps for design improvements. It is neither possible to account for multiple real-world constraints up front in design nor is it possible to know what the performance will be with a given design. Because unmanned vehicles are sized and optimized for particular missions, modern low-fidelity conceptual design and sizing tools that have been used for the design of large helicopters can also be used for the design of small multi-rotor craft.

However, there are aerodynamic features of these multi-rotor vehicles that can be difficult to account for with these low-fidelity tools, unless there is a method to calibrate the tools. Accurate prediction of rotor-craft performance continues to be challenging. The flows are inherently unsteady, nonlinear, and complex. A rotor blade can encounter its own tip vortex and the tip vortices of other blades. It is even more difficult when there are aerodynamic interactions between multiple rotors and fuselage because of the close proximity of all of these components. High-fidelity computational fluid dynamics (CFD) methods may offer an advantage over low-fidelity tools when investigations of interactional aerodynamics of multi-rotor vehicles are required. High-fidelity CFD can also provide information to calibrate low-fidelity design tools to account for aerodynamic interactions. Small multi-rotor configurations often have low aerodynamic efficiencies both in hover and in cruise. However, compared to single rotor systems, multi-rotor vehicles offer an advantage in lifting capacity because the size of a single rotor is limited by the tip speed and structural mechanics.

The Objective of the presented work is to demonstrate a high-fidelity computational simulation capability to study the aerodynamics of complete multi-rotor systems both in hover and in forward flight, that is ignoring the rotor blades.

10.2. Model and Mesh

Many Models have been used for the Aerodynamic Analysis, most of them were edited specifically just for the case of aerodynamic study. we will begin listing all the Model and Mesh trials until the recent final version of it.

1. The first Solid Model was inserted with the rotor blades and all holes left open as it is in the original manufactured Model, as in the following figure.

10. Numerical Analysis of The Drone

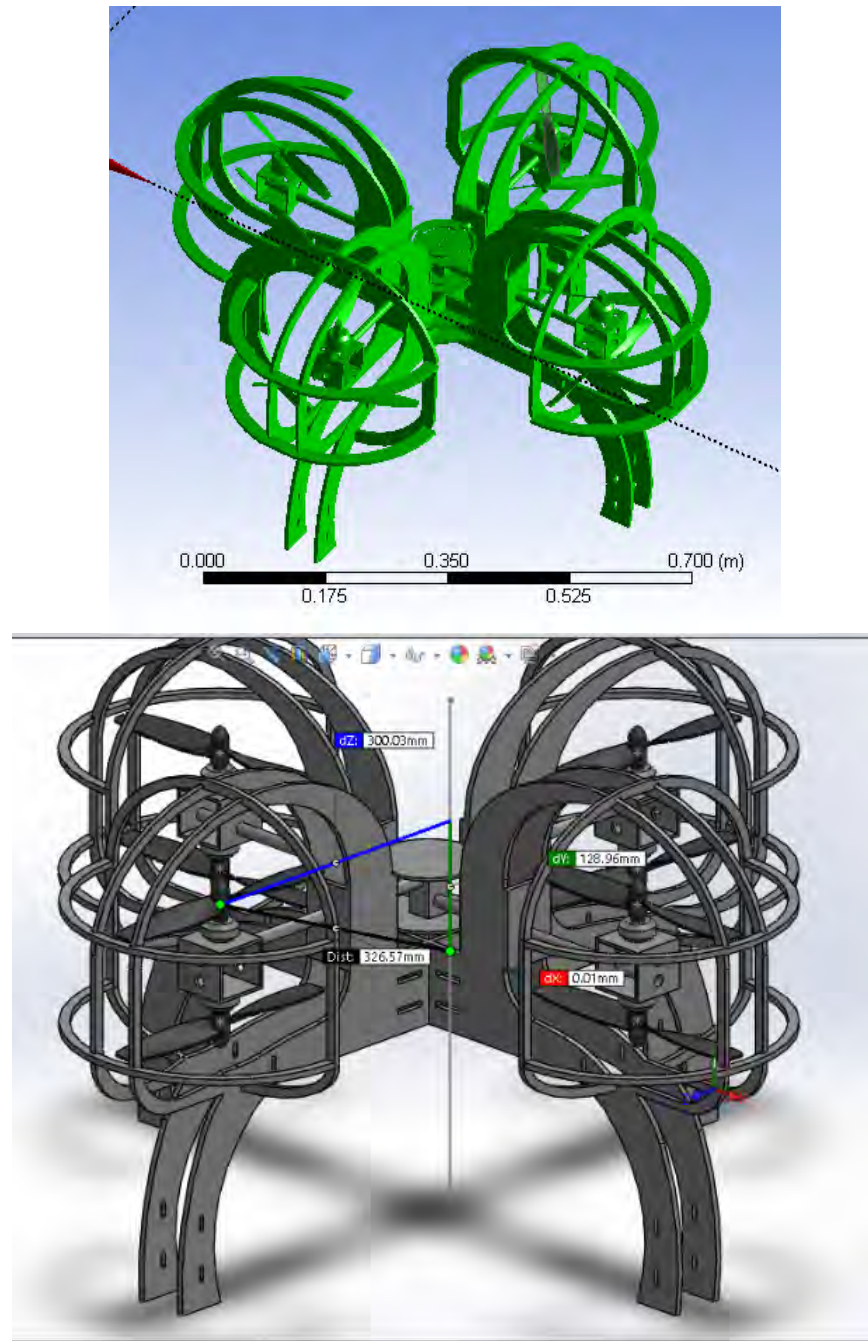


Figure 10.1.: First Model

we couldn't create the Mesh for this Model, it was inserted as 78 Parts, where we should cut the 78 parts from the control volume using Boolean →cut material , which is a very exhausting process and didn't work well either, so we transferred into Model 2.

2. A special model were made for the analysis, A model that didn't contain the rotor blades, also it's mainly a skin, for the whole Drone Body, we have closed every small orifices and removed tolerance that may affect the mesh quality.

10. Numerical Analysis of The Drone

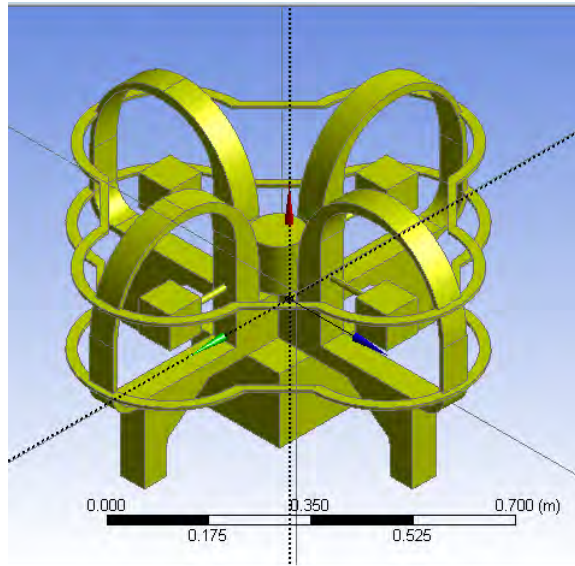


Figure 10.2.: Second Model

the control volume was created as a box that has edge length of 4 meters measured from the c.g. of the drone. That was created and combined using SolidWorks in order to eliminate the errors in the Ansys Design modeler **import** settings. which has greatly affected the creation of the mesh as we will see.

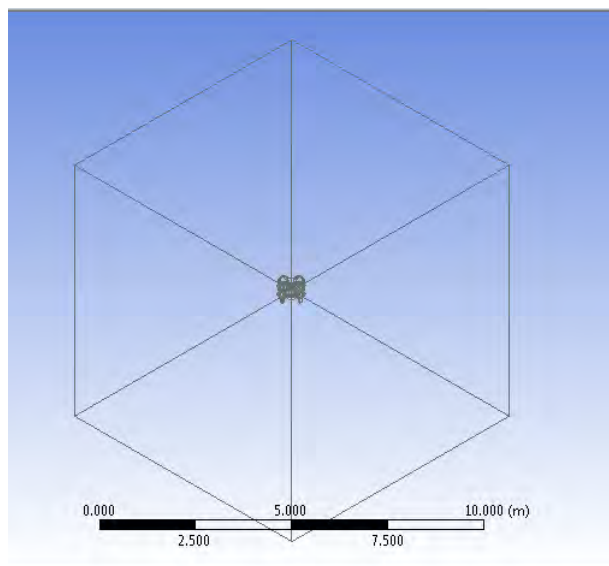


Figure 10.3.: control volume

- Mesh:

The Mesh creation was too primitive, that it was just a trial. We didn't use any advanced size function, as we will be using sphere of influence around the Drone body. The sphere of influence used as the following settings, Using a radius of 2 meters has enabled us cover all the Drone body

10. Numerical Analysis of The Drone

and more mesh cells! Also choosing the element size of 0.007 m was the least we could choose, due to computational limitations.

Details of "Face Sizing" - Sizing	
Scoping Method	Geometry Selection
Geometry	202 Faces
Definition	
Suppressed	No
Type	Sphere of Influence
Sphere Center	Global Coordinate System
<input type="checkbox"/> Sphere Radius	2. m
<input type="checkbox"/> Element Size	7.e-002 m

Figure 10.4.: Sphere of influence

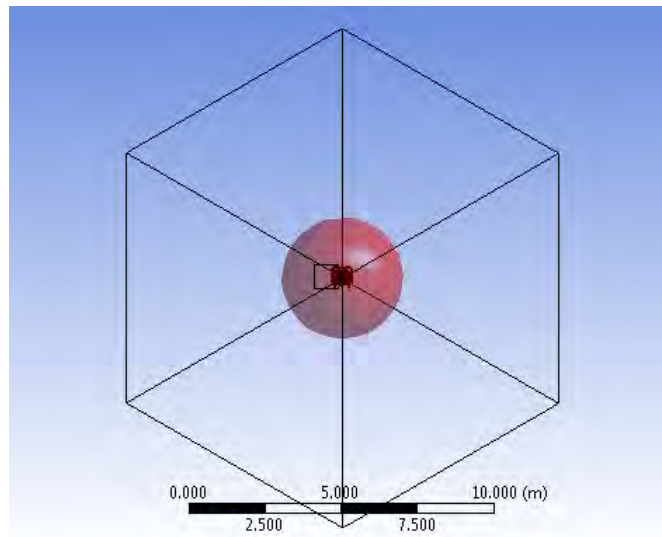


Figure 10.5.: Sphere of influence in mesh

The mesh generated was too coarse, as we can see in the following pictures. Although it was 240,593 elements. which may take days to be solved. but we made sure that we kept the skewness less than 0.9.

10. Numerical Analysis of The Drone

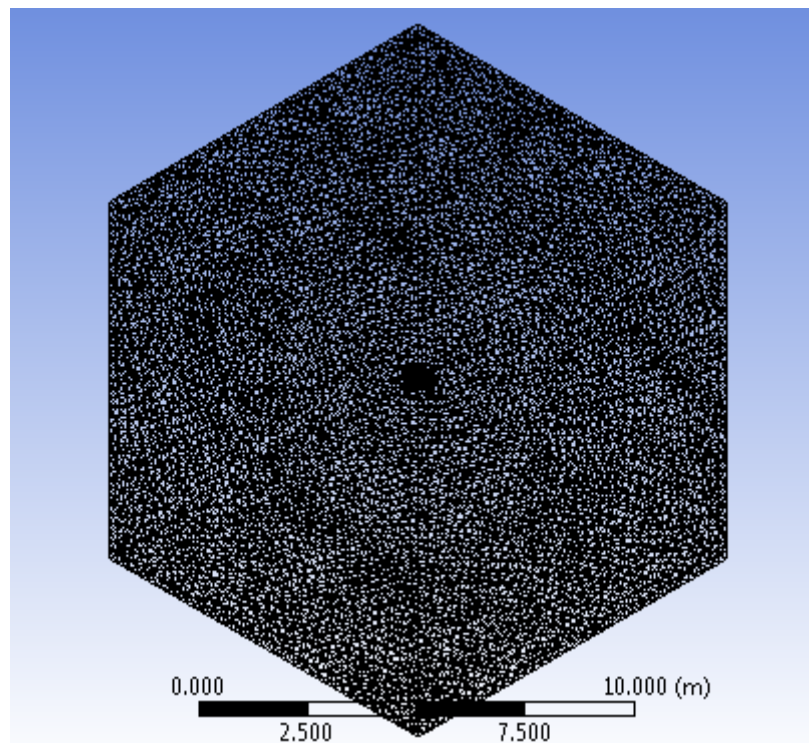


Figure 10.6.: 3D view of Mesh

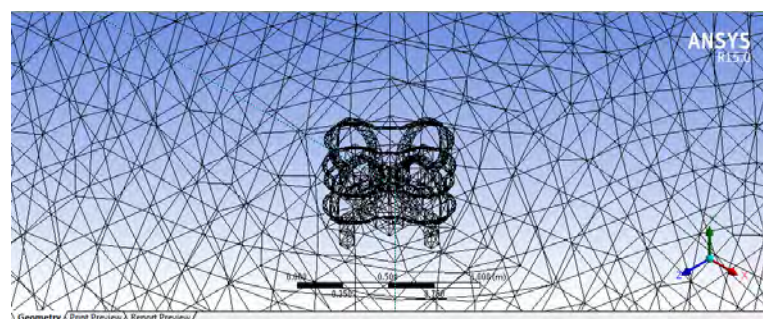


Figure 10.7.: Mesh

10. Numerical Analysis of The Drone

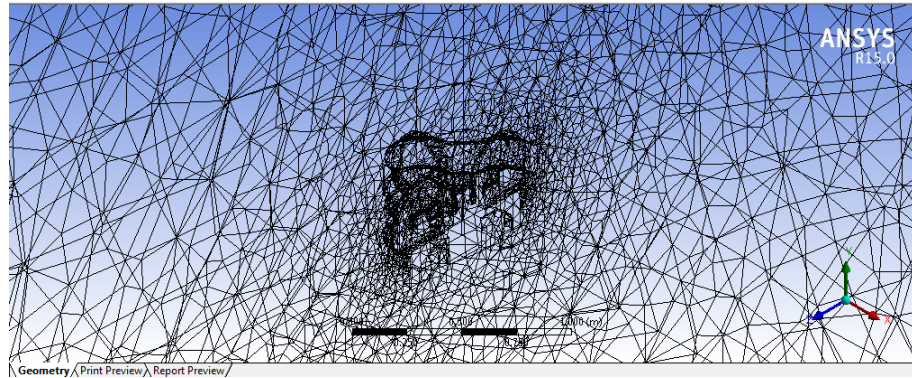


Figure 10.8.: Section plane in Mesh

3. A much better model was generated to be used on a super computer, The model Geometry is as the same as the previous one. but a different technique was used, and that will be illustrated later. That has greatly helped in creating the mesh, as we could create a mesh that is **15,093,577** elements , and a **max. skewness ratio of 0.84**. The mesh is as in the following pictures.

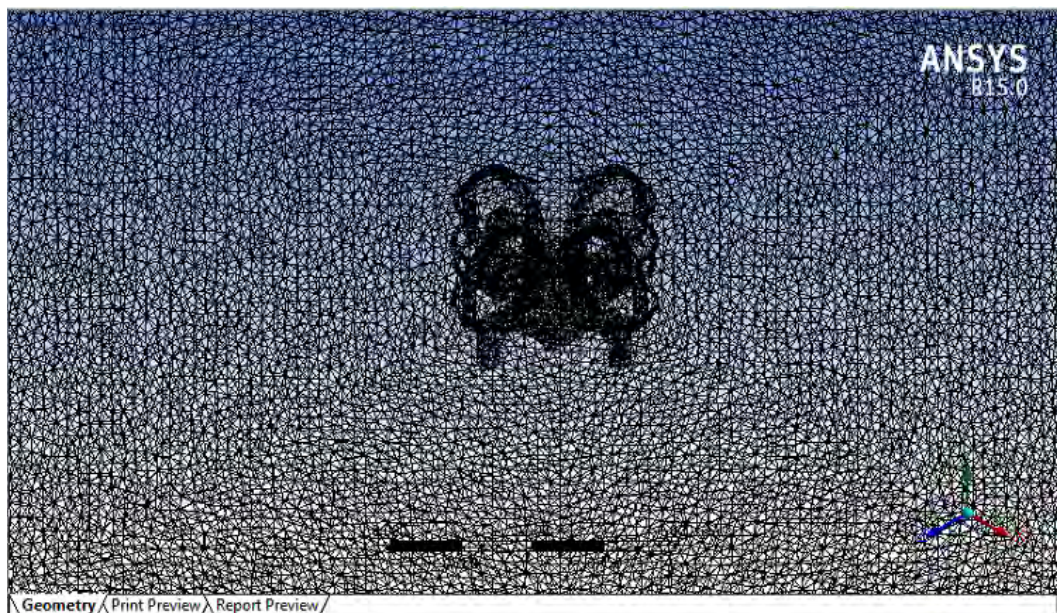


Figure 10.9.: 3D Mesh of Third Model

10. Numerical Analysis of The Drone

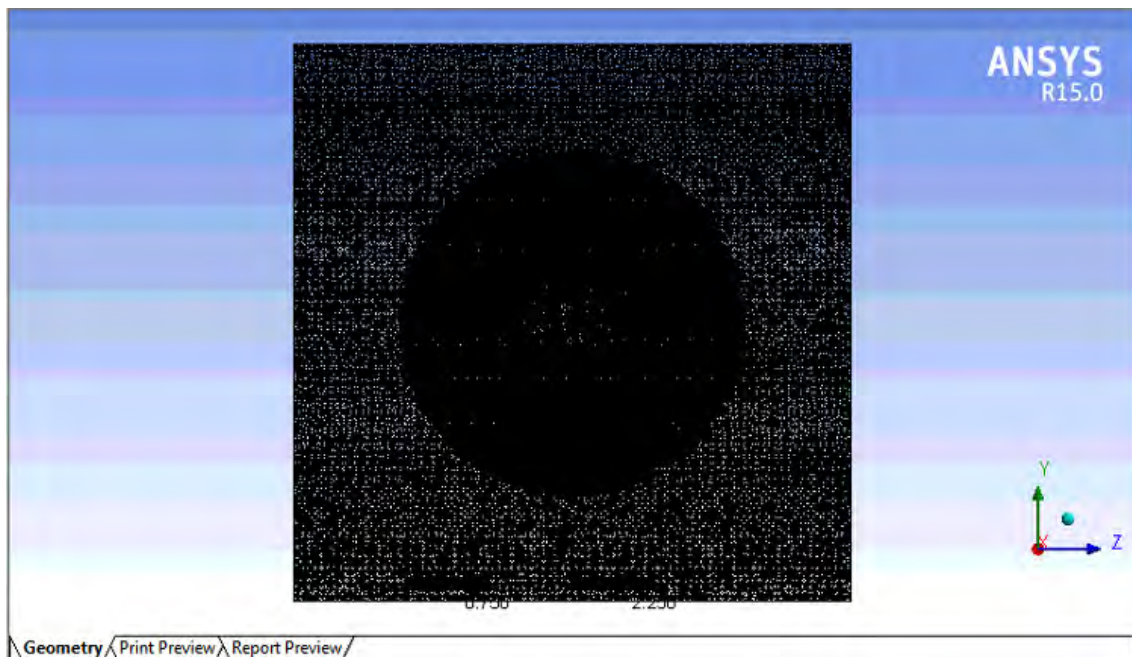


Figure 10.10.: view from Y-Z plane of Mesh

A section plane for the mesh is as in the following picture,

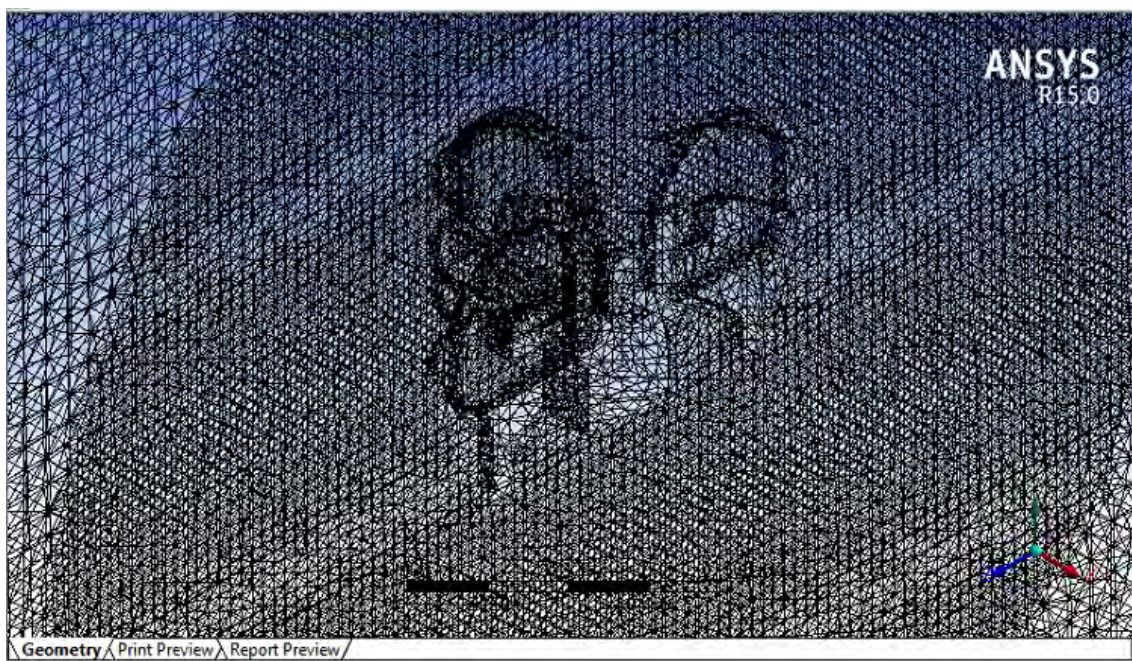


Figure 10.11.: Section plane in Third Model

11. Take-off Mode Analysis.

11.1. First Model Full Analysis

11.1.1. Geometry

- The first Model is created using import setting in Ansys design modeler, we inserted the combined part as a one-part body. as follows

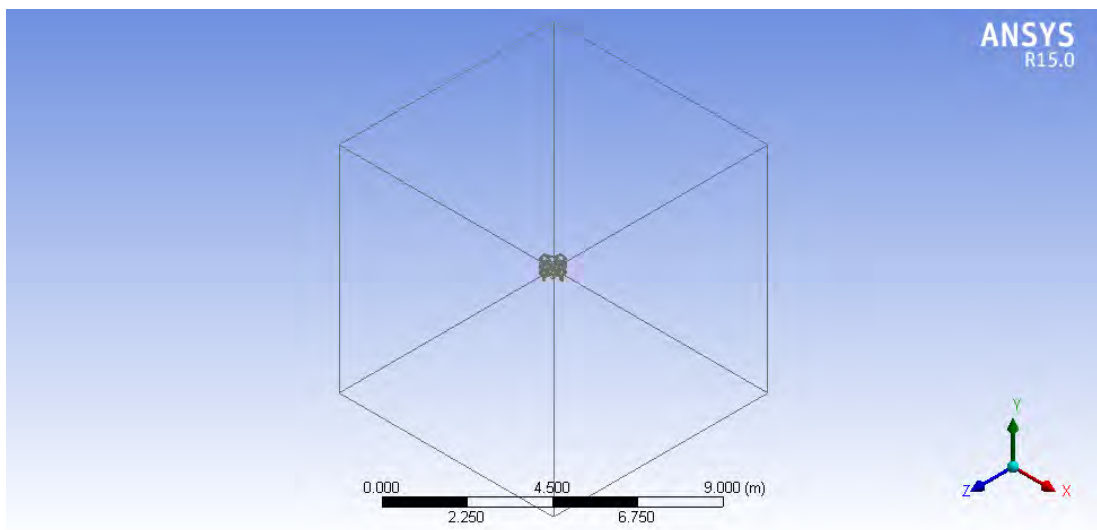


Figure 11.1.: First Model Geometry

- Then, The control volume is created using the **Extrude** option in Ansys design modeler, Extruding a cubic box with edge length of 4 meters.
- Using the **Boolean** option to **cut** the **material** of the drone from the outside control volume.

11.1.2. Mesh

The mesh created for the first model was intentionally created coarse, to obtain a fast solution, then we can improve it. The mesh options for this model is as follows,

- A sphere of Influence was created with element size of 0.05 meters, The sphere center is the global coordinate system located in the CG of the Drone, with a radius of 0.8 meters.
- Another Sphere of Influence was created with element size of 0.1 meters, The sphere center is the global coordinate system located in the CG of the Drone, with a radius of 1.5 meters.

11. Take-off Mode Analysis.

- From **Mesh** option, Insert **Method** → choose “**Tetrahedrons**”
- For algorithm → choose **patch independent**
- From defined by → choose **max. element size** → we have chosen the max. element size is **0.4**, in order to decrease **the skewness**. The final mesh settings is as follows, Skewness = **0.946**, Number of elements = **628,236**.

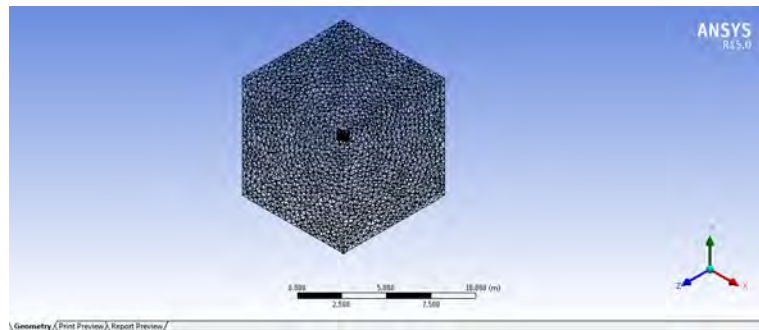


Figure 11.2.: 3D Model of First Mesh

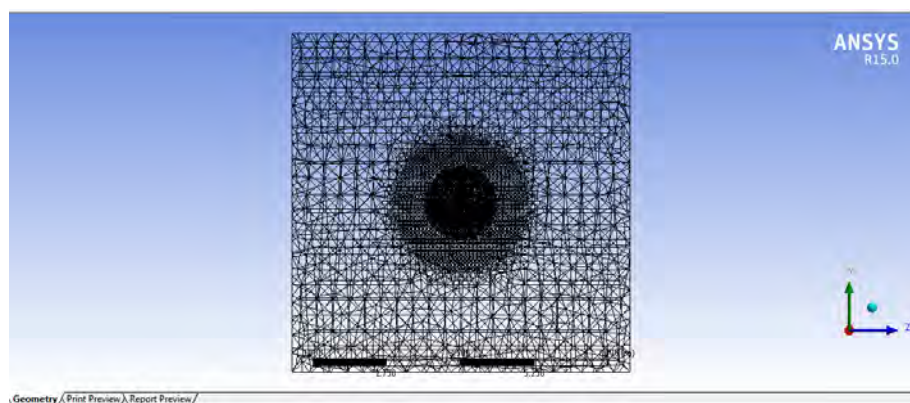


Figure 11.3.: view from Y-Z plane for First Model

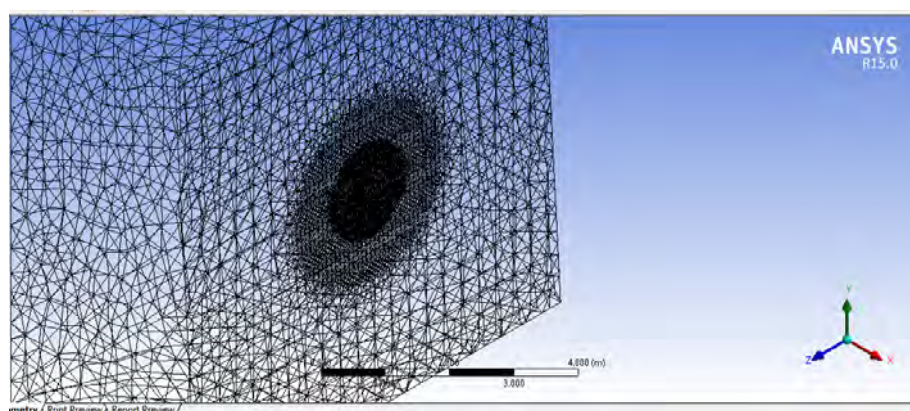


Figure 11.4.: section plane for First Model

11. Take-off Mode Analysis.

11.1.3. Setup

11.1.3.1. Model

The model chosen for this case is K-omega shear stress transport model, an brief explanation about that model can be found in Appendix A

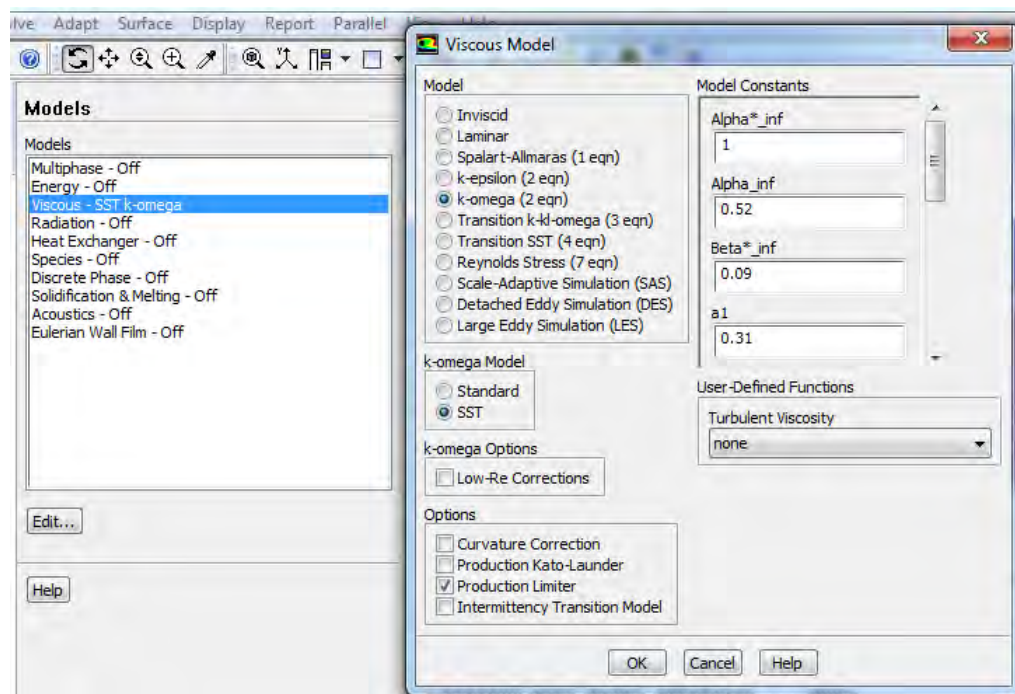


Figure 11.5.: Model

11.1.3.2. Material

The material chosen is Air with the following properties,

$$\text{Density} = 1.225 \text{ kg/m}^3$$

$$\text{Viscosity} = 1.789 \times 10^{-5} \text{ kg/m.s}$$

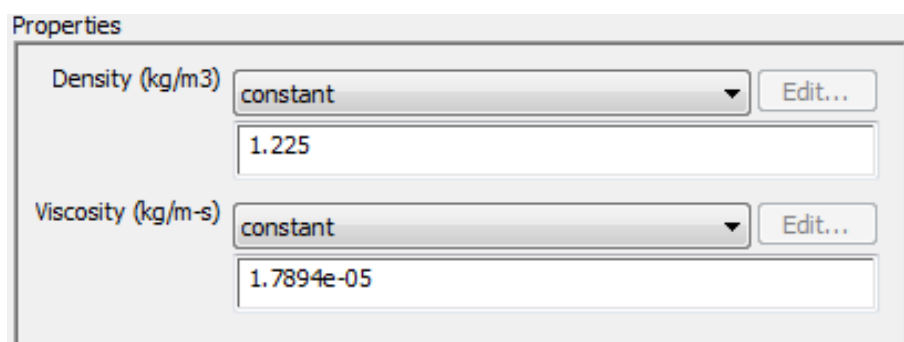


Figure 11.6.: Material

11. Take-off Mode Analysis.

11.1.3.3. Boundary Conditions

The boundary conditions cannot be set in the Fluent setup, unless named selections were created in the Mesh step. That's what we will illustrate now;

1. Inlet : For our case in the Take-off phase, the inlet is the upper surface above the Drone wall. The inlet boundary is set to “ **velocity inlet** ” with various velocities set by the supervisor in order to simulate the real case of the drone flying in the best aspects. Those velocities are [0.1 m/s , 0.5 m/s , 1 m/s , 2 m/s , 5 m/s , 6 m/s , 10 m/s]
2. Outlet: The outlet is the lower surface below the drone wall. The outlet boundary is set to “ **pressure-outlet** ” type, with **gauge pressure** = 0 pascal.
3. Drone wall: is all faces that are projected to air. The wall boundary is set to “ **wall** ” type. that's treated as a **stationary wall** and **no-slip condition** is true on it.
4. Far-field: The air around the Drone, but very far away from its walls. that can represent the velocity v_∞ , The far-field boundaries are treated as the inlet, that the type is set to “ **velocity inlet** ” , with the various velocities mentioned above.

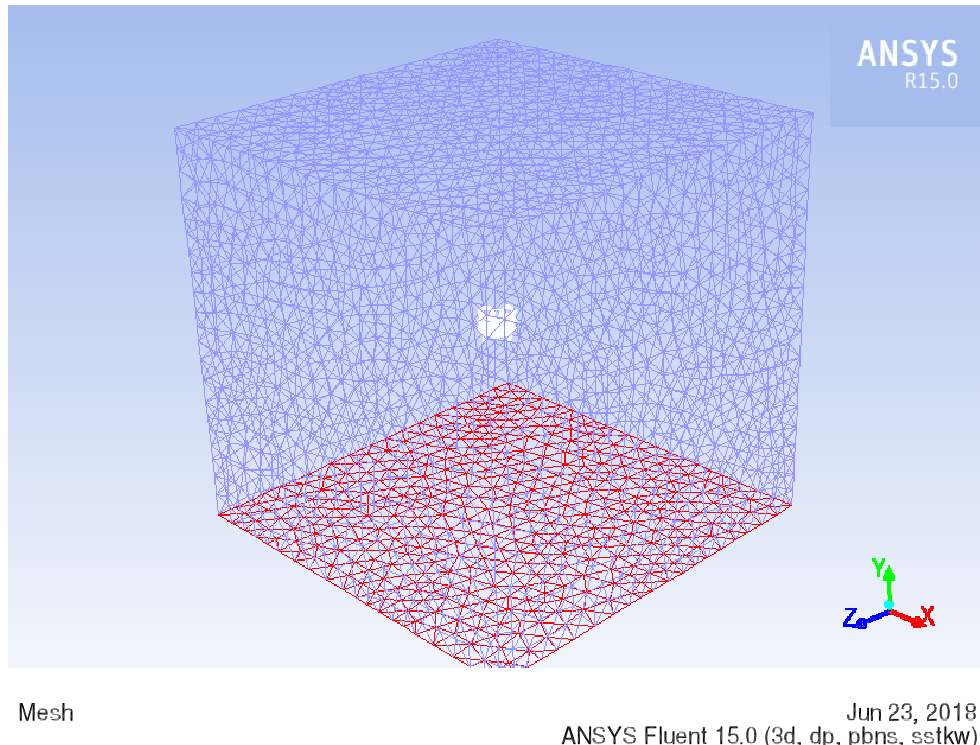


Figure 11.7.: Boundary conditions

11. Take-off Mode Analysis.

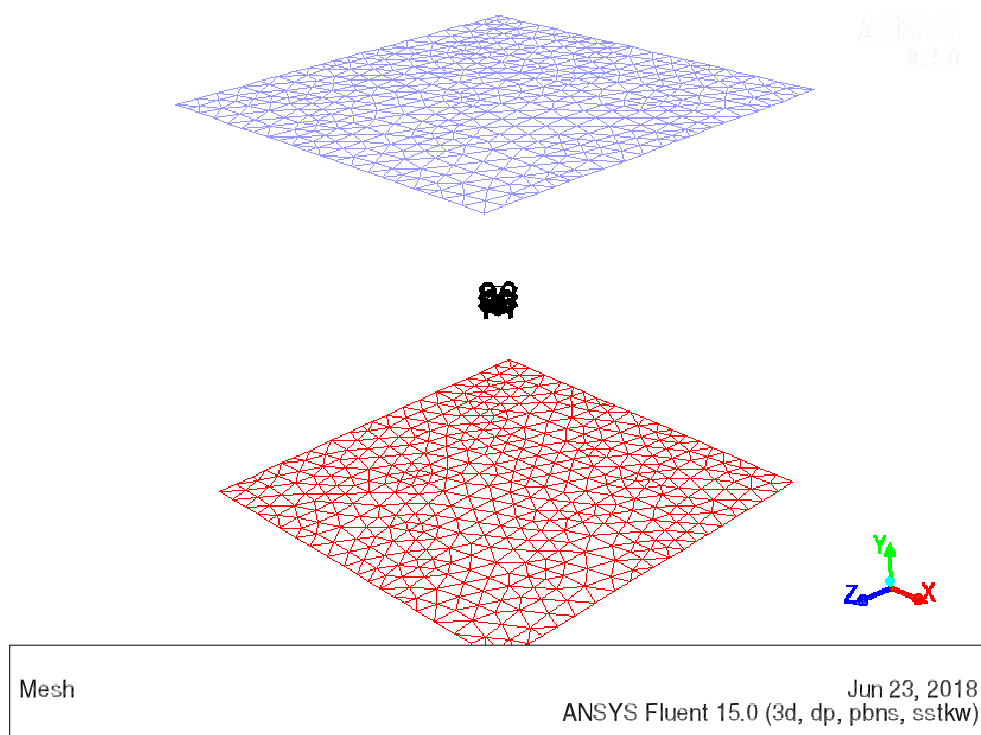


Figure 11.8.: Inlet and outlet only

11.1.4. Solution

11.1.5. Solution Methods

The solution methods have lots of variant options, of course that depends on the equations the program solve and other factors, that will be illustrated clearly in Appendix A. For our case we use the following Solution Method,

The scheme → Coupled.

Gradient → Least squares cell based.

Pressure → Second order.

Momentum → Second Order Upwind.

Turbulent Kinetic Energy → First Order Upwind.

Specific Dissipation Rate → First Order Upwind.

11. Take-off Mode Analysis.

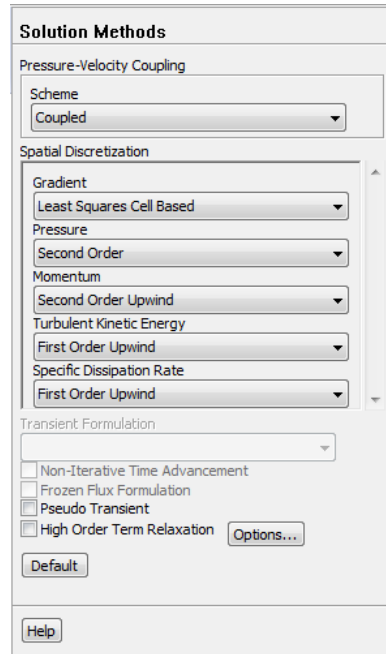


Figure 11.9.: solution method

11.1.6. Results

To be added later

11.2. Second Model Full Analysis

11.2.1. Geomtry

- The Second Model is created using import setting in Ansys design modeler, we inserted the combined part as a one-part body. as follows

11. Take-off Mode Analysis.

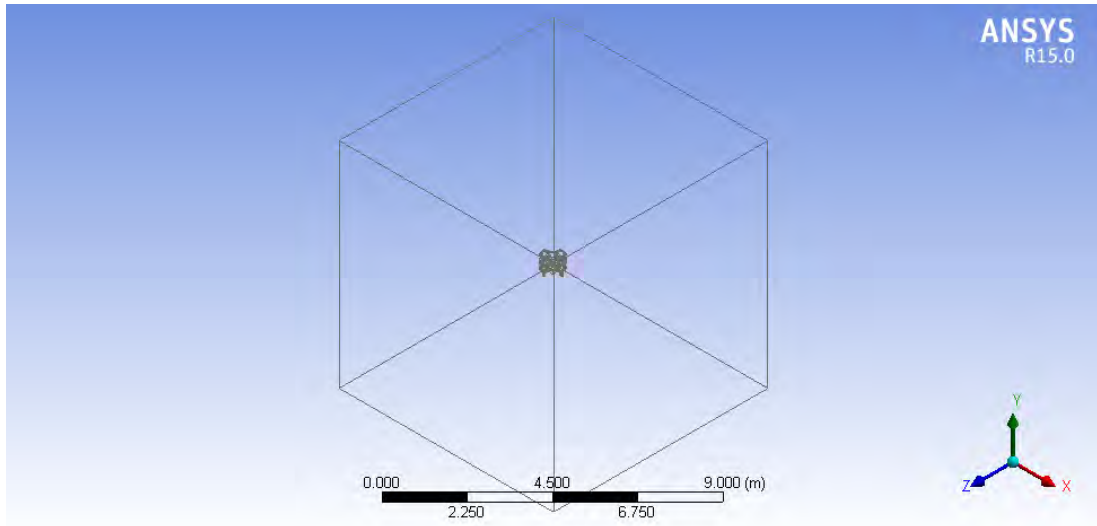


Figure 11.10.: Second Model Geometry

- Then, The control volume is created using the **Extrude** option in Ansys design modeler, Extruding a cubic box with edge length of 4 meters.
- Using the **Boolean** option to **cut** the **material** of the drone from the outside control volume.

11.2.2. Mesh

The mesh created for the Second model was much better than the First model. The mesh options for this model is as follows,

- A sphere of Influence was created with element size of 0.03 meters, The sphere center is the global coordinate system located in the CG of the Drone, with a radius of 0.5 meters.
- Another Sphere of Influence was created with element size of 0.04 meters, The sphere center is the global coordinate system located in the CG of the Drone, with a radius of 1 meters.
- Another Sphere of Influence was created with element size of 0.05 meters, The sphere center is the global coordinate system located in the CG of the Drone, with a radius of 1.5 meters.
- Another Sphere of Influence was created with element size of 0.06 meters, The sphere center is the global coordinate system located in the CG of the Drone, with a radius of 2 meters.
- From **Mesh** option, Insert **Method** →choose “**Tetrahedrons**“
- For algorithm → choose **patch independent**
- From defined by → choose **max. element size** → we have chosen the max. element size is **0.1**, in order to decrease **the skewness**. The final mesh settings is as follows, Skewness = **0.84**, Number of elements = **15,093,577**

11. Take-off Mode Analysis.

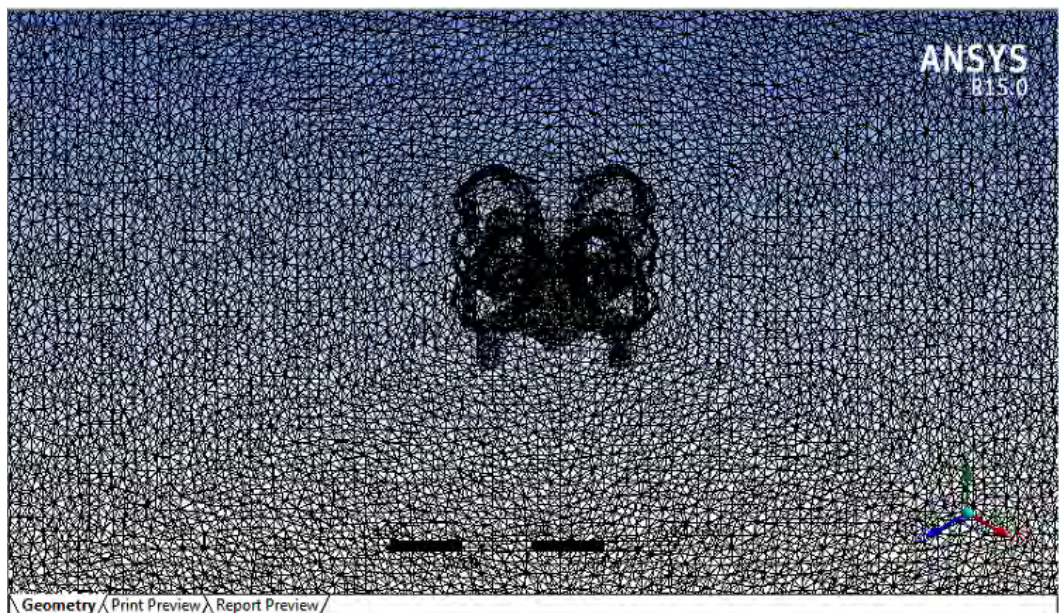


Figure 11.11.: 3D Mesh of Second Model

1.

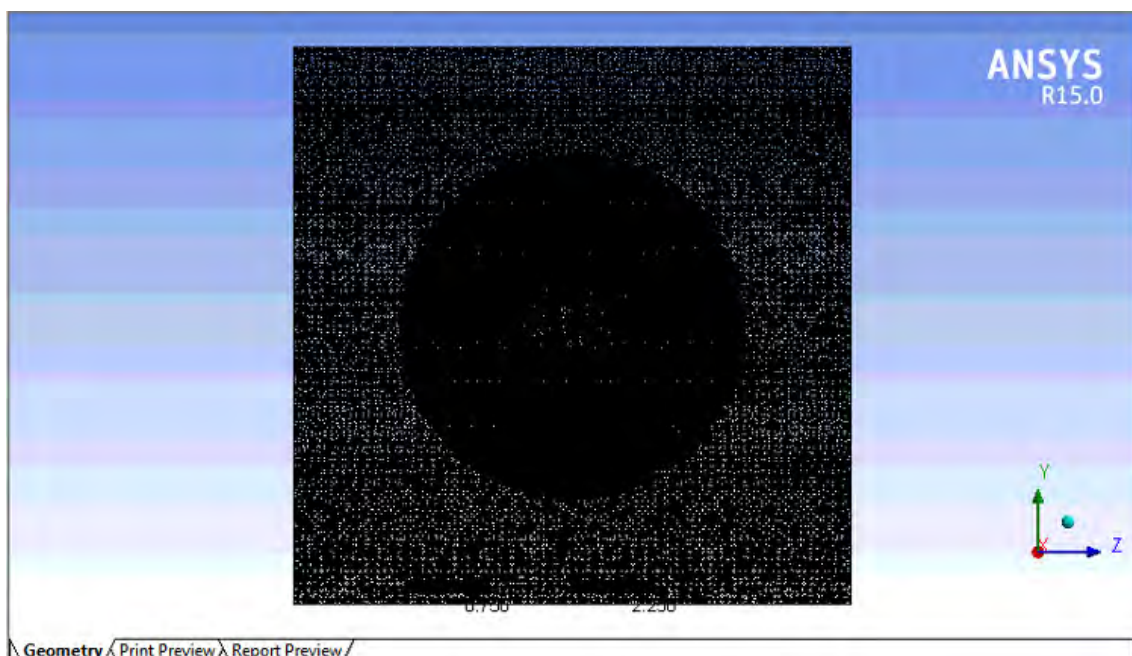


Figure 11.12.: view from Y-Z plane of Mesh

A section plane for the mesh is as in the following picture,

11. Take-off Mode Analysis.

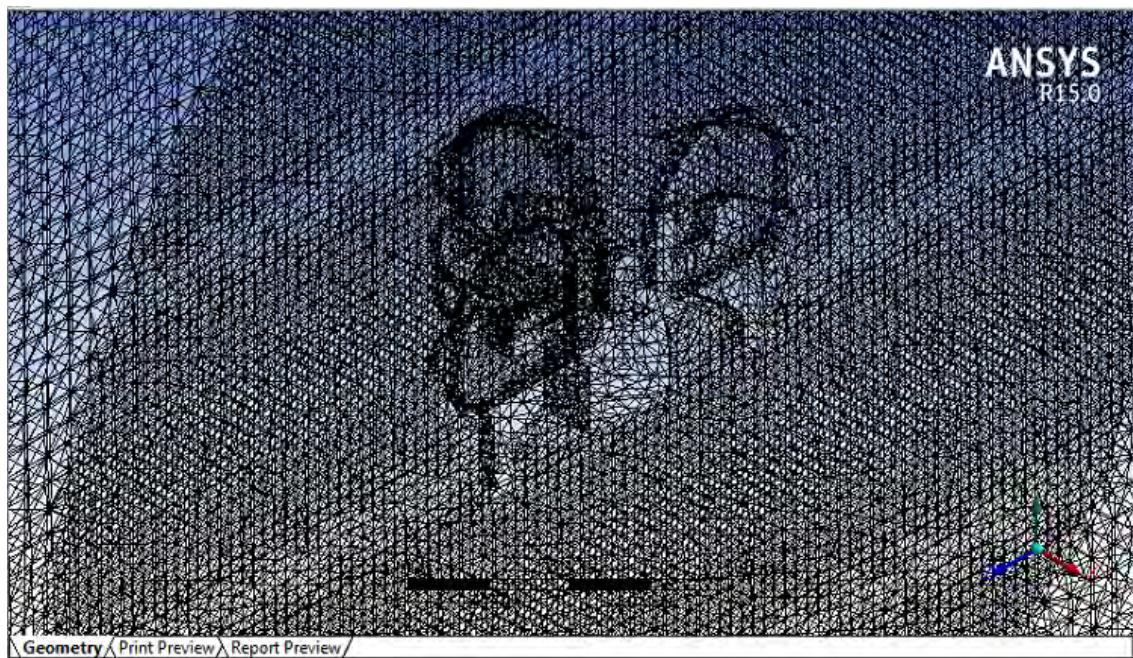


Figure 11.13.: Section plane in Second Model

11.2.3. Setup and solution

The same as Model 1

11.2.4. Results

to be added later on

12. Forward Flight Mode Analysis

Bibliography

- [1] Ardupilot, “Choosing a Ground Station,” <http://ardupilot.org/copter/docs/common-choosing-a-ground-station.html>, [Online; accessed July-2017].
- [2] Jimdo, “Drones User Manuals,” <https://dronesusermanuals.jimdo.com/>, [Online; accessed July-2017].
- [3] PWC, “Clarity from Above,” <https://www.pwc.pl/pl/pdf/clarity-from-above-pwc.pdf/>, [Online; accessed July-2017].
- [4] P. Lab, “Consume Camera vs Professional Multispectral Camera,” <https://publiclab.org/notes/Claytonb/07-09-2016/plant-health-ndvi-consumer-camera-vs-professional-multispectral-camera>, [Online; accessed July-2017].
- [5] I. H. Johansen, “Autopilot Design for Unmanned Aerial Vehicles, Master of Science in Engineering Cybernetics, Norwegian University of Science and Technology,” <https://daim.idi.ntnu.no/masteroppgaver/007/7001/masteroppgave.pdf>.
- [6] Y. . N. Paper, “iflyEgypt story,” <https://goo.gl/6M19S2>.
- [7] W. M. DeBusk, *Unmanned Aerial Vehicle Systems for Disaster Relief: Tornado Alley*, 2011.
- [8] I. C. of the Red Cross, “Drones for Disaster Response and Relief Operations,” <https://www.issuelab.org/resources/21683/21683.pdf>.
- [9] N. S. Nise, *CONTROL SYSTEMS ENGINEERING, Sixth Edition*, 1998.
- [10] P. Mapper, “Algorithms Used in Aerial Images,” <https://www.precisionmapper.com/algorithms>.
- [11] EUMeTrain, “Monitoring Vegetation from Space,” <http://www.eumetrain.org/data/3/36/print.htm>, [Online; accessed July-2017].
- [12] Micasense, “The MicaSense Parrot SEQUOIA ,” <https://www.micasense.com/parrotsequoia/>, [Online; accessed July-2017].
- [13] ——, “The MicaSense RedEdge,” <https://www.micasense.com/rededge/>, [Online; accessed July-2017].
- [14] Sentera, “The Sentera Double 4K,” <https://sentera.com/sensors/>, [Online; accessed July-2017].
- [15] Event38, “Custom NGB Filter Glass for Diy Camera Conversion,” <http://event38.com/product/custom-ngb-filter-glass-for-diy-camera-conversion/>, [Online; accessed July-2017].
- [16] Mapir, “Mapir’s Products and Solutions,” <https://www.mapir.camera/pages/cameras>, [Online; accessed July-2017].
- [17] ——, “Survey 3 Camera’s Specications,” <https://www.mapir.camera/collections/survey3/products/survey3n-camera-red-green-nir-rgn-ndv>, [Online; accessed July-2017].

Bibliography

- [18] ——, “Survey3w’s Specifications,” <https://www.mapir.camera/collections/survey3/products/survey3w-camera-red-green-nir-rgn-ndvi>, [Online; accessed July-2017].
- [19] the UAV guy, “Drones above the Vineyards,” <https://theuavguy.wordpress.com/2014/09/26/drones-above-the-vineyards/>, [Online; accessed July-2017].
- [20] D. Deploy, “Making Successful Maps,” <https://support.dronedeploy.com/docs/making-successful-maps>, [Online; accessed July-2017].
- [21] Mikroopter, “Mk8-3500 Agrar,” <http://www.mikroopter.de/en/products/nmk8agraren/nmk8anw>, [Online; accessed July-2017].
- [22] DJI, “Agras MG-1S,” <http://www.dji.com/mg-1s/info>, [Online; accessed July-2017].
- [23] ——, “Matrice 200 Series,” <http://www.dji.com/matrice-200-series>, [Online; accessed July-2017].
- [24] R. C. Nelson, *Flight stability and automatic control*, 1998.
- [25] Pix4d, “Ground Sampling Distance,” <https://support.pix4d.com/hc/en-us/articles/202559809-Ground-Sampling-Distance-GSD->, [Online; accessed July-2017].
- [26] ——, “Paramters Effect on Covered Area,” <https://support.pix4d.com/hc/en-us/articles/202558849>, [Online; accessed July-2017].
- [27] N. Mansurov, “Raw vs JPEG,” <https://photographylife.com/raw-vs-jpeg>, [Online; accessed July-2017].
- [28] Pix4d, “Designing the Image Acquisition Plan,” <https://support.pix4d.com/hc/en-us/articles/202557459-Step-1-Before-Starting-a-Project-1-Designing-the-Image-Acquisition-Plan-a>Selecting-the-Image> [Online; accessed July-2017].
- [29] ——, “GSD Calculator,” <https://support.pix4d.com/hc/en-us/articles/202560249>, [Online; accessed July-2017].
- [30] F. E. Egypt, “Weight Scales Analog-to-Digital Converter ,” <https://store.fut-electronics.com/products/weight-scales-analog-to-digital-converter-adc-24-bit>, [Online; accessed July-2017].
- [31] ——, “Weight Sensor Load Cell 10kg,” <https://store.fut-electronics.com/products/weight-sensor-load-cell-10kg>, [Online; accessed July-2017].
- [32] ATI, “Multi-Axis Force / Torque Sensors,” <http://www.ati-ia.com/products/ft/sensors.aspx>, [Online; accessed July-2017].

A. Camera Terminology

Introduction

There are some definitions we should be familiar with when working with camera in precision agriculture field.

Ground Sampling Distance (GSD)[25]

The Ground Sampling Distance (GSD) is the distance between two consecutive pixel centers measured on the ground. The bigger the value of the image GSD, the lower the spatial resolution of the image and the less visible details. The GSD is related to the flight height: the higher the altitude of the flight, the bigger the GSD value.

Example

- A GSD of 5 cm means that one pixel in the image represents linearly 5 cm on the ground ($5 \times 5 = 25$ square centimeters).
- A GSD of 10 m means that one pixel in the image represents linearly 10 m on the ground ($10 \times 10 = 100$ square meters).

Notes:

Even when flying at a constant height, the images of a project may not have the same GSD. This is due to terrain elevation differences and changes in the angle of the camera while shooting.

- At a defined altitude, increasing the focal length:[26]
 - A smaller area is captured, and therefore:
 - The Ground Sampling Distance (GSD) value will decrease: one pixel will capture a smaller area and therefore the image will have a higher spatial resolution.
 - The image rate needs to be increased to maintain a good overlap.
- At a defined focal length, decreasing the altitude:
 - A smaller area is captured, and therefore:
 - The GSD value will decrease: one pixel will capture a smaller area and therefore the image will have a higher spatial resolution.
 - The image rate needs to be increased to maintain a good overlap.
- Terrains:
 - Forest and dense vegetation: Flying higher helps for the reconstruction, but the spatial resolution will be lower.

A. Camera Terminology

- Buildings: Flying higher reduces the artifacts at the building edges, but the spatial resolution will be lower.

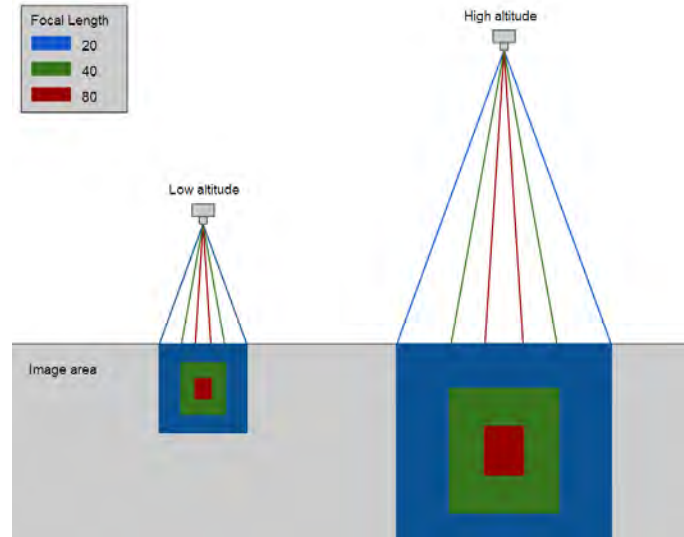


Figure A.1.: Focal length and flight height effect on area covered

- Overlap:

- Low altitude with big focal length will request a very high image rate in order to maintain a good overlap.
- For a given focal length and a given image rate, increasing the altitude will increase the overlap.

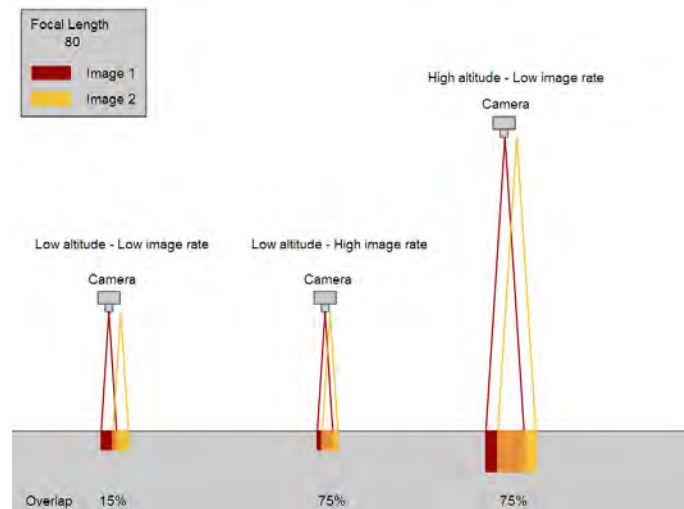


Figure A.2.: Image rate and flight height effect on overlap

A. Camera Terminology

Resolution

Resolution is a term associated with all types of photography. It has several different meanings depending on the context in which it is used.

With regard to digital cameras, resolution (also called image capture resolution) refers to the number of pixels in the camera sensor. A camera with 3 megapixels has a sensor with 3 million pixels. A pixel in a sensor is a single element of the sensor that will record the smallest element of the image. The more pixels in a sensor, the higher the resolution of the image.

With regard to digital printing, resolution refers to the number of dots in a given distance, usually dots per inch, or DPI. The more dots per inch, the higher resolution of the print.

With regard to vertical aerial photography, resolution (also called ground resolution or ground sample distance) refers to the area of ground covered by an individual pixel. In an image with 6 inch ground resolution, each pixel records the average reflected color of an area 6 inches by 6 inches. The fewer inches per pixel, the higher the resolution resolution of the image. The selection of a desired ground resolution is an important factor to decide when ordering vertical aerial images.

Examples of various ground resolutions and considerations:

- 1 meter (36 inch) resolution is considered high resolution for satellite imagery. It is useful for surveying very large areas. Details that can be seen at this resolution include roads, average color of crops and forests, buildings, large infrastructure features and large waterways.

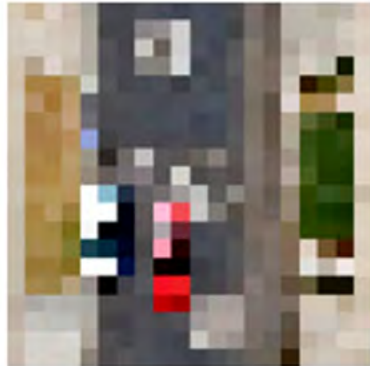


Figure A.3.: Meter resolution

- 12 inch resolution is the industry standard for most archived large area image databases including Google Earth. It displays much more detail than 1 meter resolution. Details that can be seen at this resolution include vehicles, roads and some markings, individual crop rows, large trees and details on buildings.

A. Camera Terminology



Figure A.4.: 12 inch resolution

- 6 inch resolution is considered high resolution for aerial photography. This resolution is occasionally available from archives but is usually produced on a custom basis. Details that are visible at this resolution include individual small trees and plants, individual vines and other crops, vehicle types, power poles and other infrastructure details, road markings and lettering.



Figure A.5.: 6 inch resolution

- 3 inch resolution is very high resolution for aerial imagery. Details that can be seen with this resolution include power lines and other very small infrastructure details, individual people and animals, currents and waves in water, fine details on roads including markings and skid marks.

A. Camera Terminology



Figure A.6.: 3 inch resolution

- 1 inch resolution is about the highest ground resolution available today. Street markings are very clear and legible. This resolution provides detail 9 times greater than 3 inch. Focal Flight has shot areas up to 80 square miles at this resolution providing the user the highest available detail in their imagery.

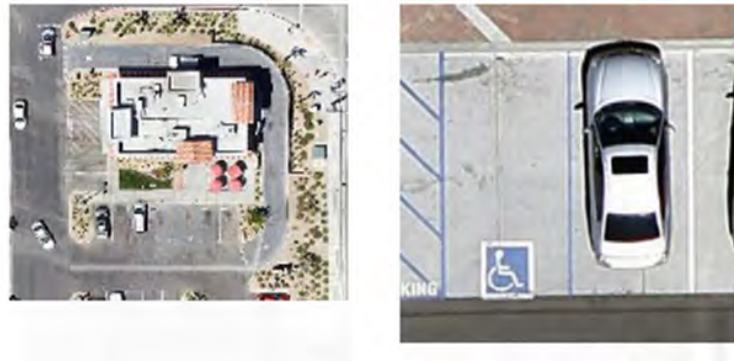


Figure A.7.: 3 inch resolution

RAW vs JPG [27]

Some Camera offers two captures modes

- 8-bit JPG mode
- 12 bit RAW+ 8 bit JPG mode

Main difference :

- From photo Graph prospective
 - When you shoot in RAW you record all of the data from the sensor.

A. Camera Terminology

- 8-bit JPEG format that can only contain up to 256 shades of Red, Green and Blue colors (total of 16 million), 12-bit RAW images contain the most amount of information with 4,096 shades of Red, Green and Blue (equivalent of 68 billion colors!) and higher.
 - RAW takes up much more camera memory and space than JPEG images. This means that memory card can store fewer images and camera buffer can quickly fill up, causing the camera frame rate to drop down significantly.
 - No image-sharpening is performed on RAW files, which means that you can use better and more complex sharpening algorithms for your photos in your PC.
 - you can post process the raw images into jpeg images but you can
 - JPEG images are fully processed in camera and all settings such as White Balance, Color Saturation, Tone Curve, Sharpening and Color Space are already applied to the image. So you do not need to spend any time on post-processing the image – all you need to do is extract the image out of the memory card and it is ready to use. JPEG images are much smaller than RAW images and therefore consume a lot less storage and need much less processing power. Due to the smaller size, cameras can write JPEG files much faster, which increases the number of pictures that can fit in temporary camera buffer. This means that compared to RAW, you can potentially shoot at higher frames per second and for longer periods of time.
- From our application prospective
 - JPEG images are (mostly) lossy compressed images of the original, thought for visualization purposes, not for analysis.

Example:



Figure A.8.: JPEG image vs RAW image

A. Camera Terminology

We recommend shooting in Raw + jpg mode.

Recommended Overlap [28]

The recommended overlap for most cases is at least 75% frontal overlap (with respect to the flight direction) and at least 60% side overlap (between flying tracks). It is recommended to take the images with a regular grid pattern . The camera should be maintained as much possible at a constant height over the terrain / object to ensure the desired GSD.

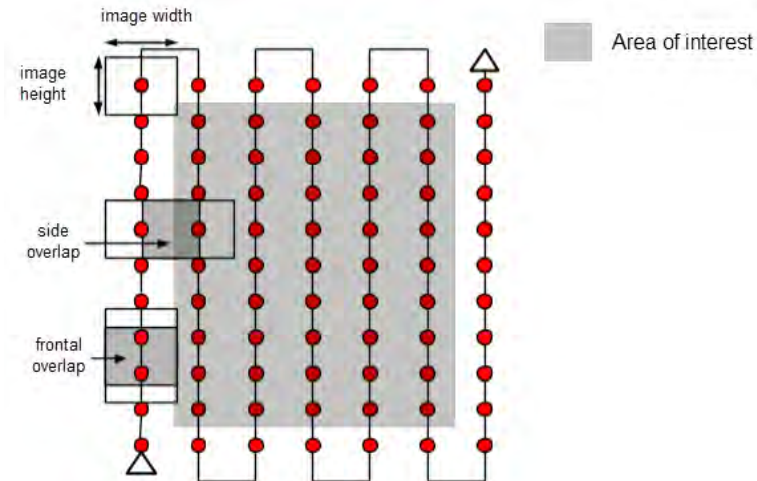


Figure A.9.: Ideal image acquisition plan

Computing the Image Rate for a given Frontal Overlap

The image shooting rate to achieve a given frontal overlap depends on the speed of the UAV/plane, the GSD and the pixel resolution of the camera.

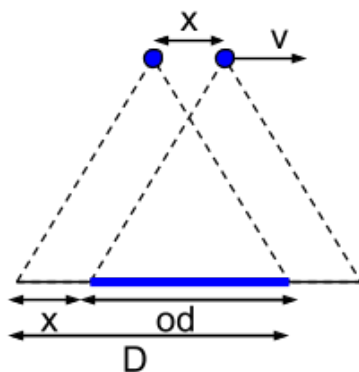


Figure A.10.: Overlap

A. Camera Terminology

From figure A.10, we obtain the following equations:

$$\begin{aligned} od &= overlap * D \\ x &= D - od \\ t &= x/v \end{aligned}$$

Where

D = distance covered on the ground by one image in the flight direction [m]

$overlap$ = percentage of desired frontal overlap between two images

od = overlap between two images in the flight direction [m]

x = distance between two camera positions in the flight direction [m]

v = flight speed [m/s]

t = elapsed time between two images (image rate) [s]

Two cases are possible:

- Camera oriented with the sensor width (long dimension) perpendicular to the flight direction (usual case)

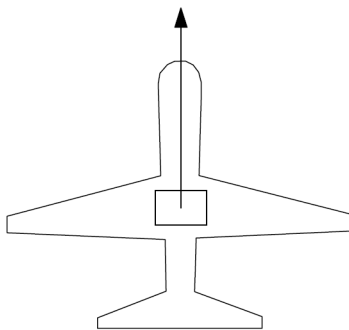


Figure A.11.: Sensor width placed perpendicular to the flight direction.

$$D = D_h = (imH * GSD) / 100$$

Where:

D_h = distance covered on the ground by one image in the height direction (footprint height) [m]

imH = image height [pixel]

GSD = desired GSD [cm/pixel]

$$\begin{aligned} \therefore x &= D_h - overlap * D_h \\ x &= D_h (1 - overlap) \\ x &= ((imH * GSD) / 100) (1 - overlap) \\ t &= ((imH * GSD) / 100) (1 - overlap) / v \end{aligned}$$

Note: x is given in [m], considering that the GSD is in [cm/pixel].

- Camera oriented with the sensor width (long dimension) parallel to the flight direction

A. Camera Terminology

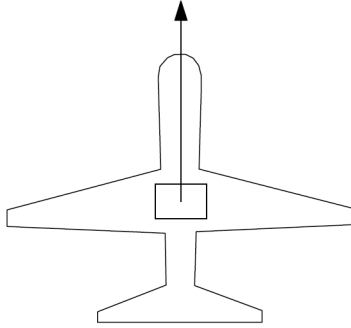


Figure A.12.: Sensor width placed perpendicular to the flight direction.

$$D = D_w = (imW * GSD) / 100$$

Where:

D_w = distance covered on the ground by one image in the width direction (footprint width) [m]

imW = image width [pixel]

GSD = desired GSD [cm/pixel]

$$\begin{aligned} \therefore x &= D_w - overlap * D_w \\ x &= D_w (1 - overlap) \\ x &= ((imW * GSD) / 100) (1 - overlap) \\ t &= ((imW * GSD) / 100) (1 - overlap) / v \end{aligned}$$

Calculating Flight Height , Flight Velocity

There are relations between camera specification, flight height and GSD.

The following relations were derived by pix4d [29]

$$\begin{aligned} GSD &= (SW * H * 100) / (FL * imW) \\ D_w &= GSD * imW / 100 \\ D_h &= GSD * imH / 100 \\ Ox &= Ovelap_{front} * D_h \\ x &= D_h - Ox \\ Oy &= Ovelap_{side} * D_w \\ y &= D_w - Oy \\ Max\ velocity &= CEIL(H/20) * 5 * 0.44704 \\ v &= f * Max\ velocity \\ t &= x/v \end{aligned}$$

Where:

H: Flight height (m).

Max velocity: The max velocity at this height (m/sec).

f: Percentage of max velocity.

v: Flight velocity (m/sec).

B. Ground Control Station

B. Ground Control Station

Program Sequence Diagram

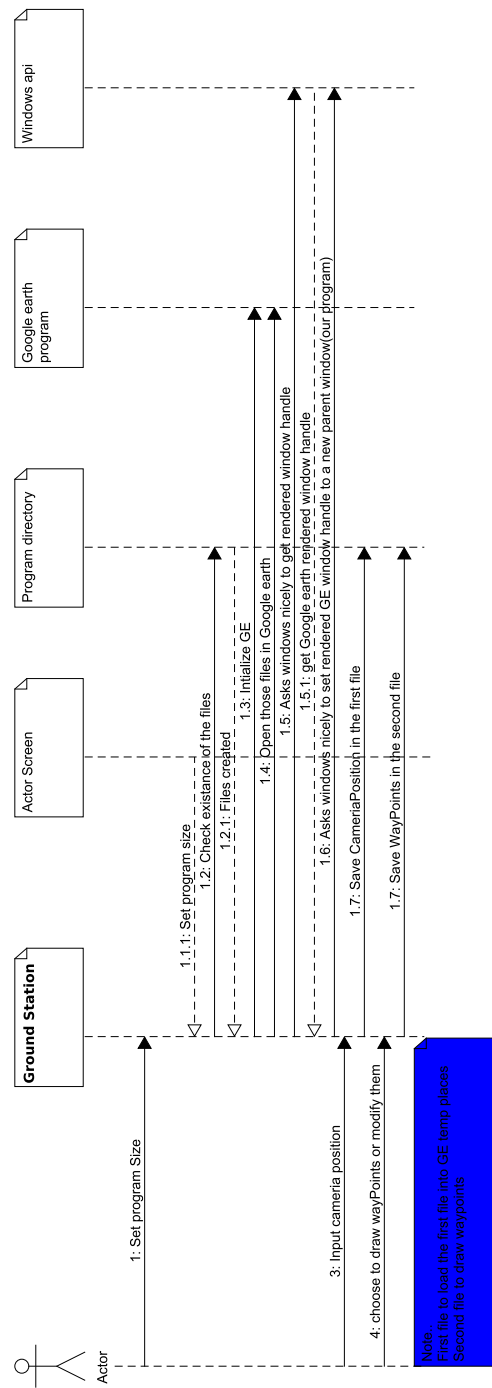


Figure B.1.: Program sequence diagram

B. Ground Control Station

Google earth

Google Earth for PC enables you to explore the globe. Fly through 3D cities like London, Tokyo and Rome. Dive in to view the world at street level with integrated Street View. Find stories about what it means to live here from the BBC, NASA, Sesame Street, and more.

the program version that is used with our program is `GoogleEarthWin_5.2.1.1588` as officially google earth doesn't support API after version 5.2¹

you can find the version that is used by following this link [GoogleEarthWin_5.2.1](#)

KML

I had to learn kml syntax in order to fully control Google earth.

i focused on three examples to create way points on google earth

- kml Placemark
- kml Path
- kml NetworkLink

and by understanding them. I could build complex things like used in the program.

Introduction

KML is a file format used to display geographic data in an Earth browser such as Google Earth. KML uses a tag-based structure with nested elements and attributes and is based on the XML standard.

KML Placemark

A Placemark is one of the most commonly used features in Google Earth. It marks a position on the Earth's surface, using a yellow pushpin as the icon. The simplest Placemark includes only a `<Point>` element, which specifies the location of the Placemark. You can specify a name and a custom icon for the Placemark, and you can also add other geometry elements to it.

Open the KML Samples file in Google Earth and expand the Placemarks subfolder. This folder includes three different types of placemark: simple, floating, and extruded. The KML code for the simple placemark looks like this:

¹Today we're announcing that the Google Earth 5.2 client will be the last version that supports the COM API. Earth 5.2 and older clients will continue to support the COM API while these versions are supported. Future releases will no longer have COM API bindings. We believe that the JavaScript API provides the best mechanism for reaching the most developers.

B. Ground Control Station

Algorithm B.1 Placemark.kml

```
<?xml version="1.0" encoding="UTF-8"?>
<kml xmlns="http://www.opengis.net/kml/2.2">
    <Placemark> <name>Simple placemark</name>
        <description>Attached to the ground. Intelligently places itself at
        <Point>
            <coordinates>-122.0822035425683,37.42228990140251,0</coordinates>
        </Point>
    </Placemark>
</kml>
```

The structure of this file breaks down as follows:

- An XML header. This is line 1 in every KML file. No spaces or other characters can appear before this line.
- A KML namespace declaration. This is line 2 in every KML 2.2 file.
- A Placemark object that contains the following elements:
 - A name that is used as the label for the Placemark
 - A description that appears in the "balloon" attached to the Placemark
 - A Point that specifies the position of the Placemark on the Earth's surface (longitude, latitude, and optional altitude)



Figure B.2.: Placemark example

B. Ground Control Station

KML Style

Once you've created features within Google Earth and examined the KML code Google Earth generates, you'll notice how styles are an important part of how your data is displayed. Power users will want to learn how to define their own styles.

If you define a Style at the beginning of a KML Document and also define an ID for it, you can use this style in Geometry, Placemarks, and Overlays that are defined elsewhere in the Document. Because more than one element can use the same Style, styles defined and used in this way are referred to as shared styles. You define a given Style once, and then you can reference it multiple times, using the `<styleUrl>` element. If the Style definition is within the same file, precede the Style ID with a # sign. If the Style definition is in an external file, include the complete URL in the `<styleUrl>` element.

B. Ground Control Station

Example

Algorithm B.2 Style.kml

```
<?xml version="1.0" encoding="UTF-8"?>
<kml xmlns="http://www.opengis.net/kml/2.2">
<Document>
<Style id="transBluePoly">
<LineStyle>
<width>1.5</width>
</LineStyle>
<PolyStyle>
<color>7dff0000</color>
</PolyStyle>
</Style>
<Placemark>
<name>Building 41</name>
<styleUrl>#transBluePoly</styleUrl>
<Polygon>
<extrude>1</extrude>
<altitudeMode>relativeToGround</altitudeMode>
<outerBoundaryIs>
<LinearRing>
<coordinates>
-122.0857412771483,37.42227033155257,17
-122.0858169768481,37.42231408832346,17
-122.085852582875,37.42230337469744,17
-122.0858799945639,37.42225686138789,17
-122.0858860101409,37.4222311076138,17
-122.0858069157288,37.42220250173855,17
-122.0858379542653,37.42214027058678,17
-122.0856732640519,37.42208690214408,17
-122.0856022926407,37.42214885429042,17
-122.0855902778436,37.422128290487,17
-122.0855841672237,37.42208171967246,17
-122.0854852065741,37.42210455874995,17
-122.0855067264352,37.42214267949824,17
-122.0854430712915,37.42212783846172,17
-122.0850990714904,37.42251282407603,17
-122.0856769818632,37.42281815323651,17
-122.0860162273783,37.42244918858722,17
-122.0857260327004,37.42229239604253,17
-122.0857412771483,37.42227033155257,17
</coordinates>
</LinearRing>
</outerBoundaryIs>
</Polygon>
</Placemark>
</Document>
</kml>
```

B. Ground Control Station

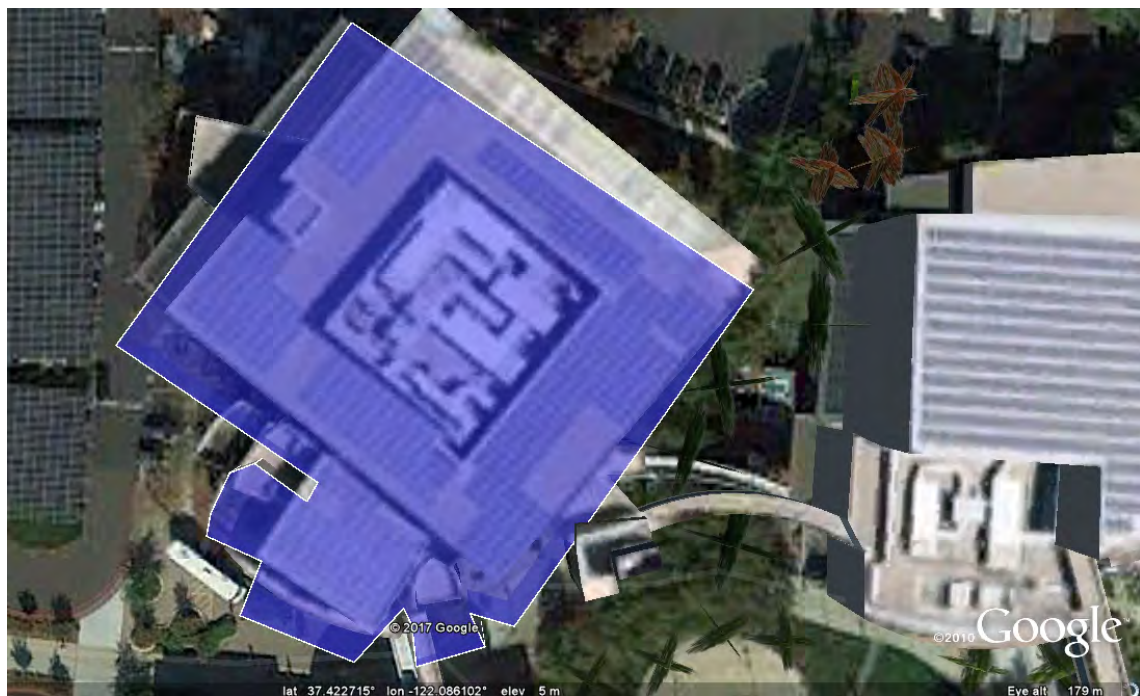


Figure B.3.: Style example

KML Path

Many different types of paths can be created in Google Earth, and it is easy to be very creative with your data. In KML, a path is created by a <LineString> element. Take a look at the "Absolute Extruded" example in the Paths folder and you can see how the shape has been generated by the following code:

B. Ground Control Station

Algorithm B.3 Path.kml

```
<?xml version="1.0" encoding="UTF-8"?>
<kml xmlns="http://www.opengis.net/kml/2.2">
<Document>
<name>Paths</name>
<description>Examples of paths. Note that the tessellate tag is by default set to 0. If you want to create tessellated lines, they must be authored (or edited) directly in KML.</description>
<Style id="yellowLineGreenPoly">
<LineStyle>
<color>7f00ffff</color>
<width>4</width>
</LineStyle>
<PolyStyle>
<color>7f00ff00</color>
</PolyStyle>
</Style>
<Placemark>
<name>Absolute Extruded</name>
<description>Transparent green wall with yellow outlines</description>
<styleUrl>#yellowLineGreenPoly</styleUrl>
<LineString>
<extrude>1</extrude>
<tessellate>1</tessellate>
<altitudeMode>absolute</altitudeMode>
<coordinates>
-112.2550785337791,36.07954952145647,2357
-112.2549277039738,36.08117083492122,2357
-112.2552505069063,36.08260761307279,2357
-112.2564540158376,36.08395660588506,2357
-112.2580238976449,36.08511401044813,2357
-112.2595218489022,36.08584355239394,2357
-112.2608216347552,36.08612634548589,2357
-112.262073428656,36.08626019085147,2357
-112.2633204928495,36.08621519860091,2357
-112.2644963846444,36.08627897945274,2357
-112.2656969554589,36.08649599090644,2357
</coordinates>
</LineString>
</Placemark>
</Document>
</kml>
```

B. Ground Control Station



Figure B.4.: Path example

KML Network link

A network link contains a `<Link>` element with an `<href>` (a hypertext reference) that loads a file. The `<href>` can be a local file specification or an absolute URL. Despite the name, a `<NetworkLink>` does not necessarily load files from the network.

The `<href>` in a link specifies the location of any of the following:

- An image file used by icons in icon styles, ground overlays, and screen overlays
- A model file used in the `<Model>` element
- A KML or KMZ file loaded by a Network Link

The specified file can be either a local file or a file on a remote server. In their simplest form, network links are a useful way to split one large KML file into smaller, more manageable files on the same computer.

So far, all of our examples have required that the KML code be delivered to Google Earth from the local machine. Network links give you the power to serve content from a remote location and are commonly used to distribute data to large numbers of users. In this way, if the data needs to be amended, it has to be changed only at the source location, and all users receive the updated data automatically.

B. Ground Control Station

Algorithm B.4 Network link.kml

```
<kml xmlns="http://www.opengis.net/kml/2.2">
<Document>
<name>Open Document</name>
<open>1</open>
<NetworkLink>
<name>Open NetworkLink</name>
<open>1</open>
<description>NetworkLink open to fetched content</description>
<Link>
<href>placemark.kml</href>
</Link>
</NetworkLink>
<NetworkLink>
<name>non-Open NetworkLink</name>
<open>0</open>
<description>NetworkLink not open</description>
<Link>
<href>placemark.kml</href>
</Link>
</NetworkLink>
</Document>
</kml>
```

Algorithm B.5 Placemark.kml

```
<kml xmlns="http://www.opengis.net/kml/2.2">
<Placemark id="p">
<name>P</name>
<Point>
<coordinates>1,1</coordinates>
</Point>
</Placemark>
</kml>
```

B. Ground Control Station

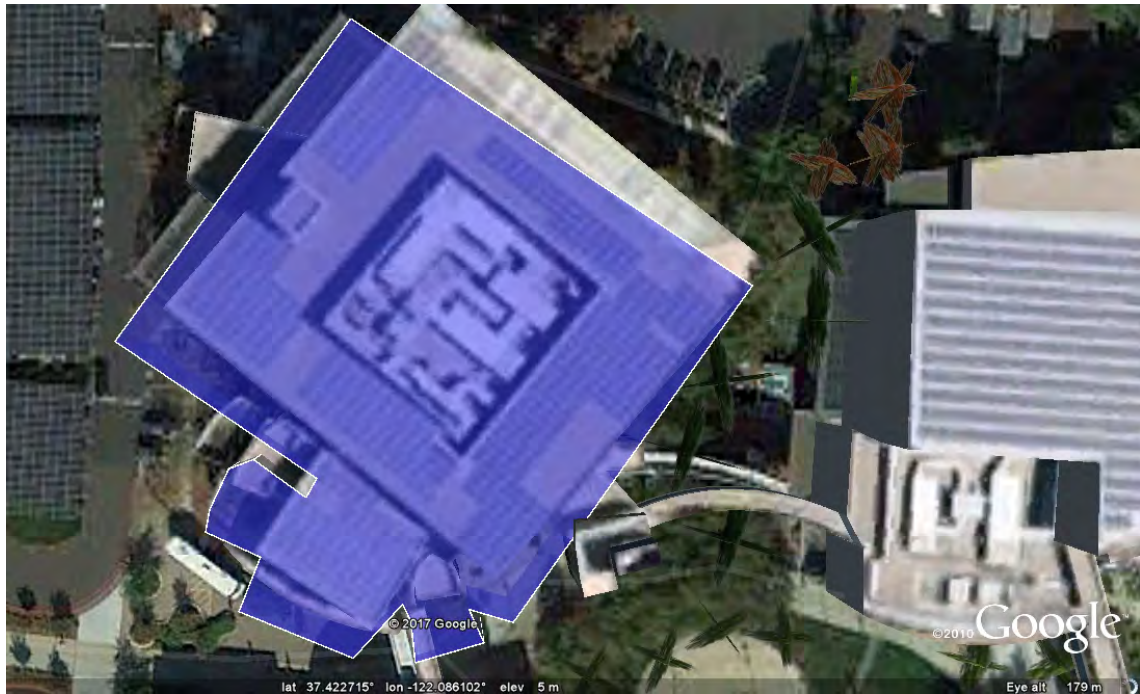


Figure B.5.: Network link example

B.1. Windows API

theses Windows API functions were used in the program to get google earth rendered window handle

FindWindowEx Function

Retrieves a handle to a window whose class name and window name match the specified strings. The function searches child windows, beginning with the one following the specified child window. This function does not perform a case-sensitive search.

GetWindowLong Function

Retrieves information about the specified window. The function also retrieves the 32-bit (DWORD) value at the specified offset into the extra window memory.

SetWindowLong Function

Changes an attribute of the specified window. The function also sets the 32-bit (long) value at the specified offset into the extra window memory.

SetLayeredWindowAttributes Function

Sets the opacity and transparency color key of a layered window.

B. Ground Control Station

MoveWindow Function

Changes the position and dimensions of the specified window. For a top-level window, the position and dimensions are relative to the upper-left corner of the screen. For a child window, they are relative to the upper-left corner of the parent window's client area.

ShowWindow Function

Sets the specified window's show state.

SetParent Function

Changes the parent window of the specified child window.

B.2. Spline path

We wanted to create spline path like the ones generated by professional GCS

Spline Path Algorithm

- Specify four points to specify the required area of interest

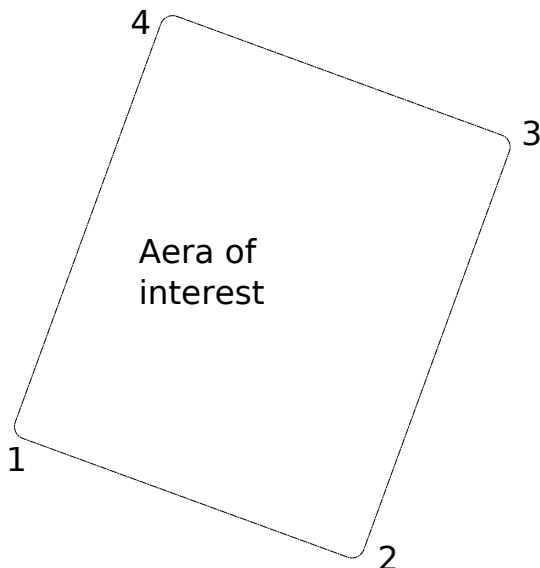


Figure B.6.: Aera of interest

- Specify your required height & from relations from [appendix A](#), you will get the required X , Y & required velocity to the multi rotor.
- Calculate the inclination of line $\overrightarrow{12}$, line $\overrightarrow{14}$ & line $\overrightarrow{23}$
- Calculate max distance between point 2 & point 3 and point 1 & point 3

B. Ground Control Station

- Get number of rows
 $n_{row} = \frac{\max distance}{Y}$
- For $i = 1 : n_{row}$
 - get direction
 - * if i equals odd number then $dir = 1$;
 - * if i equals even number then $dir = -1$
 - move from point 1 distance $i * Y$ in the direction of line $\overrightarrow{14}$ & get this point (longitude & latitude)(P_i^*)
 - move from point 2 distance $i * Y$ in the direction of line $\overrightarrow{23}$ & get this point(longitude & latitude)(P_{2i}^*)
 - get number of points in each row
 $n_{columns} = \frac{distance(P_i^*, P_{2i}^*)}{X}$
 - for $i = 1 : n_{columns}$
 - * move from P_i^* to P_i distance $dir * X$ in the direction of line $\overrightarrow{12}$
 - end
 - move from $P_{n_{columns}}$ distance Y in the direction of line $\overrightarrow{23}$
 - end

Example

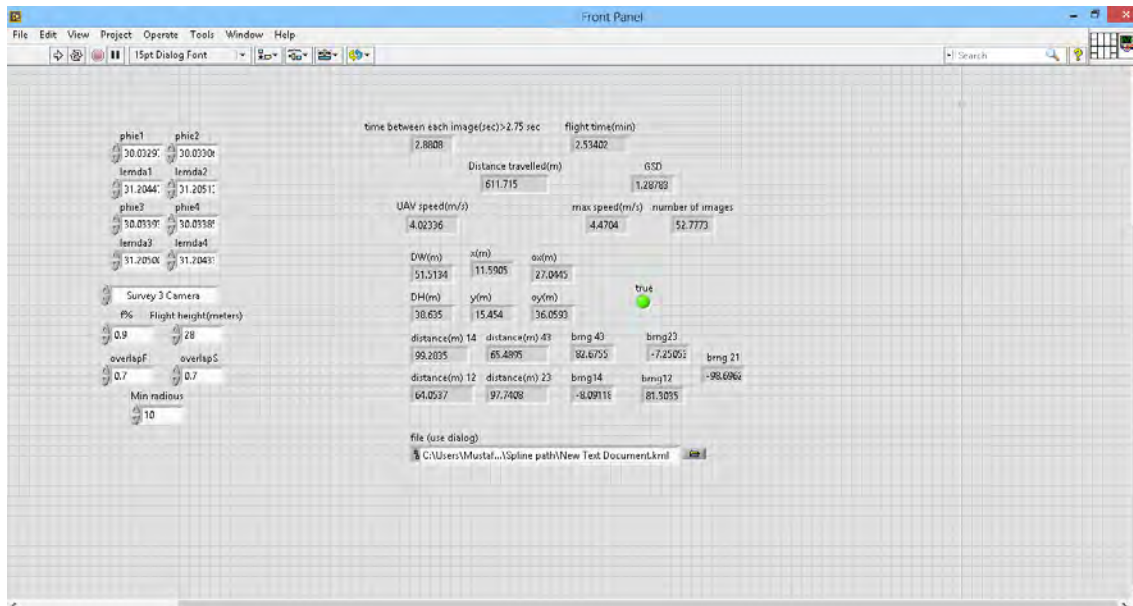


Figure B.7.: Front panel #1

B. Ground Control Station



Figure B.8.: Block diagram #1

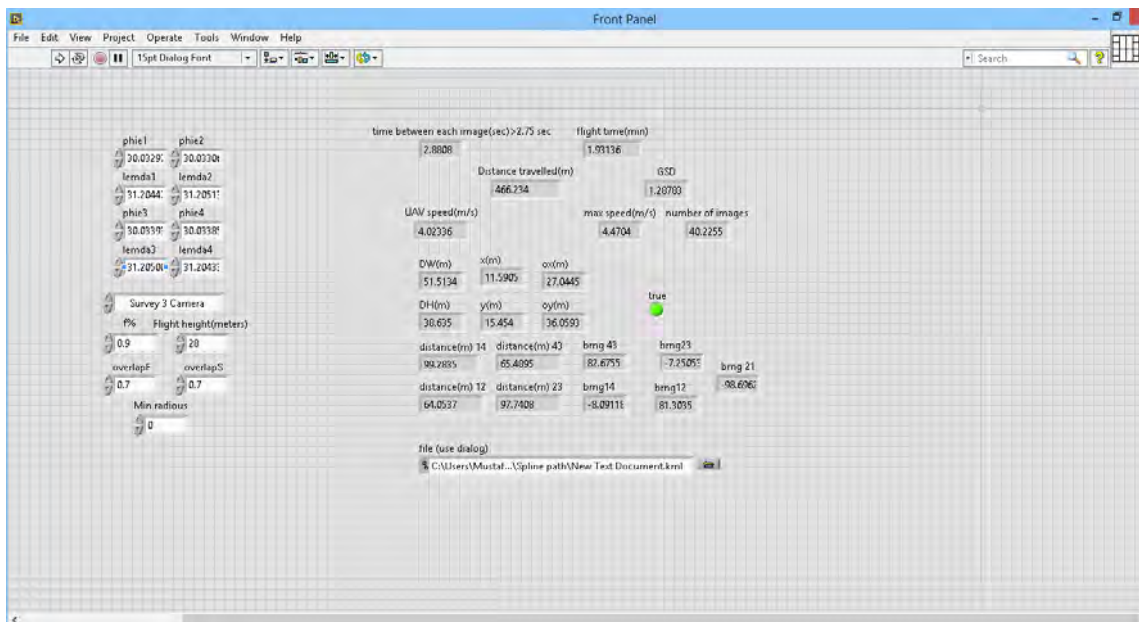


Figure B.9.: Front panel #2

B. Ground Control Station



Figure B.10.: Block diagram #2

B.3. Manual

- First install the attached google earth program then open the application.exe file
- Wait until google earth opens then switch to application.exe 's window
- Click on the left and the right button of the mouse
- Click OK button then google earth will atomically goes to it's default location(our collage longitude and latitude)

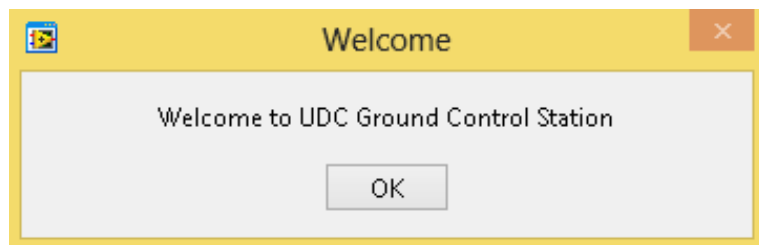


Figure B.11.: Dialog box #1

B.3.1. Make path

- Click on the left and the right button of the mouse

B. Ground Control Station

- Click Create Path button

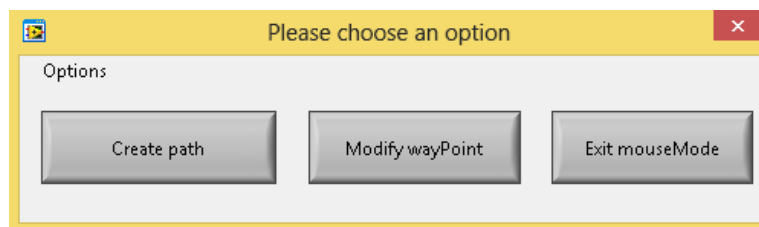


Figure B.12.: Dialog box #2

- Click on the right button to choose it your home point
- Enter your altitude at that point

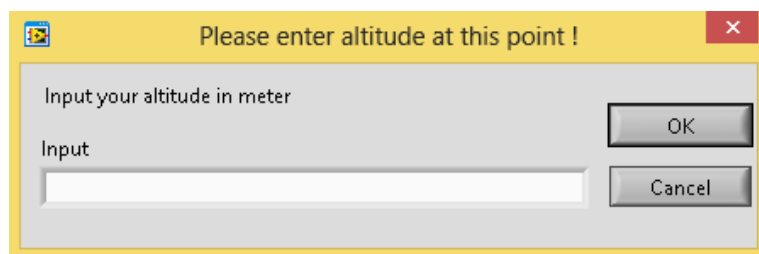


Figure B.13.: Dialog box #3

- Click OK button
- Click on the right mouse to specify different way points and each time you click, you'll have to specify the required altitude at that point

B. Ground Control Station



Figure B.14.: Screen shoot #1

1. Note that
 - a) the red point is your start & end point
 - b) green point is way point that is not your home point
 - c) blue point is the closest point to the airplane at that moment

B.3.2. Modify way point

- Go close to your desired unwanted way point
- Click Modify way Point button

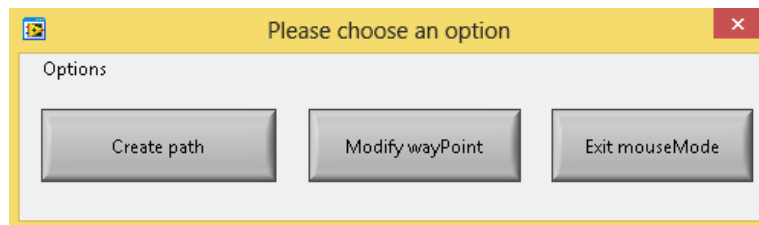


Figure B.15.: Dialog box #2

- The way point will begin to move with the mouse until you click on the right mouse button

B. Ground Control Station



Figure B.16.: Screen shoot #2

- Enter your new altitude at that point

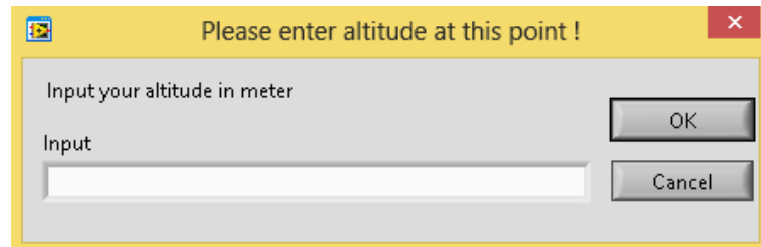


Figure B.17.: Dialog box #3

- That's now your new point have been added to the way point array successfully

B. Ground Control Station



Figure B.18.: Screen shoot #3

B.3.3. Make circle path

- Go to menu bar and Click on Options then choose DrawCircle from the drop-down menu

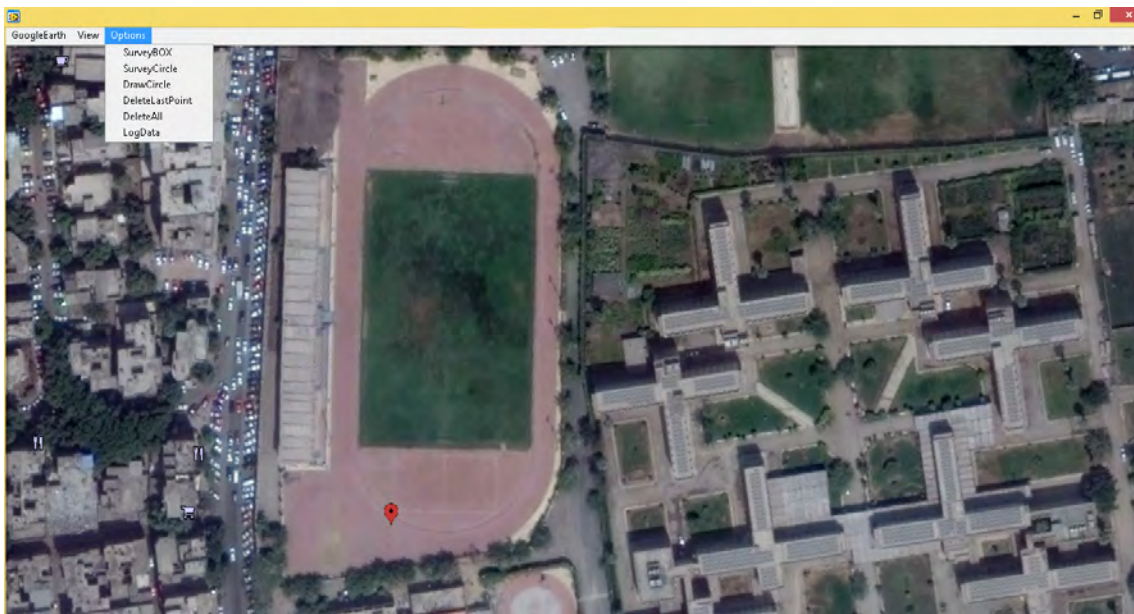


Figure B.19.: Screen shoot #4

B. Ground Control Station

- Choose your circumference point of the circle then choose your center point
- Choose the altitude of all the circle point then number of number of circles and if you want to rotate clock wise or anti-clock wise

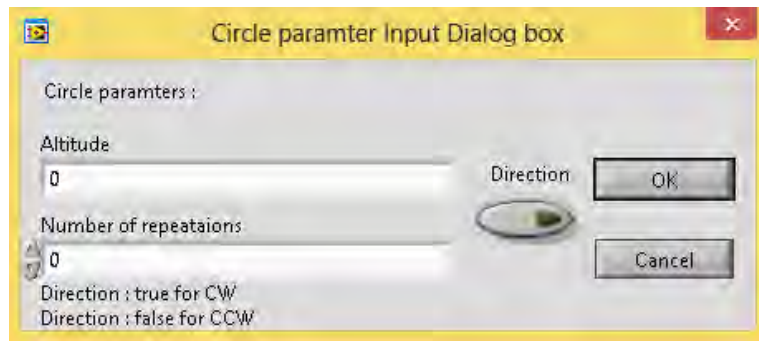


Figure B.20.: Dialog box #4

- The result will be like this



Figure B.21.: Screen shoot #5

B.3.4. Make spline path

- Go to menu bar and Click on Options then choose SurveyBox or SurveyCircle according to the shape of the area of interest from the drop-down menu

B. Ground Control Station

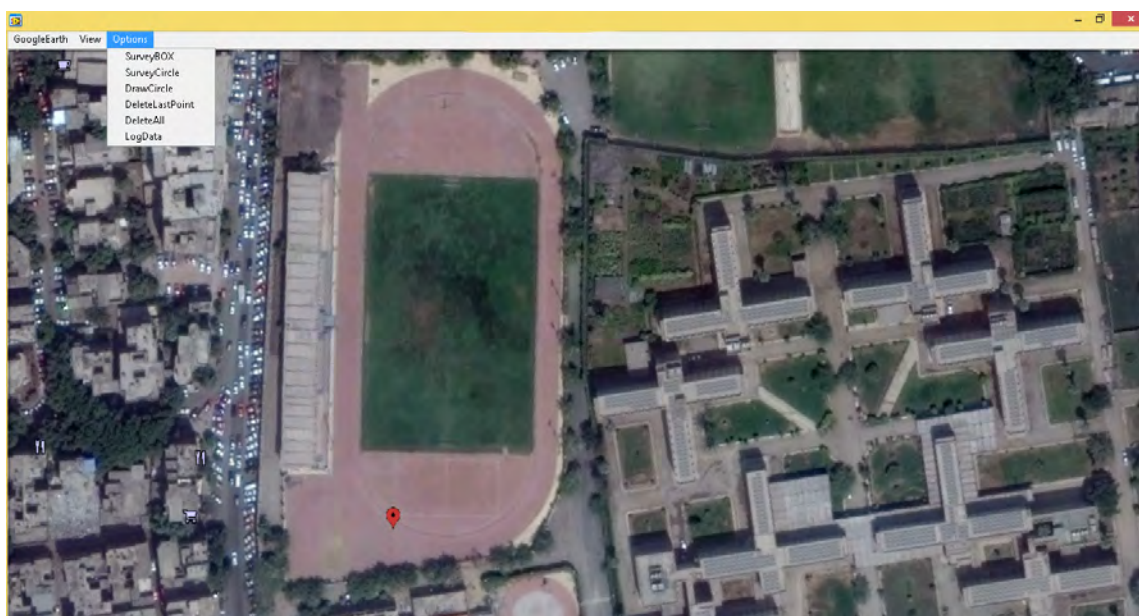


Figure B.22.: Screen shoot #4

- Enter Spline path parameters

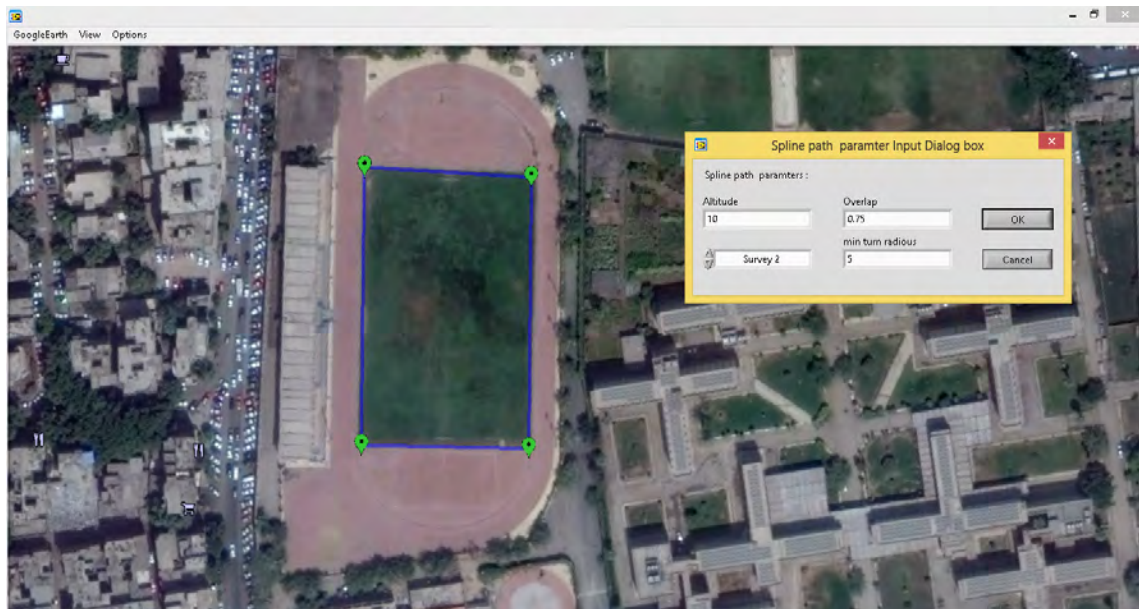


Figure B.23.: Screen shoot #6

- The result is

B. Ground Control Station

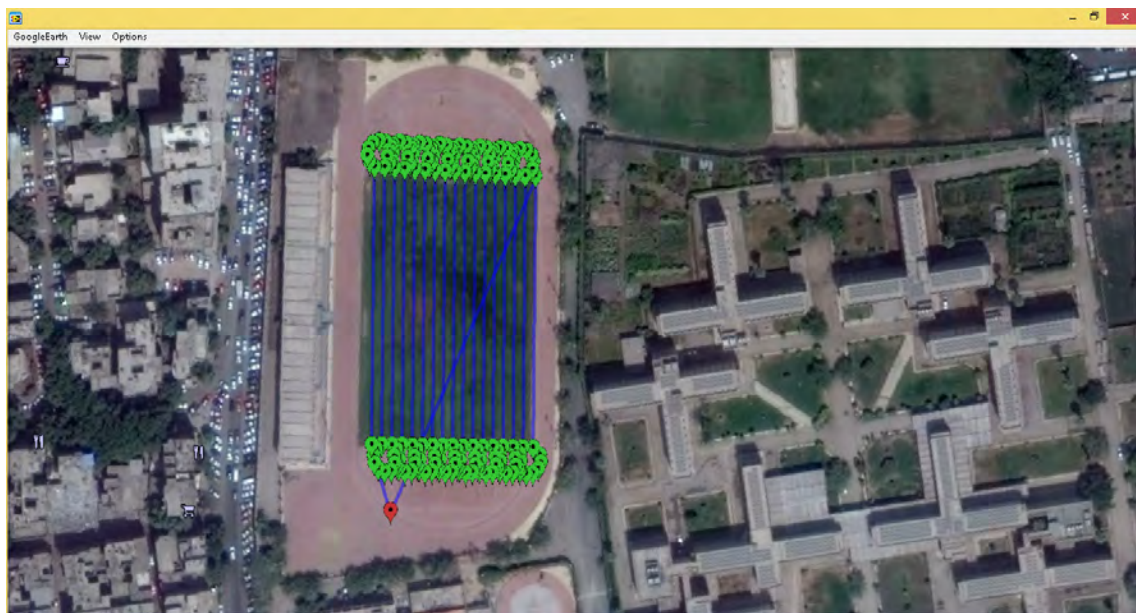


Figure B.24.: Screen shoot #7

B.3.5. Delete last point

- Go to menu bar and Click on Options then choose DeleteLastPoint from the drop-down menu

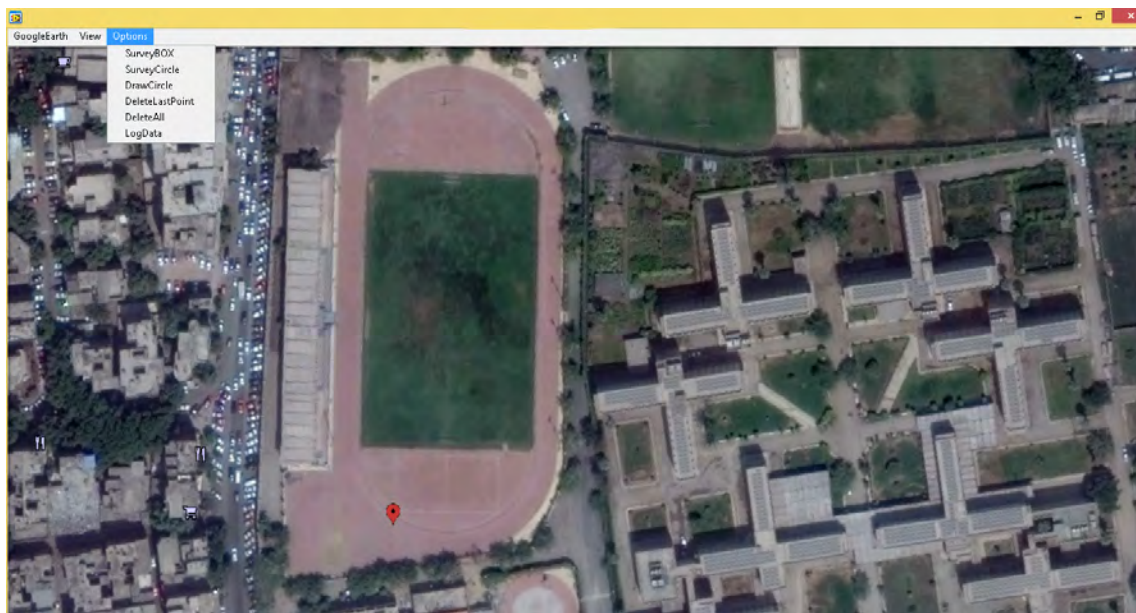


Figure B.25.: Screen shoot #4

B. Ground Control Station

B.3.6. Delete all points

- Go to menu bar and Click on Options then choose DeleteAll from the drop-down menu

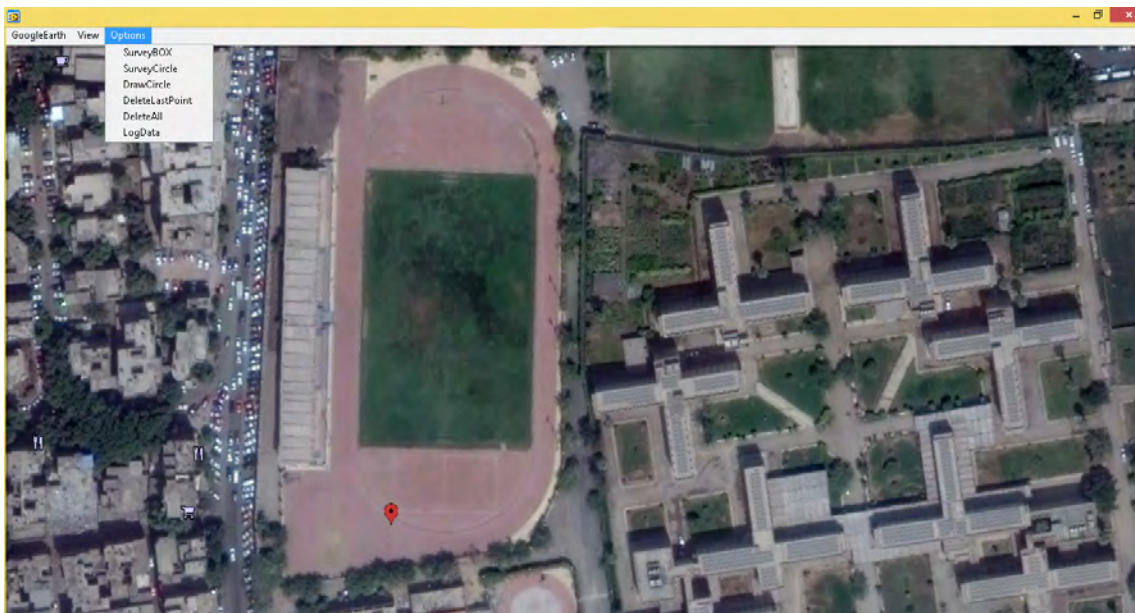


Figure B.26.: Screen shoot #4

B.3.7. Refresh maps

- To refresh maps just click on GoogleEarth then choose Refresh from the drop-down menu

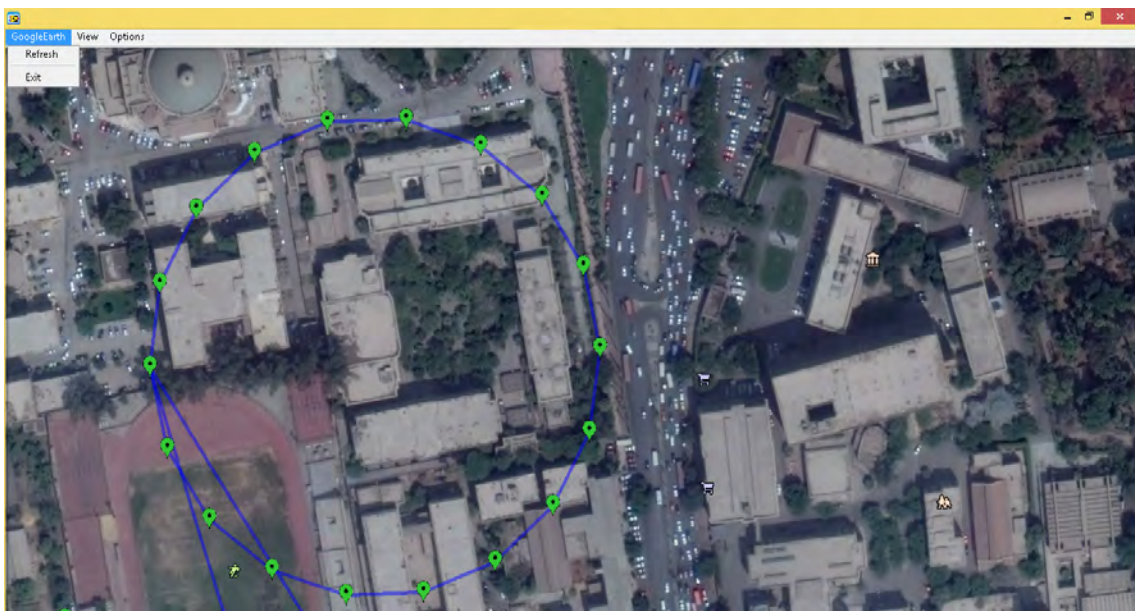


Figure B.27.: Screen shoot #8

B. Ground Control Station

B.3.8. Close the program

- To close the program just click on GoogleEarth then choose Exit from the drop-down menu

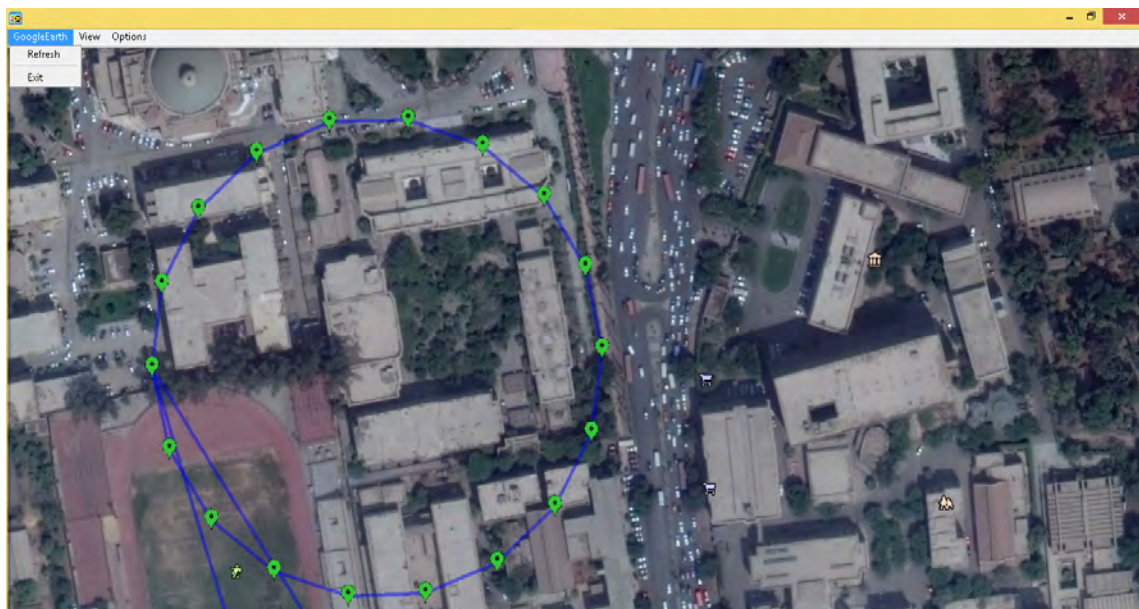


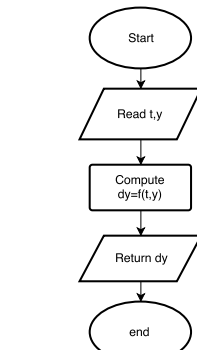
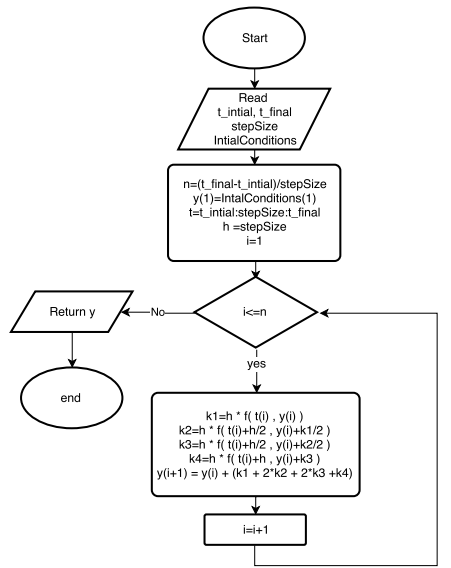
Figure B.28.: Screen shoot #8

C. Numerical Solution of differential equations using Runge-Kutta 4th order

Runge-Kutta 4th order

$$\begin{aligned}
 k_1 &= h f(x_n, y_n) \\
 k_2 &= h f\left(x_n + \frac{h}{2}, y_n + \frac{k_1}{2}\right) \\
 k_3 &= h f\left(x_n + \frac{h}{2}, y_n + \frac{k_2}{2}\right) \\
 k_4 &= h f(x_n + h, y_n + k_3) \\
 y_{n+1} &= y_n + \frac{1}{6}(k_1 + 2k_2 + 2k_3 + k_4)
 \end{aligned}$$

Flow Chart



Flow chart of function

Flow chart of Runge-Kutta Method

Figure C.1.: RK4 flow chart

C. Numerical Solution of differential equations using Runge-Kutta 4th order

C.1. Mat-lab code Implementation

```

function [ t,y ] = RK4(func,stepSize,timeSpan,intialValues)
h = stepSize;% step size
t = timeSpan(1):h:timeSpan(2);% time span
y = zeros(length(intialValues),length(t));
for i=1:length(intialValues)
    y(i,1)= intialValues(i); % The initial value of y at time t(1)
end
for i=1:(length(t)-1) % Runge Kutta forth order
    k1 = h * func( t(i) , y(:,i) );
    k2 = h * func( t(i)+0.5*h , y(:,i)+0.5*k1 );
    k3 = h * func( t(i)+0.5*h , y(:,i)+0.5*k2 );
    k4 = h * func( t(i)+h , y(:,i)+k3 );
    y(:,i+1) = y(:,i) + (1/6)*(k1 + 2*k2 + 2*k3 + k4);
end
y=y';
end

```

Testing

we compared the output of this function with the analytical solution of this differential equation

$$t^2 \frac{d^2y}{dt^2} - 2t \frac{dy}{dt} + 2y = t^3 \log(t)$$

the analytical solution of the previous differential equation is

$$Y(t) = \frac{7}{4} * t + \frac{t^3}{2} * \log(t) - \frac{3}{4} * t^3 \quad \text{for } 1 \leq t \leq 2$$

where $y'(1) = 0$, $y(1) = 1$

Solution procedure

first write the second order differential equation as a system of first order differential equations

$$\begin{aligned} & \text{let } y_1 = y \\ & \quad y_2 = y' \\ & \therefore y'_2 = \frac{2y_2}{t} - \frac{2y_1}{t^2} + t \log(t) \end{aligned}$$

Function Mat-lab code

```

function dy = f( t,y )
dy = zeros(2,1);
dy(1) = y(2);
dy(2) = 2*y(2)./t - 2*y(1)./(t.^2) + t.*log(t);
end

```

Testing Runge-kutta Mat-lab code

C. Numerical Solution of differential equations using Runge-Kutta 4th order

```

clc
clear all
close all
step = 0.01; % stepSize
timeSpan = [1, 2]; % timeSpan
initialConditions = [1, 0]; % y(1) = 1, y'(1) = 0, Initial conditions
[t, y] = RK4(@f, step, timeSpan, initialConditions);
Y = (7/4)*t + (t.^3/2).*log(t) - (3/4)*t.^3; % -- The analytic solution
figure
hold on
plot(t, Y, 'b', 'LineWidth', 5); % Plot the analytic solution in thick blue
plot(t, y(:, 1), 'r', 'LineWidth', 2); % Plot the RK4 solution in thin red
grid on
legend('analytic', 'RK4');
xlabel('Time')
ylabel('y')
title('Solution to (t^2)*y'' - 2*t*y' + 2*y = (t^3)*log(t)');

```

Comparing the two solutions

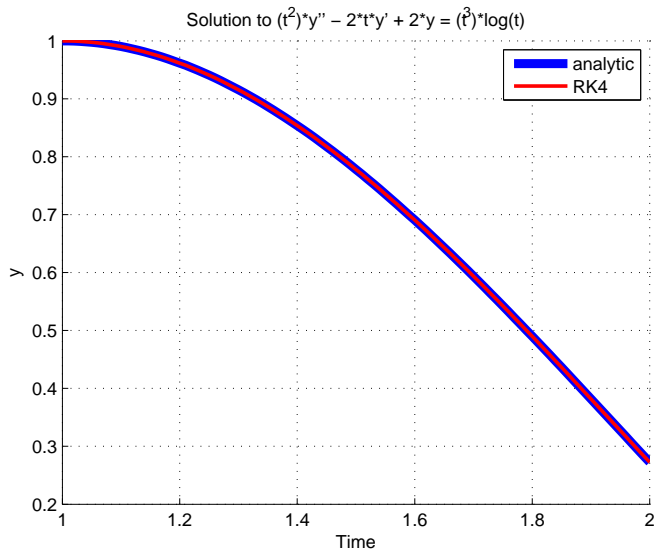


Figure C.2.: Analytic solution vs numerical solution

D. Moment of Inertia Estimation Using a Bifilar Pendulum

Overview

A bifilar pendulum consists of suspending a system from two parallel wires, or filars, that allow it to rotate freely about a given axis. The experiment is to measure the moment of inertia for the axis of rotation parallel to the filars. A small moment is then applied to the system to measure its period of oscillation, Taking into considerations the damping associated with the rotational motion due to aerodynamic drag and viscous damping, a nonlinear differential equation is introduced. This could be simplified, assuming small angular motion and omitting the damping, to produce the following equation:

$$I = \frac{mgb^2T^2}{4l^2\pi^2}$$

where;

m : Mass of the system.

g : Acceleration of gravity (9.79).

T : Periodic time of the motion.

b , l: Geometry related parameters.

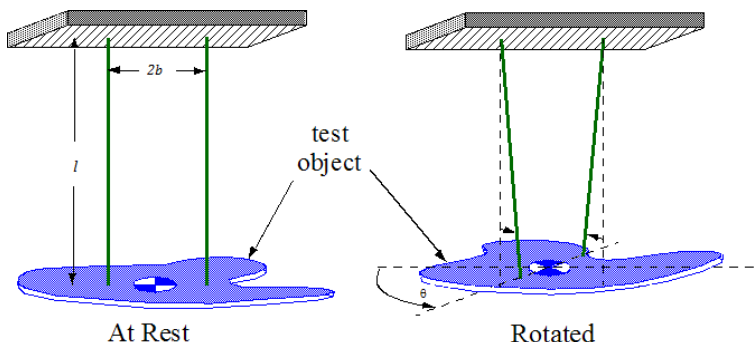


Figure D.1.: Bifilar Pendulum Experiment installation

Secondly, in order to measure the periodic time, apply a small angular displacement on the system, after hanging it with ropes as shown in D.1 and calculate the time and number of full cycles made till rest. Note that, it is not required to count the full cycles till rest. Ten to fifteen ($10 \rightarrow 15$) cycles are sufficient for the averaging, to avoid taking the damping and air drag in count.

It is important to make sure that the system is rotating without translating about the axis at which the moment of inertia is required.

D. Moment of Inertia Estimation Using a Bifilar Pendulum

It is important to verify that the center of gravity of the system is aligned with the points of suspension (i.e. the plane of the filars); a misalignment can lead to significant errors. The error associated with a misaligned center of gravity can be bound by the parallel-axis theorem.

After that, it is easy to estimate the periodic time from its definition by dividing the total time by the number of cycles ($T = \frac{\text{Time}}{\text{cycles}}$).

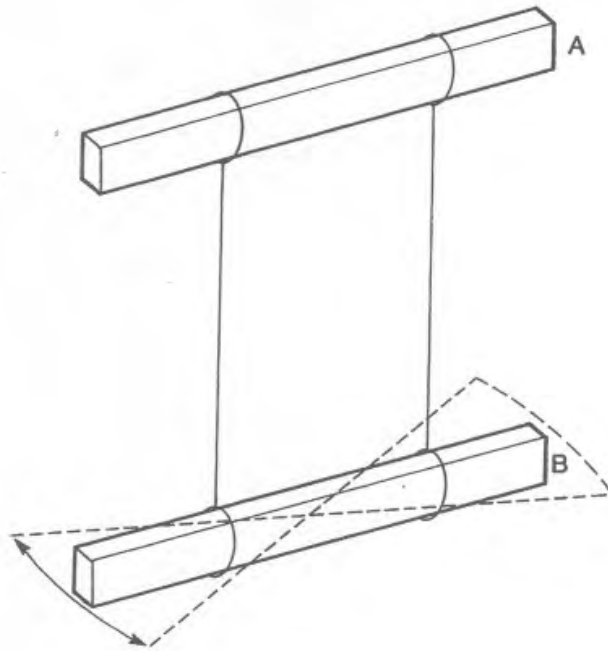


Figure D.2.: Bifilar Pendulum Experiment cycles

Finally, the last step is to substitute into the bifilar pendulum equation and calculate the moment of inertia.

D. Moment of Inertia Estimation Using a Bifilar Pendulum

Moment of inertia of a rod with square cross section

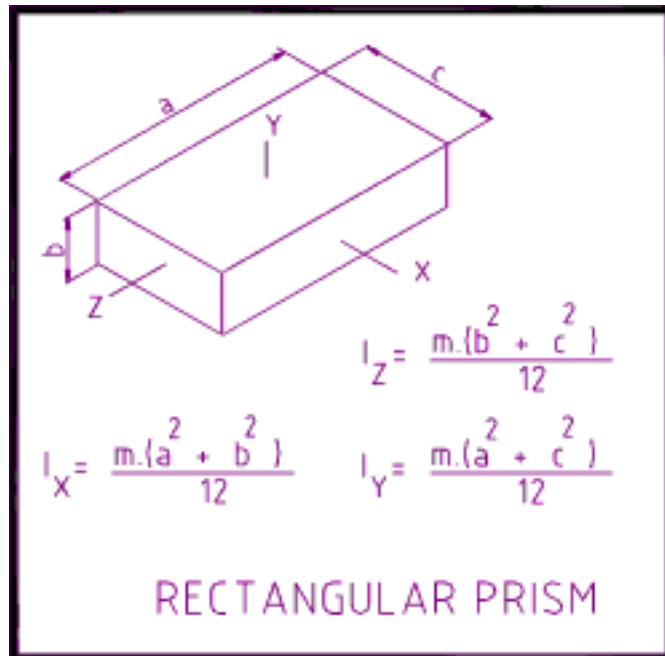


Figure D.3.: Rectangular prism

mass	0.23 kg
a	0.235 m
b	0.04 m
c	0.04 m

$$I_{\text{exact}} = m \frac{a^2 + c^2}{12} = 0.001089 \text{ kg.m}^2$$

Trial	Average Period (seconds)	Length of filar (L) (meters)	Moment of inertia ((kg-m ²)
1	2.3825	1.31	0.001044
2	2.3613	1.31	0.001026

Table D.1.: Bifilar testing data

Predicted	0.001089 kg.m ²
Experimental	0.001035 kg.m ²

Percent Error: +4.9586%

Table D.2.: Moment of Inertia Results

D. Moment of Inertia Estimation Using a Bifilar Pendulum

Moment of inertia of a quad

mass	1.66 kg
------	---------

Measuring I_{xx} & I_{yy}

from system symmetry

$$I_{xx} = I_{yy}$$

Trial	Average Period (seconds)	Length of filar (L) (meters)	Moment of inertia ($\text{kg}\cdot\text{m}^2$)
1	3.7467	1.32	0.0187
2	3.6329	1.32	0.0175

Predicted	0.0181 $\text{kg}\cdot\text{m}^2$
-----------	-----------------------------------

Measuring I_{zz}

Trial	Average Period (seconds)	Length of filar (L) (meters)	Moment of inertia ($\text{kg}\cdot\text{m}^2$)
1	5.2393	1.31	0.0361
2	5.2129	1.31	0.0357

Predicted	0.0359 $\text{kg}\cdot\text{m}^2$
-----------	-----------------------------------

E. Measuring Motors' Parameters

We used two methods to get motors' constants

- First Method: Using Load cell to measure thrust of each motors, We couldn't measure the torque constants so we went to the second method.
- Second method: Using ATI Multi-Axis Force / Torque Sensor.

E.1. First Method

We measured the thrust of each motor using load cell.

Load Cell

Load Cell is a transducer that generates a voltage signal as a result of an applied force.

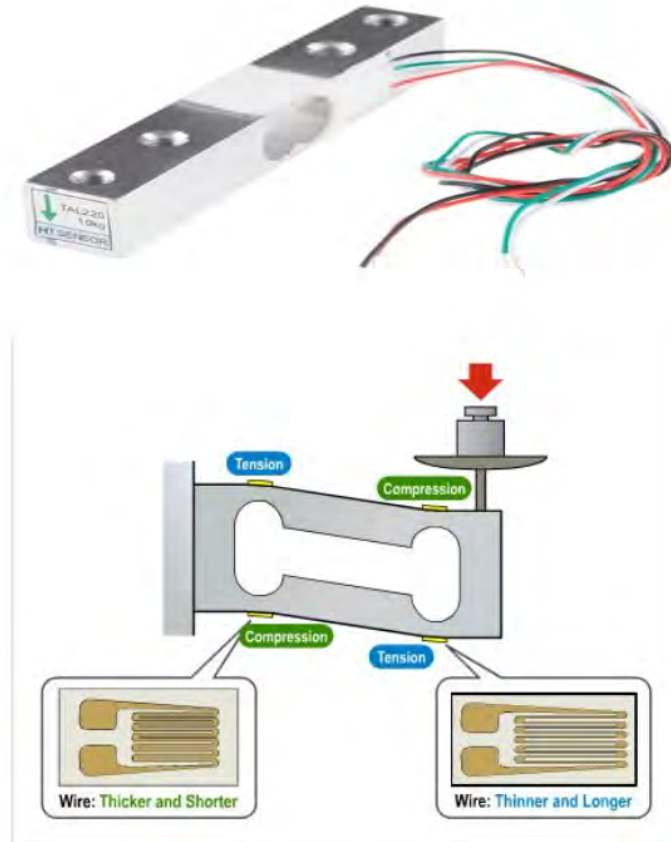


Figure E.1.: Loadcell #1

E. Measuring Motors' Parameters

We started our work using these components

- HX711 Balance Module [30]
- Arduino Uno Board and USB cable
- Load Cell, with maximum weight of 10 kg [31]

HX711 Balance Module: This module uses 24 high-precision A / D converter. This chip is designed for high-precision electronic scale and design, has two analog input channels, programmable gain of 128 integrated amplifier. The input circuit can be configured to provide a bridge voltage electrical bridge (such as pressure, load) sensor model is an ideal high-precision, low-cost sampling front-end module.

HX711 Specifications

Data Accuracy: 24 bit (24 bit analog-to-digital converter chip)
Operation supply voltage range: 4.8 ~ 5.5V
Operation supply Current: 1.6mA

Hardware Installation:

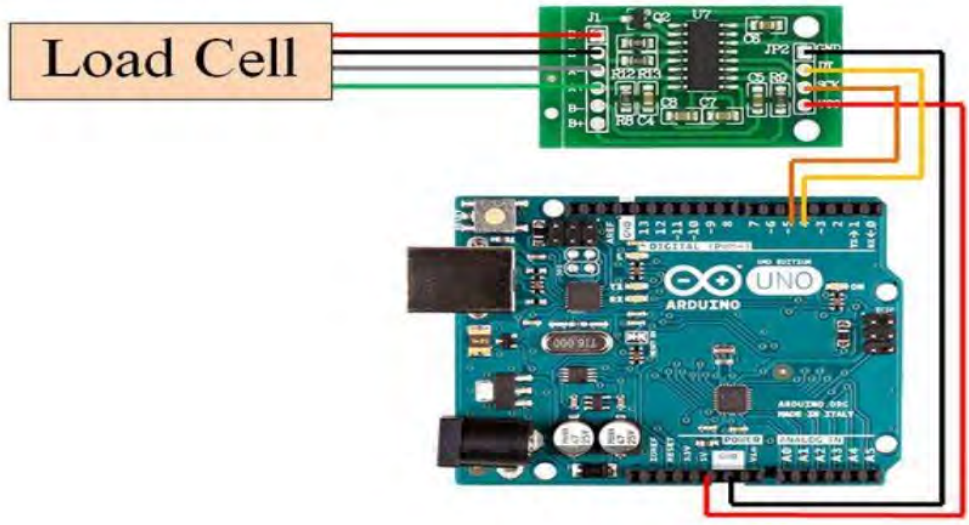


Figure E.2.: Load Cell #1

Connections:

- HX711 to Arduino Uno
 - VCC to 5V
 - GND to GND
 - SCK to D5

E. Measuring Motors' Parameters

- DT to D6
- Load Cell to HX711
 - E+ : RED
 - E- : BLACK
 - A- : WHITE
 - A+ : GREEN

We calibrated the load cell with some known weights and then remove them one by one to see if any non linearity in the sensor.

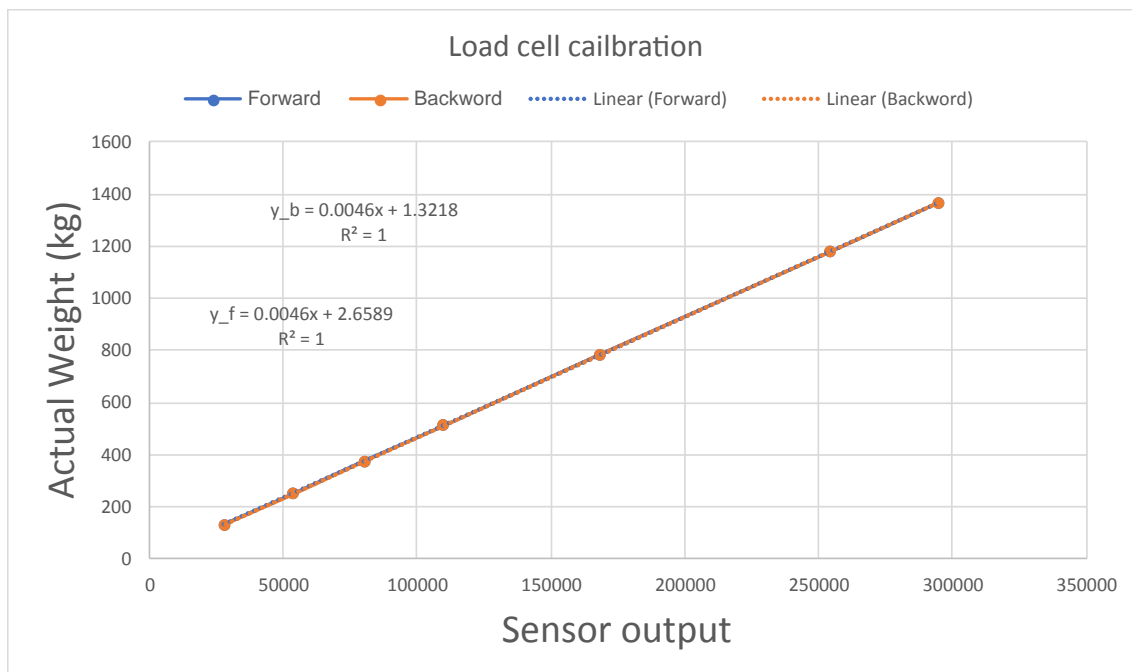


Figure E.3.: Load Cell calibration

E. Measuring Motors' Parameters

Testing each motor

Motor 1

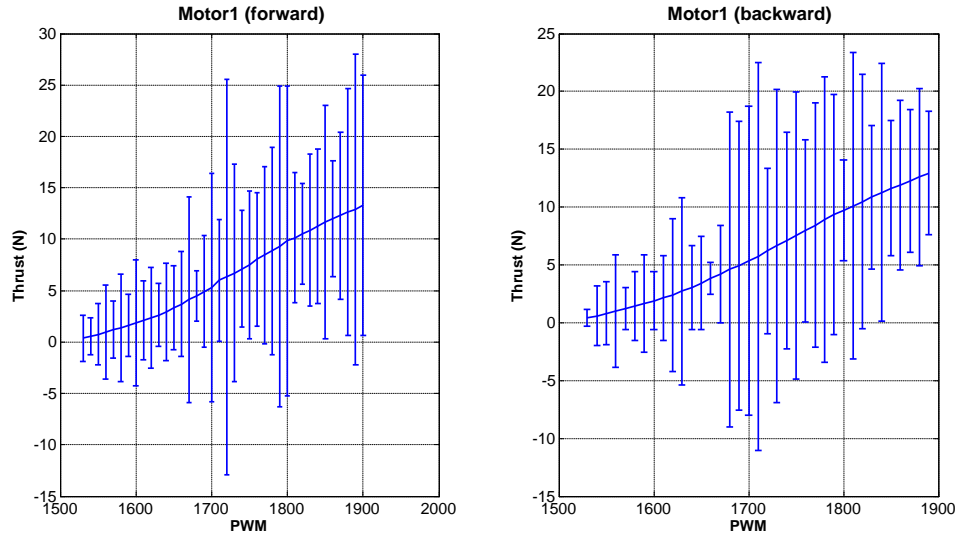


Figure E.4.: Motor 1

Motor 2

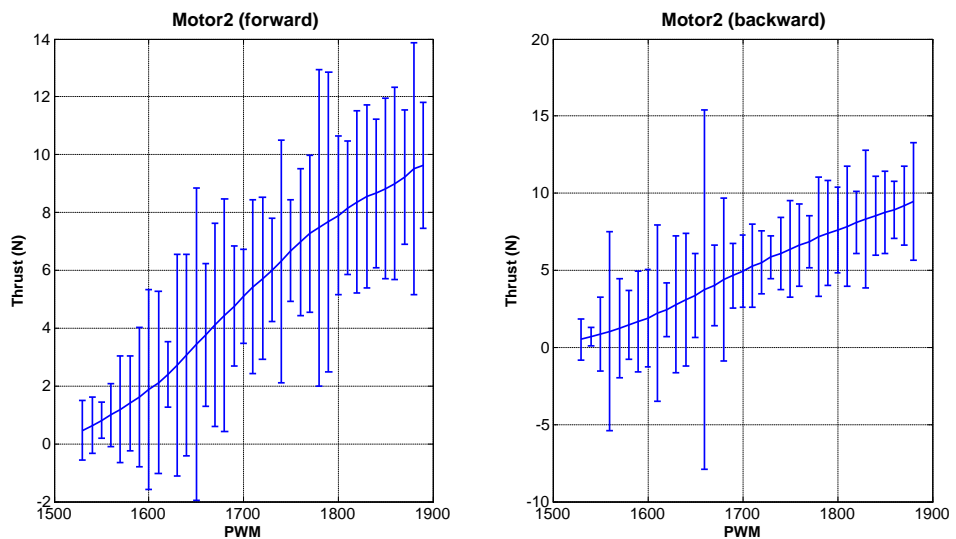


Figure E.5.: Motor 2

E. Measuring Motors' Parameters

Motor 3

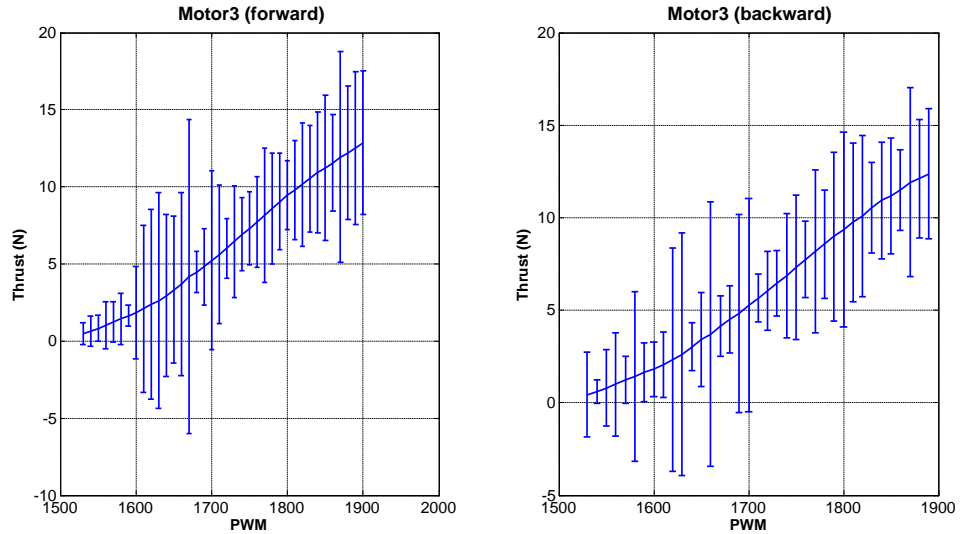


Figure E.6.: Motor 3

Motor 4

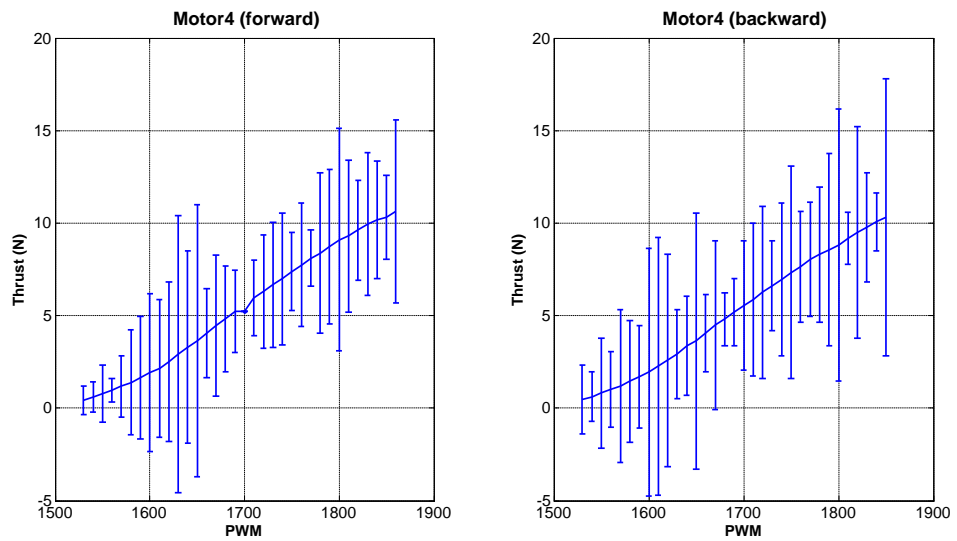


Figure E.7.: Motor 4

E. Measuring Motors' Paramters

E.2. Second Method

The ATI Multi-Axis Force/Torque Sensor system [32], is a device that measures the outputting forces and torques from all three Cartesian coordinates (x, y, and z).



Figure E.8.: Motor testing

E. Measuring Motors' Parameters

Testing each motor

Motor 1

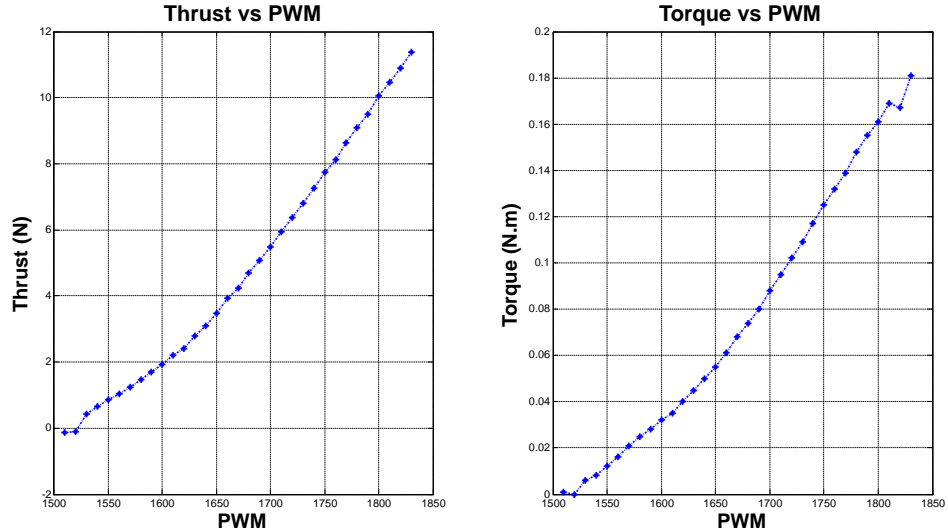


Figure E.9.: Motor 1

Motor 2

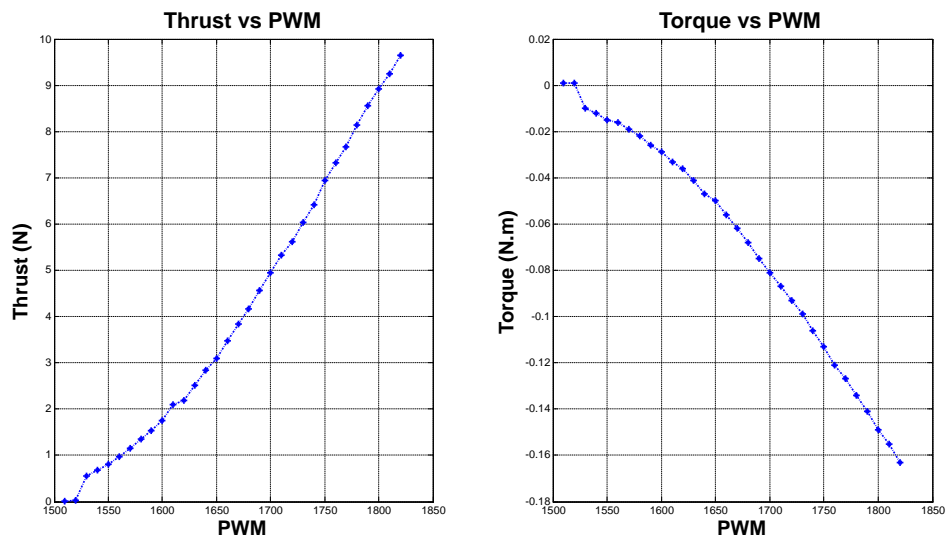


Figure E.10.: Motor 2

E. Measuring Motors' Parameters

Motor 3

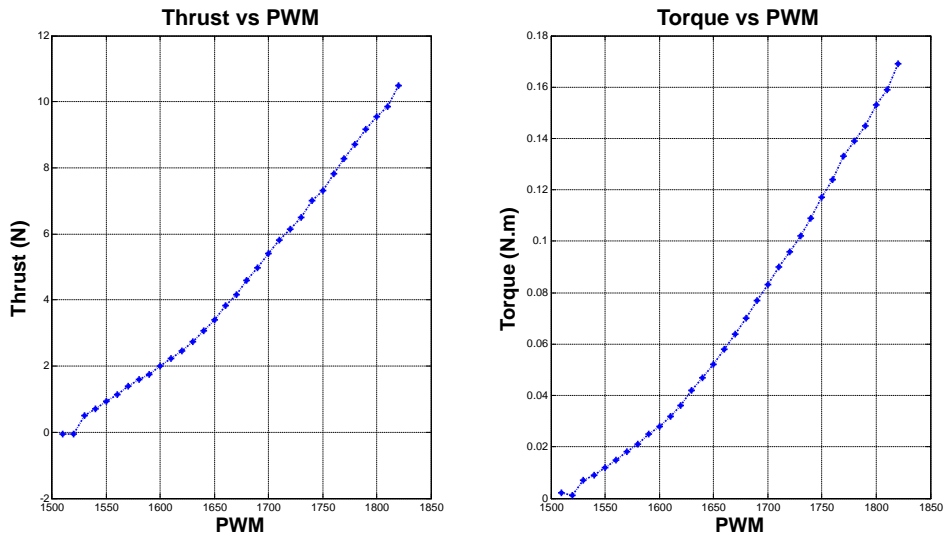


Figure E.11.: Motor 3

Motor 4

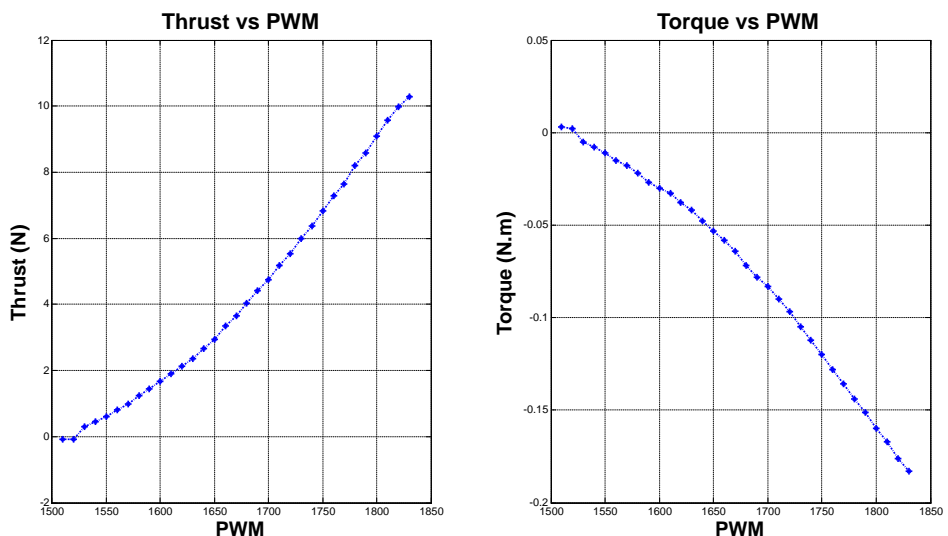


Figure E.12.: Motor 4

E. Measuring Motors' Parameters

PWM		1650	1700
Motor 1	K	0.0360	0.0417
	B	5.6250e-04	7.0000e-04
Motor 2	K	0.0308	0.0369
	B	-5.2500e-04	-6.2500e-04
Motor 3	K	0.0343	0.0394
	B	5.6250e-04	6.3750e-04
Motor 4	K	0.0316	0.0378
	B	-5.6250e-04	-6.7500e-04

Table E.1.: Motors' constants

Note:

We measured thrust constant of each motor using the two methods , but we'll take the results of the second method as it's more reliable.

E.3. Comparison

	Method 1	Method 2	Error
Motor 1	0.035	0.0360	2.77 %
Motor 2	0.0331	0.0308	7.46 %
Motor 3	0.0343	0.0343	0 %
Motor 4	0.0386	0.0316	22.15 %

Table E.2.: Comparison of motors' thrust constant using the two methods @ Nom.Thrust =1650

	Method 1	Method 2	Error (%)
Motor 1	0.0428	0.0417	2.63 %
Motor 2	0.0318	0.0369	-13.82 %
Motor 3	0.0406	0.0394	3.04 %
Motor 4	0.0370	0.0378	-2.11 %

Table E.3.: Comparison of motors' thrust constant using the two methods @ Nom.Thrust =1700

For thrust constant, we can conclude that the first method give accepted results even so the sensor is much cheaper than the one used in the second method